Intersectin1 is a component of the Reelin-VLDLR pathway to regulate neuronal migration, adult neurogenesis and synaptic plasticity in the hippocampus

Inaugural-Dissertation

to obtain the academic degree
Doctor rerum naturalium (Dr. rer. nat.)

submitted to the Department of Biology, Chemistry and Pharmacy
of Freie Universität Berlin

by
Burkhard Jakob
from Würzburg, Germany
2016

Period of doctoral studies: September 2010 to June 2016

Supervisor: Prof. Dr. Volker Haucke

Institute: Institut für Chemie und Biochemie, Freie Universität Berlin
(09/2010 to 08/2012)
Leibniz-Institut für Molekulare Pharmakologie (FMP), Berlin-Buch
(09/2012 to 06/2016)

1st Reviewer: Prof. Dr. Volker Haucke

2nd Reviewer: Prof. Dr. Thomas Willnow

Date of defense: November the 2nd, 2016

Affidavit

I declare that my PhD thesis at hand has been written independently and with no other sources and aids then quoted.

Berlin, August the 5th, 2016

Acknowledgements

I want to express my gratitude to my supervisor, Prof. Volker Haucke. Your support and guidance were crucial for the success of my PhD project.

I would particularly like to thank Gaga Kochlamazashvili for his great work with the electrophysiological recordings and Maria Jäpel for discussing ITSNs in all its facets in and outside of our subgroup meetings. I would like to give thanks to Marielle Eichhorn-Grünig, Natalia Kononenko and Arndt Pechstein for discussions and practical support.

I owe special thanks to Melanie Pritchard (Melbourne) for providing the ITSN1 KO mice and Hans Bock (Düsseldorf) and Joachim Herz (Dallas) for the ApoER2 KO mice. Many thanks also to Hans Bock, Jonathan Cooper (Seattle), Carol Mason (New York) and Bill Rebeck (Washington, D.C.) for the DNA constructs and to Tom Curran (Philadelphia) for CER and CEP4 cell lines.

Moreover, I would like to express my gratitude to the skilled and charming technicians in the AG Haucke lab: Delia Löwe, Maria Mühlbauer and Silke Zillmann. Many thanks also to Jenny Eichhorst and Burkhard Wiesner from the Imaging Facility and the MDC animal caretakers Franziska Binder, Franziska Ellert and Stephanie Rode for their help and support. Special thanks also to our endearing secretaries, Alex Chylla and Heidi Petschick, and to “our IT guy” Alex Heyne.

Furthermore, I would like to acknowledge all past and present members of the AG Haucke, including AG Krauß, AG Maritzen and AG Schmoranzer. The time in the lab would have been different, presumably worse, without you: Jelena Bacetic, Marietta Browarski, Caroline Bruns, Katrin Diesenberg, Fabian Feutlinske, Uwe Fink, Niclas Gimber, Gala Claßen, Claudia Gras, Isabelle Grass, Kira Gromova, Sabine Hahn, Lisa Jerndal, Natalie Kaempf, Christina Kath, Katharina Ketel, Peter Koch, Seong Joo Koo, Ludwig Krabben, Michael Krauß, Marijn Kuijpers, André Lampe, Wen-Ting Lo, Martin Lehmann, Gregor Lichtner, Tania López Hernández, Albert Mackintosh, Marta Maglione, Andrea Marat, Tanja Maritzen, Julia Mössinger, Jasmin Podufall, York Posor, Dmytro Puchkov, Yijian Rao, Christine Rückert, Linda Sawade, Hannah Schachtner, Claudia Schmidt, Jan Schmoranzer, Irene Schütz, Kyungyeun Song, Wiebke Stahlschmidt, Tolga Soykan, Susanne Thomsen, Dennis Vollweiter, Anela Vukoja,

Alexander Wallroth, Ingeborg Walther, Susanne Wojtke, Haibin Wang, Anna Wawrzyniak, Mirjana Weimershaus and Marnix Wieffer.

Most importantly, I want to thank my family and friends for their support and being there.

Table of contents

Summary

Intersectin1 (ITSN1) is a multi-domain scaffold protein with proposed roles in vesicular membrane traffic and cellular signaling events. However, the functional relevance of ITSN1 in mammalian organisms is still under debate. Here, we provide evidence for a so far undescribed function of ITSN1. Mouse mutants with a genetic ablation of ITSN1 (ITSN1 knockout mice) display normal viability and appearance. However, histological analysis of brains from ITSN1 knockout mice revealed marked perturbations in the hippocampus. In these mice, hippocampal layering is disrupted due to aberrant cell migration during development. In addition, the radial glia scaffold in the dentate gyrus is disorganized and neuronal precursors are ectopically localized, indicating deficits in hippocampal adult neurogenesis. Cortical and cerebellar architecture, neurogenesis in the subventricular zone (SVZ), dendritic spine morphology and axonal commissure formation are unaltered in the absence of ITSN1. This suggests that ITSN1 is specifically required for development and function of the hippocampus. A number of cell biological and biochemical experiments revealed that the alterations in ITSN1 knockout mice are not the consequence of defective ephrinB/EphB trafficking or signaling, a pathway previously linked to ITSN1. Instead, the phenotype of ITSN1 knockout mice is caused by defective signaling downstream of the large extracellular glycoprotein Reelin. Biochemical, electrophysiological and genetic data indicate that ITSN1 is specifically required for propagation of the Reelin signal through one of its major receptors, the very-low-density-lipoprotein receptor (VLDLR). ITSN1 associates physically with VLDLR and the Reelin signaling adaptor Disabled1 (Dab1). Despite its described role as endocytic scaffold protein, ITSN1 is dispensable for endocytic trafficking of Reelin receptors. However, levels of phosphorylated Dab1 are decreased in ITSN1 knockout mice indicating inefficient activation of the Reelin signaling pathway. Reelin fails to facilitate N-methyl-D-aspartate receptor (NMDAR) potentials in ITSN1 knockout mice and, as a result, cannot augment hippocampal long-term potentiation (LTP). These findings suggest that ITSN1 operates as a signaling adaptor for Reelin-VLDLR-Dab1 signaling. This notion is supported by mouse mutants deficient for the second main receptor for Reelin, apolipoprotein E receptor 2 (ApoER2). These ApoER2 knockout

mice phenotypically resemble ITSN1 knockout mice, albeit in a more severe form, suggesting that the disruptions in the absence of ITSN1 are indeed a consequence of defective Reelin signaling. Simultaneous ablation of ITSN1 and ApoER2 (ITSN1/ApoER2 double knockout mice) aggravates the defects in hippocampal morphology and neurogenesis. In addition, ITSN1/ApoER2 double knockout mice also display disrupted layering of the cerebral cortex, similar to VLDLR/ApoER2 double knockout mice. These results imply that ITSN1 and ApoER2 act in distinct pathways transmitting the Reelin signal, in agreement with the biochemical data. Taken together, our results show that ITSN1 is a component of the Reelin signaling machinery downstream of the VLDLR. This finding provides insights into the mechanisms by which Reelin fulfills its various functions for the developing and mature brain. Furthermore, our results may have implications for a variety of neurological diseases, particularly Down syndrome and Alzheimer's disease.

Zusammenfassung

Intersectin1 (ITSN1) ist ein Multidomänen-Gerüstprotein, für das Funktionen im vesikulären Membranverkehr und bei zellulären Signalkaskaden vorgeschlagen wurden. Allerdings ist die funktionelle Bedeutung von ITSN1 in Säugetierorganismen noch nicht ausdiskutiert. Hier erbringen wir den Nachweis für eine bisher unbeschriebene Funktion von ITSN1. Mausmutanten, denen ITSN1 genetisch entfernt wurde (ITSN1 Knockout Mäuse), weisen eine normale Lebensfähigkeit auf und erscheinen äußerlich normal. Histologische Analysen der Gehirne von ITSN1 Knockout Mäusen offenbarten jedoch ausgeprägte Störungen im Hippocampus. In diesen Mäusen ist die hippocampale Schichtung aufgrund fehlerhafter Zellwanderung während der Entwicklung gestört. Darüber hinaus ist das Gerüst der radialen Gliazellen im Gyrus dentatus ungeordnet und neuronale Vorläufer ektopisch lokalisiert, was auf Defizite bei der adulten Neurogenese im Hippocampus hinweist. Der Aufbau des Cortex und des Cerebellums, die Neurogenese in der subventrikulären Zone (SVZ), die Morphologie dendritischer Dornen und die Ausbildung axonaler Kommissuren sind unverändert in Abwesenheit von ITSN1. Dies deutet darauf hin, dass ITSN1 spezifisch für Entwicklung und Funktion des Hippocampus benötigt wird. Mehrere zellbiologische und biochemische Experimente zeigten, dass die Veränderungen in ITSN1 Knockout Mäusen nicht die Folge von Mängeln im Transport oder der Signalweiterleitung von ephrinB/EphB-Proteinen sind, ein Signalweg, welcher zuvor mit ITSN1 in Verbindung gebracht wurde. Der Phänotyp der ITSN1 Knockout Mäuse wird vielmehr durch Fehler im Signalweg, welcher dem großen extrazellulären Glycoprotein Reelin nachgeschaltet ist, verursacht. Biochemische, elektrophysiologische und genetische Daten zeigen, dass ITSN1 spezifisch für die Weitergabe des Reelin-Signals durch einen seiner Hauptrezeptoren, den Very-low-density-lipoprotein Rezeptor (VLDLR), benötigt wird. ITSN1 ist physisch mit VLDLR und dem Reelin-Signal-Adapterprotein Disabled1 (Dab1) assoziiert. Trotz seiner beschriebenen Funktion als endozytisches Gerüstprotein, ist ITSN1 entbehrlich für den endozytischen Transport der Reelin-Rezeptoren. Die Menge an phosphoryliertem Dab1 ist jedoch verringert in ITSN1 Knockout Mäusen, was auf eine ineffiziente Aktivierung des Reelin-Signalwegs

hinweist. Reelin gelingt es nicht, in ITSN1 Knockout Mäusen N-methyl-D-aspartate-Rezeptor (NMDAR)-Potentiale zu verstärken und es kann daher das Ausmaß der hippocampalen Langzeit-Potenzierung (LTP) nicht vergrößern. Diese Erkenntnisse legen den Schluss nahe, dass ITSN1 als Adapter für den Reelin-VLDLR-Dab1 Signalweg fungiert. Diese Vorstellung wird gestützt von Mausmutanten, denen der zweite Hauptrezeptor für Reelin, Apolipoprotein E Rezeptor 2 (ApoER2), fehlt. Diese ApoER2 Knockout Mäuse ähneln ITSN1 Knockout Mäusen phänotypisch, wenn auch in einer schwereren Ausprägung, was nahelegt, dass die Störungen in Abwesenheit von ITSN1 in der Tat die Folge eines fehlerhaften Reelin-Signalwegs sind. Die gleichzeitige Entfernung von ITSN1 und ApoER2 (ITSN1/ApoER2 Doppel-Knockout Mäuse) verschärft die Defekte hippocampaler Morphologie und Neurogenese. Darüber hinaus weisen ITSN1/ApoER2 Doppel-Knockout Mäuse eine fehlerhafte Schichtung des zerebralen Cortexes auf, ähnlich wie VLDLR/ApoER2 Doppel-Knockout Mäuse. Diese Ergebnisse lassen darauf schließen, dass ITSN1 und ApoER2 bei der Übertragung des Reelin-Signals in unterschiedlichen Signalwegen agieren, was im Einklang mit den biochemischen Daten steht. Zusammengefasst zeigen unsere Ergebnisse, dass ITSN1 eine Komponente der Maschinerie darstellt, die abhängig von VLDLR das Reelin-Signal weitergibt. Dieser Befund verschafft Einblicke in die Mechanismen, mit denen Reelin seine vielfältigen Funktionen für das sich entwickelnde und das reife Gehirn erfüllt. Des Weiteren könnten unsere Ergebnisse Folgen für eine Vielzahl an neurologischen Erkrankungen, im Besonderen Down-Syndrom und Alzheimer-Krankheit, haben.

1. Introduction

1.1 ITSNs as scaffold proteins

Scaffold and adaptor proteins are vital for many cellular processes, including proliferation, survival, differentiation, trafficking and migration. Scaffold proteins consist of multiple modular interaction domains (Good et al., 2011). This modular architecture enables scaffold proteins to interact with multiple proteins simultaneously. In doing so, scaffolds can promote the interaction and communication between different molecular components of a certain pathway. By controlling the assembly of multi-protein complexes in space and time, scaffold proteins can influence both the kinetics and the specificity of cellular signals.

Intersectin (ITSN) is a multi-domain scaffolding protein conserved throughout evolution as its orthologs can be found in all metazoan animals examined so far. ITSN is also known as Dap160 in *Drosophila* (Roos and Kelly, 1998), Ese-1/2 in mouse (Sengar et al., 1999), or EHSH-1/2 in rat (Okamoto et al., 1999). In mammals, there are two ITSN genes, ITSN1 and ITSN2, which show a high degree of similarity in both sequence and domain structure (Pucharcos et al., 2000). For both ITSN genes, alternative splicing results in two main isoforms, a ubiquitously expressed short isoform (ITSN-S) and a long isoform (ITSN-L), predominantly expressed in the nervous system (Guipponi et al., 1998; Pucharcos et al., 2001). ITSN-S consists of two Eps15 homology domains (EH1 and EH2), a coiled-coil region (CCR) and a stretch of five Src homology 3 domains (SH3A-E). The name 'intersectin' was chosen due to its potential to link EH and SH3 domain-binding proteins in a macromolecular complex (Yamabhai et al., 1998).

EH domains bind to Asn-Pro-Phe (NPF) motifs and have been found in several proteins implicated in endocytosis (Santolini et al., 1999). CCRs frequently mediate protein oligomerization (Burkhard et al., 2001). SH3 domains bind to proline-rich regions (PRR) and are commonly found in proteins regulating signaling pathways, cytoskeletal remodeling and membrane traffic (Mayer and Eck, 1995). The long isoform ITSN-L contains the same domains but also three additional domains at its C-terminus, a Dbl homology domain (DH), a pleckstrin homology domain (PH) and a C2 domain (Guipponi et al., 1998; Hussain et al., 1999; Sengar et al., 1999). The DH and

PH domain function as a guanine nucleotide exchange factor (GEF) that activates the Ras homolog gene (Rho) family GTPase Cdc42 (Hussain et al., 2001). Via its SH3 domains, ITSN can also bind to the neural Wiskott-Aldrich syndrome protein N-WASP. This interaction stimulates the ITSN1 GEF activity, thereby inducing N-WASP- and Actin-related protein-2/3 complex (Arp2/3)-dependent actin assembly (Hussain et al., 2001; McGavin et al., 2001). C2 domains are important for membrane trafficking and signaling processes by their ability to bind phosphoinositides and calcium (Corbalan-Garcia and Gomez-Fernandez, 2014). Thanks to their multi-modular structure, ITSN1 and 2 are ideally suited to act as scaffolding proteins. This work focuses on the role of ITSN1 in mammalian physiology.

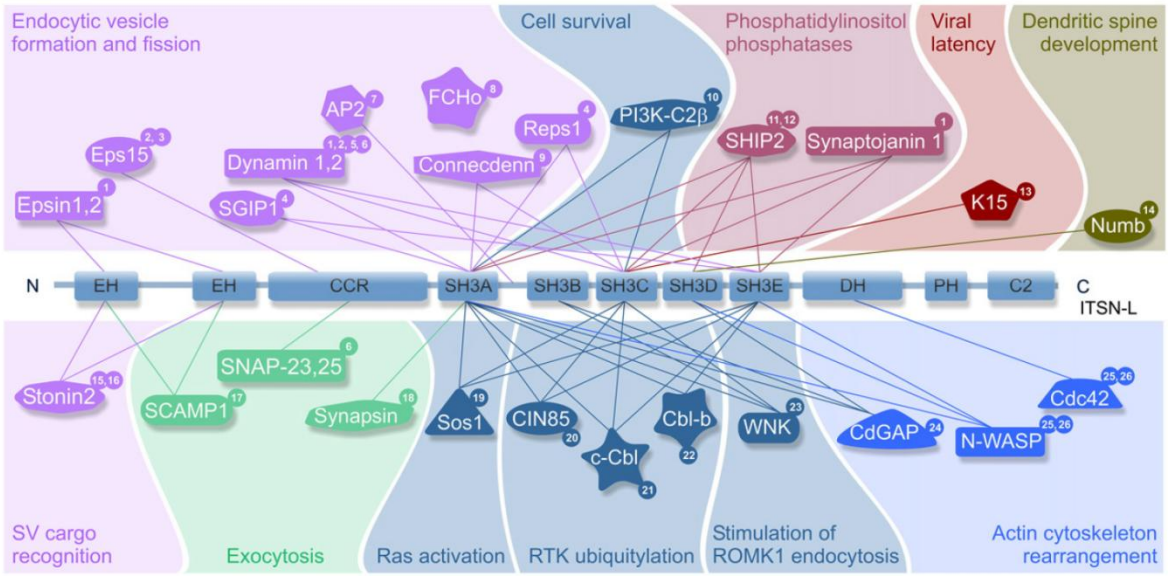

Figure 1.1 Schematic view of the ITSN domain structure and interacting proteins. ITSN consists of two EH domains followed by a coiled-coil region (CCR) and five SH3 domains. The long isoform has an extended C-terminus harboring a Dbl homology domain (DH), a pleckstrin homology domain (PH) and a C2 domain. The different domains interact with a plethora of binding partners implicating ITSN scaffold proteins in a variety of processes. Taken from Tsyba et al., 2011.

1.1.1 ITSN1 in vesicle trafficking

Eukaryotic cells are able to take up extracellular material into the cell in a process called endocytosis. There are several mechanistically distinct pathways of endocytosis, although probably considerable overlap exists between the different types. Depending on whether the coat protein clathrin is involved in formation of the endocytic vesicle, endocytic pathways are grouped into clathrin-dependent

and -independent processes (Doherty and McMahon, 2009; Hansen and Nichols, 2009).

Of the clathrin-independent pathways, caveolae-mediated endocytosis is the most commonly described process. Caveolae are invaginations of the plasma membrane with a characteristic flask-shaped morphology. Endocytosis via caveolae depends on the lipid-binding protein caveolin (Rothberg et al., 1992) and the membrane-fissioning GTPase Dynamin (Henley et al., 1998; Oh et al., 1998). Other clathrin-independent pathways like macropinocytosis, flotillin-mediated endocytosis or the CLIC/GEEC (clathrin-independent carriers/GPI-enriched early endosomal compartments) pathway are less well understood.

Clathrin-mediated endocytosis (CME) is the best understood endocytic pathway (McMahon and Boucrot, 2011). Adaptor and accessory proteins promote clathrin nucleation at phosphatidylinositol-4, 5-bisphosphate ($PI4,5P_2$)-rich sites of the plasma membrane, generating a clathrin-coated pit (CCP). Cargo is recruited into the nascent pit by the adaptor protein complex 2 (AP-2), as are further clathrin molecules. Clathrin polymerization in hexagons and pentagons facilitates membrane invagination and constriction of the neck. Clathrin-coated vesicles (CCVs) are produced by the action of the large GTPase Dynamin which mediates fission of the vesicle from the plasma membrane. The phosphoinositide phosphatase Synaptojanin 1 removes $PI4,5P_2$ and thereby releases adaptor proteins from the vesicle membrane. Finally, the clathrin coat is shed by auxilin and Hsc70.

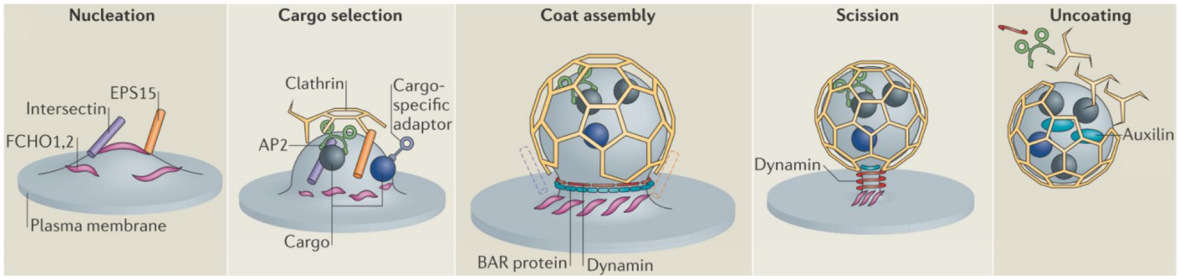

Figure 1.2 Clathrin-mediated endocytosis. The generation of clathrin-coated vesicles consists of five steps. Nucleators of clathrin-coated pits (CCPs) like FCH domain only (FCHo) proteins bind $PI4,5P_2$-rich sites of the membrane and recruit scaffold proteins like Eps15 or intersectins and adaptor protein complex 2 (AP-2). Cargo is recruited to CCPs via direct interaction with AP-2 or via cargo-specific adaptors. Clathrin molecules polymerize and form the clathrin coat around the nascent pit. Dynamin is recruited to the neck of the forming vesicle and induces membrane scission in a GTP-consuming process. Auxilin and Hsc70 disassemble the clathrin coat and release the endocytic vesicle into the cytosol. Modified from McMahon and Boucrot, 2011.

A vast number of experiments link ITSN1 to clathrin-mediated endocytosis. The EH domains of ITSN1 can interact with the endocytic accessory protein epsin and the endocytic sorting adaptor stonin 2 (Yamabhai et al., 1998; Hussain et al., 1999; Martina et al., 2001). ITSN1 can form heterodimers with the scaffolding protein Eps15 through CCR interaction (Sengar et al., 1999). Via its SH3 domains, ITSN1 can bind to the vesicle fission protein Dynamin and the phosphatase Synaptojanin 1 (Yamabhai et al., 1998; Sengar et al., 1999). Similar interactions have been described for ITSN1 orthologs in *C. elegans* and *Drosophila* (Roos and Kelly, 1998; Koh et al., 2007; Wang et al., 2008). A complex between FCHo, a nucleator of CCPs, and ITSN1 has also been described (Henne et al., 2010). ITSN1 also associates with the membrane deforming protein SH3-containing GRB2-like protein 3-interacting protein 1 (SGIP1) and the adaptor protein RalBP1-associated Eps domain-containing protein 1 (Reps1) in CCPs (Dergai et al., 2010). Furthermore, ITSN1 can directly interact with the α- and β-appendage domains of AP-2 (Pechstein et al., 2010a).

In COS-7 cells and hippocampal neurons, ITSN1 can be found in CCPs at the plasma membrane as well as in Golgi-like structures (Hussain et al., 1999; Predescu et al., 2003). Overexpression of ITSN1 inhibits the uptake of transferrin in COS-1 and COS-7 cells (Sengar et al., 1999; Pucharcos et al., 2000) as does knockdown of ITSN1 in hippocampal neurons (Thomas et al., 2009). These findings indicate a direct involvement of ITSN1 in CME. In endothelial cells, ITSN1 was also found at caveolae and ITSN1 overexpression inhibited caveolae-dependent endocytosis (Predescu et al., 2003).

ITSN1 has also been described to function in exocytic events. The CCR of ITSN1 can bind to Synaptosomal-associated protein 25 kDa (SNAP25), a Soluble NSF attachment protein receptor (SNARE) protein involved in SV release (Okamoto et al., 1999). Furthermore, the GEF activity of ITSN1-L towards Cdc42 is required for exocytosis of secretory granules in neuroendocrine cells (Malacombe et al., 2006; Momboisse et al., 2009). In line with this, exocytosis in chromaffin cells lacking ITSN1 is severely perturbed (Yu et al., 2008).

At presynaptic membranes, synaptic vesicles (SVs) are exocytosed upon arrival of an action potential. To allow sustained neurotransmission, SVs are retrieved rapidly by endocytosis and new vesicles are formed. As ITSN can associate with both endocytic and exocytic proteins, it is ideally suited for coordinating SV cycling

(Pechstein et al., 2010b; Gubar et al., 2013). Indeed, a participation of ITSN in presynaptic membrane traffic has been shown, primarily in invertebrates.

ITSN is localized to the presynapse of neuromuscular junctions in *Drosophila* and *C. elegans* (Roos and Kelly, 1998; Koh et al., 2007; Rose et al., 2007; Wang et al., 2008). In both organisms, a loss-of-function mutation in the ITSN1 ortholog leads to severe defects in SV formation (Koh et al., 2004; Marie et al., 2004; Wang et al., 2008). The number of SVs is decreased in these mutants accompanied by an aberrant SV shape. Furthermore, endocytic intermediates accumulate at the periactive zone, indicating an essential role of ITSN/Dap160 for SV formation from the plasma membrane. Dap160 seems to be important for efficient recruitment of endocytic proteins, especially Dynamin, to endocytic sites during stimulation (Marie et al., 2004; Koh et al., 2007; Winther et al., 2013). Recently, Dap160 has also been implicated in clustering of SVs by forming a functional complex with the SV-associated protein Synapsin (Winther et al., 2015).

In contrast to the pivotal function of ITSN/Dap160 at invertebrate synapses, the role of ITSN1 at mammalian synapses is less clear. Knockout (KO) of ITSN1 in mice leads to a mild effect on SV endocytosis in neurons (Yu et al., 2008) while a knockdown of ITSN1 left SV endocytosis unaltered (Thomas et al., 2009). Electrophysiological experiments did not reveal any changes in basal synaptic transmission in ITSN1 KO or ITSN1/ITSN2 double KO mice (Sengar et al., 2013). Using capacitance measurements at the calyx of Held, it could be shown that ITSN1 is specifically required for the replenishment of release-ready SVs (Sakaba et al., 2013). ITSN1 was also implicated in post-endocytic vesicle uncoating by interacting with the BAR domain protein endophilin A1 (Pechstein et al., 2015). In sum, these findings show that SV cycling in mammalian synapses is not severely perturbed in the absence of ITSN1. Therefore, ITSN1 appears to be less important for SV exo-/endocytic cycling in mammals than its orthologs are in *Drosophila* or *C. elegans*.

1.1.2 Signaling Pathways regulated by ITSN1

Besides its participation in vesicle trafficking, ITSN1 has been implicated in the regulation of intracellular signaling pathways. ITSN1 can bind to Son Of Sevenless Homolog 1 (Sos1), a GEF for the small GTPase Ras (Rat sarcoma), thereby regulating

Ras and Extracellular signal–regulated kinase (Erk) activation (Tong et al., 2000a; Tong et al., 2000b; Mohney et al., 2003). Ras-related C3 botulinum toxin substrate 1 (Rac1), a small G-protein involved in actin dynamics, is indirectly regulated by ITSN1 through association of ITSN1 with its GTPase-activating protein CdGAP (Jenna et al., 2002). Furthermore, ITSN1 forms a complex with the E3-ubiquitin ligase Cbl (Casitas B-lineage lymphoma) and stimulates the Cbl-mediated ubiquitylation and degradation of the epidermal growth factor (EGF) receptor (Martin et al., 2006). Additionally, ITSN1 can activate the transcription factor Elk1 in a c-Jun N-terminal kinase (JNK)-dependent and Erk-independent manner (Adams et al., 2000; Mohney et al., 2003). Overexpression of ITSN1 results in oncogenic transformation in fibroblasts (Adams et al., 2000; Wang et al., 2005) while knockdown of ITSN1 reduces Mek (MAPK/ERK kinase) and Erk phosphorylation and induces apoptosis (Predescu et al., 2007). ITSN1 was also shown to regulate the signaling outcome downstream of TGFβ/Alk5 (Transforming growth factor beta/Activin receptor-like kinase 5). ITSN deficiency triggers a switch, from the canonical Smad2/3 to the pathophysiological relevant Erk1/2 pathway (Bardita et al., 2015). In neural cells, ITSN1 was reported to activate a phosphoinositide 3-kinase (PI3K)-Akt pathway by interacting with PI3KC2β. Knockdown of ITSN1 in cortical neurons decreases phosphorylated Akt levels and cell survival (Das et al., 2007). In addition, ITSNs were found to bind the p85α regulatory subunit of class I PI3Ks in a yeast two-hybrid screen (Wong et al., 2012). Taken together, this data shows that ITSN1 can regulate various intracellular signaling pathways in neuronal and non-neuronal cells, thereby influencing proliferation, differentiation and survival. The functional significance of ITSN1 for these processes *in vivo* is still under debate.

1.1.3 Postsynaptic roles of ITSN1

A number of publications have described a role for ITSN1 in postsynaptic function. In *C. elegans* interneurons, ITSN was shown to regulate trafficking of the α-amino-3-hydroxy-5-methyl-4-isoxazolepropionic acid receptor (AMPAR) subunit GLR-1 (glutamate receptor 1; Glodowski et al., 2007). Additionally, ITSN1 was found to bind N-methyl-D-aspartate receptors (NMDARs) NR1 and NR2B but not AMPA receptors in rat brain tissue (Nishimura et al., 2006). A functional role of ITSN1 was

found for the development of dendritic spines, membrane protrusions in neuronal dendrites rich in filamentous actin (F-actin). Spines constitute the postsynaptic component of most excitatory synapses in the brain. The morphology of dendritic spines and their structural plasticity are vital for synaptic plasticity and learning (Yang et al., 2009). ITSN1 was shown to be localized in dendritic spines and knockdown of ITSN1 resulted in defective spine development (Thomas et al., 2009). Overexpression of full-length ITSN1 or ITSN1-SH3 domains disturbs spine formation and leads to elongated spines. The effect of ITSN1 on spine morphology seems to be linked to the receptor tyrosine kinase EphB2. ITSN1 forms a complex with EphB2 and the adaptor protein Numb. This association activates its GEF activity and thereby stimulates actin polymerization via Cdc42 and N-WASP (Irie and Yamaguchi, 2002; Nishimura et al., 2006). ITSN1 thus seems to have both pre- and postsynaptic functions, although its precise role for mammalian brain physiology is still unknown.

1.2 Hippocampal development and adult neurogenesis

The hippocampus is mainly known for its role in learning and memory processes. Malfunctioning of the hippocampus has been linked to multiple neurological disorders like Alzheimer's disease, epilepsy and schizophrenia (Engel, 2001; Harrison, 2004; Hampel et al., 2008). Investigating hippocampal development and physiology is key for a better understanding of these diseases and a prerequisite for novel therapeutic strategies.

1.2.1 Structure and formation of the hippocampus

The hippocampus (Latin for seahorse) is named after its shape. Anatomically, it is a cortical structure located in the temporal lobes of the brain. The 'hippocampus formation' consists of several components: the major part of the hippocampus proper is formed by a series of Cornu Ammonis (Ammon's horn; CA1-CA4) areas, formed by tightly packed pyramidal neurons. The CA1 region lies adjacent to the subiculum, followed by pre- and parasubiculum. The dentate gyrus (DG) forms a U- or V-shaped wedge wrapped around the CA3 region. The DG consists of three layers: a densely packed layer of small granular neurons (granular cell layer; GCL), a molecular layer (ML) containing granule cell dendrites, and a polymorph layer (also referred to as hilus). The DG receives its main input from the entorhinal cortex (EC) which is why the EC is considered a functional component of the hippocampus formation. Axons from the EC make connections with the granule neurons of the DG through the perforant pathway. Axons from the DG project to the pyramidal cells of CA3 via mossy fibers which, in turn, project to CA1 neurons via Schaffer collaterals. From CA1, information is then passed on to the subiculum and the EC. Therefore, the major connections within the hippocampus constitute a unidirectional, trisynaptic circuit.

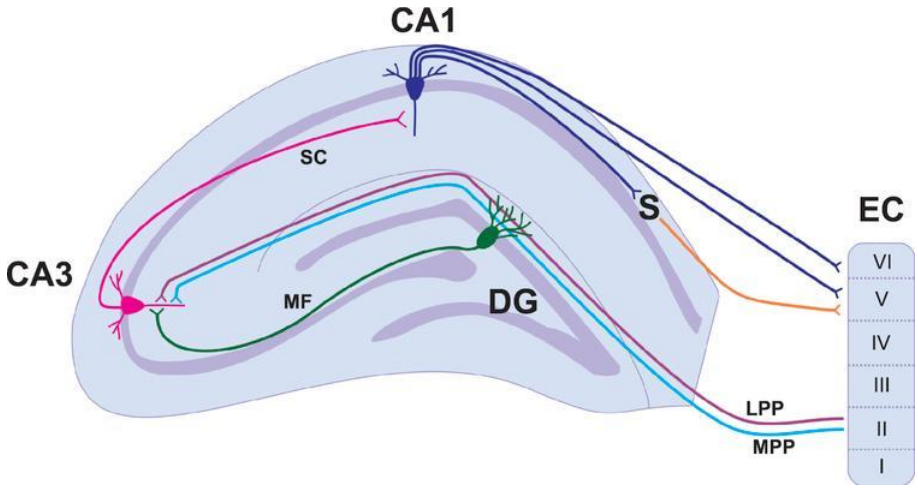

Figure 1.3 Hippocampal structure and circuitry. The basic circuitry of the hippocampus is commonly referred to as the trisynaptic circuit. Axons from layer II of the entorhinal cortex (EC) project to the granule cells of the dentate gyrus (DG) via the medial (light blue; MPP) and lateral (purple; LPP) perforant pathways. Pyramidal neurons in CA3 receive input from the DG cells via the mossy fiber pathway (green; MF). CA3 pyramidal neurons make connections with the CA1 via Schaffer collaterals (pink; SC). The CA1 pyramidal cells project to both the subiculum (S) and to deep layers V and VI of the EC. Taken from Patten et al., 2015.

As the hippocampus is a cortical structure, its development shares similarities with the formation of the neocortex (Hayashi et al., 2015). Hippocampal and cortical neurons are derived from progenitor cells in neuroepithelial ventricular zones (VZs). These progenitor cells are called radial glial cells due to their long, radially oriented process. These can give rise to neurons and glia cells but also provide a scaffold for radially migrating neurons (Rakic, 2009). In the cortex, newly generated neurons migrate out of the VZ and subventricular zone (SVZ) towards the pial surface. Later-born neurons migrate past earlier-born neurons, giving rise to the characteristic inside-out lamination pattern of the cortex (Gupta et al., 2002). Cajal-Retzius cells in the marginal zone (MZ) regulate radial migration of neurons and cortical layering by secreting soluble signaling molecules such as the glycoprotein Reelin (Ogawa et al., 1995).

Development of the hippocampus occurs in a similar way. Radial glial cells in the ammonic and dentate neuroepithelium are highly proliferative and produce pyramidal and granule neurons, respectively (Altman and Bayer, 1990b). As in the cortex, cell migration in CA and DG regions is controlled by Reelin, secreted from Cajal-Retzius cells in the MZ. In the CA region, pyramidal cells leave the neuroepithelium and form a cell band in the intermediate zone (IZ; Altman and Bayer,

1990c). After this 'sojourning', the cells leave the IZ and form the pyramidal cell layer. Sojourning has been proposed to be required for polarization and axon outgrowth.

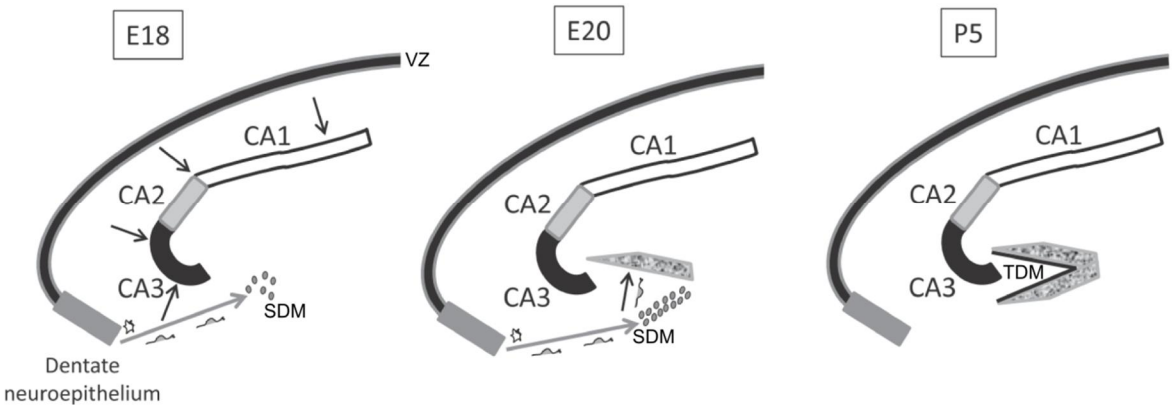

Figure 1.4 Formation of the hippocampus. Pyramidal neurons migrate from the ventricular zone (VZ) towards the pial surface (black arrows) resulting in CA layer formation. DG cells originate from a distinct area of neuroepithelium (gray box) and migrate tangentially in a subpial stream (gray arrow) towards the secondary dentate matrix (SDM). At around E20 in the mouse, the upper, supra-granular blade of the DG (mottled gray) is formed by radial migration from the SDM. By P5, both DG blades are formed and progenitors reside in a tertiary dentate matrix (TDM; hilus and subgranular zone). Modified from Khalaf-Nazzal and Francis, 2013.

DG cells are generated from the rather narrow dentate neuroepithelium (primary dentate matrix) and migrate along tangentially oriented primary radial glial cells through the subpial space (Angevine, 1965; Nakahira and Yuasa, 2005). Migrating DG cells consist of a mixture of post-mitotic neurons and precursor cells and are guided by stromal cell-derived factor 1, SDF1 (Bagri et al., 2002). These cells form the secondary dentate matrix (SDM) from which granule cells migrate radially to form the outer shell of the supra- and then the infra-granular blade of the dentate gyrus (Altman and Bayer, 1990a). In late embryonic and early postnatal days, progenitor cells from the SDM migrate into the future DG hilus region constituting the tertiary dentate matrix (TDM). Granule neurons produced in the TDM form the inner part of the GCL (Altman and Bayer, 1990a). With increasing age, the neurogenic zone becomes more and more restricted to the boundary between the hilus and the GCL, called the subgranular zone (SGZ).

1.2.2 Adult hippocampal neurogenesis

In most regions of the brain, neurons are generated during early development before neurogenesis ceases around birth (Balu and Lucki, 2009; Kempermann et al., 2015). In contrast, in the DG neurons can be generated also during adult life (Altman and Das, 1965; Kaplan and Hinds, 1977; Cameron et al., 1993). In the adult DG, different types of precursor cells reside in the SGZ. Type 1 cells are multipotent progenitors and show a radial glial cell-like morphology with a triangular soma and one apical process reaching into the GCL (Seri et al., 2001). These cells possess astrocytic properties and express the astrocyte marker glial fibrillary acidic protein (GFAP), but not S100β. They also express markers associated with neural precursors like Nestin (an intermediate filament) and the transcription factor SRY (sex determining region Y)-box 2, Sox2 (Filippov et al., 2003; Fukuda et al., 2003; Seri et al., 2004). Radial glial cells in the DG have been shown to proliferate relatively slowly (Kronenberg et al., 2003) but can divide asymmetrically, producing one new radial glial cell and one more lineage-restricted precursor cell (Kempermann et al., 2004; Encinas et al., 2011). Due to their multipotency and self-renewing capacity, radial glial cells have been considered to be *bona fide* stem cells (Palmer et al., 1997; Suh et al., 2007) although this concept has been questioned by others (Seaberg and van der Kooy, 2002; Bull and Bartlett, 2005).

Radial glia-like type 1 cells give rise to transiently amplifying neuronal progenitor cells (type 2 cells). These cells are mitotically very active and thereby expand the pool of progenitors. One subset of type 2 cells, type 2a, still expresses glial markers while another subset, type 2b, already shows neuronal features like Doublecortin (Dcx) or NeuroD expression (Steiner et al., 2006). This differentiation step marks the transition towards the neuronal lineage. Type 2b cells mature into type 3 cells which are Dcx-positive neuroblasts with limited proliferative activity. After short-distance migration into the GCL, these cells differentiate into mature granule neurons expressing neuronal markers as NeuN (neuronal nuclei) or Calbindin. Around seven weeks after birth, new neurons display properties of mature granule cells and become integrated into the hippocampal circuitry (van Praag et al., 2002).

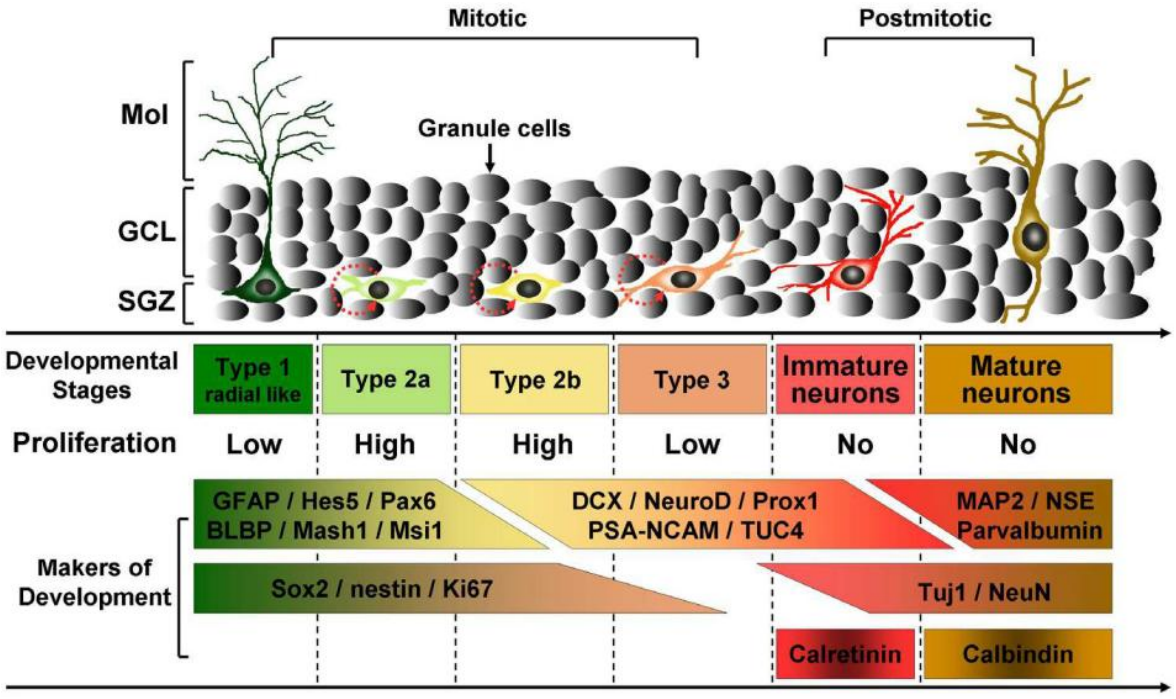

Figure 1.5 Developmental stages in the course of adult hippocampal neurogenesis. Type 1 cells with radial glia properties give rise to type 2 progenitor cells. Two subtypes of type 2 cells can be distinguished (types 2a and 2b). The neuronal fate is determined at stage type 2b. Type 3 cells exit from the cell cycle and differentiate into immature and further into mature neurons. These newborn granule cells extend their dendrites and axons to become integrated into the hippocampal network. Cells at different stages of neurogenesis can be classified according to the expression of specific markers. Taken from Zhang and Jin, 2012.

The subventricular zone (SVZ) of the lateral ventricles is the second region where neurogenesis occurs in the adult brain. The SVZ harbors slowly dividing cells with stem cell properties expressing GFAP and Nestin (Doetsch et al., 1997; Doetsch et al., 1999). These cells divide asymmetrically to generate transit amplifying cells which further differentiate into neuroblasts. Dcx-expressing neuroblasts migrate in chains along the rostral migratory stream (RMS) towards the olfactory bulb (Lois and Alvarez-Buylla, 1994), where they mature into gamma-aminobutyric acid (GABA)- and dopamine-producing interneurons (Luskin, 1993). It has been suggested that in the olfactory bulb continuous replacement of old neurons by newborn neurons is important for olfactory function (Gheusi et al., 2000). Olfaction is the primary sense for many animals, including rodents, but not for humans. Hence, SVZ neurogenesis plays a prominent role for mice but a subordinate role for humans.

In contrast, adult neurogenesis in the hippocampus is of much higher relevance for cognitive function in humans. The hippocampus is vital for learning and memory

and adult neurogenesis contributes to hippocampal plasticity required for these processes. Learning and physical exercise promote generation of new neurons in the hippocampus (Gould et al., 1999; Fabel et al., 2009). On the other hand, factors known to impair hippocampal function like stress, aging or disease can hamper neurogenesis (Warner-Schmidt and Duman, 2006; Lucassen et al., 2015). This suggests that adult neurogenesis plays an important role for hippocampal function but its specific function is still unclear (Deng et al., 2010).

1.3 Signaling pathways regulating hippocampal function

Adult hippocampal neurogenesis is regulated by a variety of extrinsic and intrinsic factors (Faigle and Song, 2013). These include growth factors like brain-derived neurotrophic factor (BDNF), Neurotrophin 3 (NT3), fibroblast growth factor 2 (FGF2), insulin-like growth factor 1 (IGF1), and vascular endothelial growth factor (VEGF) as well as morphogens, namely Wnt, Notch, sonic hedgehog protein (Shh) and bone morphogenetic protein (BMP). Neurotransmitters like GABA, Glutamate and Dopamine also influence hippocampal neurogenesis. Some of these soluble factors enter the neurogenic niche through blood vessels whereas others are synthesized locally (Suh et al., 2009). Understanding the precise mechanisms regulating adult neurogenesis might hold great potential for drug development and future treatments of neurological diseases.

1.3.1 Ephrin/Eph signaling

The microenvironment allowing for adult neurogenesis is not only determined by soluble signaling molecules but also by direct interactions between progenitors and their neighboring cells. Eph receptors and ephrins are cell surface proteins that are involved in local cell-to-cell communication. Eph receptors and ephrin ligands are typically expressed on neighboring cells, interacting with each other. Formation of ephrin/Eph complexes triggers intracellular signaling cascades in both the Eph- and the ephrin-expressing cell. Signaling downstream of Eph receptors and ephrins is referred to as forward and reverse, respectively. Mediating repulsion between neighboring cells during development is considered the canonical function of Eph/ephrin signaling. In doing so, Eph/ephrin complexes regulate various developmental processes including migration and cell positioning, axon guidance, tissue boundary formation and development of the vascular system (Pasquale, 2008). Axon guidance by various ephrins and Eph receptors is vital for the formation of axonal commissures like the corpus callosum (Mendes et al., 2006). In addition, there is a growing body of evidence suggesting additional roles for Eph/ephrin signaling in

the adult brain, e.g. for synapse plasticity (Lai and Ip, 2009) or adult neurogenesis (Laussu et al., 2014).

Ephrins and Eph receptors can be grouped into two subclasses, A and B, according to their sequence homologies and binding characteristics (Gale et al., 1996). Generally, ephrin-A ligands interact with EphA receptors while ephrin-B ligands bind to EphB receptors, although certain promiscuity exists between the subclasses (Kullander et al., 2003; Himanen et al., 2004).

Eph receptors constitute the largest subfamily of receptor tyrosine kinases (RTKs). Structurally, they possess a multi-domain extracellular region that includes a highly conserved ephrin-binding domain (Labrador et al., 1997; Himanen et al., 2001), a cysteine-rich region and two fibronectin type III repeats. The intracellular region of Eph receptors contains a tyrosine kinase domain, a sterile-α motif (SAM) as well as a PDZ (PSD-95/Dlg1/ZO1)-binding motif. The SAM domain can promote receptor oligomerization (Qiao and Bowie, 2005) while the PDZ-binding motif is required for co-clustering of Eph receptors with PDZ domain-containing proteins like AMPA-type glutamate receptors at the plasma membrane (Torres et al., 1998; Kayser et al., 2006).

Ephrins consist of an N-terminal Eph receptor-binding domain, separated from the membrane by a linker region of variable length. EphrinAs are linked to the cell surface by a glycosylphosphatidylinositol (GPI) anchor, whereas class B ephrins have a transmembrane region and a short cytoplasmic domain of about 80 amino acids which harbors a PDZ-binding motif (Torres et al., 1998; Song et al., 2002).

Binding to ephrins to Eph receptors leads to autophosphorylation of the receptor followed by phosphorylation of downstream effector proteins (Wybenga-Groot et al., 2001). Autophosphorylated Eph receptors recruit SH2 (Src homology 2) domain-containing adaptor proteins like noncatalytic region of tyrosine kinase α (Nckα; Hu et al., 2009) and CT10 Regulator of Kinase (Crk; Noren et al., 2006; Huang et al., 2008). A well-known mechanisms by which Eph receptors modulate adhesion, cell shape and migration is the regulation of small G-proteins of the Rho family, including RhoA, Rac1 and Cdc42 (Lisabeth et al., 2013). Eph receptors can influence the activation status of these G-proteins by regulating a variety of GEFs and GAPs (GTPase-activating proteins) although the precise mechanisms that determine the signaling outcome are not fully understood.

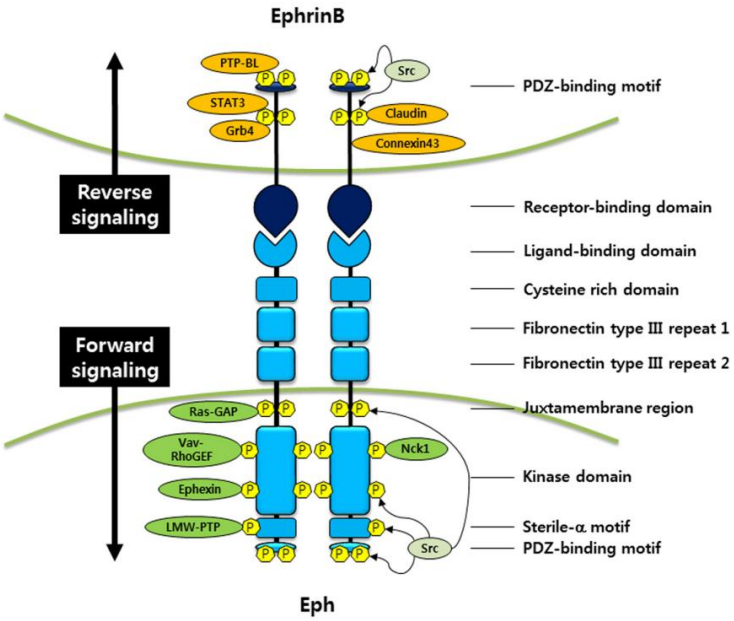

Figure 1.6 Domain structure of EphB receptors and ephrinBs and signaling effectors. EphB receptors bind to ephrinB ligands expressed by neighboring cells. Ligand binding induces forward signaling in the EphB-expressing cell and reverse signaling in the ephrinB-expressing cell. Forward and reverse signaling involves tyrosine phosphorylation of EphB and ephrinB, respectively, and recruitment of downstream effector proteins, e.g. GEFs or GAPs. Therefore, EphB/ephrinB signaling leads to remodeling of the actin cytoskeleton and as a result modulates cell adhesion and migration. Taken from Park and Lee, 2015.

By providing a repulsive cue, Eph receptor signaling can guide migrating neurons and their axonal processes during development of the nervous system. This process involves the dynamic regulation of the cytoskeleton by small G-proteins. RhoA activation by the GEF Ephexin1 has been shown to induce collapse of axonal growth cones downstream of EphA receptors (Shamah et al., 2001; Sahin et al., 2005). Inactivation of Rac1 by the Rac GAP α2-chimaerin also induces growth cone collapse (Shi et al., 2007; Wegmeyer et al., 2007). On the other hand, Rac1 activation by GEFs of the Vav family has been implicated in growth cone collapse by mediating endocytic uptake of adhesive ephrin/Eph complexes (Cowan et al., 2005; Yoo et al., 2011). Removal or disruption of ephrin/Eph complexes is a prerequisite for cellular detachment and repulsion. This can occur either by proteolytic cleavage of ephrins/Eph receptors or by endocytic removal. Internalization of ligand/receptor complexes, which can be taken up either by the ephrin- or the Eph-expressing cell, is called 'transendocytosis'. It requires mechanical force generated by actin

polymerization and is coordinated by small G-proteins like Rac1 (Marston et al., 2003; Zimmer et al., 2003).

Eph receptors also control actin dynamics during the development of dendritic spines. Activation of EphA4 induces retraction of dendritic spines in an ephexin-dependent manner (Murai et al., 2003; Fu et al., 2007). In contrast, ephrinB/EphB-dependent activation of Rac1 by the Rac GEFs Tiam1 (T-cell lymphoma invasion and metastasis 1) and Kalirin is required for spine formation and maturation (Penzes et al., 2003; Tolias et al., 2007). A similar role for dendritic spine morphogenesis has been described for EphB2-dependent activation of Cdc42 and N-WASP (Irie and Yamaguchi, 2002). Interestingly, ITSN1 associates with EphB2 suggesting a possible role for the Cdc42 GEF activity of ITSN1 in EphB2-mediated signaling. An alternative pathway for EphB-induced dendritic spine morphogenesis entails RhoA activation through focal adhesion kinase (Moeller et al., 2006). Furthermore, EphB receptor signaling can induce Ephexin5 ubiquitylation and degradation which decreases RhoA activity and thereby promotes formation of excitatory synapses (Margolis et al., 2010).

Eph receptor signaling has been shown to control diverse kinase signaling pathways. Depending on the different subclasses and the cellular context, Eph signaling can suppress or activate kinase signaling cascades. This provides Eph receptors with both tumor-suppressing and -promoting properties.

Like other RTKs, Eph receptors can activate the Ras-Erk pathway. Ephrin-stimulated EphB1 can activate Erk which increases cell motility (Vindis et al., 2003). This process involves recruitment of the adaptor proteins p52Shc and Grb2 (growth factor receptor-bound protein 2) as well as phosphorylation of the kinase Src. Similarly, activation of EphB2 forward signaling by ephrinB1 promotes cell repulsion in an Erk-dependent manner (Poliakov et al., 2008). EphrinB1-induced EphB signaling can promote proliferation and regulate gene transcription via Erk activation (Bush and Soriano, 2010).

Interestingly, Eph receptor forward signaling can also inhibit the Ras-Erk pathway. For example, EphB4 signaling can promote Erk activation in breast cancer cell while inhibiting Erk in endothelial cells (Xiao et al., 2012). Of note, Eph receptors have even been shown to often override the activating effects of other RTKs on Erk (Miao et al., 2001). For example, suppression of Erk activation by ephrinA/EphA

signaling in myoblasts shifts the response to IGF1 towards myogenic differentiation (Minami et al., 2011). EphrinA5 can suppress Erk activity and thereby inhibit the Tyrosine receptor kinase B (TrkB)-dependent effects on growth cone dynamics, neurite branching and gene expression (Meier et al., 2011). Mechanistically, Eph-dependent inactivation of the Ras/Erk-pathway involves p120-RasGAP (Elowe et al., 2001). The effects of Eph receptor signaling on integrin activity and cellular adhesion are mediated by p120-RasGAP-dependent inhibition of Ras (Dail et al., 2006). Integrin function is also regulated by Rap1 (Ras-related protein 1), another member of the Ras protein family. Activated EphB2 can inhibit Rap1 and thereby induce cell retraction (Riedl et al., 2005). In neurons, ephrinA/EphA4-dependent Rap1 inactivation has been shown to induce growth cone collapse (Richter et al., 2007).

Eph receptors can also regulate the activity of the serine/threonine kinase Akt. Unlike other RTKs, Eph receptor forward signaling can suppress Akt activation. Ephrin-dependent stimulation of EphA2 causes dephosphorylation of Akt, thereby inhibiting cell growth (Menges and McCance, 2008; Miao et al., 2009). Remarkably, EphA2-depdendent dephosphorylation of Akt can counteract the oncogenic effects of a constitutively active Akt pathway in cancer cells (Yang et al., 2011). Similarly, activation of EphB3 can inhibit Akt and thereby suppress cancer cell migration and metastasis (Li et al., 2012).

Like for the Ras-Erk cascade, Eph receptors can both inhibit and activate the Akt pathway, depending on the cellular context. Stimulation of pancreatic cancer cells with ephrinA2 lead to activation of Akt (Chang et al., 2008). In malignant T lymphocytes, ephrinB-dependent EphB signaling induces Akt activation and suppresses apoptosis (Maddigan et al., 2011). In sum, this shows that Eph receptor forward signaling controls numerous processes during development and maturity in various tissues.

Ephrin/Eph receptor interaction also elicits signaling in the ephrin-expressing cell (‘reverse signaling’). The A subclass of ephrins lacks a cytosolic region but can still activate intracellular signaling pathways. EphrinA effects on axon guidance and branching have been shown to be mediated by the neurotrophin receptors p75 and TrkB (Lim et al., 2008; Marler et al., 2008). The receptor tyrosine kinase Ret is essential for motor axon attraction caused by ephrinA reverse signaling (Bonanomi et al., 2012). Probably further transmembrane proteins are responsible for transmission

of the diverse ephrinA reverse signaling effects. EphrinA3 can modulate synaptic plasticity in the adult hippocampus by increasing the abundance of glial glutamate transporters (Carmona et al., 2009; Filosa et al., 2009). EphrinA5 can activate the Src family kinase Fyn to modulate cell adhesion and invasiveness (Davy et al., 1999; Campbell et al., 2006) or EGF receptor ubiquitylation and degradation (Li et al., 2009). Furthermore, ephrinA5 is required for insulin secretion from pancreatic beta cells (Konstantinova et al., 2007). In Jurkat immune cells EphrinA4 can activate Src family kinases as well as Akt, thereby inhibiting apoptosis (Holen et al., 2008).

Ephrins of the B subclass harbor an intracellular domain but lack enzymatic activity. Upon binding to EphB receptors they activate Src family kinases and a regulatory phosphotyrosine phosphatase (PTP-BL). EphrinBs are phosphorylated by Src family kinases (SFKs) and later dephosphorylated by PTP-BL (Cowan and Henkemeyer, 2001; Palmer et al., 2002). Additionally, ephrinBs have been shown to be a substrate for phosphorylation by FGF and PDGF (platelet-derived growth factor) receptors (Bruckner et al., 1997; Chong et al., 2000). Phosphorylated ephrinB molecules are recognized by SH2 domain-containing proteins like the adaptor protein Nckβ. Via this interaction, EphrinB signaling controls synapse formation, spine morphogenesis and axonal pruning (Segura et al., 2007; Xu and Henkemeyer, 2009). Interestingly, tyrosine-phosphorylated ephrinB1 can recruit and activate the SH2 domain containing transcription factor signal transducer and activator of transcription 3 (STAT3; Bong et al., 2007). EphrinB reverse signaling is also mediated by recruitment of signaling proteins containing PDZ domains. Glutamate receptor-interacting proteins (GRIPs) are bound by the PDZ-binding motif of ephrinBs upon stimulation by EphB (Bruckner et al., 1999). This interaction is required to stabilize AMPA receptors at the plasma membrane (Essmann et al., 2008). The PDZ-binding site has also been shown to be essential for long-term potentiation (LTP) and long-term depression (LTD) downstream of ephrinB2 (Bouzioukh et al., 2007). Interaction between ephrinBs and the adaptor PDZ-RGS3 (regulator of G-protein signaling 3) regulates neuronal migration towards attractive cues (Lu et al., 2001) as well as self-renewal of cortical progenitors (Qiu et al., 2008). A PDZ-dependent mechanism is required for axon guidance and formation of commissural tracts by ephrinB1 (Bush and Soriano, 2009). Interaction of EphrinB2 with PDZ domain proteins induces angiogenesis and lymphangiogenesis by promoting VEGF receptor internalization

(Makinen et al., 2005; Sawamiphak et al., 2010; Wang et al., 2010). Furthermore, ephrin reverse signaling has been shown to regulate the function of tight junctions (Tanaka et al., 2005; Lee et al., 2008) and gap junctions (Davy et al., 2006). These findings reveal that ephrins and Eph receptors use bidirectional signaling to control a large variety of biological processes.

Interestingly, Ephrin/Eph receptor signaling also has a role in neurogenesis. In the SVZ, various ephrins and Eph receptors are expressed and regulate migration of neuroblasts and cell proliferation (Conover et al., 2000). EphrinB reverse signaling promotes neurogenesis by SVZ progenitors *in vitro* (Katakowski et al., 2005). EphrinA2 reverse signaling can limit the proliferation of neural progenitor cells (Holmberg et al., 2005) as can EphrinB3-dependent forward signaling (Ricard et al., 2006). Interestingly, EphrinA2 and A3 inhibit progenitor cell proliferation also by EphA7-mediated forward signaling (Jiao et al., 2008). EphA4 is required to maintain the stem cell identity of SVZ stem cells (Khodosevich et al., 2011).

Signaling from ephrin and Eph receptors has also been implicated in adult neurogenesis in the DG. EphrinB2 is expressed on astrocytes of the SGZ and instructs neuronal differentiation of progenitors. This seems to be mediated by EphB4 forward signaling (Ashton et al., 2012). Furthermore, ephrinA5 is required for proliferation of SGZ progenitors and survival of newborn neurons. Of note, genetic ablation of ephrinA5 also led to disruptions of the vasculature which could have indirect effects on neurogenesis (Hara et al., 2010). EphB1 is expressed in hippocampal progenitor cells in the SGZ and mice lacking EphB1 show reduced numbers, ectopic localization and disrupted polarity of progenitor cells (Chumley et al., 2007). These effects are mediated by EphB1 forward signaling elicited by ephrinB3-expressing mature granule cells. EphB2 has a distinct function, being required for migration of progenitors during early development of the DG (Catchpole and Henkemeyer, 2011). It was shown that ephrinB1 and EphB2 control the migration of dentate progenitor cells into the dorsal compartment of the TDM. As a result, absence of ephrinB1 or EphB2 leads to an underdeveloped lateral suprapyramidal blade of the DG. Therefore, ephrin/Eph receptor signaling regulates both early stages of hippocampal development as well as neurogenesis in adults. Interestingly, mice lacking both EphB1 and EphB2 also show lamination defects in the CA3 pyramidal cell layer

(Chumley et al., 2007). This indicates that the same pathways regulating early hippocampal development persist into adulthood to control adult neurogenesis.

1.3.2 Reelin signaling

Another signaling pathway important for hippocampal development and physiology involves the extracellular matrix protein Reelin. Reelin is a large glycoprotein regulating neuronal migration and synapse function (Forster et al., 2010; Lakatosova and Ostatnikova, 2012; Stranahan et al., 2013). The two lipoprotein receptors apolipoprotein E receptor 2 (ApoER2) and the very-low-density-lipoprotein receptor (VLDLR) were shown to be the Reelin receptors *in vivo* (D'Arcangelo et al., 1999; Hiesberger et al., 1999; Trommsdorff et al., 1999). These transmembrane proteins bind and activate the intracellular adaptor protein Disabled1 (Dab1), thereby transmitting the Reelin signal (Howell et al., 1997b; Hiesberger et al., 1999; Benhayon et al., 2003; Morimura and Ogawa, 2009).

The *reeler* mouse, a mouse mutant lacking Reelin expression, was first described in 1951 (Falconer, 1951), long before the Reelin gene and its protein product were identified (D'Arcangelo et al., 1995; DeSilva et al., 1997). *Reeler* mice show impaired motor coordination (reeling gait), tremors and ataxia. This phenotype is caused by severe neuroanatomical changes in cortex, hippocampus and cerebellum (Hamburgh, 1963). During the development of the mammalian cortex, newborn neurons migrate from the ventricular zone towards the pial surface. Later-born neurons migrate past earlier-born neurons, resulting in an 'inside-out' layering of the cortex. During early cortical development, Reelin is synthesized and secreted by Cajal-Retzius cells, neurons residing in the marginal zone of the cerebral cortex (Hirotsune et al., 1995; Schiffmann et al., 1997). Mice lacking Reelin expression exhibit a severely disorganized cortical layering and an 'outside-in' pattern of cortical neurons. Furthermore, the cerebellum of *reeler* mice is smaller and less foliated than in control animals due to malpositioning of Purkinje cells (Goffinet et al., 1984).

As mentioned above, Reelin, produced by Cajal-Retzius in the MZ, is also required for hippocampal development (Frotscher, 1998). As a consequence, the hippocampus of *reeler* mice shows defective cell lamination and dispersion of pyramidal and granular neurons (Hamburgh, 1963). The pyramidal cell layer appears

split and dispersed. Similarly, granule neurons of the DG fail to form a compact layer and are scattered throughout the DG. These findings have established Reelin as a master regulator of neuronal migration.

At later stages of development, Reelin is critical for dendrite extension and maturation of dendritic spines (Niu et al., 2004; Jossin and Goffinet, 2007; Niu et al., 2008). In adults, Reelin is mainly produced by a subset of GABAergic interneurons in cortex, hippocampus and olfactory bulb (Alcantara et al., 1998; Drakew et al., 1998; Pesold et al., 1998; Ramos-Moreno et al., 2006). Interneuron-derived Reelin has been shown to modulate synaptic plasticity (Weeber et al., 2002; Beffert et al., 2005; Chen et al., 2005). Reelin can elevate the levels of hippocampal LTP through interactions between ApoER2 and NMDARs. Moreover, Reelin signaling modulates NMDAR subunit composition during hippocampal maturation (Sinagra et al., 2005; Groc et al., 2007). Therefore, Reelin is not only an important regulator of neuronal migration during development but also controls synaptic transmission in adults (Herz and Chen, 2006).

In addition to its functions in migration and synapse function, Reelin has also been implicated in the regulation of adult neurogenesis. In the olfactory bulb, Reelin acts as a detachment signal for chain-migrating neuroblasts (Hack et al., 2002). Proliferation and neurogenesis in the SVZ are unaltered in the *reeler* mouse (Kim et al., 2002) or in mice overexpressing Reelin (Pujadas et al., 2010).

In contrast, neurogenesis in the DG is markedly disturbed in Reelin signaling mutants. In the DG of *reeler* mice, the radial glia cell scaffold is severely altered. Radial glial cells are distributed throughout the DG and their processes fail to be arranged radially (Forster et al., 2002; Weiss et al., 2003). Malformation of the radial glial scaffold in Reelin pathway mutants is accompanied by a severe disruption of DG layering. Therefore, an important question is whether the altered radial glial scaffold in *reeler* mice is a consequence of the scattered cell layers. Alternatively, the disruption of DG layers could be an indirect effect of defective generation and migration of new neurons in the absence of Reelin. Using stripe choice assays and hippocampal slice cultures, it was demonstrated that Reelin can exert direct effects on radial glial cells (Frotscher et al., 2003; Zhao et al., 2004). On the other hand, Reelin directly influences migration of immature neurons *in vitro* (Gong et al., 2007). Furthermore, conditional depletion of Dab1 in postnatal mice impairs migration and

maturation of newborn neurons (Teixeira et al., 2012). This results in ectopic accumulation of newborn neurons in the hilar region and disturbed development of the dendritic arbor. Interestingly, these defects exist in the presence of a normal radial glia scaffold indicating cell-autonomous roles for Reelin in newborn neurons of the DG. Mice with conditional deletion of Dab1 in neurons but not in glial cells show a partially altered radial glia scaffold suggesting that malpositioning of granule neurons has indeed indirect effects on radial glia cells (Brunne et al., 2013). Remarkably, in the same experiment DG cell layering was only mildly affected which indicates that radial glial cells can, in turn, influence positioning of granule cells. This demonstrates that disruption of DG layering and malformation of the radial glia scaffold in Reelin signaling mutants are interdependent processes. Reelin has also been implicated in proliferation and differentiation of progenitor cells in the DG. In adult *reeler* mice the number of proliferating cells and newly generated granule neurons is severely decreased (Zhao et al., 2007). Interestingly, no difference in proliferation, maturation or differentiation of radial glia cells between WT and *reeler* mice was seen during development of the DG (Brunne et al., 2013). This argues against a direct role of Reelin in DG progenitor cell proliferation and differentiation. Rather, this discrepancy could be explained by the different structure of the neurogenic zones in young and adult animals. Adult neurogenesis depends on the morphological and molecular properties of the neurogenic niche, the SGZ. Therefore, the disturbed morphology of the DG in *reeler* mice might indirectly affect the fate of progenitor cells. Taken together, Reelin regulates migration and neurogenesis in the DG by exerting direct and indirect effects on progenitors and postnatal neurons.

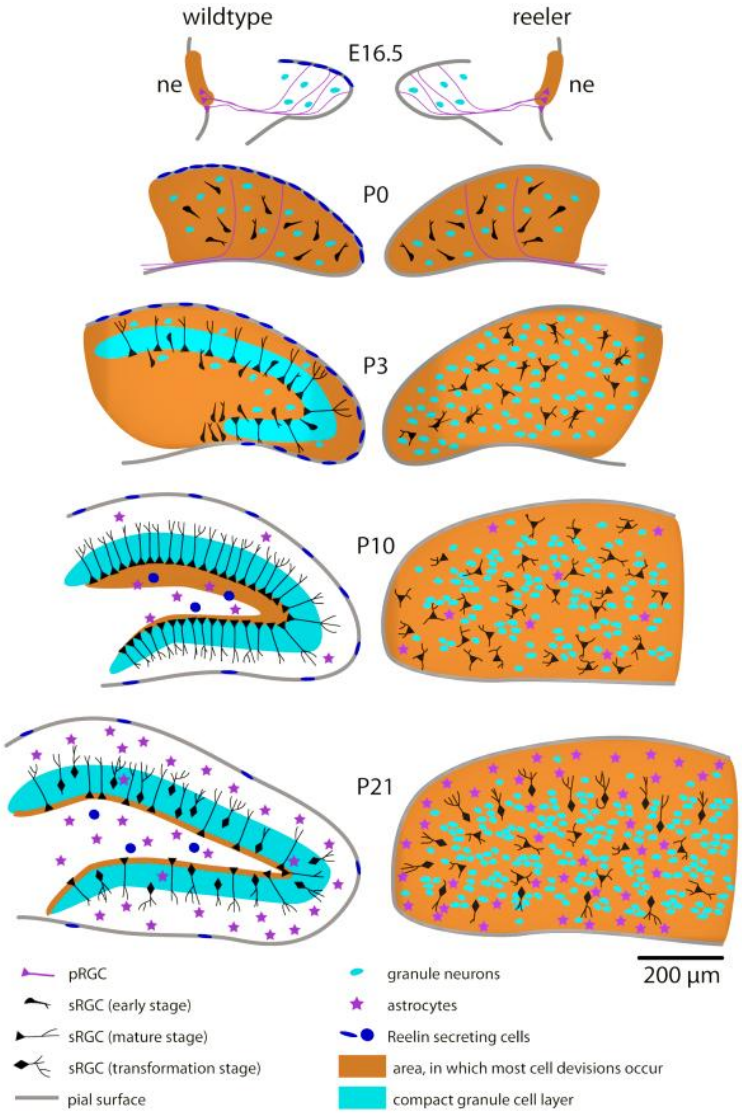

Figure 1.7 Dentate gyrus development in WT and *reeler* mice. During embryonic development, dentate gyrus (DG) cells are generated in the dentate neuroepithelium (ne) and migrate along primary radial glial cells (pRGCs) towards the secondary dentate matrix. Around P3, pRGCs disappear while the secondary radial glial cells (sRGCs) begin to form a characteristic scaffold in WT but not in *reeler* mice. Granule neurons become organized in a compact cell layer. In *reeler* mice, neurons and glial cells remain scattered throughout the DG. Proliferation gets more and more restricted to the subgranular zone in WT but not in *reeler* mice. Modified from Brunne et al., 2013.

The mouse Reelin gene consists of 65 exons and the full length protein has a relative molecular mass of ~400 kDa (Ogawa et al., 1995; Royaux et al., 1997). Structurally, it contains a signal peptide followed by an F-spondin homology domain and a hinge region. The central part consists of a stretch of eight similar domains (Reelin repeats, RRs). Each repeat has a length of 350 – 390 amino acids and is composed of two subrepeats, named A and B, separated by an EGF motif. The C-

terminal domain (CTD) of Reelin consists of a sequence of 33 mostly basic amino acids (de Bergeyck et al., 1998; Fatemi, 2005). The hinge region mediates electrostatic interactions between Reelin molecules and is responsible for the formation of soluble, string-like Reelin polymers consisting of more than 40 monomers (Utsunomiya-Tate et al., 2000). A mutant Reelin lacking the polymerization domain fails to evoke downstream signaling and a neutralizing antibody raised against the hinge region (CR-50) can block Reelin function *in vitro* and *in vivo* (Ogawa et al., 1995; Del Rio et al., 1997; Miyata et al., 1997; Nakajima et al., 1997; Utsunomiya-Tate et al., 2000). Therefore, Reelin operates as a polymer to exert its biological function. The basic CTD of Reelin has been believed to be important for secretion of Reelin into the extracellular space. The Orleans *reeler* mouse expresses a truncated version of Reelin mice lacking the CTD (de Bergeyck et al., 1997) which cannot be secreted but accumulates in the endoplasmatic reticulum (Derer et al., 2001). However, the role of the CTD in Reelin secretion has been challenged by others: Nakano et al. have shown that the CTD is not essential for secretion but is rather required for efficient activation of downstream signaling (Nakano et al., 2007). Reelin is cleaved at two sites *in vivo,* between RR 2 and 3 and between RR 6 and 7, resulting in three fragments of 400 kDa, 320 kDa and 180 kDa, respectively (Lambert de Rouvroit et al., 1999). Cleavage does not affect Reelin activity as the central fragment containing RR 3 to 6 is necessary and sufficient for receptor binding and cellular signaling (Jossin et al., 2004).

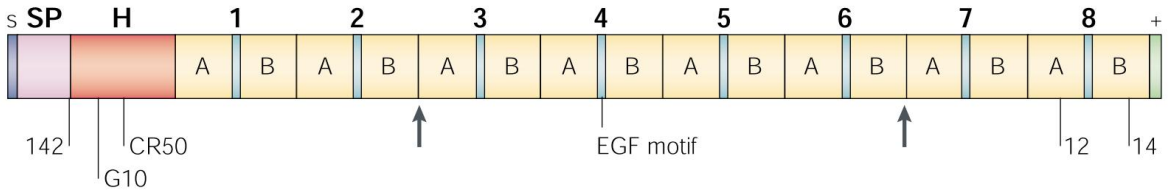

Figure 1.8 Domain structure of the Reelin protein. A signal peptide of 27 residues is followed by a region with similarity to F-spondin ('SP', amino acids 28–190). The hinge region ('H') between amino acids 191 and 500 is followed by eight repeats of about 350 amino acids (repeat 1, residues 501–860; repeat 2, 861–1220; repeat 3, 1221–1596;repeat 4, 1597–1947; repeat 5, 1948–2314; repeat 6, 2315–2661; repeat 7, 2662–3051; repeat 8, 3052–3428). Each repeat contains a central epidermal growth factor (EGF) motif, flanked by two subrepeats, A and B. The protein terminates with a basic stretch of 33 amino acids (3429–3461, +). The epitopes recognized by antibodies 142, G10, CR50, 12 and 14 are shown. The arrows point to the *in vivo* cleavage sites. Taken from Tissir and Goffinet, 2003.

Reelin elicits its effects by binding to the lipoprotein receptors ApoER2 and VLDLR (D'Arcangelo et al., 1999; Hiesberger et al., 1999; Trommsdorff et al., 1999). Reelin has a slightly stronger affinity for ApoER2 than for VLDLR (Andersen et al., 2003; Benhayon et al., 2003). VLDLR and ApoER2 are members of the low-density-lipoprotein (LDL) receptor family and are structurally similar. Both receptors contain a ligand binding domain of eight ligand binding regions, an EGF-like domain containing three cysteine-rich repeats and an O-linked glycosylation domain. The extracellular part is followed by a transmembrane region and a cytoplasmic domain containing an NPXY motif (Reddy et al., 2011). The NPXY motif mediates receptor internalization and signaling.

ApoER2 contains an alternatively spliced exon (exon 19) in its cytoplasmic tail that encodes a 59 amino acid, proline-rich domain (Clatworthy et al., 1999). Via this domain, ApoER2 can bind to the c-Jun N-terminal kinase (JNK) interacting proteins, JIP1 and JIP2, and the postsynaptic protein PSD-95 (Gotthardt et al., 2000; Stockinger et al., 2000). Exon 19 is required for Reelin-dependent modulation of LTP, NMDAR phosphorylation, and synaptic plasticity. As a result, mice lacking exon 19 show learning and memory deficits (Beffert et al., 2005). Therefore, exon 19 mediates the formation of a functional complex consisting of ApoER2, PSD-95 and NMDARs.

Interaction between Reelin and VLDLR or ApoER2 induces clustering of the receptors (Strasser et al., 2004) and binding of the intracellular adaptor protein Dab1 to VLDLR and ApoER2 (Howell et al., 1997b; Hiesberger et al., 1999; Benhayon et al., 2003; Morimura and Ogawa, 2009). This interaction is mediated by the NPXY motifs in the intracellular region of the lipoprotein receptors and the phosphotyrosine-binding (PTB) domain of Dab1. Upon binding to the receptors, Dab1 becomes tyrosine-phosphorylated by Src family kinases (SFKs) Src and Fyn (Kuo et al., 2005). Dimerization/oligomerization of Dab1 is sufficient to induce Dab1 phosphorylation (Strasser et al., 2004). Therefore, aggregation of Reelin receptors and Dab1 by multivalent Reelin polymers seems to be the trigger for signal transduction. Two mutant mice, *scrambler* and *yotari*, which show a *reeler*-like phenotype, were shown to have loss-of-function mutations in the Dab1 gene (Sweet et al., 1996; Goldowitz et al., 1997; Gonzalez et al., 1997; Sheldon et al., 1997; Yoneshima et al., 1997). Targeted disruption of the Dab1 gene results in similar defects (Howell et al., 1997b). Furthermore, the simultaneous deletion of Fyn and Src (Kuo et al., 2005) or of VLDLR

and ApoER2 (Trommsdorff et al., 1999) leads to a *reeler*-like phenotype. Therefore, VLDLR/ApoER2, Dab1 and SFKs constitute the core signaling machinery downstream of Reelin.

Dab1 contains an N-terminal protein interaction/phosphotyrosine binding (PI/PTB) domain that binds to the NPXY motif in Reelin receptors (Howell et al., 1997a). The PTB domain can bind to phosphatidylinositols, especially $PI4,5P_2$, without affecting its interaction with the NPXY motif (Stolt et al., 2003). Phosphoinositide binding by the Dab1 PTB domain is required for membrane localization of Dab1 and effective Reelin signal transduction (Huang et al., 2005; Stolt et al., 2005). The PTB domain is followed by a tyrosine-rich region harboring five highly conserved tyrosine residues (Y185, Y198, Y200, Y220, Y232). Mutation of all potentially phosphorylated tyrosine residues to phenylalanine (5F mutant) causes a *reeler*-like phenotype (Howell et al., 2000), demonstrating the crucial role of Dab1 tyrosine phosphorylation for Reelin signaling. In addition, Dab1 does not only transmit signaling but also affects Reelin receptor trafficking by promoting their plasma membrane localization (Morimura et al., 2005).

Phosphorylated Dab1 regulates a variety of downstream effectors. Its phosphotyrosine residues are recognized by SH2 domains of various downstream effectors, including PI3K, adaptor proteins Crk/CrkL (Huang et al., 2004) and Nckβ (Pramatarova et al., 2003) as well as SOCS (Feng et al., 2007). Tyrosine-phosphorylated Dab1 also binds the microtubule-associated protein Lis1 (Lissencephaly 1), albeit in a SH2 domain-independent manner (Assadi et al., 2003).

PhosphoDab1 recruits the p85 regulatory subunit of PI3K and activates the PI3K-Akt pathway, leading to inhibition of GSK3β (Beffert et al., 2002; Bock et al., 2003) and suppressed tau phosphorylation. Reelin-dependent activation of PI3K and Akt is required for normal development of the cortical plate (Jossin and Goffinet, 2007). The PI3K/Akt pathway has also been implicated in the Reelin-dependent inhibition of n-cofilin (Chai et al., 2009a; Chai et al., 2009b). Reelin activates LIM kinase 1 (LIMK1), which phosphorylates cofilin on serine 3, thereby inhibiting its actin depolymerizing activity (Arber et al., 1998; Yang et al., 1998). As phosphorylation of n-cofilin mainly occurs in the leading processes of migrating neurons, Reelin may stabilize these neuronal processes at the MZ. Furthermore, Reelin has been shown to activate Cdc42 in a PI3K-dependent manner to promote

growth cone motility and filopodia formation (Leemhuis et al., 2010). Both cofilin phosphorylation and Cdc42 activation seem to be solely mediated by ApoER2, and not by VLDLR.

Crk-family proteins (CrkL, CrkI, and CrkII) are intracellular adaptors consisting of an SH2 and one or two SH3 domains (Feller, 2001). Reelin promotes the interaction between Dab1 and Crk which is mediated by phosphotyrosines in Dab1 and Crk SH2 domain. Interestingly, simultaneous ablation of Crk and CrkL produces a reeler-like phenotype in mice (Park and Curran, 2008). Dab1 binding to Crk leads to phosphorylation of the GEF C3G, which activates its effector GTPase Rap1 (Ballif et al., 2004; Chen et al., 2004; Huang et al., 2004; Feng and Cooper, 2009). C3G-deficient mice show defects in cortical neuron migration and radial glia attachment in the cerebral cortex (Voss et al., 2008). Reelin-dependent Rap1 activation has been implicated in neuronal migration, particularly in multipolar migration in the IZ and glia-independent somal translocation (Franco et al., 2011; Jossin and Cooper, 2011). Here, Rap1 seems to increase the surface localization of N-Cadherin to regulate neuronal polarity. Thus, a Dab1-Crk-C3G-Rap1-cadherin pathway seems to play a crucial role for cortical lamination during development.

Nck (noncatalytic region of tyrosine kinase beta) adaptor proteins Nckα and Nckβ are regulators of the actin dynamics and cellular movement (Buday et al., 2002). Nckβ binds phosphorylated Dab1 and redistributes into neuronal processes upon Reelin treatment (Pramatarova et al., 2003). Peripheral Nckβ seems to alter the actin cytoskeleton although the precise mechanism is not yet understood.

Lis1, the regulatory subunit of the platelet-activating factor acetylhydrolase 1b (Pafah1b) complex, participates in microtubule dynamics and plays a key role in neuronal migration (Hirotsune et al., 1998; Wynshaw-Boris and Gambello, 2001). Dab1 and Lis1 associate in a Reelin-induced phosphorylation-dependent manner and also interact genetically (Assadi et al., 2003). Furthermore, the catalytic subunits of the Pafah1b complex, Pafah1b2 and Pafah1b3, interact biochemically with VLDLR, but not with ApoER2, which was corroborated by genetic evidence (Zhang et al., 2007). Therefore, regulation of cytoskeletal dynamics through Pafah1b components may be a unique feature of VLDLR-mediated Reelin signaling.

Moreover, there seems to be an intensive cross-talk between Reelin signaling and the Notch pathway, a major regulator of brain development. Dab1 associates with

the Notch intracellular domain (ICD), which is released by proteolytic enzymes and activates downstream molecules (Hashimoto-Torii et al., 2008). In Reelin signaling mutants, levels of Notch ICD are decreased, indicating deficient Notch signaling (Hashimoto-Torii et al., 2008; Sibbe et al., 2009). Furthermore, overexpression of Notch ICD rescued the cortical defects in the *reeler* mouse. This suggests that Notch plays a key role downstream of Reelin signaling, although the interplay between Notch and the other known signaling molecules stills needs to be investigated.

Phosphorylated Dab1 is bound by SOCS which leads to polyubiquitination by the E3 ubiquitin ligase component Culin-5 (Cul5). This modification targets phosphorylated Dab1 for proteasomal degradation and provides a negative feedback mechanism regulating Reelin responses (Feng et al., 2007).

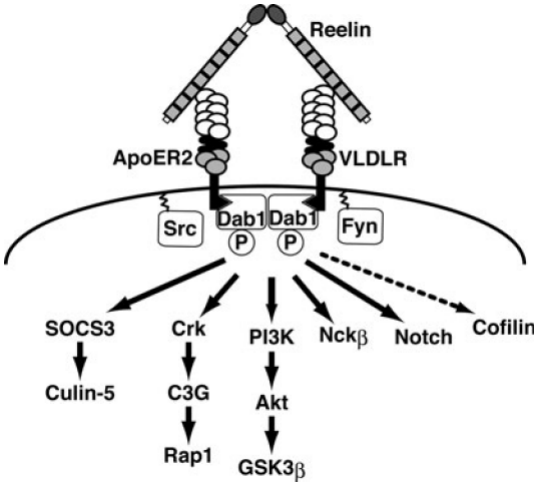

Figure 1.9 The Reelin signaling pathway. Reelin binding to ApoER2 and VLDLR leads to receptor clustering and tyrosine phosphorylation of Dab1 by Src and Fyn kinases. Phosphorylated Dab1 binds to downstream signaling molecules Crk, PI3K, and Nckβ. Binding to SOCS3 leads to proteasomal degradation of Dab1. The intracellular region of Notch also interacts with Dab1. Cofilin has been shown to be activated downstream of Reelin and Dab1. Taken from Honda et al., 2011.

Degradation of Dab1 by the proteasome is not the only possibility to modulate Reelin signaling. As mentioned above, Reelin is a substrate for extracellular metalloproteinases (Lambert de Rouvroit et al., 1999). Cleavage of Reelin plays an important role for duration and range of the signaling outcome (Koie et al., 2014).

Like Reelin itself, the Reelin receptors are also proteolytically processed. ApoER2 and VLDLR can be enzymatically cleaved by secretases (May et al., 2003; Hoe and Rebeck, 2005). Proteolysis by α-secretases generates a soluble extracellular

fragment whereas γ-secretase cleavage releases the intracellular domain into the cytosol (May et al., 2002). Receptor proteolysis occurs in a ligand-dependent manner and may therefore provide a negative feedback loop to shut down signaling response. Such a mechanism has been shown for an alternatively spliced isoform of ApoER2 which harbors a furin cleavage site (Brandes et al., 2001). Proteolytic processing by furin yields a soluble version of the complete ligand binding domain. This fragment gets secreted into the extracellular space where it acts as decoy receptor and antagonizes Reelin signaling (Koch et al., 2002). The intracellular region of ApoER2, generated by γ-secretase, can suppress signaling by inhibiting Reelin expression at a transcriptional level (Balmaceda et al., 2014). In addition, extracellular interactions with the proprotein convertase PCSK9 direct the receptors towards the lysosomal degradative pathway (Poirier et al., 2008). Similarly, the E3 ubiquitin ligase IDOL (Inducible Degrader of the LDL Receptor) targets VLDLR and ApoER2 for lysosomal degradation (Hong et al., 2010). Hence, cleavage and degradation of Reelin and its receptors by extra- and intracellular proteinases allows for modulation of the cellular signaling response.

Alternative splicing of ApoER2 and VLDLR results in a number of Reelin receptors with different properties. Four different isoforms of VLDLR can be generated by alternative splicing (Sakai et al., 2009). Interestingly, the majority of VLDLR transcripts in the adult brain lack the O-linked glycosylation domain encoded by exon 16. As cleavage by γ-secretase has been shown to be glycosylation-sensitive (Sakai et al., 2009), this suggests that signaling through ApoER2 and VLDLR can be differentially modulated by γ-secretase cleavage. ApoER2 shows excessive alternative splicing. Of the eight ligand binding regions, three are spliced out of all transcripts (Clatworthy et al., 1999). The eighth ligand binding region can be replaced with the furin cleavage site mentioned above (Brandes et al., 2001). Splicing variations in the extracellular region have been shown to influence the ligand-binding properties of ApoER2 (Hibi et al., 2009). As previously mentioned, an alternatively spliced exon (19) in ApoER2 mediates interaction with JIP1/2 and PSD-95 (Gotthardt et al., 2000; Stockinger et al., 2000). Exon 19 is crucial for Reelin-dependent LTP induction (Beffert et al., 2005).

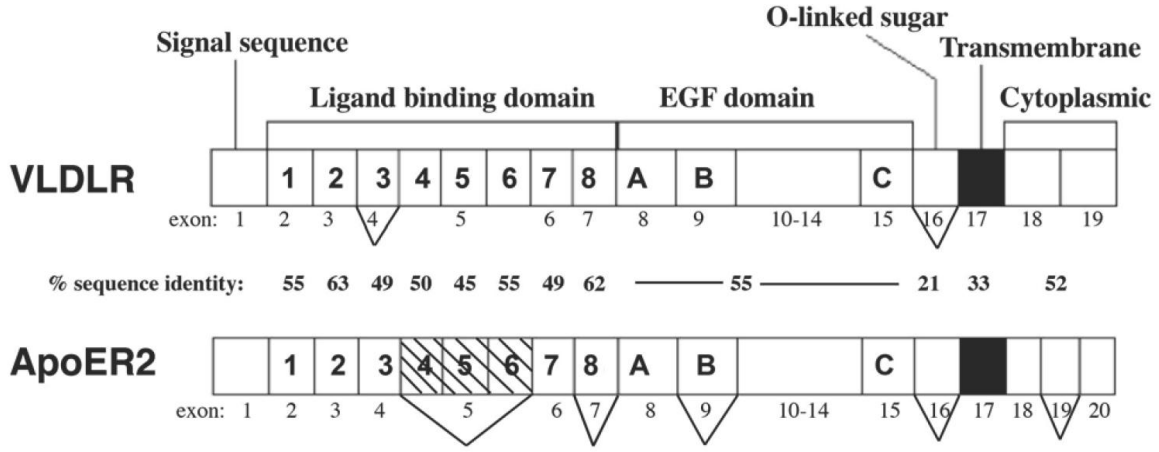

Figure 1.10 Domain structure of VLDLR and ApoER2. The signal sequence is followed by the ligand binding domain (eight ligand binding regions), an EGF domain and an O-linked glycosylation domain. The transmembrane region precedes a short cytoplasmic domain. Alternative splicing is indicated with protruding 'V's. Taken from Reddy et al., 2011.

Exon 19 and the O-glycosylated region have also been proposed to direct ApoER2 into lipid rafts (Sun and Soutar, 2003). There, ApoER2 can be endocytosed in a caveolin-dependent manner whereas VLDLR is internalized via CCPs (Riddell et al., 2001; Mayer et al., 2006). It was shown that VLDLR mediates efficient endocytosis and lysosomal degradation of Reelin. Endocytosis of ApoER2-bound Reelin occurs much slower. Interestingly, the raft association of ApoER2 is required for secretase-dependent cleavage and generation of extra- and intracellular ApoER2 fragments (Duit et al., 2010). This demonstrates that alternative splicing and differential sorting provide the molecular basis for unique functions of the Reelin receptors.

ApoER2 can also be endocytosed independently of its raft association by a clathrin-mediated process involving the adaptor protein Dab2 (Cuitino et al., 2005). Dab2 forms a complex with the endocytic proteins clathrin and AP-2 (Morris and Cooper, 2001; Mishra et al., 2002), but also with Eps15 and ITSNs (Teckchandani et al., 2012). Like its close relative Dab1, Dab2 binds to NPXY motifs. Dab2 has been shown to bind ApoER2, but not VLDLR (Yang et al., 2002). Despite its ability to activate Src kinase (Yang et al., 2002), Dab2 cannot compensate for disrupted Reelin signaling in Dab1 mutant mice (Sheldon et al., 1997). Rather, Dab2 seems to act as a cargo-specific adaptor for recruitment of lipoprotein receptors, e.g. ApoER2, into coated pits (Maurer and Cooper, 2006).

ApoER2 and VLDLR have overlapping functions for transmission of the Reelin signal across the plasma membrane. However, unique interactions and differential trafficking enable both receptors to fulfill also distinct functions in the brain. Both ApoER2 and VLDLR KOs display smaller, less foliated cerebella as well as disrupted cortical and hippocampal lamination. The cortical and hippocampal defects were more pronounced in ApoER2 KOs while VLDLR KOs showed more severe cerebellar defects. The radial alignment of cortical neurons was disrupted in ApoER2 KOs, but not VLDLR KOs (Trommsdorff et al., 1999). In the cortex of VLDLR KOs, but not of ApoER2 KOs, the MZ is invaded by numerous neurons, which suggests that VLDLR mediates a 'stop signal' function of Reelin (Dulabon et al., 2000; Hack et al., 2007). ApoER2, on the other hand, is required for migration of late-generated neurons and the development of superficial layers (Hack et al., 2007).

ApoER2 and VLDLR are closely related lipoprotein receptors and both mediate Reelin signaling in a Dab1-dependent manner. However, differences in splicing, trafficking and protein interactions also make distinct roles for these receptors possible. For example, ApoER2 can interact with PSD-95 and JIPs through a unique alternatively spliced exon and with Dab2 through its NPXY motif. VLDLR can control cytoskeletal remodeling by interacting with the Pafah1b complex. Further investigation of these receptors and their binding partners will help to better understand their roles for brain development and physiology.

1.4 Aims of this study

Although ITSN1 has been implicated in a variety of trafficking and signaling processes, its precise function in the mammalian brain remains to be elucidated. ITSN1 and its invertebrate ortholog Dap160 are mainly known for their role in endo-/exocytic membrane traffic, particularly cycling of SVs. Nevertheless, synaptic transmission is largely unaltered in mice lacking ITSN1, suggesting that ITSN1 functions might differ in vertebrates and invertebrates. There is a large body of evidence showing ITSN1 functions beyond membrane traffic, e.g. in postsynaptic development and scaffolding of intracellular signaling cascades. Whether and to what extent ITSN1 is relevant for any of these processes *in vivo* is still under debate. In mice, absence of ITSN1 has been shown to result in learning and memory deficits and disruption of axonal commissures (Sengar et al., 2013) suggesting a role of ITSN1 in higher brain functions. In addition, the ITSN1 gene is located on chromosome 21 and therefore upregulated in Down syndrome (DS) patients. DS is characterized by mental retardation and early-onset Alzheimer's disease. Hence, a better understanding of ITSN1 function might provide the basis for future therapeutic approaches.

We wanted to investigate the role of ITSN1 for brain function with a particular focus on the hippocampus. To find out about the function of ITSN1, we made use of a mouse model with a genetic ablation of ITSN1 expression (ITSN1 KO mouse). The brains of these mice were analyzed morphologically and functionally in order to investigate the role of ITSN1 *in viv*o. Based on findings from these experiments, the involvement of ITSN1 in different signaling pathways regulating brain development and physiology was investigated with histological, electrophysiological, cell biological and biochemical methods.

2. Material and Methods

2.1 Material

2.1.1 Chemicals and consumables

Chemicals and consumables were purchased from GE Healthcare, Greiner, Merck, Roth, Sarstedt, Sigma-Aldrich, Schott and Thermo Fisher Scientific.

2.1.2 Buffers, media and solutions

Deionized water from a Millipore apparatus (MilliQ H_2O) was used for all buffers and solutions. If necessary, buffers were autoclaved (121 °C, 20 min, 1 bar) or filter-sterilized (0.22 µm). pH was adjusted with HCl or NaOH.

Table 2.1 Solutions for molecular biology experiments

Solution	composition
Lysogeny broth (LB) medium	1.0 % (w/v) yeast extract 0.5 % (w/v) tryptone 0.5 % (w/v) NaCl pH 7.4
2 x YT medium	1.0 % (w/v) yeast extract 1.6 % (w/v) tryptone 0.5 % (w/v) NaCl pH 7.4
10 x Tris-Borate-EDTA (TBE) buffer	890 mM Tris 20 mM EDTA 890 mM boric acid
Tris-EDTA (TE) buffer	10 mM Tris 2 mM EDTA pH 8.0
Ampicillin stock (500 x)	50 mg/ml, sterile filtered
Kanamycin stock (200 x)	10 mg/ml, sterile filtered
Ethidium bromide stock	10 mg/ml

Tail lysis buffer	100 mM Tris pH 8.5 5 mM NaEDTA 0.2 % sodium dodecyl sulfate (SDS) 200 mM NaCl

Table 2.2 Solutions for cell biology experiments

Solution	composition
Serum-free medium (SFM) for neuronal cultures	Neurobasal-A 2 % B-27 supplement 100 U/ml penicillin 0.1 mg/ml streptomycin 1 x GlutaMAX 20 mM HEPES pH 7.4
Serum-containing medium (SCM) for HEK 293, CER, CEP4 and glial cultures	DMEM incl. GlutaMAX (4.5 g/l glucose) 10 % fetal bovine serum (heat-inactivated) 100 U/ml penicillin 0.1 mg/ml streptomycin
Digestion solution	137 mM NaCl 5 mM KCl 7 mM Na_2HPO 25 mM HEPES pH 7.4
Dissociation solution	Hank's balanced salt solution w/o Ca^{2+} or Mg^{2+} 50 mg/l $NaHCO_3$ 12 mM $MgSO_4$ 1 mM HEPES pH 7.4
10 x phosphate-buffered saline (PBS)	1.37 M NaCl 27 mM KCl 43 mM Na_2HPO_4 14 mM NaH_2PO_4 pH 7.4
PBS^{2+}	1 x PBS 1 mM $MgCl_2$ 1 mM $CaCl_2$
PFA fixative	4 % (w/v) paraformaldehyde (PFA) 4 % (w/v) sucrose in PBS pH 7.4

Goat serum dilution buffer (GSDB)	10 % goat serum (± 0.3 % Triton X-100) in 1 x PBS
Donkey serum dilution buffer (DSDB)	10 % donkey serum (± 0.3 % Triton X-100) in 1 x PBS

Table 2.3 Solution for electrophysiology experiments

Solution	composition
Artificial cerebrospinal fluid (ACSF)	120 mM NaCl 2.5 mM KCl 1.25 mM NaH_2PO_4 24 mM $NaHCO_3$ 1.5 mM $MgS0_4$ 2 mM $CaCl_2$ 25 mM glucose pH 7.35 - 7.4

Table 2.4 Solutions for protein biochemistry experiments

Solution	composition
HMK/Tx	20 mM HEPES pH 7.4 2 mM $MgCl_2$ 100 mM KCl 1 mM PMSF 0.3 % protease inhibitor cocktail 1 % Triton X-100 For phospho-samples only: 1 % phosphatase inhibitor cocktail 2 1 % phosphatase inhibitor cocktail 3
Homogenization Buffer	320 mM sucrose 4 mM HEPES pH 7.4
6 x SDS-PAGE sample buffer	375 mM Tris 60 % (v/v) glycerol 30 % (v/v) β-mercaptoethanol 18 % (w/v) SDS add bromophenol blue till deeply blue pH 6.8

4 x SDS stacking gel buffer	0.4 % (w/v) SDS 0.5 M Tris pH 6.8
4 x SDS separating gel buffer	0.4 % (w/v) SDS 1.5 M Tris pH 8.8
10 x SDS running buffer	246 mM Tris 1.92 M glycine 10 % (w/v) SDS
Semi-dry blotting buffer	1 x SDS 20 % (v/v) methanol
Coomassie stain	1 g/l Coomassie G250 10 % (v/v) acetic acid 25 % (v/v) methanol
Coomassie destain	10 % (v/v) acetic acid 25 % (v/v) methanol
Ponceau stain	0.3 % (w/v) Ponceau S 3 % (v/v) acetic acid
Ponceau destain	1 % (v/v) acetic acid
10 x Tris-buffered saline (TBS) buffer	200 mM Tris pH 7.6 1.4 M NaCl
Immunoblot blocking solution	3 % (w/v) milk powder in 1 x TBS
Immunoblot antibody dilution solution	3 % (w/v) bovine serum albumin 0.02 % (w/v) NaN_3 in 1 x TBS
2 x Bradford reagent	140 g/l Coomassie G250 200 ml 85 % H_3PO_4 100 ml ethanol (filtered)

Table 2.5 Solutions for histology experiments

Solution	composition
Fixation solution	4 % (w/v) PFA in PBS pH 7.4
Phosphate buffer 0.4 M	200 ml Na_2HPO_4 0.4 M ~30 ml NaH_2PO_4 0.4 M (until pH reaches 7.4)

Brain storage solution	20 % (v/v) glycerol 2 % (v/v) DMSO 125 mM phosphate buffer pH 7.4
Gelatin solution	0.2 % (w/v) porcine gelatin 50 mM Tris pH 7.6

2.1.3 Enzymes and kits

Restriction enzymes, calf intestinal phosphatase (CIP) and T4 DNA ligase were obtained from Fermentas. We purchased Phusion high fidelity DNA polymerase from New England Biolabs (NEB) and DreamTaq polymerase from Thermo Scientific. DNA extraction from agarose gels was performed with the NucleoSpin Gel and PCR Clean-up kit from Macherey-Nagel. For small-scale plasmid preparation (mini prep) from *Escherichia coli* (*E. coli*) we used the NucleoSpin Plasmid kit (Macherey-Nagel). For large-scale, endotoxin-free plasmid preparation (midi prep) the NucleoBond Xtra Midi EF kit (Macherey-Nagel) was used. Calcium phosphate transfection of hippocampal neurons was performed with the ProFection Mammalian Transfection System (Promega). The Cdc42 G-LISA Activation Assay was purchased from Cytoskeleton. For Golgi impregnation of brains, we made use of the FD Rapid GolgiStain Kit from FD Neurotechnologies.

2.1.4 Markers and loading dyes

DNA marker was purchased from Fermentas (GeneRuler 1kb DNA ladder) and protein markers were from Thermo Scientific (PageRuler Prestained Protein Ladder) or Serva (Triple Color Protein Standard II). DNA loading dye was obtained from Fermentas.

2.1.5 Synthetic DNA and RNA oligonucleotides

RNA oligonucleotides for RNA interference were obtained from Sigma and dissolved to a concentration of 100 µM in RNase-free water (Roth).

Table 2.6 siRNA sequences

Name	sequence (5' to 3')
human Dab2 siRNA	CAAAGGAUCUGGGUCAACAUU
scrambled siRNA	ACAACGAGCUUCCCUUCAA

DNA primers for PCR were from Biotez. Primers were stored at -20 °C for long-term and at 4 °C for short-term periods.

Table 2.7 Primer sequences

Regions overlapping with the template are highlighted with capital letters.

Name	sequence (5' to 3')
ApoEx_Hind fw	gtaa aagctt ATGGGCCGCCCAGAACTG
ApoSP_Hind rev	gtac aagctt CGCTGCGGAGAGATGCTG
ApoRest_ NotI	atca gcggccgc GATCCGCTGCCGGGCGGC
ApoER2wHA_XbaI rev	gtgc tctaga tta CTGAGCTCCTGCGTAATC
ApoER2_ICD fw	gtaa cccggg aAGGAACTGGAAGCGGAAG
ApoER2 rev	gtgc ctcgag tta GGGCAGTCCATCATCTTC
VLDLR_SP _ NotI fw	gtaa gcggccgc GGGAAGAAAGCCAAATG
VLDLR_SP_ XhoI rev	gtgc ctcgag cg AGCCAGATCATCATCTG
GST-VLDLR_EcoRI fw	gtaa gaattc AGGAATTGGCAACATAAA
GST-VLDLR_XhoI rev	gtgc ctcgag TCAAGCCAGATCATCATC
Dab2_Bam fw	gtca ggatcc ATGTCTAACGAAGTAGAA
Dab2_Xba rev	gaac tctaga CTAGGCAAAAGGATTTCC
Dab1_Bam fw	gtta ggatcc ATGTCAACTGAGACAGAA
Dab1_ Xba rev	taat tctaga CTAGCTACCGTCTTGTGG

2.1.6 Primary antibodies

Primary antibodies were usually stored with 50 % (v/v) glycerol at -20 °C to avoid repeated freeze-thaw cycles.

Table 2.8 List of primary antibodies

Antigen	host species	company/source	internal number	dilution
AP-2	mouse	BD transduction 611351	5	IB 1:500
ApoER2	rabbit	Abcam ab108208	527	IB 1:300
BrdU	rat	Abcam ab6326	342	IHC 1:200
Calbindin	mouse	Sigma C9848	-	IHC 1:2 000
Calretinin	rabbit	Abcam ab702	355	IHC 1:50
Cdc42	rabbit	Abcam ab64533	417	IB 1:1 000
CHC	mouse	TD1, homebrew	8	IB 1:500
Dab1	rabbit	Millipore ab5840	520	IB 1:1 000
Dab2	mouse	BD transduction 610464	341	IB 1:100
Dcx	rabbit	Abcam ab18723	-	IHC 1:1 000
Dcx	goat	Santa Cruz sc-8066	521	IHC 1:100
Dynamin1	mouse	#5; Zhang/de Camilli	26	IB 1:1 000
EphB2	goat	R&D AF467	401	IB 1:1 000
Epsin1	rabbit	Chen/de Camilli	156	IB 1:400
GFP	rabbit	Abcam ab6556	347	ICC 1:1 000
HA-tag	mouse	Covance MMS-101P	20	ICC 1:400
Hsc70	mouse	Thermo Scientific MA3006	170	IB 1:500
ITSN1	rabbit	1-440, homebrew	476	IP 5 - 10 µg
ITSN1	rabbit	mAC; Shupliakov	475	IB 1:500
MAP2	mouse	Sigma M9942	43	IHC 1:400
Myc-tag	rabbit	Abcam ab9106	458	IB 1:1 000
N-Cadherin	mouse	BD transduction 610920	237	IB 1:1 000
Nestin	rabbit	Covance PRB-315C	-	IHC 1:1 000
Nestin	mouse	eBioscience 14-5843-82	F-68	IHC 1:200
NeuN	mouse	Millipore MAB377	-	IHC 1:1 000
Numb	goat	Abcam ab4147	388	IB 1:1 000
pan-AKT	rabbit	Cell signaling 9272	204	IB 1:1 000
phospho-AKT	rabbit	Cell signaling 4060	74	IB 1:1 000
phospho-Cofilin	rabbit	Cell Signaling 3313	510	IB 1:100

phospho-tyrosine (4G10)	mouse	Millipore 05-321	F-92	IB 1:1 000
Reelin	mouse	Abcam ab78540	522	IB 1:500 IHC 1:500
SNAP25	mouse	Synaptic Systems 111011	334	IB 1:1 000
Synaptojanin	mouse	Cremona/di Paolo	45	IB 1:1 000
Synaptophysin	mouse	Synaptic System 101011	46	IB 1:5 000
Vinculin	mouse	Sigma V9264	418	IB 1:200
VLDLR	goat	R&D AF2258	523	IB 1:200 IHC 1:50
α-tubulin	mouse	Sigma T5168	42	ICC 1:500
β-actin	mouse	Sigma A5441	19	IB 1:1 000

IB: Immunoblot; ICC: Immunocytochemistry; IHC: Immunohistochemistry; IP: Immunoprecipitation

2.1.7 Secondary antibodies

Secondary antibodies were stored with 50 % (v/v) glycerol at -20 °C for long-term and at 4 °C for short-term periods.

Table 2.9 List of secondary antibodies

Antigen	host species	conjugated to	internal number	company/source
goat IgG	donkey	CF488A	89	Biotium 20016
goat IgG	donkey	CF568	177	Biotium 20106
goat IgG	donkey	CF647	184	Biotium 20048
goat IgG	donkey	HRP	115	Jackson 705-035-147
mouse IgG	donkey	CF488A	85	Biotium 20014
mouse IgG	donkey	CF568	96	Biotium 20105
mouse IgG	donkey	CF647	100	Biotium 20046
mouse IgG	goat	Alexa488	12	Invitrogen A11001
mouse IgG	goat	Alexa568	24	Invitrogen A11031
mouse IgG	goat	Alexa647	31	Invitrogen A21235
mouse IgG	goat	HRP	111	Jackson 115-035-003
mouse IgG	goat	IRDye 800CW	-	LI-COR P/N 926-32210

rabbit IgG	donkey	CF488A	86	Biotium 20015
rabbit IgG	donkey	CF568	97	Biotium 20098
rabbit IgG	donkey	CF647	99	Biotium 20047
rabbit IgG	goat	Alexa488	13	Invitrogen A11008
rabbit IgG	goat	Alexa568	19	Invitrogen A11011
rabbit IgG	goat	Alexa647	32	Invitrogen A21244
rabbit IgG	goat	HRP	113	Jackson 111-035-003
rabbit IgG	goat	IRDye 800CW	-	LI-COR P/N 925-32211
rat IgG	donkey	Alexa488	14	Invitrogen A21208

2.1.8 Plasmids and constructs

Plasmid DNA was stored at a concentration of 1 µg/µl at -20 °C for long-term and at 4 °C for short-term periods.

Table 2.10 List of expression constructs

Name	insert species	backbone	internal number	comment
ApoER2-HA	mouse	unknown	3745	from Bill Rebeck; UniProt: Q924X6-2
EGFP-ApoER2-HA	mouse	pcEGFP-MK	3758	
EGFP-VLDLR-HA	mouse	pcEGFP-MK	3759	origin of VLDLR construct: Hans Bock; UniProt: P98156
ephrinB2-GFP	mouse	pEGFP-N1	3744	cloned by Marielle Eichhorn-Grünig
GST	-	pGEX4T-1	2112	
GST-ApoER2-ICR	mouse	pGEX4T-1	3754	amino acids 756 - 870
GST-EH1+2	human	pGEX4T-1	STHLM G7	cloned by Arndt Pechstein
GST-SH3A	human	pGEX4T-1	STHLM H3	cloned by Arndt Pechstein
GST-SH3A +linker WT	human	pGEX4T-1	-	cloned by Arndt Pechstein
GST-SH3A +linker Mut	human	pGEX4T-1	-	cloned by Arndt Pechstein; W850A, W870A, W873A, F853A
GST-SH3A-C	mouse	pGEX4T-1	STHLM A1	cloned by Arndt Pechstein

GST-SH3A-E	human	pGEX4T-1	STHLM I8	cloned by Arndt Pechstein
GST-SH3B	human	pGEX4T-1	Arndt B1B1	cloned by Arndt Pechstein
GST-SH3B-E	human	pGEX4T-1	-	cloned by Arndt Pechstein
GST-SH3C	human	pGEX4T-1	4595	cloned by Arndt Pechstein
GST-SH3D	human	pGEX4T-1	4596	cloned by Arndt Pechstein
GST-SH3E	human	pGEX4T-1	4597	cloned by Arndt Pechstein
GST-VLDLR-ICR	mouse	pGEX4T-1	3761	amino acids 792 - 845
HA-EphB1	mouse	pCAG	4052	original construct; gift from Carol Mason
Myc-Dab1	mouse	pcMYC-MK	4601	origin of Dab1 construct: Jonathan Cooper
Myc-Dab2	mouse	pcMYC-MK	4063	origin of Dab2 construct: Jonathan Cooper

2.1.9 Bacterial strains

For cloning and amplification of plasmid DNA the *E. coli* TOP10 strain (Invitrogen) was used.

For expression of recombinant proteins we made use of the *E. coli* BL21 CodonPlus (DE3)-RP strain (Stratagene) as these bacteria express heterologous proteins at high levels.

2.1.10 Mammalian cell lines

For biochemical experiments the human embryonic kidney cell line HEK 293 was used because of its high protein content.

For Reelin purification, a 293-EBNA cell line (CER) stably transfected with the complete mouse Reelin sequence was used. In this context, 293-EBNA cells transfected with the empty vector (CEP4) served as negative control. Both CER and CEP4 cells were generously provided by Tom Curran (Children's Hospital of Philadelphia, PA, USA).

2.1.11 Software and internet resources

Table 2.11 List of programs and internet tools

Program/Website	Application	Source
Ape (A plasmid editor)	DNA sequence analysis; cloning strategies	http://biologylabs.utah.edu /jorgensen/wayned/ape/
ImageJ	image editing, analysis and quantification	https://imagej.nih.gov/ij/
GIMP	image editing	www.gimp.org/
Microsoft Office	text files, spreadsheets and presentations	Microsoft
GraphPad PRISM	statistics	GraphPad
Inkscape	illustrations and figures	www.inkscape.org/
NCBI Homepage	database for DNA/protein sequences and scientific literature	www.ncbi.nlm.nih.gov/
Genecards	information on genes/proteins	www.genecards.org/
UniProt	protein sequences and annotation	www.uniprot.org/

2.1.12 Mouse strains

The ITSN1 knockout (KO) mice were a kind gift from Dr. Melanie Pritchard (Monash University, Melbourne, Australia). Heterozygous mice were interbred to yield ITSN1 KO mice and corresponding wildtype (WT) control animals. The ApoER2 KO mice were generously provided by Prof. Hans Bock (Univ. of Düsseldorf, Germany) and Prof. Joachim Herz (Univ. of Texas Southwestern Medical Center, Dallas, TX, USA). To obtain ITSN1/ApoER2 double KO mice, ITSN1 KO mice were interbred with ApoER2 heterozygous mice. The resulting double heterozygous mice were bred to produce double and single KO mice, as well as control animals (double heterozygous).

2.2 Behavioral experiments

Studies of mouse behavior were performed in a quiet environment with low lighting. For comparability reasons, experiments were always performed at the same daytime (3 to 5 pm). All equipment used was cleaned thoroughly between experiments to avoid erroneous results due to mice sniffing each other.

2.2.1 Open field exploration

For open field exploration tests, mice were exposed to an unfamiliar open arena for a period of 8 min. The test chamber measured 60 x 40 cm. A central zone of 30 x 20 cm was marked with a black line. The total time the mice spent walking and the time spent in the center were measured manually. Additionally, the number of line crossings and wall rearing attempts were counted.

2.2.2 Novel object assay

After open field exploration, an unfamiliar object (bottle of Immu-Mount mounting medium) was placed in the center of the chamber. The mouse behavior was recorded for 5 min. The overall time spent at the novel object was measured manually, as well as the latency to the first approach. Also, the number of approaches was counted.

2.3 Molecular Biology Methods

2.3.1 Cloning strategies

Cloning strategies were developed using the free DNA editing software Ape. Primers for cloning purposes were designed with an overlap of 15 - 18 base pairs (bp) between primer and target sequence. Additional 4 nucleotides were added to the 5' end to ensure efficient cleavage by restriction enzymes. The complete DNA construct was assembled *in silico* to exclude possible mistakes, such as frame shifts or incompatibilities of restriction enzyme recognition sites.

2.3.2 Polymerase chain reaction

Polymerase chain reactions (PCRs) were used for amplification of specific DNA sequences from plasmid or genomic DNA. PCRs were usually set up in a volume of 20 µl containing 1 x polymerase reaction buffer, 200 µM of each dNTP, 500 nM of each primer, the respective template DNA and 1 unit of Phusion polymerase or 0.5 units of DreamTaq polymerase. The annealing was chosen to be equal to the melting temperature of the primers.

For cloning of protein coding sequences into expression vectors DNA sequences were amplified using plasmid DNA as a template. In this context, the proofreading polymerase Phusion was used. The following program was run in a thermocycler:

Phusion:		
	Temperature	Time
1. Initial Denaturation	95°C	30 s
2. Denaturation	95°C	10 s
3. Annealing	50 - 65°C	20 s
4. Elongation	72°C	15 - 30 s/kb
5. Final elongation	72°C	10 min
6. Storage	4°C	∞

Steps 2 to 4 were repeated for 30 cycles.

For screening of *E. coli* colonies after transformation of ligation reactions ("Colony-PCR") the DNA polymerase DreamTaq was used. Generally, primers were chosen in a way that one is specific for the insert while the other binds to the target vector. A tiny amount of bacteria picked directly from the LB agar plate provided the template DNA. For Colony-PCRs the following program was employed:

DreamTaq:		
	Temperature	Time
1. Initial Denaturation	95 °C	2 min
2. Denaturation	95 °C	30 s
3. Annealing	50 - 65 °C	30 s
4. Elongation	72 °C	1 min/kb
5. Final elongation	72 °C	10 min
6. Storage	4 °C	∞

Steps 2 to 4 were repeated for 30 cycles.

2.3.3 Agarose gel electrophoresis

Agarose was dissolved in 1 x TBE buffer to a concentration of 0.7 % to 1.5 % (w/v) by heating in a microwave. Ethidium bromide (Roth) was added to a final concentration of 100 ng/ml. The gel was cast and covered with 1 x TBE buffer after hardening. DNA samples were mixed with DNA loading dye before loading them to the agarose gel. DNA fragments were separated at 8 - 12 V per cm of electrode distance for 20 to 40 min. DNA was visualized on a UV table. If DNA was destined for ligation, the desired fragments were cut out of the gel keeping UV exposure as low and short as possible.

2.3.4 Isolation of plasmid DNA from *E. coli*

Small-scale isolation of plasmid DNA was done using the mini prep kit from Macherey-Nagel according to the manufacturer's instructions. For mini preps, 2 - 3 ml of *E. coli* overnight cultures were used. Medium-scale isolation of plasmid DNA for transfection of mammalian cells was performed with the endotoxin-free midi prep kit

from Qiagen. For this application, 100 - 200 ml of *E. coli* overnight culture were subjected to plasmid DNA isolation.

2.3.5 DNA restriction analysis

Digestion of DNA with restriction enzymes was performed for analysis of a DNA construct or to generate fragments for subcloning. 2 µg of plasmid DNA or the purified PCR product from 50 µl PCR reaction was incubated with 1 µl of the respective FastDigest enzyme (Fermentas) and 2 µl of 10 x FastDigest Green Buffer in a total reaction volume of 20 µl. Plasmid DNA was digested for 1 - 2 h at 37 °C while PCR products were digested for the maximal time specified in the user's manual. Digested fragments were verified by agarose gel electrophoresis and purified from the gel by using the NucleoSpin Clean-up kit (Macherey-Nagel) if used for cloning.

2.3.6 DNA ligation

Digested vector DNA was dephosphorylated at their 5' end by incubation with 1 unit of CIP (calf intestinal phosphatase; NEB) for 10 min at 37 °C in order to prevent self-ligation of vector DNA. Dephosphorylated plasmid DNA and digested PCR product were purified using the NucleoSpin Extract II (Macherey-Nagel). The purity and concentration of the DNA were measured photometrically. 50 ng of vector and a threefold molar excess of insert were incubated with 5 units T4 DNA ligase (Fermentas) and 4 µl of 5 x Ligation Buffer in a total reaction volume of 20 µl for 1 h at room temperature. 5 µl of the ligation reaction were used for transformation.

2.3.7 Transformation of chemically competent *E. coli*

50 µl of $CaCl_2$-competent *E. coli* (TOP10 or BL21) were thawed on ice and incubated with 5 µl of ligation reaction for 5 min on ice. Cells were heat-shocked for 45 s at 42 °C and chilled for 5 min on ice. 500 µl of LB medium without antibiotics were added and bacteria were incubated shaking for 60 min at 37 °C. Cells were plated on pre-warmed LB agar plates supplemented with appropriate antibiotics (Ampicillin or Kanamycin) for selection of positive clones.

2.3.8 Sequencing

Sequencing of plasmid DNA was carried out by MWG Biotech or Source Bioscience. 0.5 - 1 µg of DNA were sent. Sequencing results were analyzed with Ape software.

2.3.9 Cryostocks of bacterial clones

2 ml of a bacterial suspension containing a positive clone were concentrated to 0.5 ml by centrifugation and mixed in a 1:1 ratio with a 50 % glycerol solution in PBS. The mixture was transferred into cryotubes and stored at -80 °C.

2.3.10 Isolation of genomic DNA from mouse tail

Genomic DNA was isolated from mouse tissue to allow genotyping of transgenic mice. Small tail or toe biopsies were taken from pups (p0 - p3). Alternatively, ear tissue was taken from mice at the time of weaning (~3 weeks). Tissue samples were incubated in 300 µl of tail lysis buffer supplemented with Proteinase K (100 µg/ml; NEB) at 55 °C for 0.5 - 2.0 h. The debris was removed by centrifugation for 5 min at 17 000 g and DNA was precipitated by addition of an equal volume of isopropanol to the supernatant. After several inversions of the tubes, the DNA was pelleted by a centrifugation for 5 min at 17 000 g. The supernatant was removed and the pellet was washed in 500 µl 70 % ethanol. After another centrifugation the supernatant was removed carefully but meticulously. The pellet was dried in a heating block at 55 °C and then resuspended in 50 µl MilliQ H_2O. Isolated genomic DNA was used for PCR directly or stored at -20 °C.

2.3.11 Genotyping of mice

Mice from the ITSN1 and ApoER2 KO strains were genotyped by PCR.

Table 2.12 Reaction mix and primer sequences for genotyping

Reaction mix:		Primer	sequence (5' to 3')
10 x buffer	2 µl	TM218_ITSN1a_F	GTAGAGCTCTAAACTGCACCTTAG
10 x dye	2 µl	TM219_ITSN1b_F	CTGGTATGTATCGATCACCATCCA

MgCl2	2 µl
dNTPs (5 mM)	0.6 µl
Primers (10 µM)	0.75 µl
Taq	0.5 µl
DNA	1 - 2 µl
MilliQ H_2O	ad 20 µl

TM220_ITSN1c_R	GTGACAACAGTCAACACAGCATTG
ApoER2_WT fw	CCACAGTGTCACACAGGTAATGTG
ApoER2_WT rev	ACGATGACCCCAATGACAGCAGCG
ApoER2_KO rev	GCTTGTTGGAATTCAGCCAGTTACC

The following PCR programs were used for genotyping:

ITSN1 (AG55_1):		
	Temp	Time
1. Initial Denaturation	95 °C	3 min
2. Denaturation	95 °C	30 s
3. Annealing	55 °C	30 s
4. Elongation	72°C	1 min
5. Final elongation	72°C	5 min
6. Storage	4°C	∞

Steps 2 to 4 were repeated for 30 cycles.
Expected band sizes were 666 bp for WT and 544 bp for KO samples.

ApoER2_WT 55:		
	Temp	Time
1. Initial Denaturation	95 °C	2 min
2. Denaturation	95 °C	20 s
3. Annealing	55 °C	30 s
4. Elongation	72°C	1 min
5. Final elongation	72°C	10 min
6. Storage	4°C	∞

ApoER2_KO 60:		
	Temp	Time
1. Initial Denaturation	95 °C	2 min
2. Denaturation	95 °C	20 s
3. Annealing	60 °C	30 s
4. Elongation	72°C	1 min
5. Final elongation	72°C	10 min
6. Storage	4°C	∞

Steps 2 to 4 were repeated for 40 cycles.
Expected band sizes were 601 bp for WT and 420 bp for KO samples.

2.4 Cell Biology Methods

2.4.1 Hippocampal neuron preparation and culture

Coverslips were coated with Poly-L-lysine (final concentration 15 µg/ml in MilliQ H_2O) while tissue culture dishes were coated with Poly-L-ornithine (final concentration 100 µg/ml in MilliQ H_2O) for at least 1 h at 37 °C. Before application of cells, coverslips or dishes were washed twice with MilliQ H_2O and dried briefly. For preparation of hippocampal neurons, mice pups (p0 - p4) were decapitated, the brain was isolated and collected in sterile Hank's balanced salt solution (HBSS) with 20 % fetal bovine serum (FBS). Brain hemispheres were separated and brain stem, cerebellum, midbrain and thalamus were removed. The hippocampus was folded out and separated from the cortex. Isolated hippocampi were sliced into 5 - 7 pieces and collected into a 15 ml falcon tube filled with 5 ml HBSS with 20 % FBS. After settling of the tissue pieces, the supernatant was removed and the tissue was rinsed once with 5 ml HBSS with 20 % FBS and twice with 5 ml HBSS. The pieces were digested with 2 ml sterile digestion solution supplemented with 1 mg DNase (Sigma, D5025) and 12 mg Trypsin (Sigma, T1005) for 15 min at 37 °C. After that, tissue pieces were washed twice with 5 ml HBSS with 20 % FBS to block the trypsin activity and twice with HBSS. Cells were dissociated mechanically in sterile dissociation solution containing 1 mg DNase by triturating using a siliconized Pasteur pipettes with narrowed opening. 2 ml of HBSS with 20 % FBS were added to the cell suspension and cells were pelleted by centrifugation for 8 min at 200 x g and 4 °C. Cells were resuspended in 0.5 ml of SFM and counted. For immunocytochemical experiments, 50 000 cells in a volume of 50 µl were plated in the middle of an 18 mm Poly-L-lysine-coated coverslip. When cells were to be used for proteinbiochemical assays 200 000 - 500 000 cells at a concentration of 100 000 - 250 000 cells / 100 µl were plated onto Poly-L-ornithine-coated 3.5 cm tissue culture dishes. Cells were allowed to attach for 1 - 2 h and subsequently supplied with a sufficient volume of SFM. Every 4 - 5 days neurons were fed by exchanging half of the culture medium. Neuronal cells were cultured in a New Brunswick Galaxy 170 S incubator at 37 °C and with 5 % CO_2.

2.4.2 Calcium phosphate transfection of neuronal cultures

Hippocampal neurons were transfected on day 3 - 10 *in vitro* (DIV) with endotoxin-free plasmid DNA by a modified calcium phosphate transfection method using the ProFection mammalian transfection system (Promega, E1200). Osmolarity of culture medium, Neurobasal A (NBA; Invitrogen, 21103) and Ca^{2+}/Mg^{2+}-free HBSS (Invitrogen, 14170) were measured and adjusted to the same osmolarity by adding D-Mannitol (Sigma, M4125). First, medium was removed from coverslips and saved for later reuse. Cells were starved in pre-equilibrated NBA for 25 - 30 min in the incubator. DNA (1 - 10 µg for an 18 mm coverslip) was mixed with 6.25 µl of 2 M $CalCl_2$ and 50 µl water in an Eppendorf tube while 50 µl of 2 x HEPES buffer was pipetted into a 15 ml falcon tube. DNA precipitates were formed by adding the DNA/calcium mixture dropwise into HEPES buffer while vortexing gently. The solution was kept in dark for 20 min and then added dropwise to cells (100 µl / 1 well). After incubation for 20 - 25 min in the incubator, cells were washed three times with pre-equilibrated HBSS for 1 min before cells were covered with the culture medium removed earlier.

2.4.3 Antibody uptake in hippocampal neurons

Antibody uptake experiments were performed with DIV7 hippocampal neurons, transfected on DIV3 with EGFP-VLDLR-HA or EGFP-ApoER2-HA. Anti-EGFP antibody (Abcam) was diluted 1:500 in prewarmed SFM and coverslips with transfected cells were incubated upside down on antibody solution in a humidity chamber. The uptake was allowed for 15 or 30 min at 37 °C or for 30 min at 8 °C (control). Afterwards, cells were washed three times with ice-cold PBS^{2+} and fixed in PFA fixative for 5 min at room temperature. After three washes with PBS and blocking with GSDB without Triton X-100 for 30 min, the surface-bound antibody pool was stained with goat α rabbit Alexa647 (1:100; Invitrogen) for 1h. Cells were washed three times with PBS and postfixed with 2 % PFA for 10 min at room temperature before another three washes with PBS. Neurons were permeabilized and blocked simultaneously with GSDB containing Triton X-100 for 30 min. Then, internalized antibodies were stained with goat α rabbit Alexa568 (1:200; Invitrogen) for 30 min. After three washes with

PBS, coverslips were mounted on microscopy slides with Immu-Mount (Thermo Scientific).

2.4.4 Preparation of hippocampal explants

Coverslips were coated with Poly-L-lysine (final concentration 100 µg/ml in MilliQ H_2O) and Laminin (final concentration 20 µg/ml in MilliQ H_2O) for at least 2 h at 37 °C. Directly before plating coverslips were washed twice with MilliQ H_2O and SFM was added. Hippocampal explants were isolated from embryonic mice (E16 - E18). For that purpose, parental mice were mated and females were checked for a vaginal plug. About 17 days after a plug had been noted, the pregnant mouse was sacrificed by cervical dislocation. The uterus containing the mouse embryos was taken out before the embryonic brains were isolated. Brains were stored in ice-cold HBSS while genotyping of the embryos was carried out using tail biopsies. Only brains from KO animals and their WT littermates were used. From these, hippocampi were isolated and chopped into 500 µm thick pieces using a McIlwain tissue chopper (Mickle). Three pieces of hippocampal tissue were plated on a coated 18 mm coverslip.

2.4.5 Growth cone collapse assay

To examine the EphB-mediated collapse of growth cones, chimeric murine ephrinB2/human Fc region (R&D) was preclustered with a rabbit anti-human IgG Fc secondary antibody at a molar ratio of 1:2 for one hour at room temperature. Per coverslip, 1 µg of ephrinB2/Fc were used at a final concentration of 2.5 µg/ml. Clustering antibody only served as negative control. Preclustered ephrinB2/Fc or control antibody were added to hippocampal explants in SFM at DIV1 or DIV2 and incubated for 60 min in the incubator. For fixation of the explant cultures, 4 % PFA with 20 % sucrose was added on top of the culture medium to avoid collapse induction by air exposure. After 15 min, PFA/sucrose was removed and growth cones were stained with Alexa568-coupled phalloidin (1:50; Invitrogen, A12380) and mouse anti-tubulin antibody according to the standard immunostaining protocol.

2.4.6 Organotypic hippocampal slice cultures

For hippocampal slice cultures, mice pups at p5 - p7 were used. In preparation, 1.2 ml of incubation medium per well were added to a 6-well plate (4 wells per animal). Millicell culture plate inserts (Millipore, PICMORG50) were placed in each well. Dissection was performed in 3 ml ice-cold preparation medium in a 3.5 cm dish. Hippocampi were isolated very carefully from the brain to avoid damage to the hippocampal tissue. Afterwards, hippocampi were transferred to the McIlwain tissue chopper and surrounding medium was removed completely. The tissue was chopped into 300 µm thick sections and transferred on a spatula. Sections were separated by gentle rubbing with a second spatula. Slices were collected in a 3.5 cm dish with preparation medium and examined under the microscope. Only slices with smooth margins and well defined, undamaged CA1, CA3, and DG regions were used. Two slices were placed onto the previously prepared inserts in the well plates and cultured at 37 °C and 5 % CO2. Slices were checked for contamination every other day and incubation medium was fully exchanged every second day. Bromodeoxyuridine (BrdU; Sigma, B5002) was added to the medium at 20 µM between DIV14 and DIV16. At DIV18, slices were fixed with PFA fixative for 15 min, 30 min, 1 h, 2 h and overnight. Immunostaining of the slices continued according to the immunohistochemical staining protocol (chapters 2.7.6 and 2.7.7).

Table 2.13 Media for hippocampal slice cultures

Preparation medium	
Sterile MEM (2 x)	50 ml
Aqua ad iniectabilia	49 ml
GlutaMAX 200 mM	1 ml
NaOH 1 M	0.940 ml
adjust to pH 7.32 - 7.36 directly before use	

Serum-free incubation medium	
Neurobasal-A	96.25 ml
B-27 supplement	2 ml
Sterile 20 % glucose	0.5 ml
GlutaMAX 200 mM	1.25 ml
adjust to pH 7.2 - 7.3 directly before use	

All components and devices were used exclusively for slice cultures. Cleaning occurred with MilliQ H_2O only, without any detergent. All media were sterilized by filtration through a 0.22 µm sterile filter.

2.4.7 Culture of cell lines

HEK 293 cells were grown at 37 °C in presence of 5 % CO_2 in a New Brunswick Galaxy 170 S incubator in serum-containing medium (SCM). Confluent cells were passaged by washing once with PBS followed by detaching the cells from the plate using trypsin/EDTA solution (Thermo Scientific). Detached cells were resuspended in SCM and plated on a new dish in a dilution ranging from 1:3 to 1:20. For long-term storage, pelleted cells were resuspended in SCM containing 10 % DMSO and frozen with slowly decreasing temperature by placing them in a styropor box at -80 °C. The next day, cells were transferred to the gas phase of a liquid nitrogen tank.

2.4.8 Reelin production and concentration

CER cells, stably expressing full length Reelin, were cultured in 15 cm dishes in SCM. To obtain Reelin, confluent 15 cm dishes were washed meticulously with PBS three times to get rid of serum proteins. Cells were incubated with Dulbecco's modified Eagle medium (DMEM; containing 20 mM HEPES at pH 7.4) without serum and antibiotics for 24 hours. Cell supernatant was harvested and new DMEM was added for another 24 hours. Supernatants were pooled and precleared by centrifugation at 1 000 g for 5 min. To purify and simultaneously concentrate Reelin, the solution was applied to an Amicon Ultra 15 mL centrifugal filter unit (Millipore) and centrifuged at 4 000 g and 4 °C for 15 min. Protein concentration was measured with the Bradford assay before the solution was snap-frozen and stored at -20 °C. Concentrated supernatant from CEP4 cells served as negative control.

2.4.9 Calcium phosphate transfection of HEK 293 cells

HEK 293 cells were cultured in 10 cm dishes and transfected at a confluence of ~50 - 70 %. For one dish, 5 - 15 µg of plasmid DNA were mixed with 60 µl $CaCl_2$ (2.5 M) and 440 µl 0.1 x TE Buffer. The solution was added dropwise into 500 µl of 2 x HBS while vortexing gently. After 20 min, the mixture containing Ca^{2+}-DNA precipitates were added drop by drop to the HEK 293 cells. Transfections were in performed with cells in full medium containing antibiotics. Cells were harvested and lysed 48 - 72 hours after transfection.

2.4.10 Transfection of HEK 293 cells with DNA/siRNA using Jetprime

HEK 293 cells were simultaneously transfected with DNA and siRNA using a reverse transfection protocol. For a 10 cm dish, 500 pmol of siRNA and 5 µg of DNA were diluted in 1 ml Jetprime buffer. After adding 20 µl of Jetprime reagent, the solution was vortexed for 20 s and incubated for 15 min at room temperature. Meanwhile, HEK 293 cells were trypsinized and counted. 3.5 - 4.0 x 10^6 cells were plated on a 10 cm dish and the transfection mix was added immediately. Cells were harvested 72 hours after transfection.

2.4.11 Immunocytochemistry

Cells were fixed with PFA fixative for 15 min at room temperature. Residual PFA was removed by washing cells three times with PBS. Fixed cells were permeabilized and at the same time blocked with GSDB/DSDB (depending of the origin species of the secondary antibodies) for 30 min at room temperature. Triton X-100 was only added when total pools were to be detected whereas Triton X-100 was omitted for surface stainings. Afterwards, cells were incubated with primary antibodies diluted in GSDB/DSDB for 1 h at room temperature. Incubation with antibodies was performed by placing the coverslips upside down onto a drop of antibody solution on parafilm in a humidified chamber. Coverslips were transferred back into a well plate and washed three times with PBS for 5 min each. Alexa-conjugated secondary antibodies were applied at a 1:200 dilution in GSDB containing 5 µg/ml 4',6-Diamidino-2-phenylindole (DAPI) for 30 min at room temperature. After washing the coverslips three times in PBS for 5 min each and quick washing in water, the coverslips were mounted on a microscope slide with Immu-Mount reagent and dried at room temperature for 1 h.

2.4.12 Uptake of preclustered ephrinB-Fc

EphrinB1-Fc and ephrinB2-Fc chimeric proteins were preclustered with goat anti-human Fc antibodies at a 2:1 molar ratio for 1 h at room temperature in PBS. Complexes were used at a final concentration of 500 ng/ml. Uptake was allowed for 15 min at 37 °C. Cells were washed three times with PBS and then fixed with PFA fixative. After three PBS washes and blocking with DSDB without Triton X-100,

surface-bound ephrinB-Fc was stained with donkey anti-goat Alexa488 for 30 min. After another three washes, cells were postfixed with 2 % PFA for 15 min and washed again three times with PBS. Permeabilization and blocking was done with DSDB containing Triton X-100 for 30 min. Internal ephrinB-Fc was stained with donkey anti-goat Alexa568 for 30 min. Finally, cells were washed again three times and mounted in microscopy slides using Immu-Mount reagent.

2.4.13 Transendocytosis of ephrinB/EphB complexes

Hippocampal glia cultures were prepared similarly to hippocampal neurons. As culture medium, SCM was used. Cells were isolated and cultured for 2 - 3 passages before transfection with Lipofectamine 2000. 2 dishes of WT and ITSN1 KO cells each were transfected with HA-tagged EphB1 and GFP-tagged ephrinB2, respectively. The next day, WT cells, transfected with HA-EphB1, and ITSN1 KO cells, transfected with ephrinB2-GFP, were split and mixed in a 1:1 ration. Vice versa, the same was done with WT cells, transfected with ephrinB2-GFP, and ITSN1 KO cells, transfected with HA-EphB1. After one day, cells were fixed and stained for HA and GFP. Coverslips were examined for transendocytosis between neighboring transfected cells of different origin.

2.5 Electrophysiology

2 - 3 months old WT and ITSN1 KO mice were used for acute hippocampal field electrophysiology. Mice were decapitated and brains quickly sectioned into 350 µm thick sagittal slices and transferred to recover in resting chamber (22 - 24 °C) filled with artificial cerebrospinal fluid (ACSF). After recovery, slices were transferred to a submerged recording chamber supplied with continuously bubbled ACSF with solution exchange of 3 - 5 ml per min at room temperature (22 - 24 °C). CA3 - CA1 Schaffer collaterals were stimulated in stratum radiatum using a glass electrode filled with ACSF (1 - 1.5 MΩ) and a similar glass electrode (1.5 - 2.5 MΩ) placed in the distal part of the CA1 region was used to record field excitatory postsynaptic potentials (fEPSPs). Electrical pulses of 0.2 ms were delivered for stimulation of Schaffer collaterals and basal excitatory synaptic transmission was evaluated using input-output stimulus response curves. To test synaptic plasticity LTP was induced using single theta burst stimulation (TBS) comprising 8 bursts delivered every 200 ms with each burst containing 4 pulses at 100 Hz. The data were recorded at a sampling rate of 10 kHz, low-pass filtered at 3 kHz and analyzed using PatchMaster software and EPC9 amplifier (Heka Elektronics).

2.6 Proteinbiochemical Methods

2.6.1 Preparation of mouse brain extract

In order to analyze the expression levels of proteins and for protein-protein interaction studies, whole brains or isolated hippocampi were collected in a teflon homogenizer. 5 µl of ice-cold lysis buffer (HMK/Tx) were added per mg of tissue. By applying 15 strokes at 900 rpm (IKA EUROSTAR power basic) the tissue was homogenized and complete lysis was allowed by subsequent incubation on a rotating wheel for 30 min at 4 °C. Lysates were centrifuged for 10 min at 17 000 x g at 4 °C and the supernatants were collected. If the lysates were to be used for interaction studies, i.e. GST-pulldown or immunoprecipitation assays, they were cleared by ultracentrifugation for 20 min at 180 000 g and 4 °C in a TLA-110 rotor. Alternatively, if lysates were destined for immunoblotting only, sample buffer was added and they were stored at -20 °C or -80 °C (for phospho-samples).

2.6.2 Crude synaptic vesicle (LP2) preparation

For subcellular fractionation of brain tissue, 1 mouse brain was homogenized in 12 ml of ice cold homogenization buffer with 20 strokes at 900 rpm (IKA EUROSTAR power basic). After centrifugation for 10 min at 800 g, the supernatant (S1) was centrifuged again (15 min at 10 000 g). The pellet (P2) was resuspended in 12 ml ice cold homogenization buffer and centrifuged for 15 min at 10 000 g. The resulting pellet (P2') contains the crude synaptosomal fraction. The P2' fraction was resuspended in 1.2 ml homogenization buffer and synaptosomes were lysed osmotically by addition of 9 ml ice cold MilliQ H_2O and homogenization with 3 strokes at 2 000 rpm. The solution was centrifuged for 20 min at 25 000 g and the resulting supernatant (LS1) was centrifuged for 2 h at 200 000 g. The pellet containing crude synaptic vesicles (LP2) was resuspended in 50 µl homogenization buffer and stored in 1 x sample buffer at 0.25 mg/ml.

2.4.3 Preparation of cell lysates from eukaryotic cells

Total cell lysates from eukaryotic cell lines or primary hippocampal cultures were prepared using HMK/Tx lysis buffer. Cells grown on plastic dishes or glass coverslips were washed with PBS once and buffer was aspirated completely. Dishes were transferred to ice and HMK/Tx was added instantaneously. Cells were collected using a cell scraper. Confluent 10 cm dishes were harvested in a total volume of 300 to 600 µl HMK/Tx lysis buffer. To ensure complete lysis, samples were incubated for 30 min on a rotating wheel in the cold room. Clarification of lysates was achieved by centrifugation for 15 min at 17 000 g and 4 °C in a tabletop cooling centrifuge. In case only expression levels were to be analyzed, sample buffer was added to the lysates and they were stored at -20 °C or -80 °C (for phospho-samples). For interaction studies, lysates were cleared further by ultracentrifugation for 20 min at 180 000 g and 4 °C in a TLA-110 rotor.

2.6.4 Protein quantification using Bradford assay

To measure the protein concentration of cell lysates, tissue extracts and purified protein solutions, samples were diluted 1:500 to 1:10 000 in 1 000 µl of 1 x Bradford reagent. The mixture was incubated for 5 min at room temperature and OD_{595} was measured with a photometer. As blank sample, 1 x Bradford reagent with lysis buffer/PBS was used. Extinction values between 0.1 and 0.6 were accepted as reliable. Protein concentration was calculated from a BSA standard curve, covering the range of 1 µg to 10 µg.

2.6.5 Expression of GST-fusion proteins in *E. coli*

A starter culture of 50 ml LB medium containing 50 µg/ml ampicillin was inoculated with a small amount of *E. coli* bacteria from the respective cryostock. For protein expression the strain BL-21 was used. Bacteria were allowed to grow shaking at 37 °C overnight. The next day 500 ml 2 x YT protein expression medium, freshly supplemented with 50 µg/ml ampicillin, were inoculated with 20 - 40 ml overnight culture and bacteria were grown at 37 °C shaking at 180 rpm. When optical density (OD_{600}) had reached 0.7 - 0.8, the medium was cooled to 30 °C and protein expression was induced with 0.5 mM isopropyl thiogalactoside (IPTG). After 4 h of

expression at 30 °C and 180 rpm bacteria were harvested by centrifugation at 4 000 g for 15 min and resuspended in ice-cold PBS. Aliquots of the bacterial suspension (5 % - 50 %, depending on the expression yield) were stored at -20 °C for later use.

2.6.6 Affinity-purification of GST-fusion proteins

Bacterial pellets were thawed in a room temperature water bath and 1 mM PMSF, 125 units of benzonase (a DNase/RNase) and a tip-of-a-spatula lysozyme (Roth, 8259) were added. After 15 min on ice, bacterial cells were sonicated for 1 min (1 min at 30 % power, Branson digital sonifier) at 4 °C. Triton X-100 was added to a final concentration of 1 % (v/v) and lysis was allowed for 15 min on ice. Cell debris was removed by centrifugation for 15 min at 35 000 g. Afterwards, the supernatant was added to 0.25 ml (1:2 slurry) of PBS-washed GST-bind-resin (Novagen) and incubated for 1 - 2 h at 4 °C on a rotating wheel. The beads were washed 3 times with ice-cold PBS and resuspended in 1 ml PBS after last wash. The concentration of the purified GST-fusion proteins was determined using the Bradford method and by Coomassie staining.

2.6.7 GST pulldown assay

GST-pull down experiments were performed to study protein-protein interactions. 100 µg of purified GST-fusion proteins were incubated with cell or brain extract, precleared by ultracentrifugation, for 2 - 4 h at 4 °C on a rotating wheel. Unbound proteins were removed by washing the beads three times with ice-cold HMK/Tx. The fourth and final wash step was done without Triton X-100 and supernatant buffer was removed completely with a Hamilton Syringe. Elution of bound proteins was achieved by adding 40 µl of 1 x sample buffer and boiling for 5 min at 95 °C. After a brief centrifugation in a tabletop centrifuge, the supernatant was transferred to a new tube and proteins were analyzed by SDS-PAGE and immunoblotting. For detection of Dab1 in pulldowns from brain extract, bound proteins were first eluted with 500 mM NaCl and 0.5 % SDS for 30 min at room temperature. Eluate was diluted 1:10 in 20 mM HEPES pH 7.4 before Dab1 was immunoprecipitated according to the standard immunoprecipitation protocol (Chapter 2.6.9).

2.6.8 Surface biotinylation of hippocampal cultures

To investigate surface levels of plasma membrane proteins in hippocampal neurons, a surface biotinylation assay was carried out. Cells were washed twice with ice-cold PBS^{2+} and then incubated with EZ-Link Sulfo-NHS-SS-Biotin solution (0.5 mg/ml in PBS^{2+}, Thermo Fisher Scientific, 21331) for 15 min at 4 °C. Residual biotin was quenched by two washes with glycine (50 mM in PBS^{2+}) for 5 min each at 4 °C. After two washes with PBS^{2+}, cells were harvested and lysed with HMK/Tx for 30 min on rotating wheel at 4 °C. Lysates were centrifuged at 17 000 g for 15 min at 4 °C before supernatants were applied to 100 µl of pre-equilibrated streptavidin beads. The mixture was incubated for 2 h on rotating wheel at 4 °C before beads washed four times with HMK/Tx and once with lysis buffer without Triton X-100. After removing residual buffer completely, 40 µl of 1 x sample buffer were added and samples were boiled for 5 min at 95 °C. Beads were spun down by brief centrifugation and supernatants, containing the cell surface proteins, were transferred to new tubes. Proteins were separated by SDS-PAGE and detected by immunoblotting.

2.6.9 Immunoprecipitation

Co-immunoprecipitation experiments were either carried out with lysates from HEK 293 cells overexpressing the proteins of interest or from mouse brain extract. 40 µl of protein A/G PLUS Agarose beads (Santa Cruz Biotechnology) were pre-equilibrated with HMK/Tx and incubated with 1 - 10 µg of the precipitating antibody in 500 µl HMK/Tx. The mixture was incubated on a rotating wheel for 1 h at room temperature to allow coupling of antibodies to the agarose beads. Unbound antibodies were removed by washing twice with HMK/Tx and antibody-coupled beads were incubated with ultracentrifuged cell or brain extract for 2 - 4 h at 4 °C on a rotating wheel. Then, the beads were washed three times with HMK/Tx and once with HMK buffer (without Triton X-100). Residual buffer was completely removed with a Hamilton syringe and 40 µl of 1 x sample buffer, supplemented freshly with 10 % β-mercaptoethanol to break the disulfide bonds of the antibody molecules were added. After boiling for 5 min at 95 °C, the samples were centrifuged briefly in a tabletop centrifuge and the supernatant, containing the eluted proteins, was

transferred into a new tube. Proteins were detected by SDS-PAGE, followed by immunoblotting.

2.6.10 SDS polyacrylamide gel electrophoresis (SDS-PAGE)

To separate proteins based on their molecular mass sodium dodecyl sulfate (SDS) polyacrylamide gel electrophoresis (PAGE) was performed. SDS-PAGEs were carried out using Tris-glycine based buffers with a 3 % stacking and 4 % to 14 % separating gel (Table 2.12). A constant current of 10 - 20 mA was applied per gel. After electrophoresis, gels were either processed for immunoblotting or proteins were visualized by Coomassie staining.

Table 2.14 SDS polyacrylamide gels

	Separation:					**Stacking:**
	14 %	12 %	10 %	7 %	4 %	3 %
MilliQ H2O	2.0 ml	2.5 ml	3.0 ml	3.75 ml	4.5 ml	1.25 ml
4 x buffer	1.875 ml	1.875 ml	1.875 ml	1.875 ml	1.875 ml	0.625 ml
30% AA/BA mix	3.5 ml	3.0 ml	2.5 ml	1.75 ml	1.0 ml	0.33 ml
TEMED	7.5 µl	7.5 µl	7.5 µl	7.5 µl	7.5 µl	3.75 µl
10 % (w/v) APS	75 µl	75 µl	75 µl	75 µl	75 µl	37.5 µl

2.6.11 Immunoblotting

Immunoblotting (or Western Blotting) was used to detect specific proteins after separation by SDS-PAGE. Proteins were transferred using a semi-dry method (Biometra FastBlot B44) onto a nitrocellulose membrane (GE Healthcare, Amersham Protran 0.2 NC). Blotting papers (Rotilabo, Roth) were soaked in blotting buffer and placed on the blotting apparatus, followed by the rinsed membrane. The polyacrylamide gel, also rinsed in blotting buffer, was placed on top. Finally, another pre-wetted blotting paper was put on the stack. Air bubbles were removed thoroughly during the stacking procedure. Proteins were transferred with 60 mA/gel for 3 h. Then, membranes were washed twice with MilliQ H_2O and transferred proteins were stained with Ponceau stain for 5 min. Background staining was removed by washing in Ponceau destain. Membranes were cut according to the size of

the proteins to be detected. Ponceau S was washed out completely by rinsing several times in TBS. Membranes were blocked with blocking solution for 1 h. After washing the membrane with TBS three times, primary antibodies in antibody dilution solution were applied for 2 h at room temperature or, preferably, overnight at 4 °C. The membrane was washed four times for 5 min in TBS before secondary antibodies, specifically recognizing antibodies of the primary antibody species, were applied 1 h at room temperature. Secondary antibodies were used in a 1:5 000 dilution in blocking solution. When weak signals were expected, HRP (horseradish peroxidase)-conjugated secondary antibodies and ECL Substrate (LI-COR, P/N 926-80100) were used. Chemiluminescence was detected with the Biorad ChemiDoc MP Imaging system. Stronger signals were detected quantitatively with IRDye 800CW-conjugated secondary antibodies and LI-COR Odyssey Fc Imaging system.

2.6.12 Coomassie staining

Polyacrylamide gels were immersed in Coomassie stain and heated to about 60 °C in a microwave. The gel was stained for 15 min. Background staining was removed by washing with Coomassie destain, again heated to about 60 °C. The destaining procedure was repeated twice.

2.6.13 Cdc42 activity assay (G-LISA)

Quantification of active Cdc42 the G-LISA Activation Assay from Cytoskeleton was performed according to the manual. Briefly, lysates were thawed in a room temperature water bath, chilled on ice and added to the G-LISA plate. Lysis buffer and GTPase-deficient Cdc42 served as negative and positive control, respectively. Incubation took place on a cold orbital microplate shaker (300 rpm) at 4 °C for exactly 15 min. The wells were washed twice and pre-equilibrated with antigen presentation buffer before another three washes. Anti-Cdc42 antibody was added to each well and the plate was incubated on the orbital shaker (300 rpm) at room temperature for 30 min. The plate was washed three times and incubated with HRP-conjugated secondary antibody shaking at room temperature for 30 min. After three washes, HRP detection reagent was added and incubated for 15 min at 37 °C.

Reaction was stopped by addition of stop buffer and the absorbance at 485 nm was measured immediately.

2.7 Histological Methods

2.7.1 Perfusion of mice

Mice were narcotized by intraperitoneal injection of a Ketamin/Xylazin mixture (1.2 % Ketamin, 0.16 % Xylazin in PBS). Per 10 g of body weight, 100 µl of anesthetic solution were applied. Anesthetized mice were fixed on a styropor board and abdominal fur was removed. Skin and abdominal wall were incised beneath the rib cage before the diaphragm was cut along the entire length of the rib cage. Afterwards, the rib cage was cut up to the collarbone and removed. The left ventricle was penetrated with a 15-gauge blunt-tipped perfusion needle connected to a PeriStarPRO pump (WPI). The needle and the attached tube were fixed and the superior vena cava was cut to create an outlet. Mice were perfused at a constant speed of 1.0 ml/min, first with ice-cold PBS + heparin for about 15 min, then with ice-cold fixation solution for about 10 min. The perfused animal was disconnected from the apparatus, the brain was isolated from the skull and incubated in fixation solution overnight at 4 °C. The next day, brains were transferred to brain storage solution.

2.7.2 Cryosectioning of brains

Brains were glued to the platform of a Microm HM 430 (Thermo Scientific) using Tissu-Tek (VWR, 25608-930). Temperature was lowered to -40 °C to freeze the brain completely. Horizontal or sagittal sections with a thickness of 40 µm were cut with a sliding blade. Per brain, 6 series of sections were collected in cryotubes containing brain storage solution. Sections were stored at -80 °C.

2.7.3 Nissl staining

One series of sections (i.e. every sixth slice of a brain) was thawed and mounted on SuperFrost Plus slides (Thermo Scientific, 10143352) in gelatin solution at 41 °C. Sections were allowed to dry overnight. Then, sections were immersed briefly in water, followed by Cresyl violet (0.1 % w/v Cresyl violet in MilliQ H_2O) staining for 10 min in the dark. Afterwards slices were dehydrated by incubation in solutions with increasing ethanol concentrations (50 %, 70 %, 80 %, 90 % v/v) for 2 min each.

Sections were destained with 96 % (v/v) ethanol with 0.5 % (v/v) acetic acid for 30 s, followed by two incubations in pure ethanol for 2 min each. Sections were transferred to Xylene and finally coverslips were mounted onto the slides with Entellan (Millipore, 107961).

2.7.4 Estimation of DG volume

For DG volume determination, every sixth section was stained with the Nissl method. Images from all sections containing DG were recorded, the DG was outlined and the area was measured using ImageJ software. Volume was estimated using the formula $\sum A \times h \times n$, with $\sum A$ being the sum of the area measured on each section, h being the section thickness (40 µm) and n being the section interval (6).

2.7.5 Golgi staining

Golgi impregnation of brains was performed with the FD Rapid GolgiStainKit by FD NeuroTechnologies according to the manual. Briefly, animals were perfused with PBS containing heparin followed by brief perfusion with fixation solution for less than 5 min. The tissue was immersed into impregnation solution (1:1 mixture of Solution A and B, prepared at least 24 h prior to perfusion). The next days, impregnation solution was replaced with fresh solution and the brains were incubated for 2 - 3 weeks in the dark. Then, tissue was transferred into solution C and stored at 4 °C in the dark at least for 2 - 7 days. Solution C was renewed after 24 h. For sectioning, a Leica VT1000M vibratome was used and brains were cut into 200 µm thick slices while immersed in solution C. Slices were transferred directly onto SuperFrost Plus slides, coated before with 0.5 % (w/v) gelatin, and allowed to dry at room temperature. For staining, slides were rinsed with MilliQ H_2O twice for 2 min each before sections were placed in a 1:1:2 mixture of solutions D:E:MilliQ H_2O for 10 min. After 2 washing steps in MilliQ H_2O for 4 min each, tissue was dehydrogenated by immersion in ethanol solutions with increasing ethanol content (50 %, 75 %, 95 % and 4 x 100 %) for 4 min each. Sections were cleared in xylene 3 times, 4 min each, and coverslips were mounted onto the sections with Entellan.

2.7.6 Immunohistochemical staining

Sections were thawed and collected in phosphate buffer (125 mM). Only sections containing a complete cross section of the hippocampus were used. All washing and incubation steps took place on a standard 1000 orbital shaker (VWR) at 100 rpm. Samples were washed three times in phosphate buffer for 15 - 20 min each and afterwards permeabilized with phosphate buffer, freshly supplemented with 0.3 % Triton X-100. Permeabilization was carried out for 2 - 3 h, during which the buffer was exchanged every 20 min. For blocking, 5 % serum (goat and/or donkey, depending of the origin species of the secondary antibodies) in phosphate buffer with 0.3 % Triton X-100 was applied for 1 h. Primary antibodies were diluted in phosphate buffer with 0.3 % Triton X-100 and incubated together with the sections for 2 - 3 days in the cold room. Then, sections were washed for 3 h in phosphate buffer with 0.3 % Triton X-100, changing the solution every 15 min. Secondary antibodies were incubated either at 4 °C overnight or 2 h at room temperature. After three washes in phosphate buffer, sections were mounted with 41 °C warm gelatin solution (0.2 % porcine skin gelatin in 50 mM TrisHCl pH 7.4) onto microscope slides. After drying for 10 min at 41 °C, coverslips were mounted on top with Immu-Mount. Stained brain slices were analyzed with Zeiss laser scanning confocal microscopes LSM710 or LSM780.

2.7.7 BrdU labelling of dividing cells *in vivo*

To quantify the number of dividing cells in adult brains, mice at the age of 2 months were injected intraperitoneally with a 10 mg/ml solution of BrdU in PBS (50 µg/g body weight). Injection was repeated twice with a two-hour interval. Mice were perfused two hours after the last injection. Brains were cut and stored according to the standard protocol. For the immunohistochemical staining of BrdU, the staining protocol was complemented with the following steps: after the initial washing in phosphate buffer, slices were incubated in 2 N HCl at 37 °C for 45 min to denature DNA. Slices were washed twice with 0.1 m borate buffer (pH 8.5) and twice with phosphate buffer for 15 min each to neutralize the acidic pH. Then, the standard staining procedure continued with permeabilization of the slices.

2.7.8 Quantification of Nestin-positive processes and Dcx-positive cells

The DG area of immunostained brain sections was imaged with a 10 x objective and a laser scanning confocal microscope. Images were recorded as stacks with a distance of 0.3 µm to cover the whole slice in the z dimension. Stacks were projected onto one image and the region of interest was outlined manually. Nestin-positive processes and Dcx-positive cell bodies were quantified using the ImageJ particle analysis tool.

3. Results

3.1. ITSN1 KO mice show hippocampus-specific deficits

3.1.1 Absence of ITSN1 in mice has no overt effect on viability, health or behavior

To study the role of intersectin1 (ITSN1) in brain development and physiology we made use of the ITSN1 knockout (KO) mouse, created in the lab of Melanie Pritchard (Yu et al., 2008). These mice are macroscopically indistinguishable from their wildtype (WT) littermates (Fig. 3.1a) and mice heterozygous for the mutant allele produced offspring at the expected Mendelian ratio, i.e. ~25% KO animals (Fig. 3.1b). The ITSN1 KO animals were of similar size as their WT siblings and displayed similar weight gain (Fig. 3.1c).

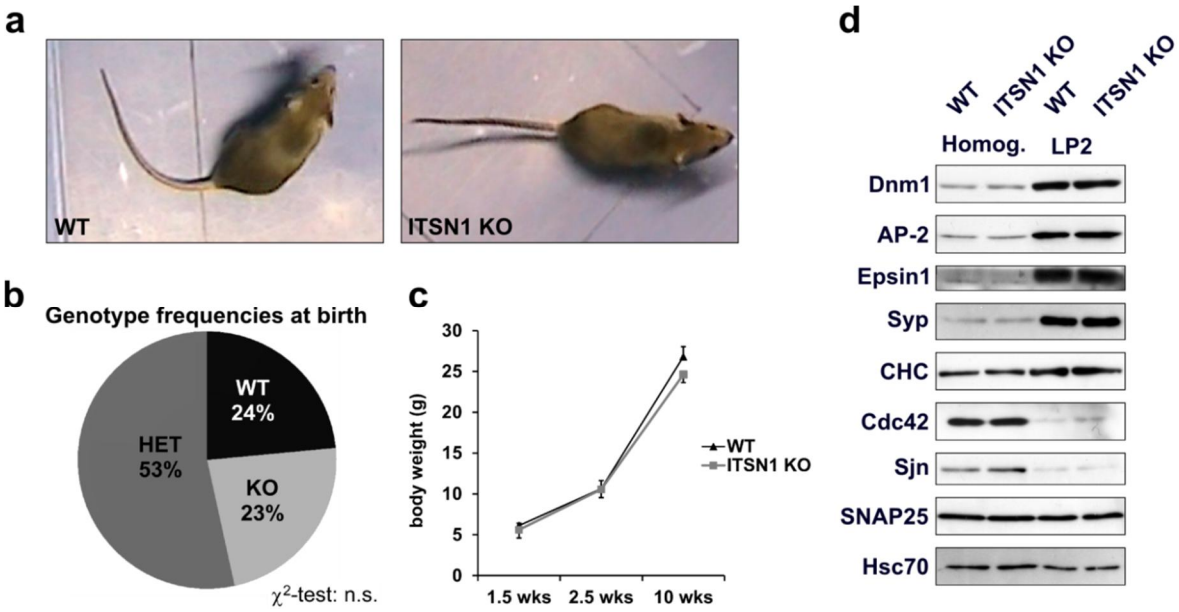

Figure 3.1 Mendelian inheritance and unchanged body weight of ITSN1 KO mice. (a) Example images of a WT mouse and its ITSN1 KO littermate. **(b)** Heterozygous mating produced offspring at Mendelian frequencies (number of animals: WT: 55, KO: 54, Heterozygotes (HET): 125; chi-square test: not significant). **(c)** Body weight of female mice (WT and ITSN1 KO littermates) was measured at 1.5, 2.5 and 10 weeks. No significant difference was detected (mean +/- SEM; $p > 0.05$; two-tailed t-test for unpaired samples). **(d)** Brain homogenates and crude synaptic vesicles (LP2) from WT and ITSN1 KO brains were analyzed for level changes of various ITSN1 interactors. None of the proteins checked

showed an altered pattern in ITSN1 KO brain tissue. Dnm1: Dynamin1; AP-2: adaptor protein complex 2; Syp: Synaptophysin; CHC: clathrin heavy chain; Sjn: Synaptojanin; SNAP25: Synaptosomal-associated protein 25 kDa; Hsc70: heat shock cognate 70 kDa.

ITSN1 has been implicated in vesicular trafficking, especially SV exo-/endocytosis (Pechstein et al., 2010b). Therefore, we investigated whether genetic ablation of ITSN1 affects either the total levels or the subcellular distribution of proteins involved in SV cycling. To that end, protein levels in brain homogenate and the crude synaptic vesicle fraction (LP2) from WT and ITSN1 KO mice were analyzed. The list of examined proteins entailed endocytic players like AP-2 or Dynamin1, but also the exocytic protein SNAP25 or the actin-regulating small G-protein Cdc42. Of the proteins analyzed, none showed a significant change, neither in whole brain homogenates nor in the crude synaptic vesicle fraction (Fig. 3.1d). This implies that these proteins do not rely on ITSN1 to be stably expressed although most of them have been shown to bind ITSN1.

We wanted to investigate the effect of ITSN1-deficiency on general activity and exploratory behavior. WT and ITSN1 KO mice were placed into a novel environment, a rectangular box with an outlined central rectangle. The walking time and the time in the center were measured along with the number of line crossings and rearing attempts at the wall. No significant differences between WT and ITSN1 KO mice were observed (Fig. 3.2a). ITSN1-deficient mice showed only a mild tendency towards more active behavior, indicated by a slightly increased walking time and a higher number of line crossings. To further analyze exploratory and anxiety-related behavior, mice were confronted with a novel object. Time at the object, latency to the first approach, as well as the total number of approaches were measured. Again, ITSN1 KO mice did not show substantial changes in behavior compared to control animals (Fig. 3.2b). Animals lacking ITSN1 were slightly more explorative, as seen in a tendency towards more approaches, but this effect was statistically not significant.

In sum, we concluded that a lack of ITSN1 expression in mice has no major effect on viability, health or behavior.

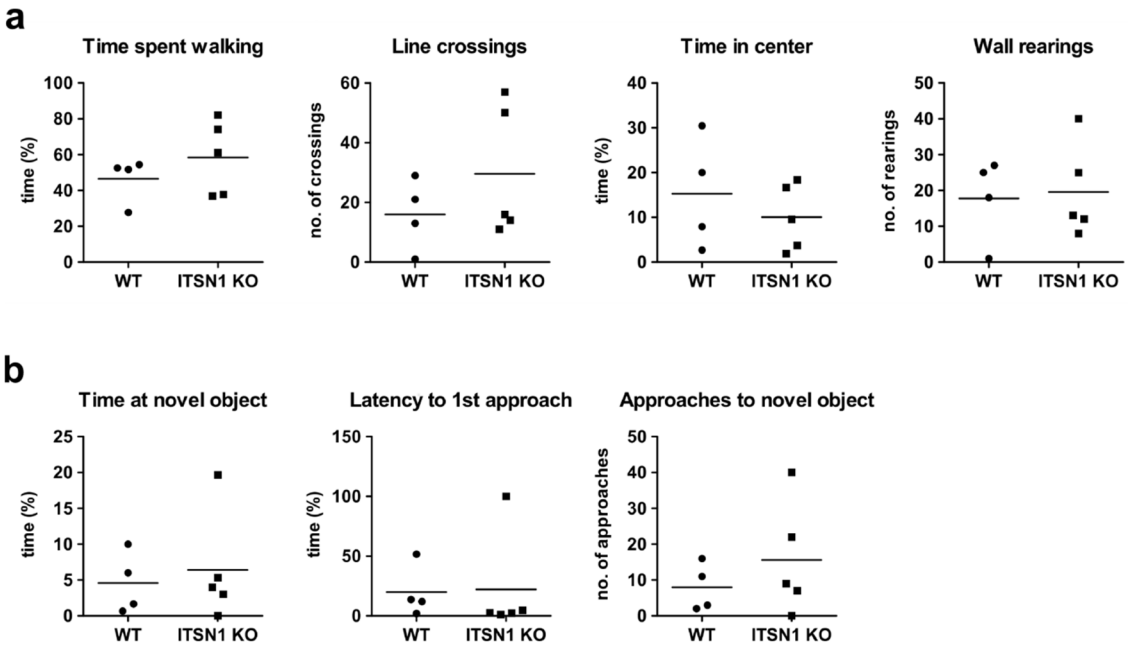

Figure 3.2 No obvious changes in behavior of ITSN1 KO mice. (a) Absence of ITSN1 has no major effect on activity during open field exploration. During an 8 min period, the walking time and the time spent in the center were measured and the number of line crossings and wall rearing attempts were counted. **(b)** No significant difference was noted between WT and ITSN1 KO mice in a novel object assay. Mouse behavior towards a novel object was recorded for 5 min. The time at the object, the latency to the first approach and the total number of approaches were measured. Circles/squares represent single animals and the horizontal line indicates the mean; N = 4 for WT and 5 for ITSN1 KO; $p > 0.05$; two-tailed t-test for unpaired samples.

3.1.2 Neuronal migration deficits in hippocampi of ITSN1 KO mice

To find out if ITSN1 plays a role in brain development and morphology, we examined Nissl-stained brain sections of adult (2 months old) ITSN1 KO mice and WT control animals. While overall brain size and morphology appeared normal, there were obvious morphological changes in the hippocampi of ITSN1 KO mice (Fig. 3.3). First, the dentate gyrus (DG) was altered in shape, showing a more rectangular, rather than triangular form when compared to the corresponding region in control littermates. This phenotype became more overt in horizontal than in coronal or sagittal sections. Such a shape is most likely the consequence of disturbed guidance of progenitor cells during perinatal development of the DG (Altman and Bayer, 1990a). Misdirected migration of DG progenitors from the secondary dentate matrix could ultimately results in a deformed DG. A second alteration in ITSN1-deficient hippocampi pertains to the pyramidal cell layer in cornu ammonis (CA) regions. There, the pyramidal cells were less densely packed than in the WT hippocampi. This

dispersion was most obvious in the CA3 but also extended to the CA1 region. Depending on the expressivity of the phenotype, the pyramidal cell layer was even split into two distinct layers. This shows that not only the granular neurons in the DG but also the pyramidal neurons in the CA region do not migrate properly in the absence of ITSN1. Therefore, ITSN1 has a so far undescribed role in neuronal migration during hippocampal development.

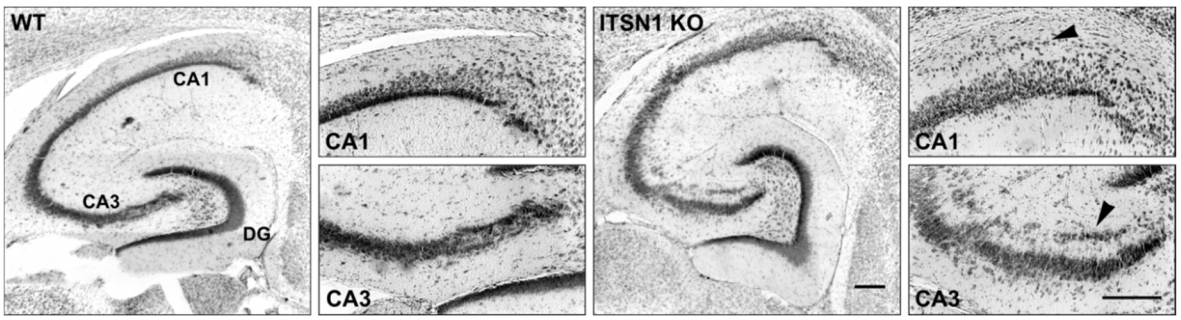

Figure 3.3 Hippocampal lamination defects in ITSN1 KO mice. Nissl-stained horizontal sections of hippocampi from WT and ITSN1 KO mice reveal morphological changes in the absence of ITSN1. The shape of the dentate gyrus (DG) is changed and the pyramidal cell layers in CA1 and CA3 are dispersed. Arrowheads indicate the separation of pyramidal cells into two distinct layers, both in CA1 and CA3. Scale bars: 200 µm.

3.1.3 Alterations in adult hippocampal neurogenesis in ITSN1 KO mice

The altered positioning of hippocampal cells in ITSN1 KO mice indicates that ITSN1 acts during embryonic and early postnatal development of the hippocampus. The dentate gyrus is one of the few regions where neurogenesis and migration of immature neurons persists into adulthood (Altman and Das, 1965; Kaplan and Hinds, 1977; Cameron et al., 1993). As many signaling pathways controlling early hippocampal development also regulate adult neurogenesis (Faigle and Song, 2013), we asked whether ITSN1 also has a function in this process. Radial glial cells residing in the subgranular zone (SGZ) of the DG possess one long radial process spanning the granular cell layer (GCL). These cells act as a scaffold for migration of newborn neurons but also exhibit properties of neural stem cells (Palmer et al., 1997). Radial glial cells express certain marker proteins like Nestin or GFAP. Strikingly, when we compared Nestin-positive processes in the GCL from ITSN1 KO brains with WT controls, we found that these processes were severely disorganized (Fig. 3.4a) and

their number was reduced by around 50% (Fig. 3.4b). Therefore, ITSN1 plays an important role for the establishment or maintenance of the radial glial scaffold in the adult DG.

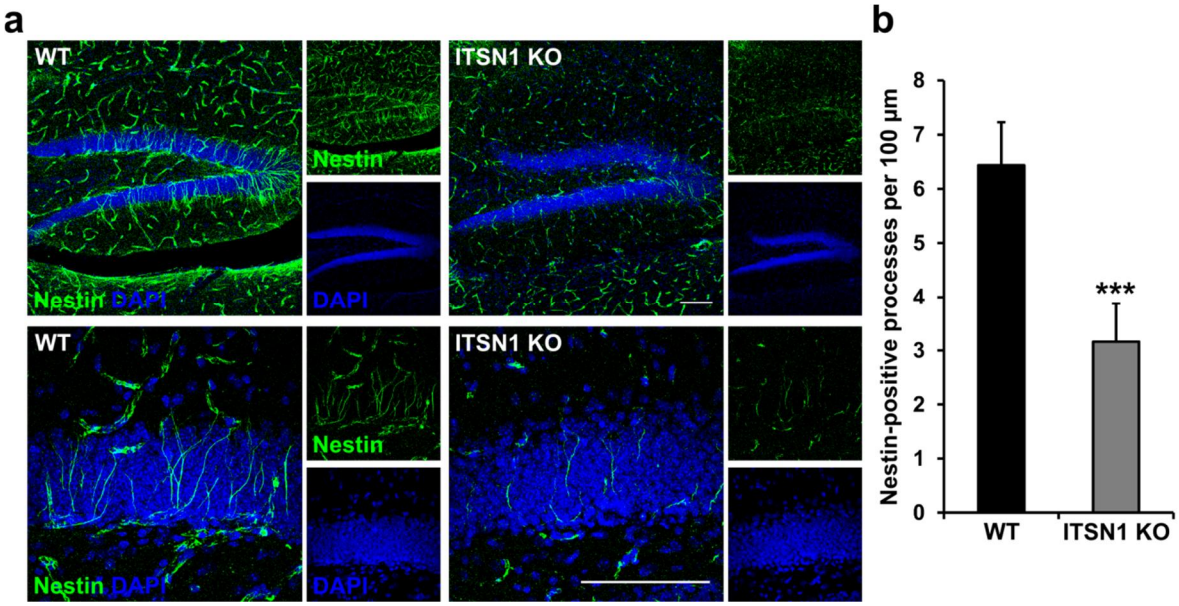

Figure 3.4 Disorganized radial glial cell scaffold in the dentate gyrus of ITSN1 KO mice. **(a)** Immunohistochemical staining for the radial glial cell marker Nestin in sagittal sections of WT and ITSN1 KO. Scale bars: 100 µm. **(b)** Quantification of Nestin-positive processes in the DG shows that the number of radial glial cell processes in ITSN1 KO brains is reduced to less than 50 % of the WT level (mean + SEM; N = 8 littermate couples; ***p < 0.001; two-tailed t-test for paired samples).

Radial glial cells can give rise to Doublecortin (Dcx)-positive precursors during differentiation into mature granular cells. Therefore, we analyzed if Dcx-positive cells were also affected in ITSN1 KO mice. Interestingly, we found an accumulation of Dcx-positive precursors in the hilar region of ITSN1 KO mice (Fig. 3.5). In WT control animals, Dcx-positive cells were found almost exclusively in the SGZ and the GCL. This suggests that in the absence of ITSN1 generation of new neurons is not as restricted to the SGZ as in WT mice. Instead, Dcx-positive progenitors/neuroblasts are generated for several weeks after birth in the hilus of ITSN1 KO mice. This suggests that the hilus retains the neurogenic properties of the tertiary dentate matrix in ITSN1 KO animals. Taken together with the altered radial glia scaffold, this suggests an essential function of ITSN1 for the development of the neurogenic niche in the adult hippocampus.

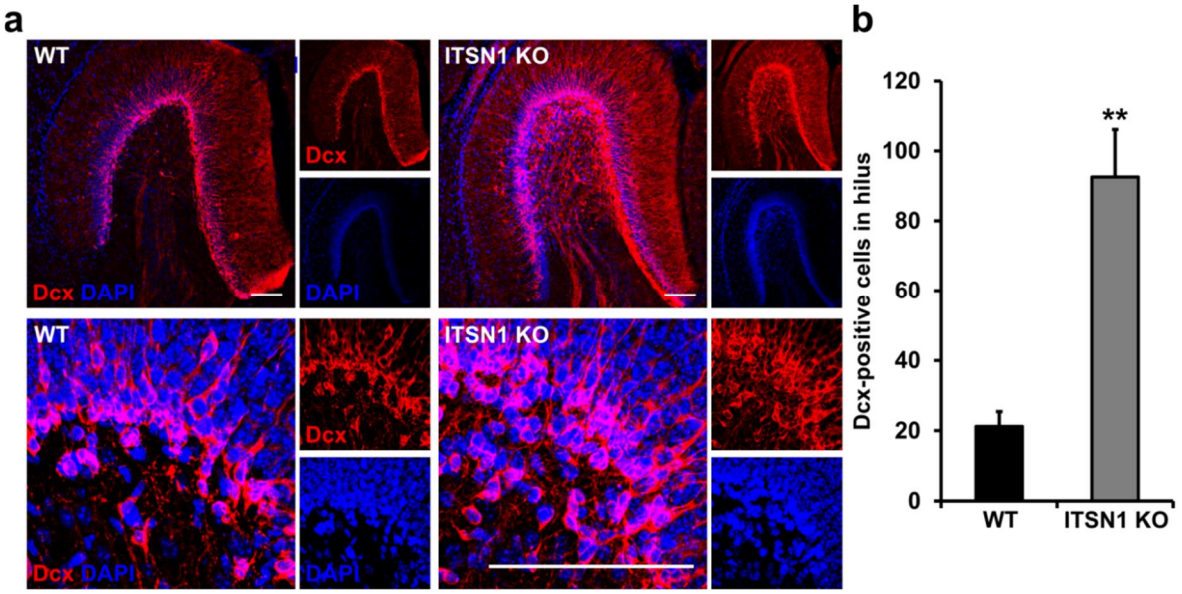

Figure 3.5 Accumulation of Dcx-positive cells in the hippocampal hilus region of ITSN1 KO mice. **(a)** Immunohistochemical staining for Dcx in sagittal sections of WT and ITSN1 KO brains. The number of Dcx-positive cells ectopically localized in the hilar region is elevated in ITSN1 KO brains. Scale bars: 100 µm. **(b)** Quantification shows a striking increase of Dcx-positive cells in the hilus of ITSN1 KO brains. (mean + SEM; N = 4 littermate couples; **p < 0.01; two-tailed t-test for paired samples).

Neurogenesis in the adult brain relies on the distinct organization of the neurogenic zone (Balu and Lucki, 2009). Therefore, we wanted to test if the disrupted radial glial scaffold and the ectopic accumulation of Dcx-positive cells in ITSN1 KO mice affects the generation of mature neurons and ultimately leads to a smaller DG. Immunofluorescence (IF) staining for Calbindin, a marker for mature granular neurons in the DG, gave no indication of a reduced granular cell number in ITSN1 KO mice (Fig. 3.6a). Furthermore, ITSN1 deficiency had no effect on the volume of the DG, based on stereological analysis of Nissl-stained brain sections (Fig. 3.6b). These findings imply that the disturbed organization of radial glial and neuronal progenitor cells does not translate into a smaller number of mature neurons. As a result, absence of ITSN1 affects the shape but not the size of the DG.

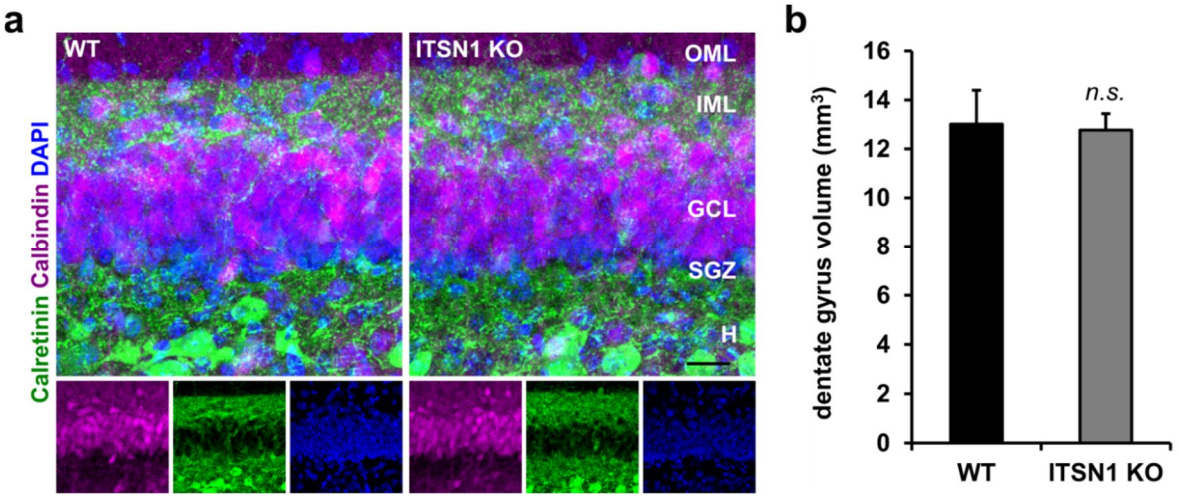

Figure 3.6 Granular cell number and dentate gyrus size are unchanged in ITSN1 KO mice. **(a)** Immunohistochemical staining for Calbindin and Calretinin in the DG of WT and ITSN1 KO brains shows no obvious reduction of Calbindin-positive mature granular neurons. Scale bar: 20 µm. OML/IML: outer/inner molecular layer; GCL: granular cell layer; SGZ: subgranular zone; H: hilus. **(b)** The volume of the DG was estimated by stereological analysis (Cavalieri method) of Nissl-stained brain sections. The DG volume in ITSN1 KO brains was similar to WT controls (mean + SEM; N = 5 littermate couples; $p > 0.05$; two-tailed t-test for paired samples).

We wanted to investigate how proliferation in the DG is affected by the described perturbations of the neurogenic zone. To that end, we injected the nucleotide analogue BrdU into 2 months old mice and sacrificed them the same day. BrdU gets incorporated into the DNA of dividing cells and can be detected with IF. This allows the quantification of dividing cells at a certain time point (Ming and Song, 2005). Colabeling with other markers (e.g. Dcx) provides insight into the proliferation of the respective cell population (Fig. 3.7a). Interestingly, the number of BrdU-positive cells was significantly increased in the DG of ITSN1 KO mice. The same held true for Dcx-/BrdU-positive cells which were also more numerous in mutant brains (Fig. 3.7b). This suggests that the disruption of the radial glial scaffold is balanced by increased proliferation during differentiation. Ultimately, this results in a normal number of mature neurons and, therefore, a regularly sized DG. Interestingly, in ITSN1 KO brains BrdU-positive cells were not as restricted to the SGZ as in WT littermates (Fig. 3.7c). A significantly higher number of dividing cells were found ectopically in the molecular layer (ML) or the hilus of the DG (Fig. 3.7d). This finding suggests that ITSN1 is required for the correct localization of newborn neural cells in the DG. Ectopic localization of newborn cells is most likely the consequence of the disorganized arrangement of radial glial cells in ITSN1 KO mice. In sum, these

findings support the notion of ITSN1 as a regulator of migration and neurogenesis in the hippocampus.

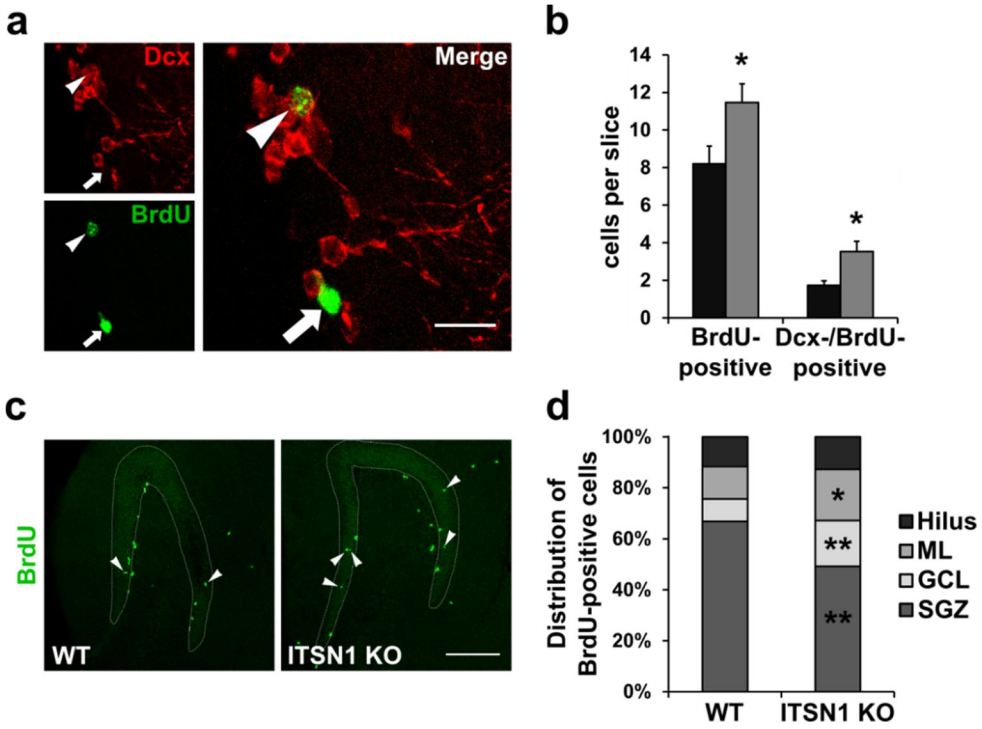

Figure 3.7 Elevated proliferation during hippocampal adult neurogenesis in ITSN1 KO animals. **(a-b)** Increased number of dividing cells in the SGZ of ITSN1 KO mice. **(a)** Brain sections from 2 months old, BrdU-injected mice were stained for BrdU and Dcx. SGZ cells, positive for BrdU only (arrow) or double positive for BrdU and Dcx (arrow head), were counted. Scale bar: 20 µm. **(b)** Both BrdU-positive and Dcx-/BrdU-positive cells were more numerous in hippocampi from ITSN1 KO mice when compared to WT littermates (mean + SEM; N = 5 littermate couples; *p < 0.05; two-tailed t-test for paired samples). **(c-d)** More BrdU-positive cells are ectopically localized in ITSN1 KO mice. **(c)** Brain sections from 2 months old, BrdU-injected mice were stained for BrdU. Arrow heads indicate BrdU-positive cells in the granular layer. Scale bar: 200 µm. **(d)** The relative distribution of BrdU-positive cells shows that in ITSN1 KO mice significantly more dividing cells are located in the molecular layer (ML), the granular cell layer (GCL) and less in the subgranular zone (SGZ). N = 4 littermate couples; **p < 0.01 for cells in GL and SGZ, *p < 0.05 for ML; two-tailed t-test for paired samples.

In order to find out whether the same ITSN1-dependent mechanisms regulating hippocampal neurogenesis can also be investigated *ex vivo*, we turned to organotypic hippocampal slice cultures (OHSCs). These cultures possess many morphological and functional features of the hippocampal network (Gahwiler et al., 1997 and Fig. 3.8a). Furthermore, the culture of these slices easily allows manipulations (e.g. drug treatments) providing an excellent tool to investigate hippocampal biology. Incubation of OHSCs with BrdU for 48 h followed by IF revealed that labeling of

dividing cells can be easily achieved with this method and that many cells are proliferating *ex vivo* (Fig. 3.8b). Additionally, a substantial number of Dcx-/BrdU-positive cells could be detected and this number was elevated in slices from ITSN1 KO mice compared to WT littermates (Fig. 3.8c). This suggests that the same pathways that regulate neurogenesis *in vivo* also operate in OHSCs and that ITSN1 also plays a role for neurogenesis in this model system.

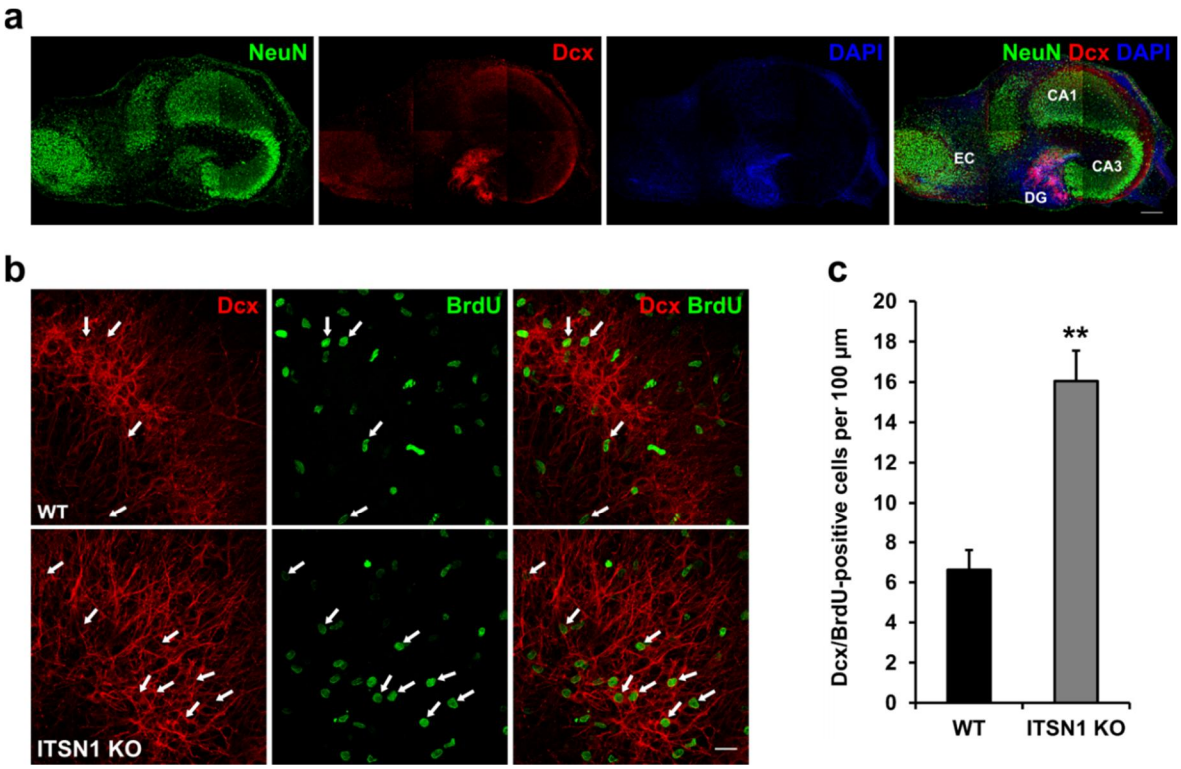

Figure 3.8 Increased proliferation during hippocampal neurogenesis in organotypic hippocampal slice cultures of ITSN1 KO mice. (a) Example images of a hippocampal slice after culture, fixation and immunostaining for the granule cell marker NeuN and the progenitor marker Dcx. Scale bar: 200 µm. EC: entorhinal cortex. **(b-c)** The number of dividing progenitors is elevated in slice cultures from ITSN1 KO mice. **(b)** BrdU application to the culture medium results in labeling of dividing cells. Slices were stained for Dcx and BrdU. Dcx-/BrdU-positive cells (arrows) were counted in slices from WT and ITSN1 KO mice. Scale bar: 20 µm. **(c)** The number of Dcx-/BrdU-positive cells is strongly increased in cultured slices from ITSN1 KO mice when compared to WT slices (mean + SEM; N = 4 littermate couples; **p < 0.01; two-tailed t-test for paired samples).

The DG is not the only area where neurogenesis occurs in the adult brain. Another region is the subventricular zone (SVZ). Neuronal precursors generated here migrate along the rostral migratory stream (RMS) to the olfactory bulb (OB) where they finally differentiate into GABAergic interneurons (Luskin, 1993; Lois and Alvarez-Buylla, 1994). To elucidate if the absence of ITSN1 leads to similar effects on

neurogenesis in the SVZ-RMS-OB as in the hippocampus, brain sections were stained for Nestin as stem cell marker and Dcx as a marker for migrating neurons. No evidence for a reduction of stem cells or migrating neurons in brains from ITSN1 KO mice could be found. Furthermore, the morphology of both cell populations appeared unaffected in the absence of ITSN1 (Fig. 3.9). This could indicate that the pathway regulated by ITSN1 is solely important for neurogenesis in the DG but not in the SVZ-RMS. An alternative explanation would be that the function of ITSN1 in the DG can be fulfilled by another protein in the SVZ-RMS.

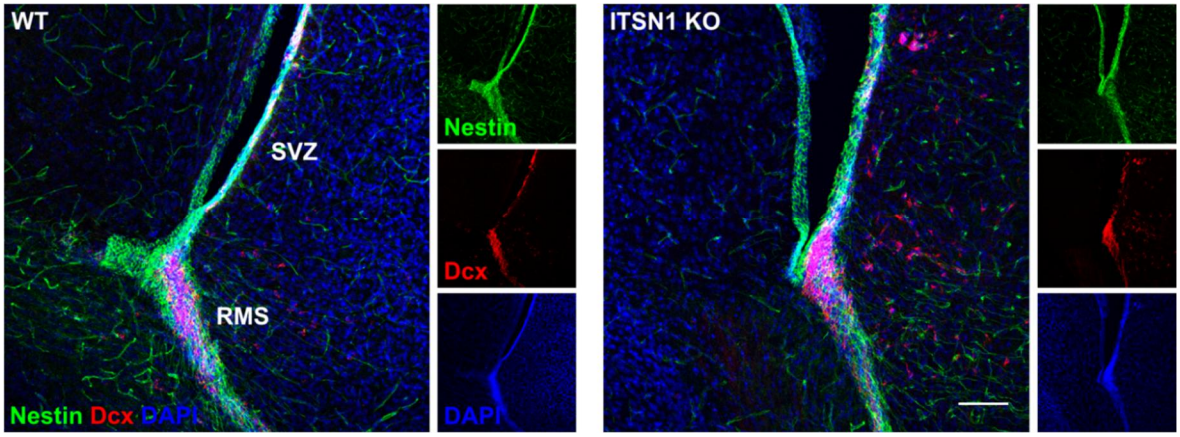

Figure 3.9 Absence of ITSN1 does not affect migration along the rostral-migratory stream to the olfactory bulb. Immunohistochemical staining for Nestin and Dcx shows that ITSN1 deficiency has no effect of on numbers or morphology of stem or progenitor cell in the SVZ-RMS system. Scale bar: 100 µm.

3.2 ITSN1 is part of the Reelin signaling pathway

3.2.1 EphrinB/EphB endocytosis and signaling are unaltered in ITSN1 KO mice

It has been shown that ITSN1 can bind to EphB2 and that this interaction activates the ITSN1 GEF activity towards Cdc42 (Irie and Yamaguchi, 2002; Nishimura et al., 2006). As EphB2 and other Eph receptors have been implicated in hippocampal development and adult neurogenesis we investigated if defects in EphB signaling might be the underlying cause of the hippocampal phenotype in ITSN1 KO mice. Surprisingly, we could not detect binding between ITSN1 and EphB2, neither by immunoprecipitation with an ITSN1-specific antibody from brain extract (Fig. 3.10a) nor by GST-pulldown with different ITSN1 domains (Fig. 3.10b). AP-2 and the EphB2-interacting protein Numb were bound efficiently by ITSN1.

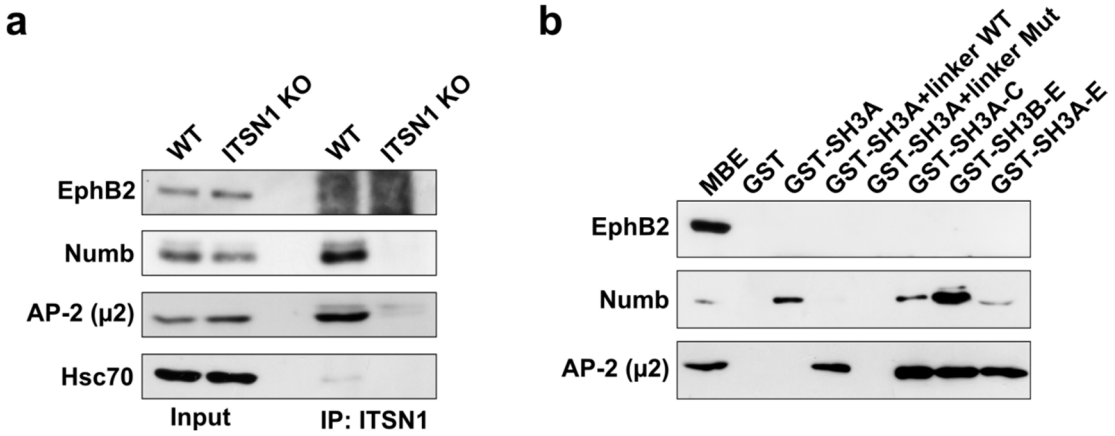

Figure 3.10 ITSN1 does not bind to EphB2. (a) ITSN1 was immunoprecipitated from WT mouse brain extract using the polyclonal antibody 1-440. Extract from an ITSN1 KO littermate served as specificity control. The association of ITSN1 with the endocytic proteins Numb and AP-2 used as a positive control was readily detected. A complex of ITSN1 and EphB2 could not be observed. **(b)** GST-pulldown from MBE with different domains of ITSN1. ITSN1 SH3 domains were found to associate with control proteins (Numb and AP2). No interaction between ITSN1 SH3 domains and EphB2 was detected.

To find out if ITSN1 is required for endocytosis of EphB receptors, the extracellular region of ephrinB1 and B2, fused to the human Fc region, were clustered with an anti-Fc antibody and added onto hippocampal neurons from WT and ITSN1 KO mice. Comparison between WT and ITSN1 KO cells showed no significant

difference regarding the amount of internalized clustered ephrinB-Fc molecules after 15 min (Fig. 3.11). This implies that ITSN1 is not essential for endocytosis of EphB receptors bound to solubilized ligand molecules.

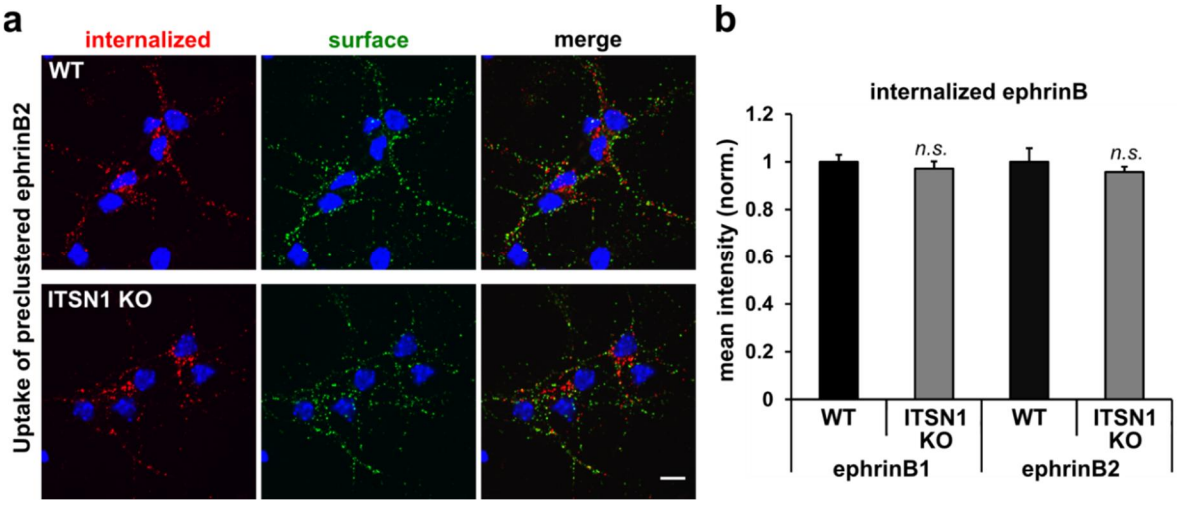

Figure 3.11 Uptake of clustered ephrinB is unaffected by loss of ITSN1. (a) EphrinB1-Fc or ephrinB2-Fc were preclustered with a goat anti-Fc antibody at a 2:1 molar ratio. Hippocampal neurons were incubated with preclustered ephrinB for 15 min at 37 °C to allow endocytosis. Neurons were washed, fixed and stained for surface and internal ephrinB-Fc with fluorescently labeled donkey anti-goat antibodies. Scale bar: 10 µm. **(b)** Quantification of internalized ephrinB2-Fc punctae reveals no difference between WT and ITSN1 KO neurons regarding the uptake of preclustered ephrinB1-Fc or ephrinB2-Fc (mean + SEM; N = 3; $p > 0.05$; two-tailed t-test for paired samples).

The uptake of preclustered ephrinB-Fc chimeric proteins might not sufficiently reflect the *in vivo* situation. As both ephrinB and EphB molecules are transmembrane proteins, endocytosis of ephrinB/EphB complexes requires uptake of parts of a neighboring cell, a process called 'transendocytosis' (Marston et al., 2003; Zimmer et al., 2003). This process requires mechanical force generated by actin filaments. ITSN1 and its Cdc42 GEF activity might be a regulator of transendocytosis by inducing local actin polymerization at ephrinB/EphB contact sites. To investigate the involvement of ITSN1 in ephrinB/EphB transendocytosis, glia cells from WT and ITSN1 KO mice were transfected with tagged EphB1 or ephrinB2. Cells of different genotype and differently transfected were mixed and stained for the overexpressed proteins. The presence of ephrinB2 clusters in a cell overexpressing EphB1 was taken as evidence for a transendocytic event, as were EphB1 clusters in a cell overexpressing ephrinB2. Of note, such events were only observed in neighboring cells expressing different constructs but not between cells overexpressing the same protein or untransfected

cells highlighting the specificity of this assay for ephrinB/EphB complexes. Strikingly, deficiency for ITSN1 did not interfere with transendocytosis as ITSN1 KO cells were still able to internalize ephrinB/EphB complexes (Fig. 3.12). Uptake of such complexes was seen in ITSN1 KO cells overexpressing ephrinB2 as well as in cells overexpressing EphB1. This proves that ITSN1 is not required for transendocytosis into either EphB- or ephrinB-expressing cells.

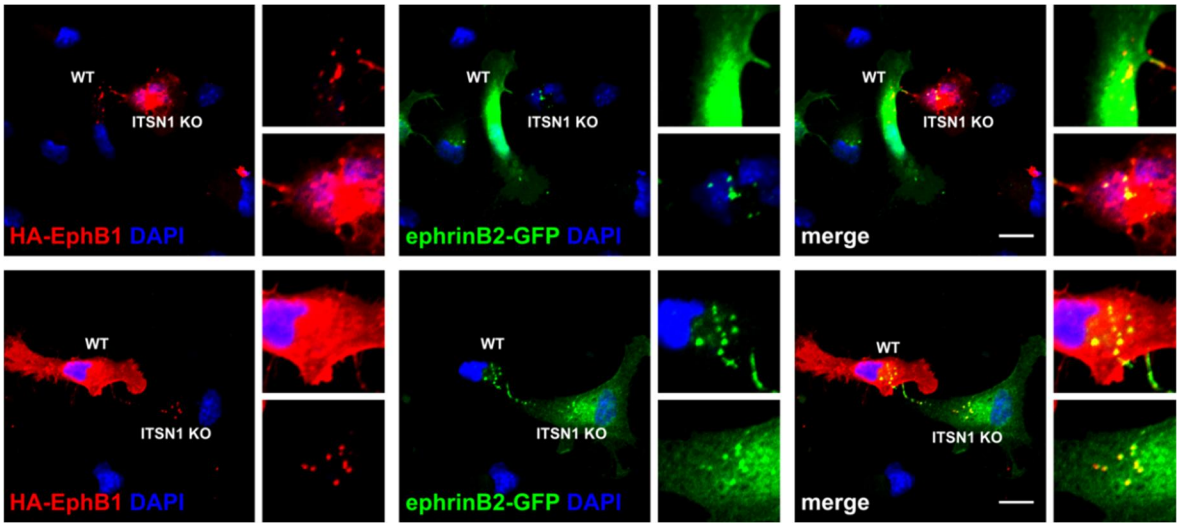

Figure 3.12 EphrinB/EphB-transendocytosis does not depend on ITSN1. Glial cultures from WT and ITSN1 KO littermates were transfected either with HA-tagged EphB1 (HA-EphB1) or GFP-tagged ephrinB2 (ephrinB2-GFP). After 1 day, cells with different genotypes and expressing different constructs were split, combined and seeded on coverslips. The next day, cells were stained for HA and GFP. Microscopic analysis revealed that in neighboring cells expressing different constructs, ephrinB2-EphB1 complexes can be internalized. This transendocytosis can occur in both directions and is independent of the genotype as ITSN1 KO cells also show punctae positive for HA-EphB1 and ephrinB2-GFP. Scale bar: 10 µm.

In order to find out if ITSN1 plays a role in EphB-mediated forward signaling, we checked the extent of ephrinB2-induced growth cone collapse in ITSN1 KO neurons (Srivastava et al., 2013). Hippocampal explants from WT and ITSN1 KO embryos were stimulated with preclustered ephrinB2-Fc before collapsed and uncollapsed growth cones were counted (Fig. 3.13a). No significant difference in the percentage of collapsed growth cones could be detected between axons from WT and ITSN1 KO neurons (Fig. 3.13b). Additionally, the levels of active Cdc42 were unchanged in hippocampal neuron lysates from ITSN1 KO mice, as measured with an ELISA detecting GTP-bound Cdc42 (Fig. 3.13c). This indicates that EphB forward

signaling is unperturbed in ITSN1 KO cells and that the absence of ITSN1 does not change the steady-state levels of active Cdc42.

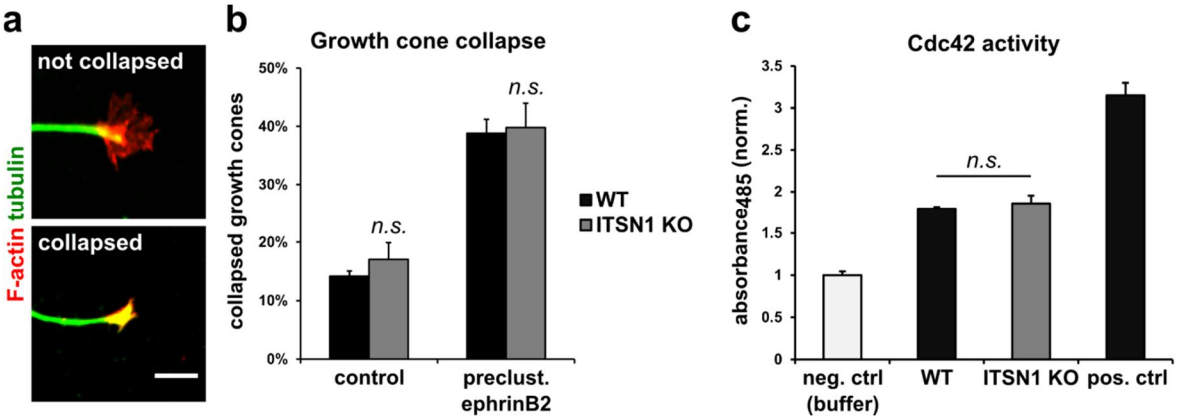

Figure 3.13 EphB-mediated forward signaling is unchanged in ITSN1 KO mice. (a-b) Genetic ablation of ITSN1 has no effect on ephrinB2-dependent growth cone collapse. **(a)** Example images of growth cones in embryonic hippocampal explant cultures. Scale bar: 5 µm. **(b)** Explants from WT and ITSN1 KO embryos were incubated with preclustered ephrinB2-Fc or clustering antibody alone (control) for 60 min at 37 °C. After fixation and staining for tubulin and F-actin, collapsed and non-collapsed growth cones were counted. The fraction of collapsed growth cones was unaltered in the absence of ITSN1 (mean + SEM; N = 4; $p > 0.05$; two-tailed t-test for paired samples). **(c)** The levels of active, GTP-bound Cdc42 were measured in hippocampal neuron lysates from WT and ITSN1 KO mice. Relative levels of active Cdc42 were quantified with a commercial ELISA kit using the photometric absorbance at a wavelength of 485 nm as readout. No significant difference between WT and ITSN1 KO lysates was found (mean + SEM; N = 3; $p > 0.05$; two-tailed t-test for paired samples).

ITSN1 and Cdc42 have been reported to be important modulators of dendritic spine morphology (Irie and Yamaguchi, 2002; Nishimura et al., 2006; Thomas et al., 2009). To investigate a possible involvement of ITSN1 in dendritic spine formation we analyzed the morphology of spines in apical dendrites of CA1 pyramidal neurons. To that end, Golgi-impregnated brain sections from WT and ITSN1 KO brains were examined and the dendritic spines were sorted into three categories based on their shape (mushroom, stubby and thin; Fig. 3.14a,b). The morphology of spines in hippocampi from ITSN1 KO mice was similar to WT control ruling out a vital role for ITSN1 in dendritic spine development *in vivo*. Similarly, dendritic spines of hippocampal neurons from ITSN1 KO mice did not show an altered morphology *in vitro* (Fig. 3.14c). Spines, visualized by Alexa568-conjugated phalloidin, had a similar size and length in WT and ITSN1 KO neurons, corroborating the *in vivo* data (Fig. 3.14d,e).

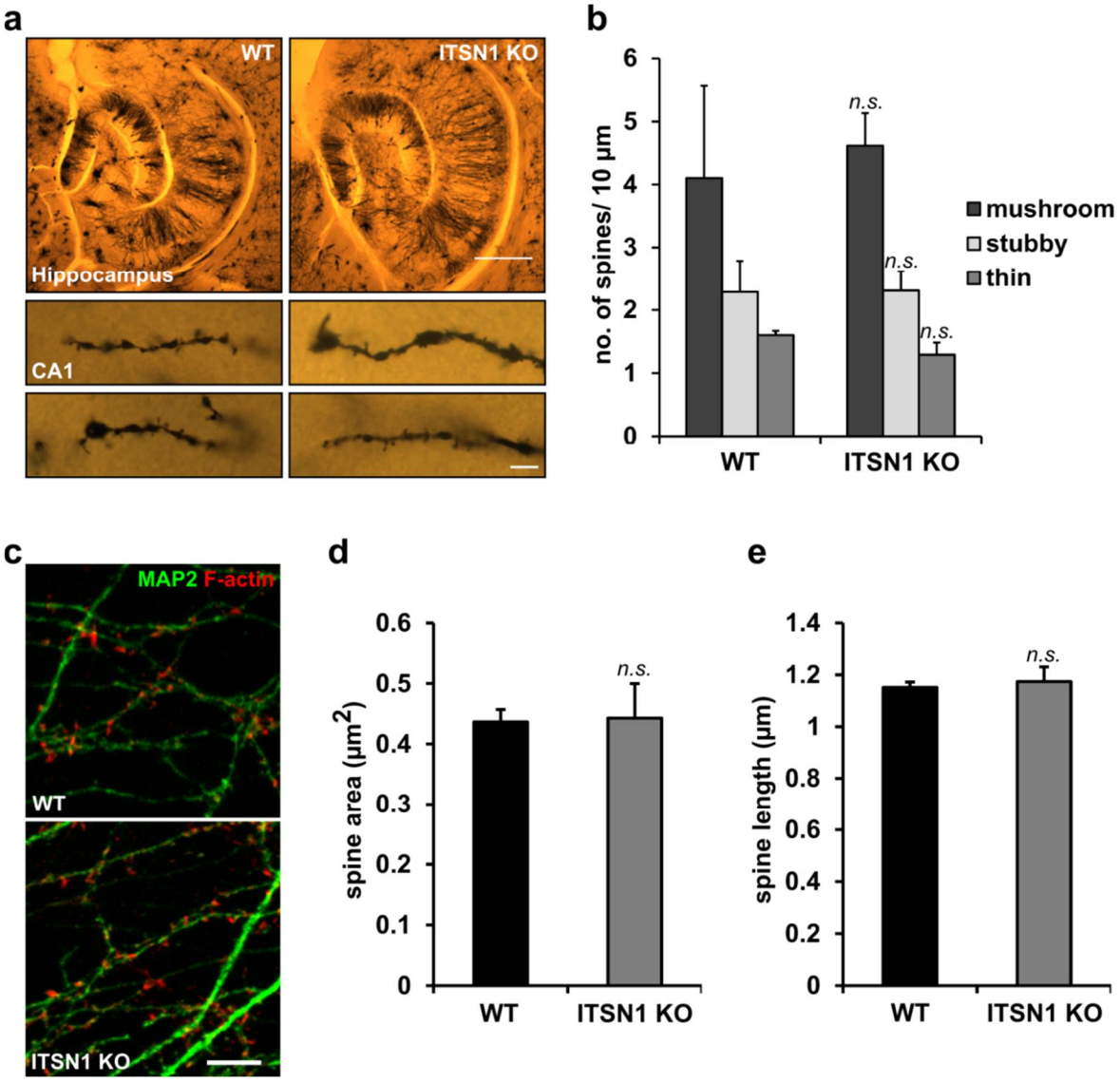

Figure 3.14 ITSN1 deficiency has no major effect on dendritic spine morphology *in vivo* and *in vitro*. (a-b) Dendritic spine morphology *in vivo*. **(a)** Golgi-stained horizontal sections of 6 months old brains from WT and ITSN1 KO littermates show no obvious effect of ITSN1 deficiency on dendritic spine morphology. Scale bars: 500 and 5 µm, respectively. **(b)** Spines in apical distal dendrites of CA1 pyramidal neurons were counted according to their morphology (mushroom, thin and stubby). Numbers are mean + SEM; N = 3 littermate couples; $p > 0.05$; two-tailed t-test for paired samples. **(c-e)** Dendritic spine morphology *in vitro*. **(c)** Dendritic spines were visualized in hippocampal neuron cultures from WT and ITSN1 KO pups by Alexa568-conjugated phalloidin which stains F-actin-rich structures as dendritic spines. MAP2 immunostaining was used as a dendritic marker. Scale bar: 5 µm. **(d)** The area covered by spines as well as their length **(e)** was not affected in neurons lacking ITSN1 (mean + SEM; N = 3; $p > 0.05$; two-tailed t-test for paired samples).

Another ITSN1 KO mouse model, created by a gene-trap approach, showed defects in brain hemisphere connectivity due to insufficient commissure formation (Sengar et al., 2013). Furthermore, a variety of ephrins and Eph receptors has been implicated in the development of axonal commissures (Mendes et al., 2006). To check

if absence of ITSN1 has a detrimental effect on commissure formation, we analyzed a large number of Nissl-stained brain sections from WT and ITSN1 KO mice. Generally, axonal tracts formed normally in ITSN1-deficient brains (41 out of 42 animals). Only one mouse brain failed to connect the hemispheres through corpus callosum and hippocampal commissure (Fig. 3.15). As defects in commissure formation can also be found in WT mouse strains at a sizeable number (Wahlsten, 1982), the phenotype of this single mouse was considered insignificant. Thus, we concluded that ITSN1 does not play a fundamental role for the formation of axonal commissures.

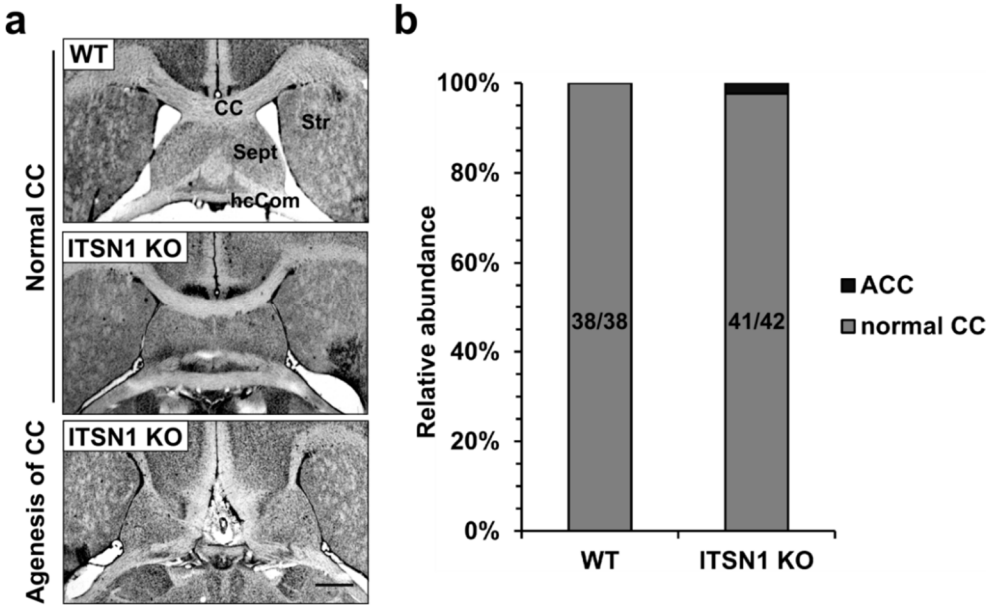

Figure 3.15 ITSN1 is dispensable for the formation of forebrain commissures. (a) Example images of Nissl-stained horizontal sections of hippocampi from WT (upper) and ITSN1 KO with corpus callosum (middle) and ITSN1 KO without the corpus callosum (lower). Absence of ITSN1 does not lead to a general disruption of axonal tracts. CC: corpus callosum; Sept: septum; Str: striatum; hcCom: hippocampal commissure. Scale bar: 500 µm. **(b)** Only 1 out of 42 ITSN1 KO animals analyzed showed agenesis of the corpus callosum (ACC).

Taken together, this data shows that ITSN1 is dispensable for endocytosis of EphB receptors as well as for EphB-mediated forward signaling. EphB-dependent processes as ephrinB2-induced growth cone collapse, dendritic spine development or axonal commissure formation are not affected by absence of ITSN1. This renders the phenotype seen in ITSN1 KO mice unlikely to be a consequence of disturbed EphB signaling.

3.2.2 ITSN1 binds Reelin pathway components

As the hippocampal phenotype seen in ITSN1 KO mice is most likely not a consequence of altered EphB signaling, we turned towards other possible explanations. Reelin signaling is crucial for hippocampal layer formation and also known to regulate hippocampal neurogenesis (Forster et al., 2010). Therefore, we investigated a possible role of ITSN1 in Reelin signaling through its main receptors, ApoER2 and VLDLR. Strikingly, we found that ITSN1 can bind to the intracellular region of VLDLR in a GST-pulldown assay from mouse brain extract. An association of ITSN1 with the intracellular regions of ApoER2 could not be detected (Fig. 3.16a). The same conclusion was drawn from pulldown assays from HEK293 cells overexpressing VLDLR-HA or ApoER2-HA. GST-tagged ITSN1 SH3 domains pulled down overexpressed VLDLR but hardly any overexpressed ApoER2 (Fig. 3.16b). A GST-pulldown with single ITSN1 SH3 domains showed that a single SH3 domain is sufficient for this interaction and that, of the five ITSN1 SH3 domains, SH3B binds most efficiently (Fig. 3.16c).

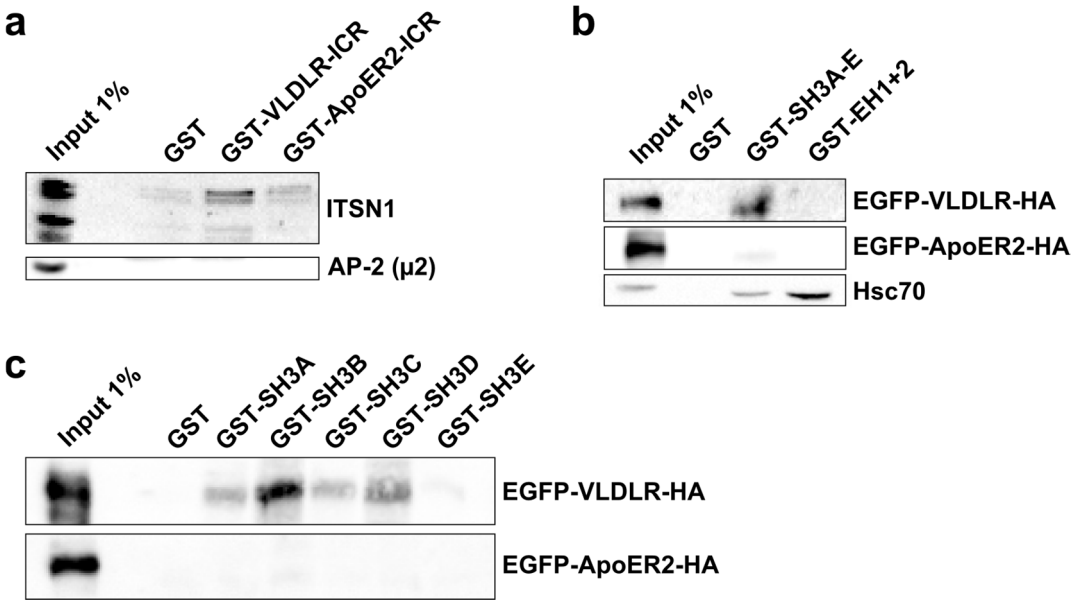

Figure 3.16 ITSN1 binds to VLDLR. (a) GST-pulldown with the intracellular regions (ICRs) of the Reelin receptors, VLDLR or ApoER2, from mouse brain extract reveals that ITSN1 associates with VLDLR but hardly with ApoER2. **(b)** GST-pulldown with ITSN1 SH3 or EH domains from HEK cells overexpressing HA-tagged VLDLR or ApoER2 shows that ITSN1 binding to VLDLR is mediated by its SH3 domains. **(c)** GST-pulldown with single ITSN1 SH3 domains from HEK cells, transfected with VLDLR-HA or ApoER2-HA, proves that single SH3 domains are sufficient for VLDLR-ITSN1 interaction. Of the ITSN1 SH3 domains, VLDLR binds most efficiently to SH3B.

Next, we analyzed whether the absence of ITSN1 has any effect on the levels of the Reelin pathway core components. Interestingly, total levels of Reelin are slightly elevated in brains from ITSN1 KO mice which could be detected by immunohistochemistry and in brain lysates (Fig. 3.17a,b). Notably, this increase is mainly caused by the 180 kDa fragment. As this fragment is generated after endocytosis and subsequent resecretion (Hibi and Hattori, 2009), this increase could be explained by altered trafficking of Reelin in the absence of ITSN1. Alternatively, the higher levels might be due to enhanced synthesis of Reelin. In contrast to Reelin, the levels of its receptors, VLDLR and ApoER2, were not changed in ITSN1 KO brains. The total levels of the signaling adaptor Dab1 were also unaltered (Fig. 3.17c). This indicates that ITSN1 regulates Reelin levels whereas the cellular components of the Reelin signaling apparatus remain unaffected.

Staining of brain slices for VLDLR and GFAP, a marker for astrocytes but also for DG stem cells, revealed that VLDLR is highly expressed in neural stem cells of the hippocampus (Fig. 3.17d). This finding supports the notion that Reelin-VLDLR signaling has an important function for adult neurogenesis in the DG.

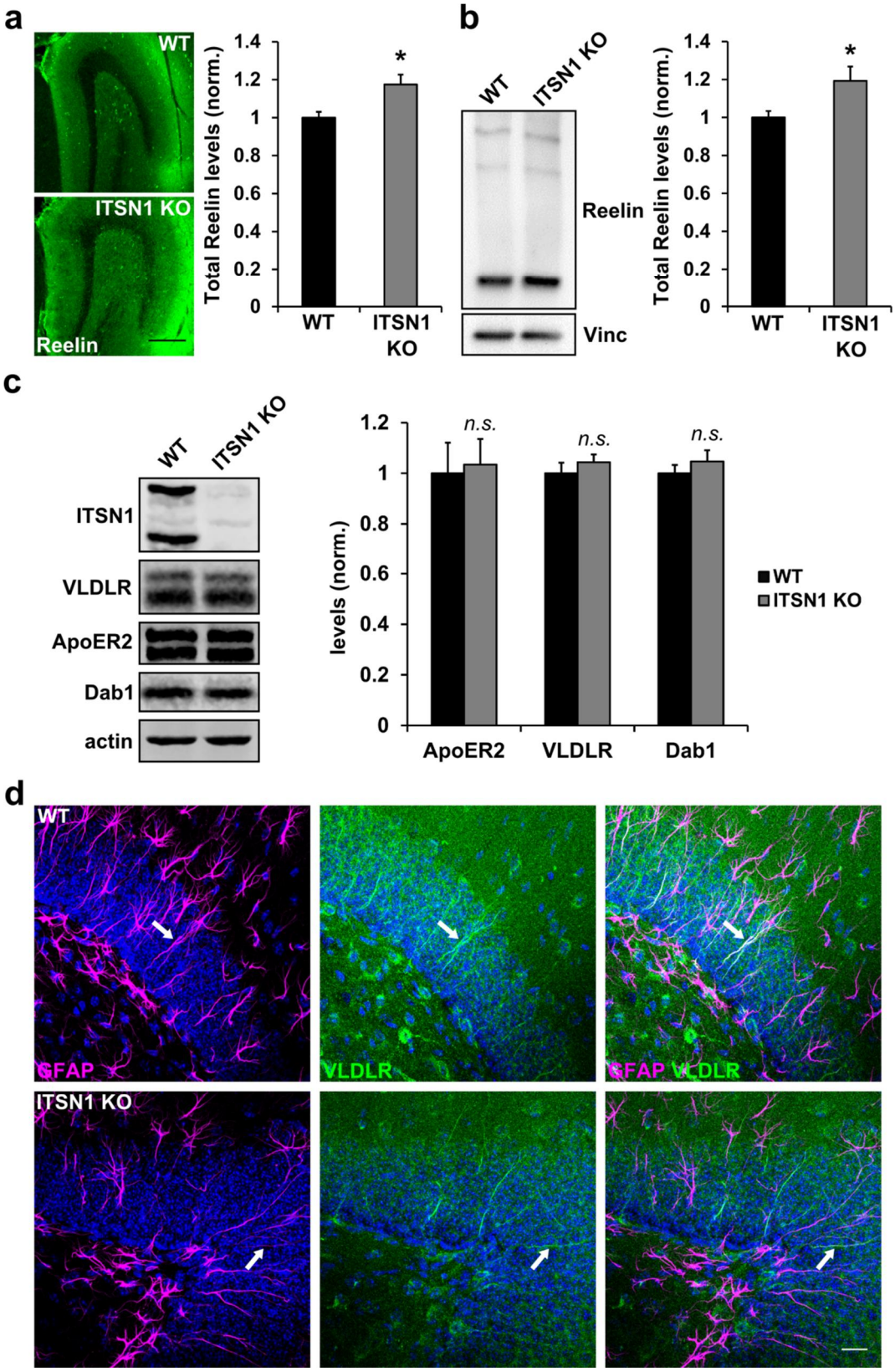

Figure 3.17 Total levels of Reelin are increased in hippocampi of ITSN1 KO mice whereas Reelin receptor levels are unchanged. (a-b) Reelin levels are elevated in hippocampi of ITSN1 KO mice. **(a)** Immunohistochemical staining for Reelin in horizontal brain sections shows a small but significant increase in ITSN1 KO mice (normalized mean gray value + SEM; N = 3 littermate couples; *p < 0.05;

two-tailed t-test for paired samples). Scale bar: 100 µm. **(b)** Hippocampal lysates from ITSN1 KO mice also show a significant increase in Reelin levels (normalized mean gray value + SEM; N = 5 littermate couples; *p < 0.05; two-tailed t-test for paired samples). Loading control: Vinculin (Vinc). **(c)** The total levels of the Reelin pathway components VLDLR, ApoER2 and Dab1 are unchanged in hippocampal lysates from ITSN1 KO mice (normalized mean gray value + SEM; N = 5 littermate couples; p > 0.05; two-tailed t-test for paired samples). **(d)** Co-labeling of VLDLR and GFAP, a marker for stem cells in the DG, in brain sections reveals that VLDLR is highly expressed in neuronal stem cells of the DG (arrows). Scale bar: 20 µm.

Due to the well-established role of ITSN1 in endocytosis, we analyzed the effect of ITSN1 deficiency on Reelin receptor surface levels. Cell surface biotinylation of hippocampal neurons did not show a difference regarding surface levels of VLDLR or ApoER2 in the absence of ITSN1 (Fig. 3.18a). Immunofluorescence staining of hippocampal neurons with a VLDLR-specific antibody under non-permeabilizing conditions confirmed the finding that loss of ITSN1 does not alter the surface pool of VLDLR (Fig. 3.18b). Additionally, an antibody uptake assay with hippocampal neurons overexpressing EGFP-tagged VLDLR or ApoER2 showed no effect of ITSN1 deficiency (Fig. 3.18c). Both WT and ITSN1 KO cells internalized similar amounts of an anti-GFP antibody with the same slope (Fig. 3.18d,e). This data suggests that ITSN1 is not required for correct endocytic trafficking of the Reelin receptors ApoER2 and VLDLR.

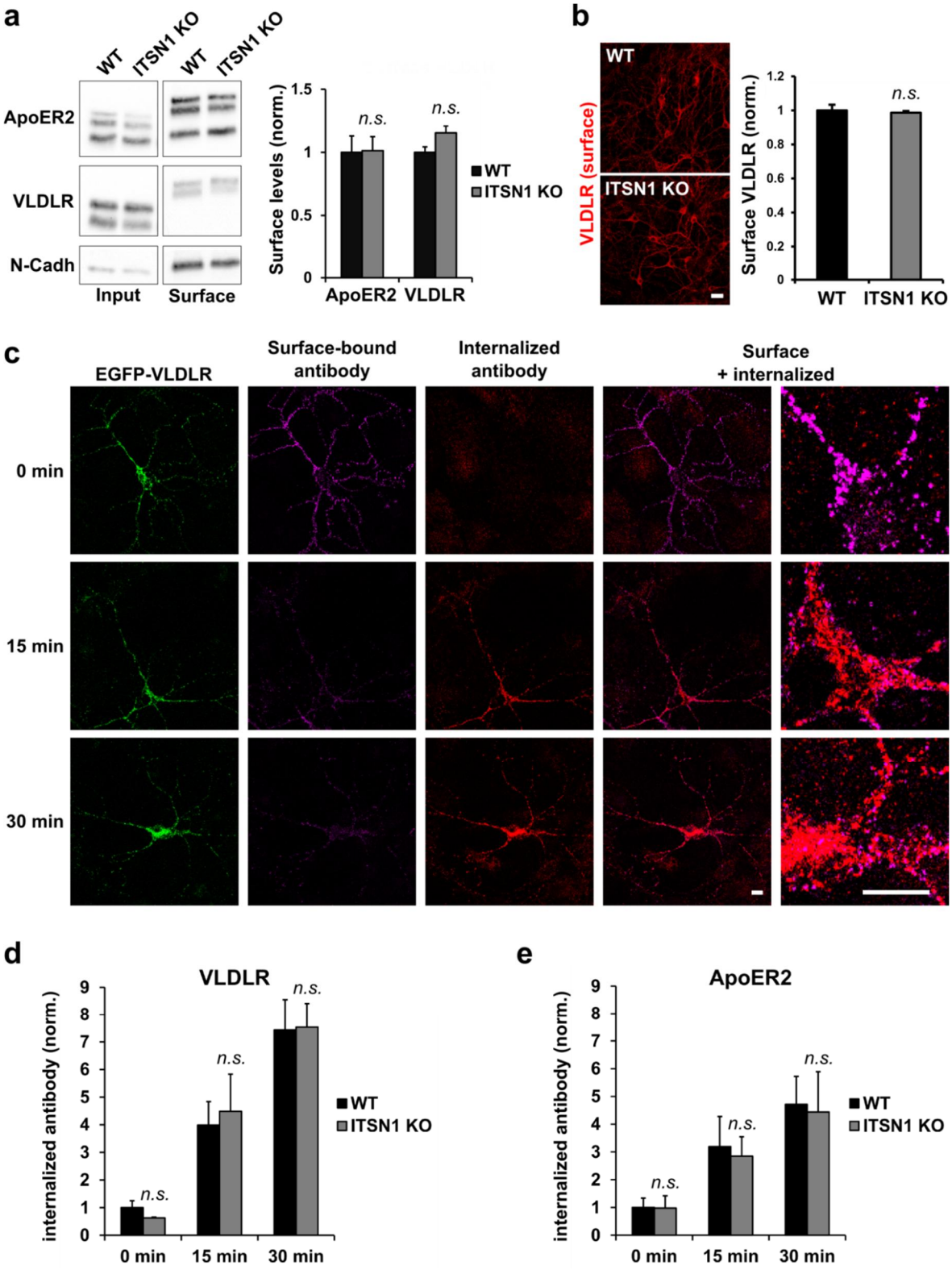

Figure 3.18 Endocytosis of ApoER2 and VLDLR does not require ITSN1. (a-b) Steady-state surface levels of Reelin receptors are unchanged in the absence of ITSN1. **(a)** Surface biotinylation of hippocampal neurons from WT and ITSN1 KO mice shows that surface levels of ApoER2 and VLDLR are unchanged in the absence of ITSN1. Values were normalized to N-Cadherin (N-Cadh) surface levels (mean + SEM; N = 3; $p > 0.05$; two-tailed t-test for paired samples). **(b)** Immunofluorescence staining of hippocampal neurons under non-permeabilizing conditions shows that surface levels of VLDLR are

unaltered in ITSN1 KO neurons (normalized mean gray value + SEM; N = 3; p > 0.05; two-tailed t-test for paired samples). Scale bar: 20 µm. **(c-e)** ITSN1 is dispensable for Reelin receptor endocytosis in antibody uptake experiments. **(c)** Example images from an antibody uptake experiment. Hippocampal neurons were transfected with EGFP-VLDLR or EGFP-ApoER2. Cells were incubated with rabbit anti-GFP antibody for 15 or 30 min at 37 °C to allow uptake or 30 min at 4 °C as control. After fixation, the remaining surface pool was stained with Alexa647-conjugated anti-rabbit secondary antibodies while the internalized fraction was visualized with Alexa568. Scale bars: 10 µm. **(d, e)** The quantification shows that both GFP-VLDLR and GFP-ApoER2 become internalized over time yet the internalization process is independent of ITSN1 (normalized mean gray value + SEM; N = 3; p > 0.05; two-tailed t-test for paired samples).

Dab2 is an endocytic adaptor binding to receptors of the LDLR family, particularly ApoER2 (Yang et al., 2002; Cuitino et al., 2005). Additionally, Dab2 has been shown to bind to ITSN1 (Teckchandani et al., 2012). This being the case, we sought to investigate a possible involvement of Dab2 in the ITSN1-VLDLR interaction. First, we could confirm the interaction between ITSN1 and Dab2 using a GST-pulldown with ITSN1 SH3 or EH domains from HEK293 cells overexpressing Myc-tagged Dab2 (Fig. 3.19a). Interestingly, the SH3 domains bound to Myc-Dab2 much more efficiently than did the EH domains, in contrast to previous data (Teckchandani et al., 2012). Dab2 also bound to the intracellular regions of ApoER2 and, much stronger, VLDLR in pulldown experiments from mouse brain extract (Fig. 3.19b). To find out if the binding of ITSN1 to VLDLR was mediated by Dab2, we performed a GST-pulldown with ITSN1 SH3 domains from HEK293 cells overexpressing HA-tagged VLDLR. The efficiency of the VLDLR-SH3 binding was compared between cells in which Dab2 levels had been decreased by an siRNA-mediated knockdown and control cells (scrambled siRNA). Interestingly, reduction of Dab2 to non-detectable levels had no effect on the interaction between VLDLR-HA and GST-SH3A-E (Fig. 3.19c). As Dab2 is strongly down-regulated during development while ITSN1 is not (Fig. 3.19d), comparing the pulldown efficiency from tissue of different age provides an alternative way to probe for the Dab2 dependency of the VLDLR-ITSN1 interaction. The GST-tagged intracellular region of VLDLR was able to pull down ITSN1 from brain tissue at the age of 1 day and 3 months to a similar extent (Fig. 3.19e). This indicates that the endocytic adaptor Dab2, despite its ability to bind VLDLR and ITSN1, does not mediate the interaction between VLDLR and ITSN1. This is in agreement with the fact that endocytosis of VLDLR and ApoER2 is

unaltered in ITSN1 KO mice and strongly suggests that a possible involvement of ITSN1 in Reelin signaling is not related to endocytosis of Reelin receptors.

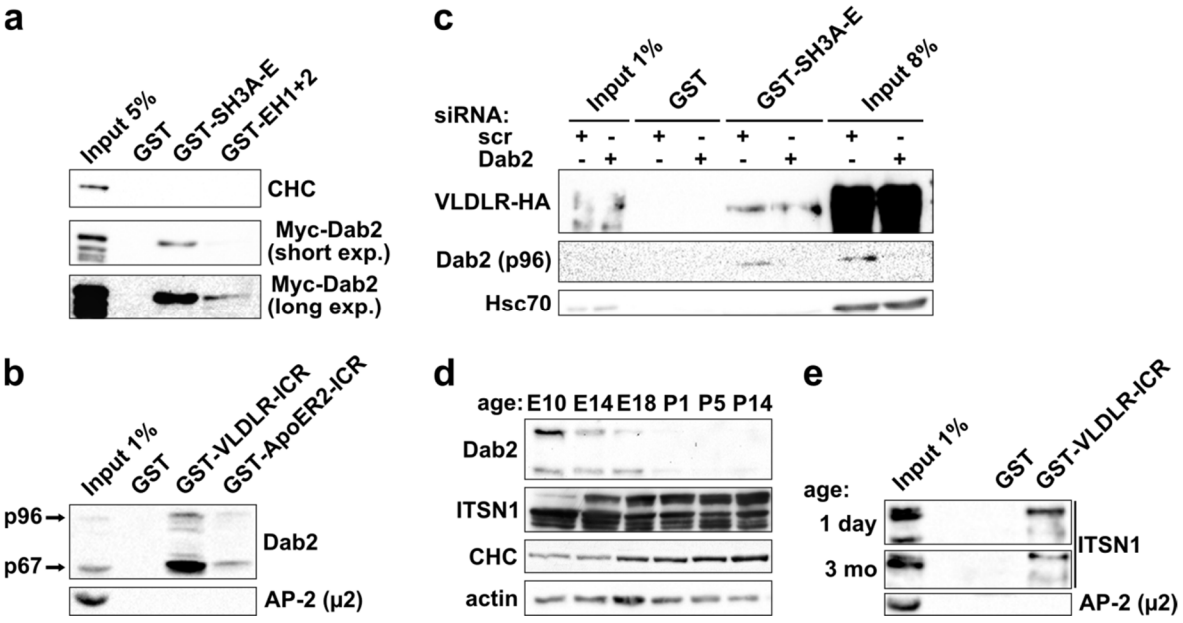

Figure 3.19 Binding of ITSN1 to VLDLR is independent of Dab2. (a) GST-pulldown with ITSN1 SH3 or EH domains from HEK cells overexpressing Myc-Dab2 shows that ITSN1 can bind Dab2, preferably with its SH3 domains. **(b)** GST-pulldown with the intracellular regions of VLDLR or ApoER2 from mouse brain extract shows that both Reelin receptors bind Dab2, with VLDLR binding more efficiently. **(c)** GST-pulldown with ITSN1 SH3 domains. HEK cells were transfected with VLDLR-HA and simultaneously with an siRNA against Dab2 (or scrambled siRNA for control). Interaction between ITSN1 SH3 domains and HA-tagged VLDLR can be observed regardless of Dab2 levels. **(d)** Lysates from brain tissue at different developmental stages reveals early and continuous expression of ITSN1 while Dab2 expression is strongly down-regulated during development. **(e)** GST-pulldown with the intracellular region of VLDLR from brain extract of mice at the age of 1 day versus 3 months. The ITSN1-VLDLR interaction is not decreasing with age and is therefore independent of Dab2 expression.

3.2.3 ITSN1 mediates Reelin signaling

ITSN1 interacts with VLDLR but is apparently dispensable for endocytic trafficking of Reelin receptors. Therefore, we sought to investigate whether ITSN1 was instead involved in propagation of the Reelin signal towards downstream signaling molecules. To that end, we checked for a possible interaction of ITSN1 with Dab1, the signaling adaptor for ApoER2 and VLDLR. Strikingly, both ITSN1 SH3 and EH domains were able to bind Myc-tagged Dab1 in a pulldown assay from overexpressing HEK293 cells. The GST-tagged intracellular regions of VLDLR and ApoER2 were also able to bind Myc-Dab1 (Fig. 3.20a). Interaction of ITSN1 domains

and Dab1 could also be seen in GST-pulldowns from mouse brain extract, followed by elution and immunoprecipitation of Dab1 to reduce unspecific background (Fig. 3.20b). This suggests that ITSN1 not only can bind to VLDLR but also to Dab1, which has a pivotal role in signaling downstream of the Reelin receptors. This places ITSN1 at the core of the Reelin signaling complex.

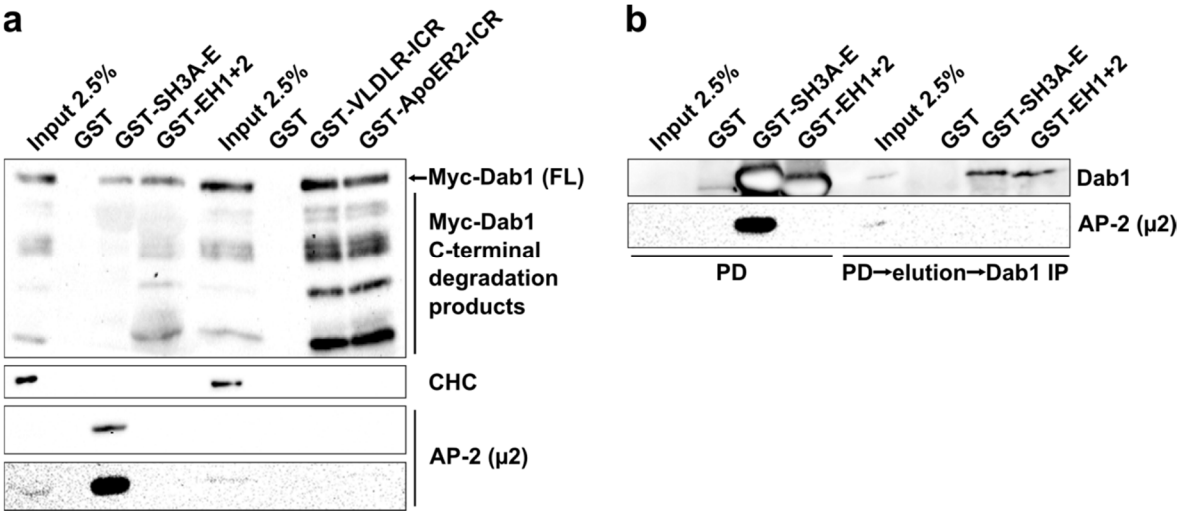

Figure 3.20 ITSN1 binds to Dab1. (a) GST-pulldown with ITSN1 SH3 or EH domains from HEK cells overexpressing Myc-tagged Dab1 shows that ITSN1 can form a complex with Dab1 both via its SH3 and its EH domains. Dab1 also binds to the intracellular regions of VLDLR and ApoER2 with similar efficiency. FL: full length. **(b)** GST-pulldown (PD) with ITSN1 SH3 or EH domains from MBE also reveals the ITSN1-Dab1 interaction. Due to high unspecific background (left), signals for Dab1 could only be seen after elution and subsequent immunoprecipitation (IP) of Dab1 (right).

We investigated if the absence of ITSN1 has an effect on the activation status of its interaction partner Dab1. For that purpose, Dab1 was immunoprecipitated from hippocampal lysates of WT and ITSN1 KO origin and the samples were probed with a phospho-tyrosine-specific antibody (Fig. 3.21a). Interestingly, the levels of phosphorylated Dab1 were reduced to about 79 % of control animals implying that signaling downstream of the Reelin receptors is indeed partially impaired in mice lacking ITSN1 (Fig. 3.21c). In contrast, the levels of phosphorylated Akt or cofilin, known downstream effectors of Reelin signaling, were not changed significantly in the absence of ITSN1 (Fig. 3.21b,c). This suggests that the reduction of phospho-Dab1 levels in ITSN1 KO mice does not translate into an altered activation status of these downstream signaling molecules.

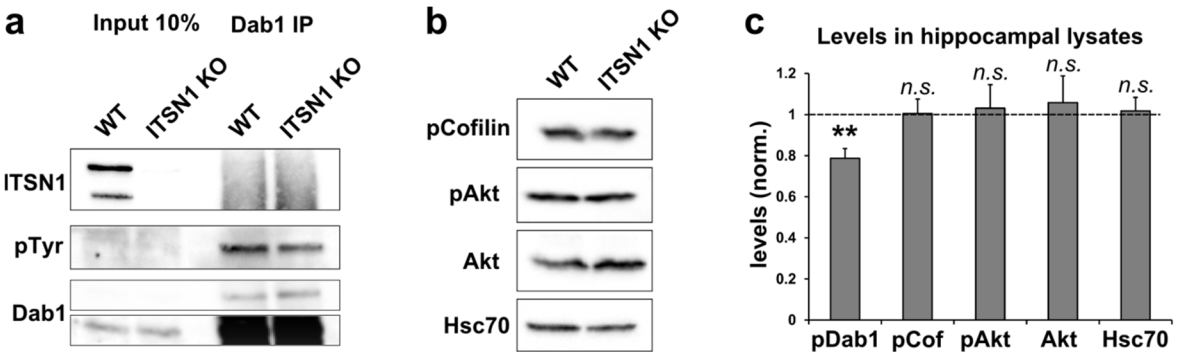

Figure 3.21 Levels of phosphorylated Dab1 are reduced in ITSN1 KO mice. (a) Levels of phosphorylated Dab1 (pDab1) in hippocampi of WT and ITSN1 KO mice were assessed by immunoprecipitation of Dab1 from hippocampal lysates followed by immunoblotting with an antibody specific for phospho-tyrosine (pTyr). **(b)** The phosphorylation status of known downstream effectors of Reelin signaling, cofilin (pCof) and Akt (pAKT), was measured with antibodies raised against specific phosphorylated sites in the respective proteins. **(c)** Quantification revealed a significant reduction of pDab1 levels to 78.7 ± 4.8 % in hippocampi from ITSN1 KO mice. Shown are ITSN1 KO levels normalized to WT, indicated by the dotted line (mean + SEM; N = 8 littermate couples; **p < 0.01; one-sample t-test). Neither AKT nor Cofilin showed a significant change regarding their phosphorylation status (mean + SEM; N = 6 littermate couples; p > 0.05; one-sample t-test).

Reelin has been shown to augment hippocampal long-term potentiation (LTP) in acute hippocampal slices (Weeber et al., 2002; Beffert et al., 2005). This process depends on both ApoER2 and VLDLR as genetic ablation of ApoER2 or VLDLR completely abrogates Reelin effects on LTP. To investigate a possible involvement of ITSN1 in Reelin-dependent modulation of synaptic plasticity, we analyzed LTP induction in WT and ITSN1 KO mice in control or Reelin-conditioned medium. All electrophysiological experiments were conducted by Dr. Gaga Kochlamazashvili (FMP Berlin, Germany). Single theta-burst stimulation (TBS) of CA1 Schaffer collaterals induced reliable LTP in hippocampal slices from WT mice (Fig. 3.22a,c). In ITSN1 KO slices, LTP induction was similar to WT slices under control conditions (Fig. 3.22b,c). This finding is in agreement with the normal dendritic spine morphology in ITSN1 KO brains described above. Application of Reelin-conditioned medium to slices from WT mice strongly facilitated LTP induction in agreement with previous publications (Fig. 3.22a,c and Weeber et al., 2002). In contrast, Reelin failed to augment LTP in slices from ITSN1 KO mice (Fig. 3.22b,c). These results suggest that ITSN1 is dispensable for LTP formation but specifically required for Reelin-dependent augmentation of LTP.

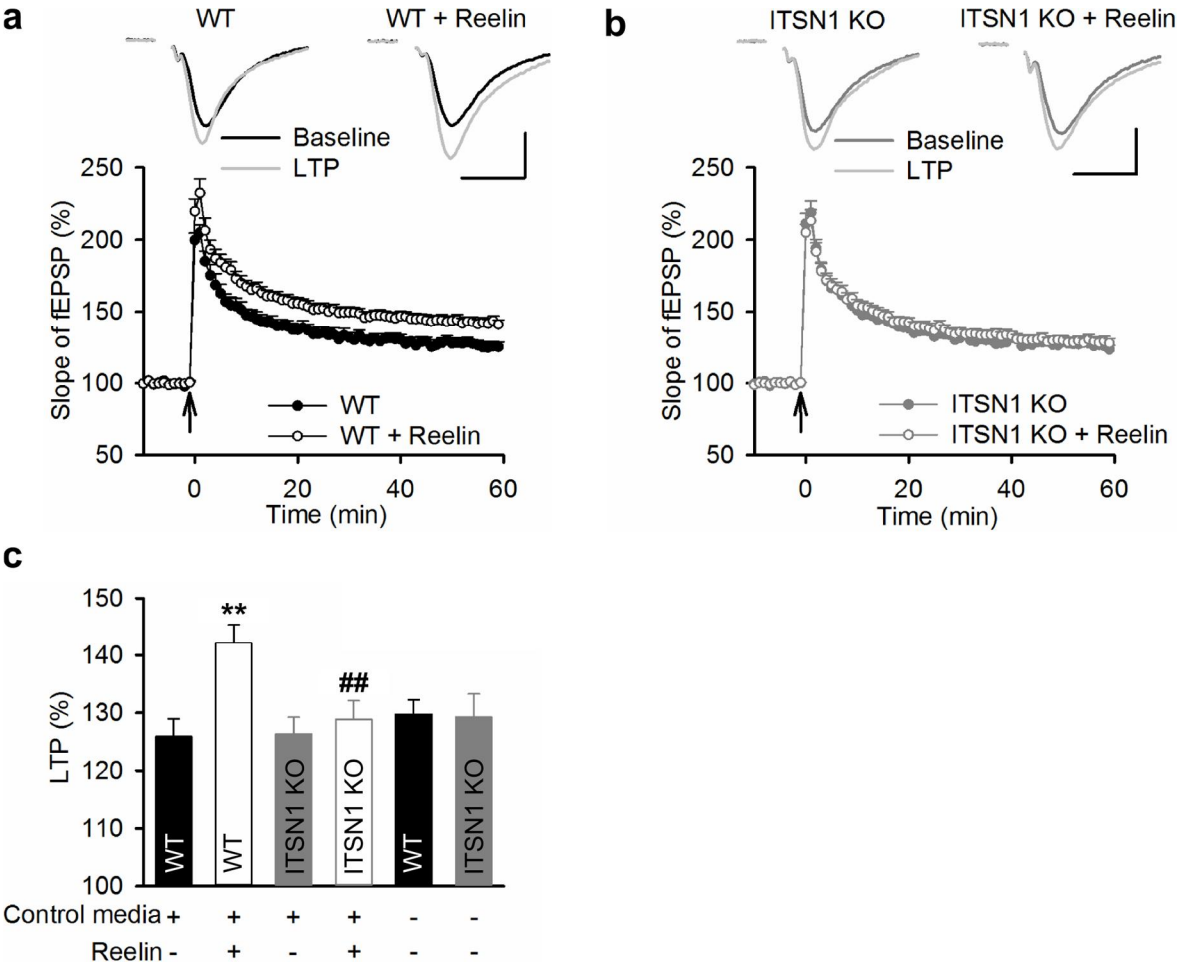

Figure 3.22 ITSN1 is required for Reelin-dependent facilitation of LTP. (a-b) Normal LTP induced by a single theta burst stimulation (TBS) in slices perfused with control medium of WT (n = 7, N = 7; 125.8 + 3.1 %) and ITSN1 KO (n = 6, N = 6; 126.3 + 2.9 %) mice. **(a)** LTP in WT slices was strongly facilitated when medium containing Reelin (5 µg/ml for 15 min before TBS) was applied (n = 12, N = 8; 142.1 + 3.1 %). **(b)** Application of Reelin did not facilitate LTP in ITSN1 KO mice (n = 12, N = 8; 128.8 + 3.3 %). Representative traces are the average of 30 elicited field excitatory postsynaptic potentials (fEPSPs) recorded 10 min before (black) and 50–60 min after LTP induction (grey). Scale bars: 0.5 mV and 10 ms. The delivery of TBS is indicated by the arrow. **(c)** Mean (+ SEM) LTP levels recorded 50–60 min after LTP induction in the presence or absence of control medium and or Reelin. **p < 0.01, significant difference between control medium and Reelin-treated WT slices; ##p < 0.01 significant difference between Reelin-treated WT and ITSN1 KO slices (two-tailed t-test for unpaired samples). Experiments were performed by Dr. Gaga Kochlamazashvili (FMP Berlin, Germany).

In order to better understand the differential effect of Reelin on WT and ITSN1 KO slices we analyzed N-methyl-D-aspartate receptor (NMDAR) potentials. NMDAR-mediated potentials were measured during the late phase of TBS-elicited field excitatory postsynaptic potentials (fEPSPs; Fig. 3.23a). Slices from WT and ITSN1 KO mice showed similar amplitudes of NMDAR potentials in control conditions. In contrast, Reelin application facilitated NMDAR potentials in slices from WT mice but

not from ITSN1 KO mice (Fig. 3.23b,c). These findings are in agreement with previous publications showing Reelin-induced facilitation of NMDAR potentials (Beffert et al., 2005; Chen et al., 2005). Furthermore, this data corroborates an essential role of ITSN1 for Reelin-dependent modulation of synaptic plasticity.

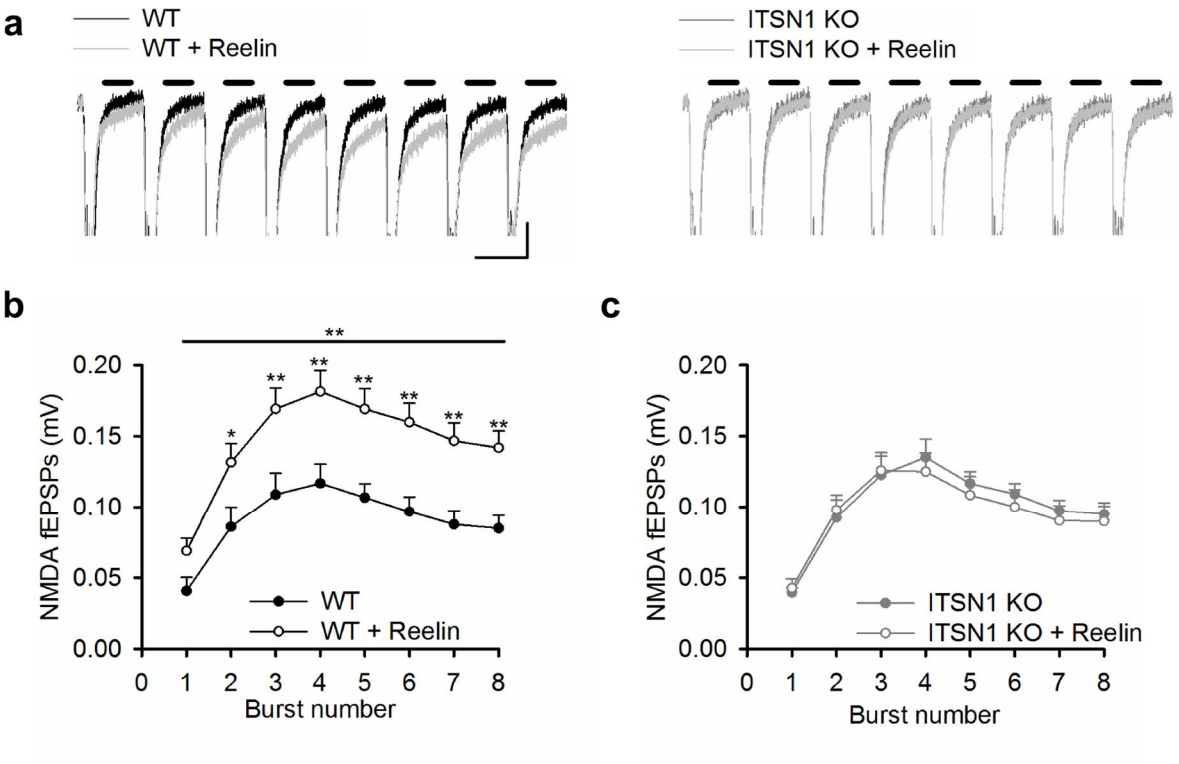

Figure 3.23 ITSN1 is required for Reelin-dependent facilitation of NMDAR-mediated fEPSPs. **(a)** Representative fEPSPs elicited by a single theta burst stimulation (TBS) for WT and ITSN1 KO in control medium (black and dark grey, respectively) and in Reelin-treated conditions (light grey). Horizontal lines indicate the time intervals, 80–180 ms after the beginning of each theta-burst, in which the mean amplitudes of the late NMDAR-mediated responses were measured. Scale bars: 0.5 mV and 200 ms. **(b-c)** Late NMDAR-mediated responses during TBS in control medium revealed normal levels of NMDAR depolarization in ITSN1 KO as compared to WT mice (P = 0.483; Two way repeated measures ANOVA). **(b)** Reelin-dependent facilitation of NMDAR responses during TBS in WT slices compared to control (P = 0.007; Two way repeated measures ANOVA with Newman-Keuls post hoc analysis; *p < 0.05, **p < 0.01). **(c)** Lack of Reelin facilitation of NMDAR responses during TBS in ITSN1 KO slices compared to control (P = 0.835; Two way repeated measures ANOVA). Experiments were performed by Dr. Gaga Kochlamazashvili (FMP Berlin, Germany).

In sum, this data shows that ITSN1 has so far unknown functions for migration, neurogenesis and synaptic plasticity in the hippocampus. The described defects in ITSN1 KO mice seem to be caused by disturbed Reelin signaling. Interestingly, this effect is not a result of altered endocytosis of Reelin receptors. Instead, ITSN1 seems

to act as a molecular scaffold connecting Reelin receptors and the signaling adaptor Dab1.

3.2.4 ITSN1/ApoER2 double KO mice phenocopy VLDLR/ApoER2 double KO mice

Deficits in Reelin-dependent signaling are the most plausible explanation for the hippocampal phenotype observed in ITSN1 KO mice. The biochemical interaction studies suggest a strong preference of ITSN1 for VLDLR over ApoER2. To analyze the relationship between ITSN1 and the Reelin receptors, we made use of a mouse line lacking ApoER2 expression (ApoER2 KO mice; Trommsdorff et al., 1999). Nissl-stained sections of hippocampi from ApoER2 KO mice showed similar alterations as hippocampi from ITSN1 KO mice (Fig. 3.24). First, the morphology of the DG was altered, acquiring a more rectangular shape. Additionally, the granular neurons in the medial infrapyramidal blade of the DG appeared more dispersed in the ApoER2 KO mice than in ITSN1 KO or control animals. The pyramidal neurons of CA3 and CA1 showed a similar dispersion in ApoER2 KO mice as in ITSN1 KO mice, albeit to a stronger extent. This indicates that absence of a Reelin receptor can result in a hippocampal morphology very similar to hippocampi of ITSN1 KO mice. Remarkably, absence of both ITSN1 and ApoER2 lead to an aggravation of the defects. Mice deficient for ITSN1 and ApoER2 (ITSN1/ApoER2 DKOs) showed a severely altered DG shape. Furthermore, neurons in CA3 were widely scattered while the CA1 pyramidal layer was split into three distinct layers. Such hippocampal morphology has been described for mice lacking both Reelin receptors (VLDLR/ApoER2 double KO mice), Reelin (*reeler*) or Dab1 (*scrambler*, *yotari*). Taken together with the fact that the phenotypes of ITSN1 KO and ApoER2 KO mice are additive and therefore independent, this strongly suggests a role of ITSN1 in Reelin signaling downstream of the VLDLR.

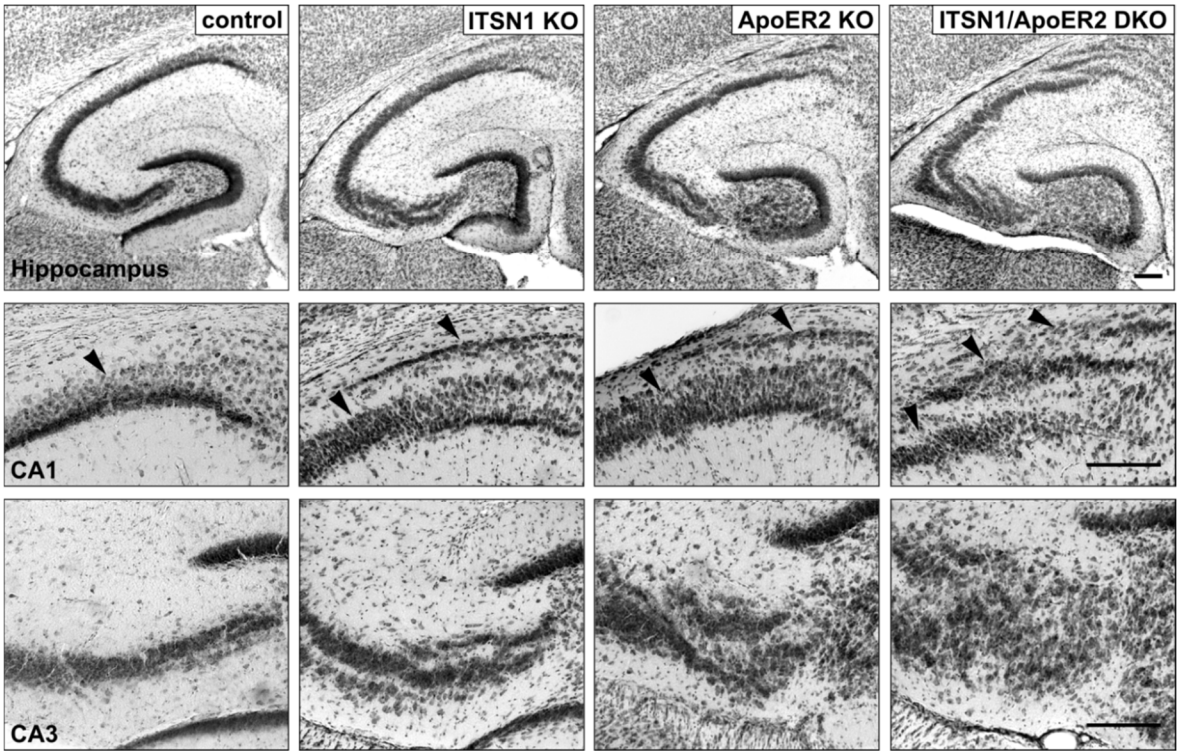

Figure 3.24 Deficiency for ApoER2 aggravates the migration phenotype in hippocampi of ITSN1 KO mice. Nissl-stained horizontal sections of hippocampi from ITSN1 KO, ApoER2 KO and ITSN1/ApoER2 DKO mice. Mice heterozygous for ITSN1 and ApoER2 served as control. Deficiency of ITSN1 and/or ApoER2 leads to an altered shape of the DG and neuronal dispersion in CA1 and CA3. The hippocampal morphology is severely altered in ApoER2 KO mice while ITSN1 KO mice show a milder version of the phenotype. The lack of both ITSN1 and ApoER2 leads to an even stronger dispersal in CA1 and CA3. In ITSN1/ApoER2 DKOs, the pyramidal cells in CA1 are split into three distinct layers (arrow heads). Scale bars: 200 µm.

In order to investigate if the additive effects of ITSN1 and ApoER2 deficiency seen for hippocampal morphology also pertain to neurogenesis, we quantified the processes of Nestin-positive radial glial cells in the DGs of single and double KO animals. Interestingly, their number was reduced to a similar degree in ITSN1 KO and ApoER2 KO mice (Fig. 3.25). This provides evidence that an impairment of Reelin signaling results in a disrupted radial glial scaffold. Lack of both ITSN1 and ApoER2 lead to an even stronger reduction of Nestin-positive processes, further supporting the notion of ITSN1 playing a vital part in VLDLR-mediated Reelin signaling.

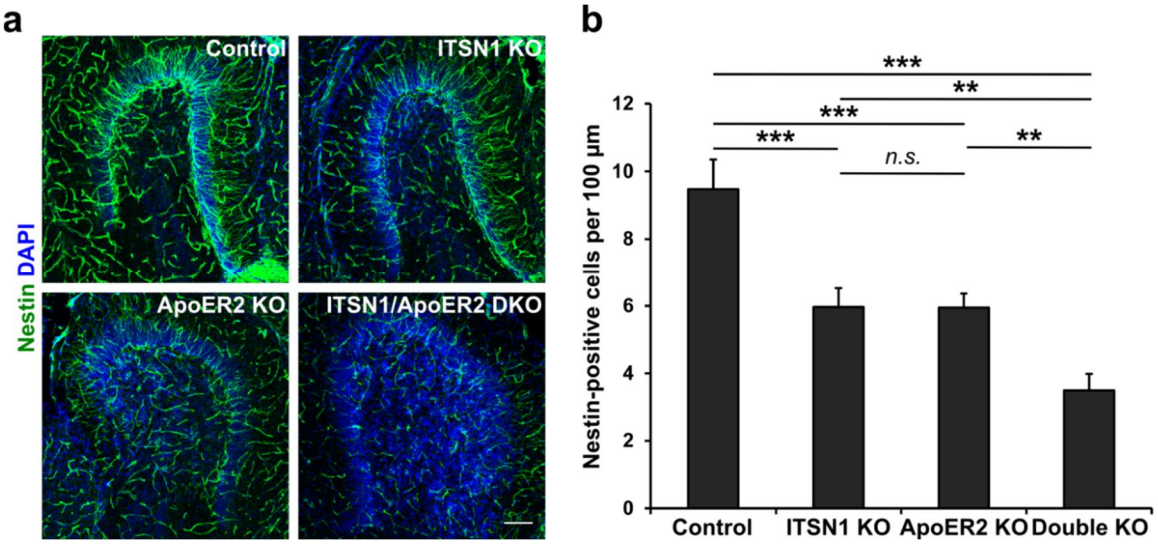

Figure 3.25 The number of Nestin-positive processes is further reduced in hippocampi of ITSN1/ApoER2 double KO mice compared to the single KOs. (a) Immunohistochemical staining for Nestin in horizontal sections of brains from different mouse mutants. Double heterozygous mice were used as control. Scale bar: 100 µm. **(b)** The number of Nestin-positive cells in the DG is reduced to a similar extent in ITSN1 KO and ApoER2 brains. These effects are additive since the number is further reduced in ITSN1/ApoER2 DKO mice (mean + SEM; n = 16, 20, 13 and 20 brains slices from 4, 5, 4, and 5 mice each; $P < 0.0001$; one-way ANOVA with Newman-Keuls post hoc analysis; $^{**}p < 0.01$, $^{***}p < 0.001$).

Deficiency of ITSN1 led to an accumulation of Dcx-positive newborn neurons in the hilus region. ApoER2 KO mice showed a similar ectopic localization of Dcx-positive cells, albeit to a stronger extent, indicating that deficits in Reelin signaling are the underlying cause of this pattern (Fig. 3.26). Interestingly, the number of hilar ectopic Dcx-positive cells was further increased in ITSN1/ApoER2 DKO mice. These findings further corroborate the idea that ITSN1 and ApoER2 both participate in Reelin signaling but are components of different signaling branches.

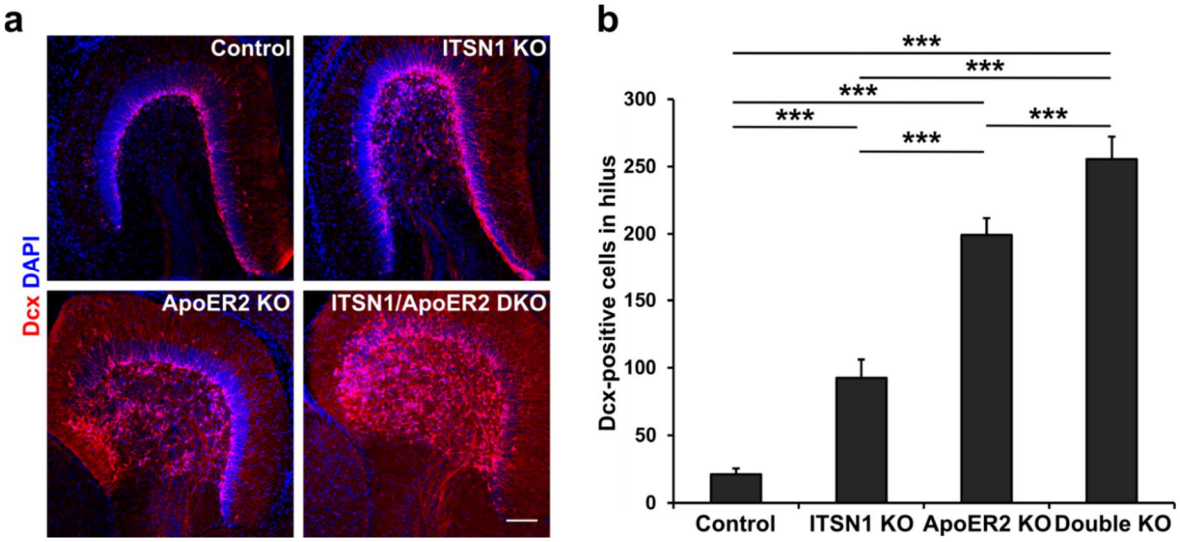

Figure 3.26 The number of Dcx-positive cells in the hilar region is further increased in hippocampi of ITSN1/ApoER2 double KO mice compared to the single KOs. **(a)** Immunohistochemical staining for Dcx in horizontal sections of brains from different mouse mutants. Double heterozygous mice were used as control. Scale bar: 100 µm. **(b)** The number of Dcx-positive cells in the hilus is elevated in ITSN1 KO and ApoER2 KO brains. The number is further increased in ITSN1/ApoER2 DKO mice (mean + SEM; n = 16, 20, 13 and 20 brains slices from 4, 4, 5, and 5 mice each; $P < 0.0001$; one-way ANOVA with Newman-Keuls post hoc analysis; ***$p < 0.001$).

Both VLDLR and ApoER2 have been implicated in cerebellar development, with loss of VLDLR being more detrimental (Trommsdorff et al., 1999). Cerebella of VLDLR- or ApoER2-deficient mice have been described as smaller and less foliated than in WT animals. To find out if ITSN1 plays a role for cerebellar development, Nissl-stained horizontal brain sections from ITSN1 KO, ApoER2 KO and ITSN1/ApoER2 DKO mice were compared with control animals. Surprisingly, no overt difference was detected between the different mouse strains (Fig. 3.27). The previously described decrease in cerebellar size in ApoER2 KO mice could not be confirmed. Similarly, the cerebellum of ITSN1/ApoER2 DKO mice is fully formed and not comparable with the rudimentary cerebellum seen in VLDLR/ApoER2 DKO mice. This suggests that ITSN1 is dispensable for cerebellar development, most likely because its function in VLDLR signaling can be assumed by another protein in this context.

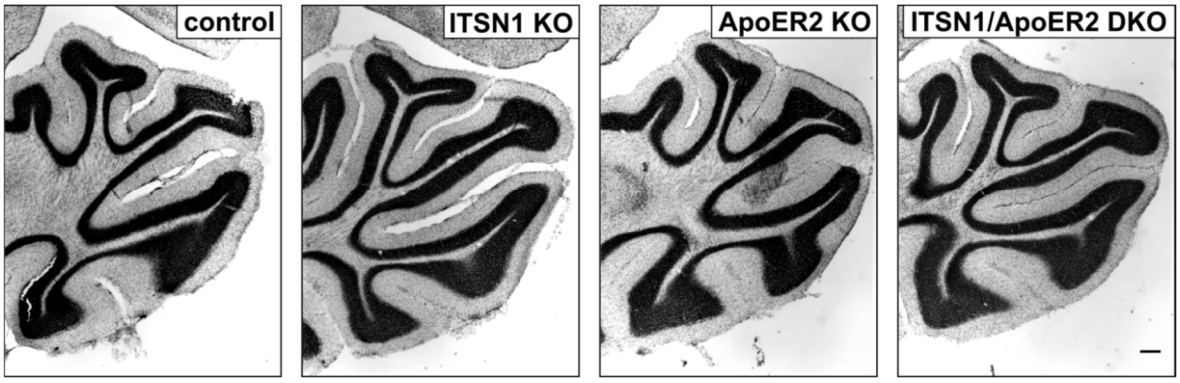

Figure 3.27 Absence of ITSN1 and/or ApoER2 does not have a notable effect on cerebellar morphology. Nissl-stained horizontal sections of cerebella from different mouse mutants. Absence of ITSN1 and/or ApoER2 has no obvious effect on shape or size of the cerebellum when compared to double heterozygous animals (control). Scale bar: 200 µm.

Reelin signaling has been shown to be essential for the development of a layered cerebral cortex. In ITSN1 KO, ApoER2 KO and ITSN1/ApoER2 DKO mice, overall cortical layering was comparable with control animals (Fig. 3.28a). Nissl staining revealed that cortical layer I was largely devoid of neuronal cells in control, ITSN1 KO or ApoER2 KO animals (Fig. 3.28b). In contrast, in ITSN1/ApoER2 DKO mice, a vast number of neuronal cell bodies were seen in layer I. Such an ectopic accumulation of neurons in layer I has also been described for VLDLR/ApoER2 DKO mice due to excessive migration of late-born neurons (Trommsdorff et al., 1999). In the cortex, MAP2-positive dendritic processes are usually arranged in a radial pattern. In ApoER2 KO mouse this radial arrangement of cortical dendrites is poorly developed (Fig. 3.28c). Interestingly, in ITSN1/ApoER2 DKO mice the radial pattern was completely absent and appeared similar to the previously described phenotype of VLDLR/ApoER2 DKO mice (Trommsdorff et al., 1999). These findings indicate a role for ITSN1 for in Reelin/VLDLR-dependent cortical layering.

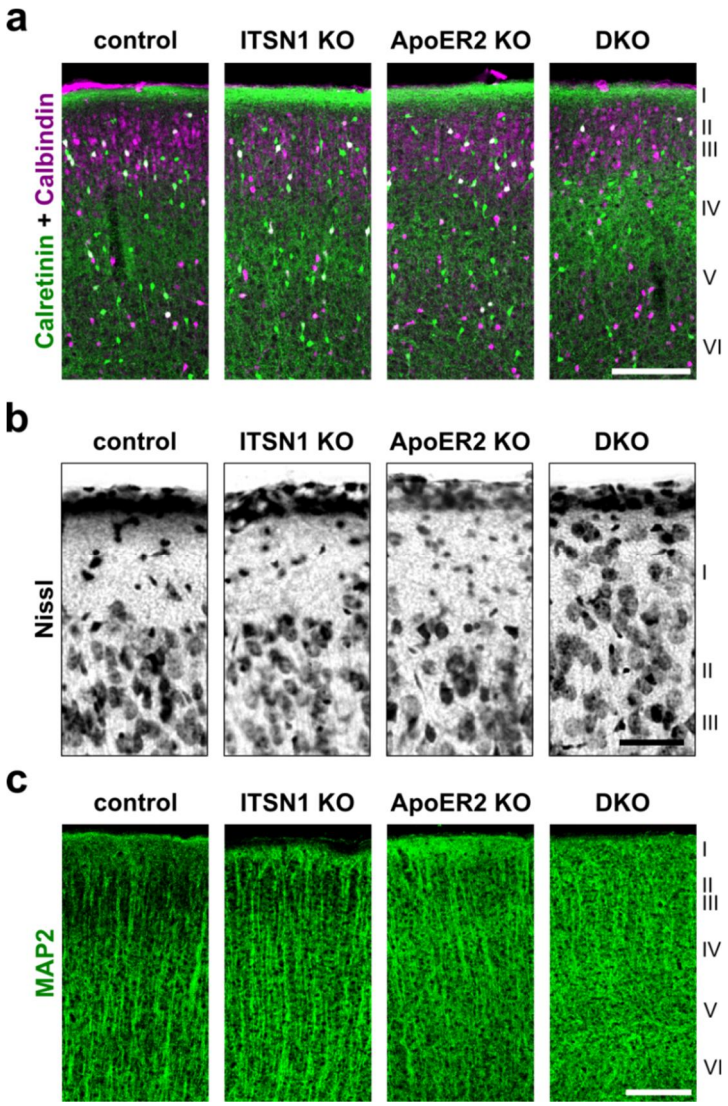

Figure 3.28 ApoER2/ITSN1 double KO mice have defects in cortical layer and bundle formation. **(a)** Immunohistochemical staining for Calbindin and Calretinin in horizontal sections from different mouse mutants shows no difference in overall cortical layering. Scale bar: 200 µm. **(b)** Nissl-staining reveals an elevated number of neuronal cell bodies in cortical layer I of ITSN1/ApoER2 DKO mice. Scale bar: 50 µm. **(c)** MAP2-positive dendritic processes show a radial arrangement in the cortex of control and ITSN1 KO mice. This pattern is incompletely formed in ApoER2 KO mice and completely absent in ITSN1/ApoER2 DKO mice. Scale bar: 200 µm. Double heterozygous mice served as control.

Taken together, the biochemical, electrophysiological and genetical data presented here provide evidence for a so far undescribed function of ITSN1 in Reelin signaling through the VLDLR.

4. Discussion

4.1 A novel role for ITSN1

Scaffolding during clathrin-mediated endocytosis (CME) has been considered the canonical function of intersectin 1 (ITSN1) but additional roles of ITSN1 in signaling and trafficking have been described (Hunter et al., 2013). In the present work, we describe a novel role for ITSN1 in Reelin signaling through the very-low-density-lipoprotein receptor (VLDLR). We demonstrate that ITSN1 regulates neuronal migration and adult neurogenesis in the hippocampus, processes known to be controlled by Reelin. Furthermore, electrophysiological measurements revealed a function for ITSN1 in Reelin-dependent modulation of synaptic plasticity in the hippocampus. Specifically, ITSN1 participates in Reelin signaling downstream of the VLDLR, shown by biochemical and genetic approaches. These data provides evidence for a so far unidentified role of ITSN1 in brain development and physiology, which may have implications for neurological diseases.

4.2 ITSN1 KO mice display defects in neuronal migration, adult neurogenesis and synaptic plasticity

Perturbation of ITSN1 expression in mice results in a rather mild phenotype with no obvious impairment to health or fitness (Fig 3.1). In contrast, genetic ablation of essential endocytic proteins like Clathrin, Dynamin1 or AP-2 leads to premature lethality (Bazinet et al., 1993; Mitsunari et al., 2005; Ferguson et al., 2007). This suggests that expression of ITSN1 is not essential for such a vital process as clathrin-mediated endocytosis.

Morphological analysis of ITSN1 KO brains revealed disrupted lamination of the hippocampus (Fig. 3.3). This finding suggests that ITSN1 acts during development of hippocampal layers, a so far undescribed function of ITSN1. A similar, albeit much stronger, phenotype is displayed by mice lacking the expression of Reelin protein (*reeler*). Reelin is required for the formation of distinct layers in Cornu Ammonis (CA) regions and the dentate gyrus (DG). Mice lacking expression of the Reelin receptors, ApoER2 (apolipoprotein E receptor 2) and VLDLR, exhibit milder versions of hippocampal cell dispersion than *reeler* mice. Notably, hippocampi of VLDLR KO mice appeared strikingly similar to those of ITSN1 KO mice (Trommsdorff et al., 1999). This result gave first indication that ITSN1 might be part of the Reelin signaling machinery controlling neuronal migration and hippocampal development.

The idea of ITSN1 as a component of the Reelin pathway was corroborated by the finding that adult neurogenesis in the DG is affected in ITSN1 KO mice. In the absence of ITSN1, the radial glia scaffold is disrupted and neural progenitors accumulate ectopically in the hilus (Figs. 3.4 and 3.5). Furthermore, dividing progenitor cells in ITSN1 KO mice are mislocalized as revealed by BrdU injections and stainings (Fig 3.7c-d). Similar observations were made in Reelin signaling mutants (Teixeira et al., 2012). Reelin influence on hippocampal neurogenesis seems to be mediated by indirect, migration-dependent and direct, cell-autonomous effects (Teixeira et al., 2012; Brunne et al., 2013). A direct influence of Reelin on DG radial glial cells is in line with strong expression of VLDLR in these cells (Fig 3.17d).

Interestingly, the disruptions in adult neurogenesis do not result in a reduced number of adult neurons or a smaller DG (Fig. 3.6). The reason for this appears to be a

compensatory increase in proliferation, shown by BrdU-positive cells (Fig 3.7a-b), which also extends to organotypic hippocampal slice cultures (Fig. 3.8). This finding differs from *reeler* mice, where proliferation in the hippocampus is decreased (Zhao et al., 2007). Notably, the defect in *reeler* mice can be explained by the severe disruption of the neurogenic zone which affects precursor proliferation indirectly (Brunne et al., 2013). DG formation and the radial glia scaffold are much less affected in ITSN1 KO than in *reeler* mice. Therefore, the disruptions in the radial glia scaffold can probably be more easily compensated for in ITSN1 KO mice. Proliferation in the subgranular zone is regulated by a variety of cues (Faigle and Song, 2013) which makes homeostatic control a likely explanation for the increased BrdU incorporation in ITSN1 KO mice.

An essential function for ITSN1 in Reelin-induced signaling was demonstrated by long-term potentiation (LTP) measurements in Schaffer collateral synapses (Fig. 3.22). LTP induction by theta burst stimulation (TBS) in slices from ITSN1 KO mice is indistinguishable from wildtype (WT) slices when perfused with control medium. This is in agreement with previous data showing unaltered LTP in the absence of ITSN1 (Sengar et al., 2013). In contrast, ITSN1 is specifically required for augmentation of LTP by Reelin-conditioned medium. Reelin effects on synaptic plasticity depend on the presence of both Reelin receptors as genetic ablation of VLDLR or ApoER2 completely abrogate Reelin-induced LTP augmentation (Weeber et al., 2002). Notably, ApoER2 KO mice show perturbed LTP induction in control conditions, in contrast to VLDLR KO mice (Weeber et al., 2002). Therefore, normal LTP induction in control conditions and impaired LTP augmentation upon stimulation in ITSN1 KO mice are compatible with a VLDLR-specific role for ITSN1 in Reelin signaling.

The Reelin effect on LTP is mediated by elevated N-methyl-D-aspartate receptor (NMDAR) potentials, which remain unaffected in ITSN1 KO slices upon Reelin treatment (Fig. 3.23). Reelin binding to VLDLR or ApoER2 activates Src family kinases (SFKs) such as Src and Fyn (Arnaud et al., 2003b; Bock and Herz, 2003). Src and Fyn have been shown to phosphorylate NMDARs and thereby modulate their function (Suzuki and Okumura-Noji, 1995; Miyakawa et al., 1997). SFK-dependent phosphorylation of NMDARs is considered the molecular basis for control of NMDAR currents by Reelin signaling (Chen et al., 2005). As SFK activation represents an early

step of the Reelin signaling cascade occurring at the plasma membrane, the defects in Reelin-induced LTP elevation in ITSN1 KO mice suggest a functional role for ITSN1 in early, membrane-localized Reelin signaling events. Taken together with the interaction data showing an association of ITSN1 with VLDLR and its adaptor Dab1, this implies a high position for ITSN1 in the Reelin-VLDLR signaling hierarchy. Interestingly, ITSN1 has been shown to bind NMDAR components (Nishimura et al., 2006). This would enable ITSN1 to bring the Reelin signaling machinery, VLDLR, Dab1 and, possibly, SFKs, in close proximity to NMDARs. In doing so, ITSN1 could promote efficient phosphorylation of NMDARs thereby fulfilling the function of a classical scaffold protein.

Basal synaptic transmission is unaffected in ITSN1 KO mice (own unpresented observations and Sengar et al., 2013). In contrast, the invertebrate ortholog Dap160 is required for synaptic vesicle (SV) recycling and normal synaptic transmission (Marie et al., 2004; Wang et al., 2008). This implies that ITSN1 has, if at all, only a minor role for SV cycling in vertebrates. Alternatively, the function of ITSN1 in SV exo-/endocytosis could be assumed by other proteins in the mammalian synapse. An obvious candidate for this role is its close relative, ITSN2. Future studies will reveal the individual contributions of ITSN1 and ITSN2 to SV trafficking and synaptic function.

4.3 EphB signaling is unperturbed in ITSN1 KO mice

Synaptic transmission depends on both pre- and postsynaptic processes. ITSN1 has been shown to be a regulator of postsynaptic development, namely dendritic spine maturation (Thomas et al., 2009). Activation of Cdc42 by ITSN1 can promote actin polymerization and influence spine morphology. It has been suggested that ITSN1 acts as an effector of EphB forward signaling in this context to regulate dendritic spine formation (Irie and Yamaguchi, 2002; Nishimura et al., 2006). Notably, EphB receptors have also been implicated in hippocampal lamination and adult neurogenesis (Chumley et al., 2007; Catchpole and Henkemeyer, 2011). Therefore, an important question was whether the phenotype displayed by ITSN1 KO mice could be caused by defects in EphB forward signaling.

Interestingly, dendritic spines were unaffected morphologically in the absence of ITSN1 (Fig 3.14). In line with this, the levels of active, GTP-loaded Cdc42 were similar in the absence of ITSN1 (Fig. 3.13c). This is in agreement with normal synaptic transmission and LTP levels discussed above. Furthermore, we could not confirm the previously described association of ITSN1 and EphB2 (Fig. 3.10). Despite its described role in endocytosis, ITSN1 is also dispensable for the internalization of soluble or membrane-associated ephrinB ligands (Figs. 3.11 and 3.12).

EphB-mediated forward signaling, assessed by ephrinB-induced collapse of growth cones, was unaltered in hippocampal explants from ITSN1 KO mice when compared to WT littermates (Fig. 3.13a-b). Defective axon guidance by ephrins and Eph receptors leads to malformations of axonal commissures as the corpus callosum (Mendes et al., 2006). It is worth mentioning that ITSN1 also has been implicated in commissure formation, supported by data from a different ITSN1 KO mouse, created by a gene-trap approach (Sengar et al., 2013). In contrast to the published data, we could not confirm an essential role of ITSN1 for commissure formation (Fig 3.15). It is noteworthy that agenesis of the corpus callosum is a phenotype frequently found in a variety of WT mouse strains, including the 129Sv strain employed by Sengar et al. (Wahlsten, 1982). Therefore, further research is required to shed light on the contribution of ITSN1 to hemisphere connectivity.

Ephrins/Eph receptors have been implicated in adult neurogenesis in both the DG and the subventricular zone (SVZ; Laussu et al., 2014). In contrast, Reelin

signaling is not required for neurogenesis in the SVZ (Kim et al., 2002). Notably, the neurogenesis defects in ITSN1 KO mice only pertain to the DG whereas neurogenesis in the SVZ remains unaltered (Fig. 3.9). This is compatible with the idea that ephrin/Eph receptor signaling remains unperturbed in the absence of ITSN1.

In sum, the data presented in this work does not support a fundamental role of ITSN1 for ephrin/Eph receptor-dependent processes as spine development, corpus callosum formation or SVZ neurogenesis. Any alteration observed in ITSN1 KO mice can be attributed to defective Reelin signaling through the VLDLR in the absence of ITSN1.

Remarkably, a certain crosstalk between ephrinB/EphB signaling and Reelin signal transduction seems to exist (Senturk et al., 2011; Bouche et al., 2013). EphrinBs have been shown to associate with Reelin, ApoER, VLDLR and Dab1. Furthermore, ephrinBs are required for Reelin-induced Dab1 phosphorylation by SFKs (Senturk et al., 2011) although this finding was questioned by others (Bouche et al., 2013). Notably, Reelin also interacts with EphB receptors and activates EphB forward signaling (Bouche et al., 2013). Furthermore, disruption of EphB2 forward signaling seems to affect Reelin expression during hippocampal development (Catchpole and Henkemeyer, 2011). These results suggest a complex interplay between Reelin and ephrinB/EphB signaling pathways. ApoER2, VLDLR, EphBs and ephrinBs all seem to interact with extracellular Reelin. Therefore, these transmembrane proteins likely operate in close proximity or even associate in macromolecular complexes. It appears plausible that such a complex formation has an impact on the different signaling pathways.

Additionally, many downstream effector molecules are shared by ephrinB/EphB and Reelin signaling, e.g. SFKs, Akt or small G-proteins. In line with this, there is also considerable overlap in the processes regulated by ephrinB/EphB and Reelin signaling, i.e. neuronal migration, neurogenesis and synaptic plasticity. This implies that these signaling pathways are indeed physically and functionally connected. The practical relevance of this crosstalk and a possible involvement of ITSN1 remain to be elucidated.

4.4 ITSN1 is a component of the Reelin-VLDLR signaling pathway

Biochemical interaction studies revealed that ITSN1 associates with the signaling adaptor Dab1 and the Reelin receptor VLDLR, but not ApoER2 (Figs. 3.16 and 3.20). ITSN1 SH3 domains can mediate the association with both VLDLR and Dab1. In addition, ITSN1 EH domains provide a second interaction site for Dab1. Interestingly, ITSN1 SH3s only bind to full-length Dab1, but not to Dab1 fragments with C-terminal deletions (Fig 3.20a). This suggests that the binding site for ITSN1 SH3s lies near the C-terminus of Dab1. Notably, Dab1 harbors a proline-rich region (PRR) near its C-terminus, suggesting a classical SH3-PRR interaction. In contrast, VLDLR and ApoER2 bind to Dab1 fragments with C-terminal deletions, as do the ITSN1 EH domains. This is in agreement with the described association of the NPXY motif in Reelin receptors with the N-terminal PTB domain of Dab1 (Howell et al., 1997a). This indicates that different Dab1 domains can mediate the interaction with VLDLR/ApoER2 and ITSN1, respectively, allowing for simultaneous binding of Dab1 to Reelin receptors and ITSN1. This suggests that ITSN1 is indeed part of a complex consisting of ITSN1, VLDLR, Dab1 and possibly other components.

The idea of ITSN1 as a crucial element for Reelin-VLDLR signaling is corroborated by genetic data. ApoER2 KO mice show similar perturbations of hippocampal morphology (Fig. 3.24) and neurogenesis (Figs. 3. 25 and 3.26) as ITSN1 KO mice, albeit to a stronger degree. This suggests that the observed phenotype in ITSN1 KO mice can indeed be attributed to disruptions in the Reelin pathway. Genetic ablation of ITSN1 and ApoER2 aggravates the adverse effects on hippocampal lamination, neurogenesis and also disrupts cortical layering (Figs. 3.24-3.26 and 3.28). These findings provide evidence that ITSN1 and ApoER2 operate in distinct pathways, supporting the biochemical findings. A mutant mouse lacking both ITSN1 and VLDLR expression could further substantiate this conclusion. If the phenotype of such an ITSN1/VLDLR DKO mouse was comparable to VLDLR KO mice this would give definite proof of a functional role for ITSN1 in VLDLR receptor signaling.

The question remains why ITSN1 is specifically needed for VLDLR to mediate Reelin signaling, while ApoER2-dependent Reelin signaling does not require ITSN1. A

possible explanation for this difference could be that ApoER2 has a higher intrinsic affinity for Dab1 and therefore does not require Dab1 recruitment by ITSN1 to elicit a signaling response. However, Dab1 seems to bind VLDLR and ApoER2 with similar strength in HEK293 cells that do not express ITSN1 (Fig. 3.20a and Trommsdorff et al., 1999). Alternatively, recruitment of Dab1 molecules to Reelin receptors could be important for efficient signal transduction *in vivo* (see below). In this scenario, ITSN1 would assist VLDLR-dependent signaling whereas other, yet unidentified scaffold or adaptor proteins would aid the ApoER2-dependent branch. Another explanation is that ITSN1 bridges the VLDLR-Dab1 complex with downstream effector proteins specific for VLDLR signaling (see below). Further investigation of the VLDLR-Dab1-ITSN1 pathway is required to distinguish between these hypotheses.

As ITSN1 is widely accepted as endocytic protein, a possible explanation for the observed phenotype in ITSN1 KO mice is altered trafficking of Reelin receptors, particularly VLDLR. Additionally, ITSN1 has been shown to interact with Dab2, an endocytic adaptor for lipoprotein receptors (Teckchandani et al., 2012). Strikingly, endocytosis of Reelin receptors can occur independently of ITSN1, as shown by surface biotinylation and antibody uptake assays (Fig 3.18). This renders the defects in ITSN1 KO mice unlikely to be the consequence of altered endocytic trafficking of Reelin receptors.

Interestingly, Dab2 associated with ITSN1 SH3 and EH domains, with the SH3 interaction being considerably stronger (Fig. 3.19a). This is contrary to the published observation that the Dab2-ITSN1 interaction relies on NPF motifs in Dab2 and the EH domains in ITSN1 (Teckchandani et al., 2012). Dab2 also binds to both Reelin receptors, with a strong preference for VLDLR (Fig. 3.19b), which conflicts with previous data showing ApoER2-specific binding of Dab2 (Yang et al., 2002; Cuitino et al., 2005). Based on our findings, we hypothesized that the SH3-mediated interaction of ITSN1 with VLDLR is indirect and mediated by Dab2. However, complex formation between ITSN1 and VLDLR is independent of Dab2 (Fig 3.19c-e). This suggests that Dab2 is dispensable for ITSN1 recruitment to VLDLR and is compatible with an endocytosis-independent function of ITSN1 for Reelin signaling.

Remarkably, lack of ITSN1 expression does not cause defects in all brain regions known to rely on Reelin function. The disruptions in brain development and function in ITSN1 KO mice seem to be restricted to the hippocampal area while cortical or

cerebellar development is not affected in ITSN1 KO mice (Figs. 3.27 and 3.28). In contrast, Reelin signaling is crucial for the development of the cerebral cortex and the cerebellum. Therefore, one important question is, why ITSN1 is only required for Reelin-dependent processes in the hippocampus, but not in other brain regions. It is conceivable that the role of ITSN1 in the hippocampus is assumed by different proteins in other brain regions. ITSN1 and its close relative ITSN2 are differentially expressed in the nervous system (Pucharcos et al., 2001). Due to their sequence similarity, it is easily conceivably that ITSN1 and ITSN2 have similar roles for Reelin receptor signaling but fulfill this function in different brain areas. Disruption of Reelin signaling results in smaller and less foliated cerebella (Goffinet et al., 1984; Miyata et al., 1997; Trommsdorff et al., 1999). Regarding the Reelin receptors, genetic ablation of VLDLR causes a much stronger disruption of cerebellar development than of ApoER2 (Trommsdorff et al., 1999). The cerebellar disruptions in Reelin pathway mutants are due to failed migration of Purkinje cells (Larouche et al., 2008). In line with this, VLDLR is much stronger expressed in Purkinje cells than ApoER2. Interestingly, also ITSN2 is abundantly expressed in Purkinje cells (Pucharcos et al., 2001). Therefore, it is plausible that ITSN2, and not ITSN1, mediates Reelin-VLDLR signaling in cerebellar Purkinje cells. Examination of ITSN2 KO and ITSN1/ITSN2 DKO mice would shed light on the particular role of the two ITSN genes for cerebellar development.

It is noteworthy that in our hands ApoER2 KO mice did not display any obvious alterations in cerebellar morphology in horizontal sections (Fig 3.27). Possibly, sagittal sectioning would be required to reveal the rather subtle cerebellar defects described for ApoER2 KO mice (Trommsdorff et al., 1999). This approach is also advised for a thorough analysis of potential cerebellar disruptions in ITSN1 KO, ITSN2 KO and ITSN1/ITSN2 DKO animals.

Additional explanations for the hippocampus-specific defects in ITSN1 KO mice exist. Reelin signaling seems to be only mildly affected in the absence of ITSN1, indicated by a ~20% reduction in levels of phosphorylated Dab1 (Fig. 3.21a). Nevertheless, this rather small decrease leads to marked disruptions in hippocampal development, neurogenesis and synaptic plasticity while cortex and cerebellum remain apparently unperturbed. This could indicate that the hippocampus-specific processes are more sensitive to disruptions in Reelin signaling than cortical or

cerebellar development (see below). It is also possible that deficient Reelin-VLDLR signaling can be compensated for by other signaling pathways in these regions. The best candidate for such a homeostatic mechanism would of course be ApoER2-dependent Reelin signaling. ITSN1 and ApoER2 operate in distinct pathways, shown by biochemical and genetic data (Figs. 3.16, 3.24-3.26 and 3.28). The fact that simultaneous ablation of ITSN1 and ApoER2 aggravates the phenotype not only in the hippocampus (Figs. 3.24-3.26) but also in the cortex (Fig. 3.28) suggests that ITSN1 has indeed a role for cortical development. This function is masked in the presence of ApoER2 but becomes apparent in its absence. This suggests that Reelin-ApoER2 signaling can counteract the adverse effects of ITSN1 deficiency in the cortex but not in the hippocampus.

It is conceivable that Reelin activates distinct downstream pathways and that ITSN1 is only required for a specific branch of Reelin-VLDLR signaling. It has been suggested that distinct Reelin signaling mechanisms underlie the different Reelin functions for brain development and function (Lee and D'Arcangelo, 2016). A possible differential requirement of ITSN1 for the activation of these signaling branches remains to be elucidated.

4.5 A function for ITSN1 in Reelin signal transmission

What is the mechanism by which ITSN1 mediates Reelin signaling through VLDLR? VLDLR binds Dab1 in the absence of ITSN1 (Fig. 3.20a and Trommsdorff et al., 1999). Therefore, it is rather surprising that ITSN1 is required for VLDLR-Dab1 signaling *in vivo*. The effect of ITSN1 on Reelin signaling could be, in principle, qualitative or quantitative. ITSN1 could bridge phosphorylated Dab1 with effector proteins further downstream in the signaling cascade, thereby controlling the signaling outcome. As a matter of fact, ITSN1 has been linked to a number of different cellular signaling pathways. ITSN1 participates in activation of Akt in a PI3KC2β-dependent manner (Das et al., 2007) whereas Reelin-Dab1 signaling activates a class I PI3K-Akt pathway (Beffert et al., 2002; Bock et al., 2003). Notably, ITSN1 is also capable of binding to p85, the regulatory subunit of class I PI3Ks (Wong et al., 2012). Surprisingly, the levels of phosphorylated Akt are unaltered in ITSN1 KO mice, despite decreased Dab1 activation (Fig 3.21). This could indicate that ITSN1 is only required for Akt-independent branches of Reelin signaling. Alternatively, normal Akt phosphorylation levels in ITSN1 KO mice could be achieved by increased activity of a different receptor. Given the importance of Akt and its variety of upstream activators (Franke, 2008), it is not unlikely that the levels of phosphorylated Akt are controlled by homeostatic mechanisms. In the case of the ITSN1 KO mouse, increased activation of the PI3K-Akt pathway by ApoER2 appears as a possible way to achieve homeostatic control. Assessing phosphoAkt levels in ITSN1/ApoER2 DKO mice should shed light on this question.

Reelin signaling induces the phosphorylation of cofilin, thereby inhibiting its activity (Chai et al., 2009a; Chai et al., 2009b). This effect is apparently exclusively mediated by ApoER2, as levels of phosphorylated cofilin are only decreased in ApoER2 KO but not in VLDLR KO mice (Chai et al., 2009a; Chai et al., 2009b). Similarly, the amount of phosphorylated cofilin was not changed in ITSN1 KO mice (Fig 3.21b-c), in agreement with a VLDLR-specific role for ITSN1 in Reelin signaling.

Cdc42, a known binding partner of ITSN1, has also been shown to be a downstream effector of Reelin signaling. Nevertheless, impaired Cdc42 activation is

unlikely to cause the observed phenotype, as the levels of active Cdc42 are unaltered in neurons from ITSN1 KO mice (Fig. 3.13c). Cdc42 activation seems to be specifically mediated by ApoER2 and not VLDLR (Leemhuis et al., 2010). Therefore, unchanged levels of active Cdc42 in ITSN1 KO mice are compatible with an exclusive requirement of ITSN1 for the VLDLR branch of Reelin signaling.

VLDLR interacts with Lis1 and the Pafah1b complex thereby regulating microtubule dynamics (Assadi et al., 2003; Zhang et al., 2007). Lis1 also forms a complex with DISC1 (Disrupted in Schizophrenia 1), an important schizophrenia risk factor (Camargo et al., 2007). Interestingly, ITSN1 also associates with DISC1 (Wong et al., 2012) suggesting a possible role for ITSN1 in the control of microtubule dynamics downstream of VLDLR. In line with this, a function of ITSN1 for microtubular stability has been proposed based on its interaction with the microtubule stabilizer STOP (or MAP6) in neurons (Morderer et al., 2012). It is therefore conceivable that ITSN1 participates in Reelin-VLDLR-dependent remodeling of the microtubule cytoskeleton.

ITSN1 has been implicated in ubiquitylation and degradation of growth factor receptors through activation of the E3 ubiquitin ligase Cbl (Martin et al., 2006). Inefficient degradation of Reelin receptors or Dab1 could therefore contribute to the observed defects in ITSN1 KO mice. However, total levels of ApoER2, VLDLR and Dab1 are unchanged in the absence of ITSN1 (Fig. 3.17c), arguing against a role of ITSN1 in Reelin receptor or Dab1 degradation. In line with this, ApoER2, VLDLR and Dab1 have been shown to be ubiquitylated by other E3 ligases than Cbl (Arnaud et al., 2003a; Feng et al., 2007; Hong et al., 2010).

Reelin-dependent phosphorylation of Dab1 induces its ubiquitylation and subsequent degradation (Feng et al., 2007). As a consequence, amounts of Dab1 are greatly increased in mutants of the Reelin signaling machinery (Rice et al., 1998; Trommsdorff et al., 1999). Surprisingly, the total levels of Dab1 are unaltered in ITSN1 KO mice (Fig. 3.17c), despite a reduction in phosphorylated Dab1 (Fig 3.21). One explanation could be that the decrease in phosphoDab1 levels is not strong enough to result in a conspicuous elevation of total Dab1. Increased activation of the ApoER2 signaling pathway in ITSN1 KO mice might ensure sufficient Dab1 phosphorylation to prevent an accumulation of Dab1 molecules. In line with this hypothesis, total Dab1 levels are only mildly increased in VLDLR KO mice but strongly

elevated in VLDLR/ApoER2 DKO animals (Trommsdorff et al., 1999). Examination of phosphoDab1 and total Dab1 levels in ApoER2 KO and ITSN1/ApoER2 DKO mice should reveal whether ApoER2 indeed fulfills a compensatory function in ITSN1 KO mice.

As mentioned above, ITSN1 is crucial for Reelin-dependent LTP elevation via NMDARs (Figs. 3.22 and 3.23) and is also physically associated with NMDARs (Nishimura et al., 2006). As both Dab1 and NMDARs are phosphorylated by SFKs (Arnaud et al., 2003b; Bock and Herz, 2003; Chen et al., 2005), this suggests a hierarchically high position of ITSN1 in the Reelin signaling cascade. It would be worth investigating whether ITSN1 forms a complex with SFKs to fulfill its function in Reelin signal transduction.

Instead of linking active VLDLR and Dab1 with effector proteins, ITSN1 binding to Dab1 and VLDLR might ensure high local concentrations of Dab1 at the site of Dab1 phosphorylation. A single ITSN1 molecule harbors at least two binding sites for Dab1 (Fig 3.20). Additionally, through coiled-coil-mediated interaction, ITSN1 can likely form oligomers and thereby recruit further Dab1 molecules. Interestingly, oligomeric Dab1 has been shown to be the substrate for SFKs (Strasser et al., 2004). Hence, ITSN1 could function as a scaffold providing a sufficient amount of Dab1 molecules in close vicinity to VLDLR and SFKs.

Interesting insights into Reelin-Dab1 signal transduction come from mice expressing mutant forms of Dab1. A single point mutation in the PTB domain of Dab1 ($Dab1^{F158V}$) strongly decreases its binding affinity to ApoER2 or VLDLR cytoplasmic domains (Herrick and Cooper, 2004). Surprisingly, mice homozygous for this mutation display no defects whereas $Dab1^{F158V/-}$ hemizygous animals show only a very subtle phenotype. Such a gene dose dependency is not seen for WT Dab1. This implies that an adequate number of Dab1 molecules in immediate proximity of Reelin receptors are paramount for efficient signaling. Similar conclusions can be drawn from mouse mutants expressing only a certain splice isoform of Dab1, p45, which lacks the C-terminal region of full-length Dab1, p80 (Herrick and Cooper, 2002). $Dab1^{p45/p45}$ mice show no discernable phenotype while $Dab1^{p45/-}$ animals have minor defects. This suggests that both $Dab1^{F158V}$ and $Dab1^{p45}$ are hypomorphic alleles which are quantitatively less effective at signaling. Notably, the Dab1 C-terminus seems to provide the interaction site for ITSN1 SH3 domains (Fig 3.20a). Hence, $Dab1^{p45}$

probably has a reduced affinity to ITSN1 and, as a result, fails to be efficiently recruited to VLDLR. This could, at least partially, explain the phenotype of Dab1$^{p45/-}$ mice.

Disruptions in Dab1$^{p45/-}$ animals are restricted to the hippocampus and the cortical marginal zone/layer I. Interestingly, ITSN1 seems to be specifically needed for the proper formation of these brain regions (Fig. 3.3 and 3.28). This is in line with the notion of ITSN1 aiding the recruitment of Dab1 to VLDLR. Region-specific defects have also been described for Dab1$^{F158V/-}$ mice which only show ectopic accumulation of neurons in layer I. Remarkably, migration of early cortical plate neurons is unaffected in Dab1$^{p45/-}$ and Dab1$^{F158V/-}$ mice resulting in normal overall cortical layering, similar to ITSN1 KO mice (Fig. 3.28a). This implies that highly efficient Reelin signaling is vital for migration of late-born cortical neurons and hippocampal lamination but less important for cerebellar development and migration of early-born cortical neurons. These different requirements could explain the tissue-specific effects of ITSN1 deficiency discussed above. In this model, ITSN1 would provide high local concentrations of Dab1, thereby ensuring efficient signal transduction. Lack of ITSN1 expression would only affect the development of brain regions with a requirement for efficient Reelin signaling. These comprise cortical layer I and the hippocampus but not the cerebellum, in agreement with the observed phenotype in ITSN1 KO mice (Fig. 3.3 and 3.27-3.28). Differential requirements for signal efficiency also explain why the rather mild decrease in levels of phosphorylated Dab1 (Fig. 3.21a) elicits discernable defects in ITSN1 KO mice.

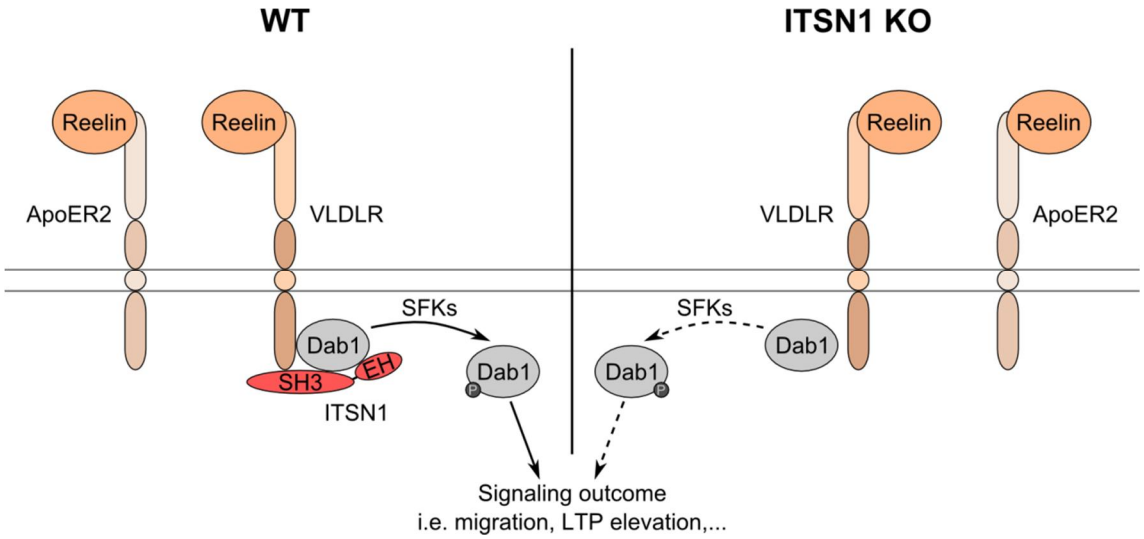

Figure 4.1 Model of ITSN1 function in VLDLR-mediated Reelin signaling. The intracellular region of VLDLR associates with the signaling adaptor Dab1 and the scaffold protein ITSN1. Dab1 also interacts with ITSN1. Binding of Reelin to its receptors, ApoER2 and VLDLR, leads to phosphorylation of Dab1 by Src family kinases (SFKs). Phosphorylated Dab1 is required for Reelin effects on neuronal migration and synaptic plasticity. In the absence of ITSN1 (ITSN1 KO), Dab1 is less efficiently phosphorylated, which impairs efficient signal transmission downstream of VLDLR. ApoER2-dependent Reelin signaling does not rely on ITSN1.

Therefore, a scaffolding function for ITSN1 at the site of Reelin receptor and Dab1 activation, ensuring high local Dab1 concentrations, provides a mechanistical explanation for the observed phenotype of ITSN1 KO mice. This proposed role does not rule out additional functions of ITSN1 for linking phosphorylated Dab1 with downstream effector molecules. Distinguishing between these hypotheses awaits further understanding of the mechanism of VLDLR–Dab1 signal transduction.

4.6 Implications for behavior and disease

Behavioral experiments gave no indication of marked alterations of general activity and exploratory behavior in the absence of ITSN1 (Fig. 3.2). ITSN1 KO mice only showed a tendency towards a more active and explorative behavior without reaching statistical significance. This is in line with previously published data on ITSN1 KO mice showing more active behavior, albeit statistically not significant (Sengar et al., 2013). Interestingly, VLDLR KO mice show hyperactivity in open field experiments (Weeber et al., 2002). Based on the findings presented above, it is conceivable that genetic ablation of ITSN1 or VLDR results in a similar phenotype with regards to activity and explorative behavior. More thorough testing of ITSN1 KO mice is required to clarify if ITSN1 regulates general activity in a similar manner as VLDLR.

Weeber et al. also described deficits of VLDLR KO mice in associative fear-conditioned learning (Weeber et al., 2002), a process depending on hippocampal function (Kim et al., 1993; Chen et al., 1996). ITSN1 is a component of the Reelin-VLDLR signaling pathway and ITSN1 KO mice show hippocampal defects in lamination, neurogenesis and synaptic plasticity. Hence, it is plausible to hypothesize that the hippocampus-related behavioral defects seen in VLDLR KO mice may also be observed in ITSN1 KO mice. Remarkably, Sengar et al. have described deficits of ITSN1 KO mice in a fear conditioning task thereby resembling VLDLR KO mice (Sengar et al., 2013). Moreover, in the same publication the authors showed spatial memory deficits of ITSN1 KO mice in a Morris water maze test, indicating impaired hippocampal function (Morris et al., 1982). Taken together, these findings show that genetic ablation of ITSN1 results in hippocampus-related behavioral defects which can be entirely explained by involvement of ITSN1 in Reelin signaling through the VLDLR. The altered behavior in VLDLR KO and ITSN1 KO mice could be caused by defective lamination, neurogenesis, postsynaptic plasticity or a combination of these. The interplay of these processes and their functional consequences for hippocampal function and behavior in Reelin signaling mutants remain to be elucidated.

Altered Reelin expression has been associated with a variety of neurological disorders, namely schizophrenia, bipolar disorder, major depression, autism, lissencephaly and Alzheimer's disease (Folsom and Fatemi, 2013). Reelin levels are

reduced in brain tissue of patients with schizophrenia, bipolar disorder and major depression (Impagnatiello et al., 1998; Fatemi et al., 2000; Guidotti et al., 2000). Similarly, reduced abundance of the Reelin protein in specific brain regions was described for autism patients (Fatemi et al., 2001; Fatemi et al., 2005). Reelin mutations, resulting in very low serum levels of Reelin, have been associated with lissencephaly (Hong et al., 2000; Chang et al., 2007). Non- or missense mutations in the VLDLR gene have been linked to cerebellar hypoplasia and gyral simplification, the so-called disequilibrium syndrome (Schurig et al., 1981; Moheb et al., 2008; Turkmen et al., 2008; Boycott et al., 2009). Therefore, altered Reelin expression or signaling may result in different neurological diseases with miscellaneous clinical appearances. This highlights the necessity to investigate the mechanisms by which Reelin and its receptors regulate brain development and synaptic function.

Altered Reelin expression and abnormal Reelin signaling have also been linked to the pathological processes resulting in Alzheimer's disease (AD). AD is a complex neurological disease which is characterized by progressive dementia and severe neurodegeneration. Development of AD is associated with abnormal deposits of proteins. Hyperphosphorylated tau forms neurofibrillary tangles inside neurons whereas amyloid plaques can be found extracellularly (Glenner and Wong, 1984; Grundke-Iqbal et al., 1986). The main component of these plaques is the amyloid-β (Aβ) peptide. Aβ arises from sequential cleavage of the amyloid precursor protein (APP) by β- and γ-secretases (Estus et al., 1992; Haass et al., 1992). Cleavage by α-secretase results in non- amyloidogenic peptides with neuroprotective function (Furukawa et al., 1996).

Interestingly, Reelin and its effectors influence AD pathology on several levels. Dab1 can bind to APP and promote non-amyloidogenic processing (Hoe et al., 2006). Reelin stimulates the APP/Dab1 interaction which leads to reduced Aβ production. In addition, Reelin signaling controls tau phosphorylation and Reelin signaling mutants display hyperphosphorylated tau protein (Hiesberger et al., 1999; Ohkubo et al., 2003). Reelin can antagonize the suppressive effects of Aβ on synaptic plasticity (Durakoglugil et al., 2009). Notably, Reelin can be found in Aβ containing plaques (Doehner et al., 2010) and delays Aβ fibril formation (Pujadas et al., 2014). Reelin overexpression can reduce the number of plaques and overcome the detrimental effects of Aβ on neuronal survival and dendritic spine number (Pujadas et al., 2014).

On the contrary, reduction of Reelin results in earlier onset and more severe pathology in an AD mouse model (Kocherhans et al., 2010). Therefore, Reelin seems to counteract the pathological mechanisms underlying AD by different mechanisms. Interestingly, abnormal glycosylation of Reelin as well as a preferential upregulation of the N-terminal 180 kDa Reelin fragment has been observed in AD patients (Botella-Lopez et al., 2006; Botella-Lopez et al., 2010). This suggests that Reelin is differentially processed in AD which might hamper its neuroprotective ability.

Remarkably, the upregulation of Reelin in hippocampi of ITSN1 KO mice seems to be mainly due to increased levels of the N-terminal 180 kDa fragment (Fig 3.17), similar to AD patients. This implies that the mechanisms altering Reelin processing in AD patients may also operate in ITSN1 KO mice. ITSN1 is located on chromosome 21 and therefore upregulated in Down syndrome (DS) patients. DS is associated with intellectual disabilities and an increased risk of AD. Notably, Reelin levels, particularly the 180 kDa fragment, are also elevated in brains from DS patients (Botella-Lopez et al., 2010). In part, this can be explained by the increased levels of APP, also located on chromosome 21, in DS patients. Yet, overexpression of APP alone, as in the Tg2576 mouse model, did not result in elevated levels of the 180 kDa band (Botella-Lopez et al., 2010). Therefore, it is conceivable that overexpression of ITSN1 in DS patients also affects Reelin processing and signaling and thereby contributes to the development of AD. Following this hypothesis, both decreased (ITSN1 KO) and increased (DS patients) levels of ITSN1 would compromise Reelin function, resulting in developmental and pathological disruptions. In fact, different groups found increased expression of ITSN1 in non-DS AD patients highlighting its role as a genetic risk factor for AD (Blalock et al., 2004; Dunckley et al., 2006; Wilmot et al., 2008).

Given its function as scaffold protein, ITSN1 overexpression might indeed cause similar effects as ITSN1 downregulation, e.g. by sequestration of effector proteins as Dab1. Therefore, it would be particularly interesting to test whether overexpression of ITSN1 results in disruptions of Reelin-dependent processes and, possibly, AD-like alterations. Ultimately, manipulation of Reelin- and ITSN1-dependent signaling might constitute a therapeutic strategy for AD and other neurological disorders.

4.7 Future directions

Despite a large number of publications on ITSN1 and its proposed functions in a variety of cellular processes, its precise role for mammalian physiology has remained elusive. Most of the research has focused on the role of ITSN1 for membrane trafficking, especially clathrin-mediated endocytosis. Based on our findings, we suggest a novel, endocytosis-independent function of ITSN1. Its proposed role as a scaffold for VLDLR-mediated Reelin signaling expands the spectrum of ITSN1-related processes. Furthermore, these findings imply a possible mechanism by which VLDLR conveys the Reelin signal to its effector proteins.

The question remains why ITSN1 is exclusively required for VLDLR-mediated Reelin signaling. It is conceivable that another, yet unknown protein fulfills a similar function for ApoER2 signaling as ITSN1 does for VLDR. Identification of such an ApoER2-specific signaling scaffold could shed light on the differential functions of these receptors and most likely provide insights into the molecular mechanisms of Reelin-evoked signaling.

The data presented in this work are in agreement with the notion of ITSN1 acting as a scaffold for efficient transmission of the Reelin signal. Region-specific requirements for Reelin signaling efficiency could also explain the differential response of brain regions to mild Reelin signaling disruptions. Further investigation is necessary to corroborate this concept.

As both ITSN1- and Reelin-dependent processes have been linked to severe neurological diseases, our results also have potential implications for future therapeutic strategies. Considering our results and previously published data, an involvement of VLDLR-ITSN1-mediated signaling in the etiology of AD, particularly in DS patients, appears entirely possible. To support this notion, it would be worth investigating whether downregulation and overexpression of ITSN1 have a similar effect on Reelin signaling and whether this, eventually, results in an AD-like pathology. This would make the VLDLR-ITSN1 pathway a possible target for therapeutic intervention in DS patients to prevent early-onset AD and would also have implications for the large group of non-DS AD patients.

5. Bibliography

Adams, A., Thorn, J.M., Yamabhai, M., Kay, B.K. and O'Bryan, J.P. Intersectin, an adaptor protein involved in clathrin-mediated endocytosis, activates mitogenic signaling pathways. J Biol Chem 275 (2000), pp. 27414-20.

Alcantara, S., Ruiz, M., D'Arcangelo, G., Ezan, F., de Lecea, L., Curran, T., Sotelo, C. and Soriano, E. Regional and cellular patterns of reelin mRNA expression in the forebrain of the developing and adult mouse. J Neurosci 18 (1998), pp. 7779-99.

Altman, J. and Bayer, S.A. Migration and distribution of two populations of hippocampal granule cell precursors during the perinatal and postnatal periods. J Comp Neurol 301 (1990a), pp. 365-81.

Altman, J. and Bayer, S.A. Mosaic organization of the hippocampal neuroepithelium and the multiple germinal sources of dentate granule cells. J Comp Neurol 301 (1990b), pp. 325-42.

Altman, J. and Bayer, S.A. Prolonged sojourn of developing pyramidal cells in the intermediate zone of the hippocampus and their settling in the stratum pyramidale. J Comp Neurol 301 (1990c), pp. 343-64.

Altman, J. and Das, G.D. Autoradiographic and histological evidence of postnatal hippocampal neurogenesis in rats. J Comp Neurol 124 (1965), pp. 319-35.

Andersen, O.M., Benhayon, D., Curran, T. and Willnow, T.E. Differential binding of ligands to the apolipoprotein E receptor 2. Biochemistry 42 (2003), pp. 9355-64.

Angevine, J.B., Jr. Time of neuron origin in the hippocampal region. An autoradiographic study in the mouse. Exp Neurol Suppl (1965), pp. Suppl 2:1-70.

Arber, S., Barbayannis, F.A., Hanser, H., Schneider, C., Stanyon, C.A., Bernard, O. and Caroni, P. Regulation of actin dynamics through phosphorylation of cofilin by LIM-kinase. Nature 393 (1998), pp. 805-9.

Arnaud, L., Ballif, B.A. and Cooper, J.A. Regulation of protein tyrosine kinase signaling by substrate degradation during brain development. Mol Cell Biol 23 (2003a), pp. 9293-302.

Arnaud, L., Ballif, B.A., Forster, E. and Cooper, J.A. Fyn tyrosine kinase is a critical regulator of disabled-1 during brain development. Curr Biol 13 (2003b), pp. 9-17.

Ashton, R.S., Conway, A., Pangarkar, C., Bergen, J., Lim, K.I., Shah, P., Bissell, M. and Schaffer, D.V. Astrocytes regulate adult hippocampal neurogenesis through ephrin-B signaling. Nat Neurosci 15 (2012), pp. 1399-406.

Assadi, A.H., Zhang, G., Beffert, U., McNeil, R.S., Renfro, A.L., Niu, S., Quattrocchi, C.C., Antalffy, B.A., Sheldon, M., Armstrong, D.D., Wynshaw-Boris, A., Herz, J., D'Arcangelo, G. and Clark, G.D. Interaction of reelin signaling and Lis1 in brain development. Nat Genet 35 (2003), pp. 270-6.

Bagri, A., Gurney, T., He, X., Zou, Y.R., Littman, D.R., Tessier-Lavigne, M. and Pleasure, S.J. The chemokine SDF1 regulates migration of dentate granule cells. Development 129 (2002), pp. 4249-60.

Ballif, B.A., Arnaud, L., Arthur, W.T., Guris, D., Imamoto, A. and Cooper, J.A. Activation of a Dab1/CrkL/C3G/Rap1 pathway in Reelin-stimulated neurons. Curr Biol 14 (2004), pp. 606-10.

Balmaceda, V., Cuchillo-Ibanez, I., Pujadas, L., Garcia-Ayllon, M.S., Saura, C.A., Nimpf, J., Soriano, E. and Saez-Valero, J. ApoER2 processing by presenilin-1 modulates reelin expression. FASEB J 28 (2014), pp. 1543-54.

Balu, D.T. and Lucki, I. Adult hippocampal neurogenesis: regulation, functional implications, and contribution to disease pathology. Neurosci Biobehav Rev 33 (2009), pp. 232-52.

Bardita, C., Predescu, D.N., Sha, F., Patel, M., Balaji, G. and Predescu, S.A. Endocytic deficiency induced by ITSN-1s knockdown alters the Smad2/3-Erk1/2 signaling balance downstream of Alk5. J Cell Sci 128 (2015), pp. 1528-41.

Bazinet, C., Katzen, A.L., Morgan, M., Mahowald, A.P. and Lemmon, S.K. The Drosophila clathrin heavy chain gene: clathrin function is essential in a multicellular organism. Genetics 134 (1993), pp. 1119-34.

Beffert, U., Morfini, G., Bock, H.H., Reyna, H., Brady, S.T. and Herz, J. Reelin-mediated signaling locally regulates protein kinase B/Akt and glycogen synthase kinase 3beta. J Biol Chem 277 (2002), pp. 49958-64.

Beffert, U., Weeber, E.J., Durudas, A., Qiu, S., Masiulis, I., Sweatt, J.D., Li, W.P., Adelmann, G., Frotscher, M., Hammer, R.E. and Herz, J. Modulation of synaptic plasticity and memory by Reelin involves differential splicing of the lipoprotein receptor Apoer2. Neuron 47 (2005), pp. 567-79.

Benhayon, D., Magdaleno, S. and Curran, T. Binding of purified Reelin to ApoER2 and VLDLR mediates tyrosine phosphorylation of Disabled-1. Brain Res Mol Brain Res 112 (2003), pp. 33-45.

Blalock, E.M., Geddes, J.W., Chen, K.C., Porter, N.M., Markesbery, W.R. and Landfield, P.W. Incipient Alzheimer's disease: microarray correlation analyses reveal major transcriptional and tumor suppressor responses. Proc Natl Acad Sci U S A 101 (2004), pp. 2173-8.

Bock, H.H. and Herz, J. Reelin activates SRC family tyrosine kinases in neurons. Curr Biol 13 (2003), pp. 18-26.

Bock, H.H., Jossin, Y., Liu, P., Forster, E., May, P., Goffinet, A.M. and Herz, J. Phosphatidylinositol 3-kinase interacts with the adaptor protein Dab1 in response to Reelin signaling and is required for normal cortical lamination. J Biol Chem 278 (2003), pp. 38772-9.

Bonanomi, D., Chivatakarn, O., Bai, G., Abdesselem, H., Lettieri, K., Marquardt, T., Pierchala, B.A. and Pfaff, S.L. Ret is a multifunctional coreceptor that integrates diffusible- and contact-axon guidance signals. Cell 148 (2012), pp. 568-82.

Bong, Y.S., Lee, H.S., Carim-Todd, L., Mood, K., Nishanian, T.G., Tessarollo, L. and Daar, I.O. ephrinB1 signals from the cell surface to the nucleus by recruitment of STAT3. Proc Natl Acad Sci U S A 104 (2007), pp. 17305-10.

Botella-Lopez, A., Burgaya, F., Gavin, R., Garcia-Ayllon, M.S., Gomez-Tortosa, E., Pena-Casanova, J., Urena, J.M., Del Rio, J.A., Blesa, R., Soriano, E. and Saez-Valero, J. Reelin expression and glycosylation patterns are altered in Alzheimer's disease. Proc Natl Acad Sci U S A 103 (2006), pp. 5573-8.

Botella-Lopez, A., Cuchillo-Ibanez, I., Cotrufo, T., Mok, S.S., Li, Q.X., Barquero, M.S., Dierssen, M., Soriano, E. and Saez-Valero, J. Beta-amyloid controls altered Reelin expression and processing in Alzheimer's disease. Neurobiol Dis 37 (2010), pp. 682-91.

Bouche, E., Romero-Ortega, M.I., Henkemeyer, M., Catchpole, T., Leemhuis, J., Frotscher, M., May, P., Herz, J. and Bock, H.H. Reelin induces EphB activation. Cell Res 23 (2013), pp. 473-90.

Bouzioukh, F., Wilkinson, G.A., Adelmann, G., Frotscher, M., Stein, V. and Klein, R. Tyrosine phosphorylation sites in ephrinB2 are required for hippocampal long-term potentiation but not long-term depression. J Neurosci 27 (2007), pp. 11279-88.

Boycott, K.M., Bonnemann, C., Herz, J., Neuert, S., Beaulieu, C., Scott, J.N., Venkatasubramanian, A. and Parboosingh, J.S. Mutations in VLDLR as a cause for autosomal recessive cerebellar ataxia with mental retardation (dysequilibrium syndrome). J Child Neurol 24 (2009), pp. 1310-5.

Brandes, C., Kahr, L., Stockinger, W., Hiesberger, T., Schneider, W.J. and Nimpf, J. Alternative splicing in the ligand binding domain of mouse ApoE receptor-2 produces receptor variants binding reelin but not alpha 2-macroglobulin. J Biol Chem 276 (2001), pp. 22160-9.

Bruckner, K., Pablo Labrador, J., Scheiffele, P., Herb, A., Seeburg, P.H. and Klein, R. EphrinB ligands recruit GRIP family PDZ adaptor proteins into raft membrane microdomains. Neuron 22 (1999), pp. 511-24.

Bruckner, K., Pasquale, E.B. and Klein, R. Tyrosine phosphorylation of transmembrane ligands for Eph receptors. Science 275 (1997), pp. 1640-3.

Brunne, B., Franco, S., Bouche, E., Herz, J., Howell, B.W., Pahle, J., Muller, U., May, P., Frotscher, M. and Bock, H.H. Role of the postnatal radial glial scaffold for the development of the dentate gyrus as revealed by Reelin signaling mutant mice. Glia 61 (2013), pp. 1347-63.

Buday, L., Wunderlich, L. and Tamas, P. The Nck family of adapter proteins: regulators of actin cytoskeleton. Cell Signal 14 (2002), pp. 723-31.

Bull, N.D. and Bartlett, P.F. The adult mouse hippocampal progenitor is neurogenic but not a stem cell. J Neurosci 25 (2005), pp. 10815-21.

Burkhard, P., Stetefeld, J. and Strelkov, S.V. Coiled coils: a highly versatile protein folding motif. Trends Cell Biol 11 (2001), pp. 82-8.

Bush, J.O. and Soriano, P. Ephrin-B1 regulates axon guidance by reverse signaling through a PDZ-dependent mechanism. Genes Dev 23 (2009), pp. 1586-99.

Bush, J.O. and Soriano, P. Ephrin-B1 forward signaling regulates craniofacial morphogenesis by controlling cell proliferation across Eph-ephrin boundaries. Genes Dev 24 (2010), pp. 2068-80.

Camargo, L.M., Collura, V., Rain, J.C., Mizuguchi, K., Hermjakob, H., Kerrien, S., Bonnert, T.P., Whiting, P.J. and Brandon, N.J. Disrupted in Schizophrenia 1 Interactome: evidence for the close connectivity of risk genes and a potential synaptic basis for schizophrenia. Mol Psychiatry 12 (2007), pp. 74-86.

Cameron, H.A., Woolley, C.S., McEwen, B.S. and Gould, E. Differentiation of newly born neurons and glia in the dentate gyrus of the adult rat. Neuroscience 56 (1993), pp. 337-44.

Campbell, T.N., Attwell, S., Arcellana-Panlilio, M. and Robbins, S.M. Ephrin A5 expression promotes invasion and transformation of murine fibroblasts. Biochem Biophys Res Commun 350 (2006), pp. 623-8.

Carmona, M.A., Murai, K.K., Wang, L., Roberts, A.J. and Pasquale, E.B. Glial ephrin-A3 regulates hippocampal dendritic spine morphology and glutamate transport. Proc Natl Acad Sci U S A 106 (2009), pp. 12524-9.

Catchpole, T. and Henkemeyer, M. EphB2 tyrosine kinase-dependent forward signaling in migration of neuronal progenitors that populate and form a distinct region of the dentate niche. J Neurosci 31 (2011), pp. 11472-83.

Chai, X., Forster, E., Zhao, S., Bock, H.H. and Frotscher, M. Reelin acts as a stop signal for radially migrating neurons by inducing phosphorylation of n-cofilin at the leading edge. Commun Integr Biol 2 (2009a), pp. 375-7.

Chai, X., Forster, E., Zhao, S., Bock, H.H. and Frotscher, M. Reelin stabilizes the actin cytoskeleton of neuronal processes by inducing n-cofilin phosphorylation at serine3. J Neurosci 29 (2009b), pp. 288-99.

Chang, B.S., Duzcan, F., Kim, S., Cinbis, M., Aggarwal, A., Apse, K.A., Ozdel, O., Atmaca, M., Zencir, S., Bagci, H. and Walsh, C.A. The role of RELN in lissencephaly and neuropsychiatric disease. Am J Med Genet B Neuropsychiatr Genet 144B (2007), pp. 58-63.

Chang, Q., Jorgensen, C., Pawson, T. and Hedley, D.W. Effects of dasatinib on EphA2 receptor tyrosine kinase activity and downstream signalling in pancreatic cancer. Br J Cancer 99 (2008), pp. 1074-82.

Chen, C., Kim, J.J., Thompson, R.F. and Tonegawa, S. Hippocampal lesions impair contextual fear conditioning in two strains of mice. Behav Neurosci 110 (1996), pp. 1177-80.

Chen, K., Ochalski, P.G., Tran, T.S., Sahir, N., Schubert, M., Pramatarova, A. and Howell, B.W. Interaction between Dab1 and CrkII is promoted by Reelin signaling. J Cell Sci 117 (2004), pp. 4527-36.

Chen, Y., Beffert, U., Ertunc, M., Tang, T.S., Kavalali, E.T., Bezprozvanny, I. and Herz, J. Reelin modulates NMDA receptor activity in cortical neurons. J Neurosci 25 (2005), pp. 8209-16.

Chong, L.D., Park, E.K., Latimer, E., Friesel, R. and Daar, I.O. Fibroblast growth factor receptor-mediated rescue of x-ephrin B1-induced cell dissociation in Xenopus embryos. Mol Cell Biol 20 (2000), pp. 724-34.

Chumley, M.J., Catchpole, T., Silvany, R.E., Kernie, S.G. and Henkemeyer, M. EphB receptors regulate stem/progenitor cell proliferation, migration, and polarity during hippocampal neurogenesis. J Neurosci 27 (2007), pp. 13481-90.

Clatworthy, A.E., Stockinger, W., Christie, R.H., Schneider, W.J., Nimpf, J., Hyman, B.T. and Rebeck, G.W. Expression and alternate splicing of apolipoprotein E receptor 2 in brain. Neuroscience 90 (1999), pp. 903-11.

Conover, J.C., Doetsch, F., Garcia-Verdugo, J.M., Gale, N.W., Yancopoulos, G.D. and Alvarez-Buylla, A. Disruption of Eph/ephrin signaling affects migration and proliferation in the adult subventricular zone. Nat Neurosci 3 (2000), pp. 1091-7.

Corbalan-Garcia, S. and Gomez-Fernandez, J.C. Signaling through C2 domains: more than one lipid target. Biochim Biophys Acta 1838 (2014), pp. 1536-47.

Cowan, C.A. and Henkemeyer, M. The SH2/SH3 adaptor Grb4 transduces B-ephrin reverse signals. Nature 413 (2001), pp. 174-9.

Cowan, C.W., Shao, Y.R., Sahin, M., Shamah, S.M., Lin, M.Z., Greer, P.L., Gao, S., Griffith, E.C., Brugge, J.S. and Greenberg, M.E. Vav family GEFs link activated Ephs to endocytosis and axon guidance. Neuron 46 (2005), pp. 205-17.

Cuitino, L., Matute, R., Retamal, C., Bu, G., Inestrosa, N.C. and Marzolo, M.P. ApoER2 is endocytosed by a clathrin-mediated process involving the adaptor protein Dab2 independent of its Rafts' association. Traffic 6 (2005), pp. 820-38.

D'Arcangelo, G., Homayouni, R., Keshvara, L., Rice, D.S., Sheldon, M. and Curran, T. Reelin is a ligand for lipoprotein receptors. Neuron 24 (1999), pp. 471-9.

D'Arcangelo, G., Miao, G.G., Chen, S.C., Soares, H.D., Morgan, J.I. and Curran, T. A protein related to extracellular matrix proteins deleted in the mouse mutant reeler. Nature 374 (1995), pp. 719-23.

Dail, M., Richter, M., Godement, P. and Pasquale, E.B. Eph receptors inactivate R-Ras through different mechanisms to achieve cell repulsion. J Cell Sci 119 (2006), pp. 1244-54.

Das, M., Scappini, E., Martin, N.P., Wong, K.A., Dunn, S., Chen, Y.J., Miller, S.L., Domin, J. and O'Bryan, J.P. Regulation of neuron survival through an intersectin-phosphoinositide 3'-kinase C2beta-AKT pathway. Mol Cell Biol 27 (2007), pp. 7906-17.

Davy, A., Bush, J.O. and Soriano, P. Inhibition of gap junction communication at ectopic Eph/ephrin boundaries underlies craniofrontonasal syndrome. PLoS Biol 4 (2006), p. e315.

Davy, A., Gale, N.W., Murray, E.W., Klinghoffer, R.A., Soriano, P., Feuerstein, C. and Robbins, S.M. Compartmentalized signaling by GPI-anchored ephrin-A5 requires the Fyn tyrosine kinase to regulate cellular adhesion. Genes Dev 13 (1999), pp. 3125-35.

de Bergeyck, V., Naerhuyzen, B., Goffinet, A.M. and Lambert de Rouvroit, C. A panel of monoclonal antibodies against reelin, the extracellular matrix protein defective in reeler mutant mice. J Neurosci Methods 82 (1998), pp. 17-24.

de Bergeyck, V., Nakajima, K., Lambert de Rouvroit, C., Naerhuyzen, B., Goffinet, A.M., Miyata, T., Ogawa, M. and Mikoshiba, K. A truncated Reelin protein is produced but not secreted in the 'Orleans' reeler mutation (Reln[rl-Orl]). Brain Res Mol Brain Res 50 (1997), pp. 85-90.

Del Rio, J.A., Heimrich, B., Borrell, V., Forster, E., Drakew, A., Alcantara, S., Nakajima, K., Miyata, T., Ogawa, M., Mikoshiba, K., Derer, P., Frotscher, M. and Soriano, E. A role for Cajal-Retzius cells and reelin in the development of hippocampal connections. Nature 385 (1997), pp. 70-4.

Deng, W., Aimone, J.B. and Gage, F.H. New neurons and new memories: how does adult hippocampal neurogenesis affect learning and memory? Nat Rev Neurosci 11 (2010), pp. 339-50.

Derer, P., Derer, M. and Goffinet, A. Axonal secretion of Reelin by Cajal-Retzius cells: evidence from comparison of normal and Reln(Orl) mutant mice. J Comp Neurol 440 (2001), pp. 136-43.

Dergai, O., Novokhatska, O., Dergai, M., Skrypkina, I., Tsyba, L., Moreau, J. and Rynditch, A. Intersectin 1 forms complexes with SGIP1 and Reps1 in clathrin-coated pits. Biochem Biophys Res Commun 402 (2010), pp. 408-13.

DeSilva, U., D'Arcangelo, G., Braden, V.V., Chen, J., Miao, G.G., Curran, T. and Green, E.D. The human reelin gene: isolation, sequencing, and mapping on chromosome 7. Genome Res 7 (1997), pp. 157-64.

Doehner, J., Madhusudan, A., Konietzko, U., Fritschy, J.M. and Knuesel, I. Co-localization of Reelin and proteolytic AbetaPP fragments in hippocampal plaques in aged wild-type mice. J Alzheimers Dis 19 (2010), pp. 1339-57.

Doetsch, F., Caille, I., Lim, D.A., Garcia-Verdugo, J.M. and Alvarez-Buylla, A. Subventricular zone astrocytes are neural stem cells in the adult mammalian brain. Cell 97 (1999), pp. 703-16.

Doetsch, F., Garcia-Verdugo, J.M. and Alvarez-Buylla, A. Cellular composition and three-dimensional organization of the subventricular germinal zone in the adult mammalian brain. J Neurosci 17 (1997), pp. 5046-61.

Doherty, G.J. and McMahon, H.T. Mechanisms of endocytosis. Annu Rev Biochem 78 (2009), pp. 857-902.

Drakew, A., Frotscher, M., Deller, T., Ogawa, M. and Heimrich, B. Developmental distribution of a reeler gene-related antigen in the rat hippocampal formation visualized by CR-50 immunocytochemistry. Neuroscience 82 (1998), pp. 1079-86.

Duit, S., Mayer, H., Blake, S.M., Schneider, W.J. and Nimpf, J. Differential functions of ApoER2 and very low density lipoprotein receptor in Reelin signaling depend on differential sorting of the receptors. J Biol Chem 285 (2010), pp. 4896-908.

Dulabon, L., Olson, E.C., Taglienti, M.G., Eisenhuth, S., McGrath, B., Walsh, C.A., Kreidberg, J.A. and Anton, E.S. Reelin binds alpha3beta1 integrin and inhibits neuronal migration. Neuron 27 (2000), pp. 33-44.

Dunckley, T., Beach, T.G., Ramsey, K.E., Grover, A., Mastroeni, D., Walker, D.G., LaFleur, B.J., Coon, K.D., Brown, K.M., Caselli, R., Kukull, W., Higdon, R., McKeel, D., Morris, J.C., Hulette, C., Schmechel, D., Reiman, E.M., Rogers, J. and Stephan, D.A. Gene expression correlates of neurofibrillary tangles in Alzheimer's disease. Neurobiol Aging 27 (2006), pp. 1359-71.

Durakoglugil, M.S., Chen, Y., White, C.L., Kavalali, E.T. and Herz, J. Reelin signaling antagonizes beta-amyloid at the synapse. Proc Natl Acad Sci U S A 106 (2009), pp. 15938-43.

Elowe, S., Holland, S.J., Kulkarni, S. and Pawson, T. Downregulation of the Ras-mitogen-activated protein kinase pathway by the EphB2 receptor tyrosine kinase is required for ephrin-induced neurite retraction. Mol Cell Biol 21 (2001), pp. 7429-41.

Encinas, J.M., Michurina, T.V., Peunova, N., Park, J.H., Tordo, J., Peterson, D.A., Fishell, G., Koulakov, A. and Enikolopov, G. Division-coupled astrocytic differentiation and age-related depletion of neural stem cells in the adult hippocampus. Cell Stem Cell 8 (2011), pp. 566-79.

Engel, J., Jr. Mesial temporal lobe epilepsy: what have we learned? Neuroscientist 7 (2001), pp. 340-52.

Essmann, C.L., Martinez, E., Geiger, J.C., Zimmer, M., Traut, M.H., Stein, V., Klein, R. and Acker-Palmer, A. Serine phosphorylation of ephrinB2 regulates trafficking of synaptic AMPA receptors. Nat Neurosci 11 (2008), pp. 1035-43.

Estus, S., Golde, T.E., Kunishita, T., Blades, D., Lowery, D., Eisen, M., Usiak, M., Qu, X.M., Tabira, T., Greenberg, B.D. and et al. Potentially amyloidogenic, carboxyl-terminal derivatives of the amyloid protein precursor. Science 255 (1992), pp. 726-8.

Fabel, K., Wolf, S.A., Ehninger, D., Babu, H., Leal-Galicia, P. and Kempermann, G. Additive effects of physical exercise and environmental enrichment on adult hippocampal neurogenesis in mice. Front Neurosci 3 (2009), p. 50.

Faigle, R. and Song, H. Signaling mechanisms regulating adult neural stem cells and neurogenesis. Biochim Biophys Acta 1830 (2013), pp. 2435-48.

Falconer, D.S. Two new mutants, 'trembler' and 'reeler', with neurological actions in the house mouse (Mus musculus L.). J Genet 50 (1951), pp. 192-201.

Fatemi, S.H. Reelin glycoprotein: structure, biology and roles in health and disease. Mol Psychiatry 10 (2005), pp. 251-7.

Fatemi, S.H., Earle, J.A. and McMenomy, T. Reduction in Reelin immunoreactivity in hippocampus of subjects with schizophrenia, bipolar disorder and major depression. Mol Psychiatry 5 (2000), pp. 654-63, 571.

Fatemi, S.H., Snow, A.V., Stary, J.M., Araghi-Niknam, M., Reutiman, T.J., Lee, S., Brooks, A.I. and Pearce, D.A. Reelin signaling is impaired in autism. Biol Psychiatry 57 (2005), pp. 777-87.

Fatemi, S.H., Stary, J.M., Halt, A.R. and Realmuto, G.R. Dysregulation of Reelin and Bcl-2 proteins in autistic cerebellum. J Autism Dev Disord 31 (2001), pp. 529-35.

Feller, S.M. Crk family adaptors-signalling complex formation and biological roles. Oncogene 20 (2001), pp. 6348-71.

Feng, L., Allen, N.S., Simo, S. and Cooper, J.A. Cullin 5 regulates Dab1 protein levels and neuron positioning during cortical development. Genes Dev 21 (2007), pp. 2717-30.

Feng, L. and Cooper, J.A. Dual functions of Dab1 during brain development. Mol Cell Biol 29 (2009), pp. 324-32.

Ferguson, S.M., Brasnjo, G., Hayashi, M., Wolfel, M., Collesi, C., Giovedi, S., Raimondi, A., Gong, L.W., Ariel, P., Paradise, S., O'Toole, E., Flavell, R., Cremona, O., Miesenbock, G., Ryan, T.A. and De Camilli, P. A selective activity-dependent requirement for dynamin 1 in synaptic vesicle endocytosis. Science 316 (2007), pp. 570-4.

Filippov, V., Kronenberg, G., Pivneva, T., Reuter, K., Steiner, B., Wang, L.P., Yamaguchi, M., Kettenmann, H. and Kempermann, G. Subpopulation of nestin-expressing progenitor cells in the adult murine hippocampus shows electrophysiological and morphological characteristics of astrocytes. Mol Cell Neurosci 23 (2003), pp. 373-82.

Filosa, A., Paixao, S., Honsek, S.D., Carmona, M.A., Becker, L., Feddersen, B., Gaitanos, L., Rudhard, Y., Schoepfer, R., Klopstock, T., Kullander, K., Rose, C.R., Pasquale, E.B. and Klein, R. Neuron-glia communication via EphA4/ephrin-A3 modulates LTP through glial glutamate transport. Nat Neurosci 12 (2009), pp. 1285-92.

Folsom, T.D. and Fatemi, S.H. The involvement of Reelin in neurodevelopmental disorders. Neuropharmacology 68 (2013), pp. 122-35.

Forster, E., Bock, H.H., Herz, J., Chai, X., Frotscher, M. and Zhao, S. Emerging topics in Reelin function. Eur J Neurosci 31 (2010), pp. 1511-8.

Forster, E., Tielsch, A., Saum, B., Weiss, K.H., Johanssen, C., Graus-Porta, D., Muller, U. and Frotscher, M. Reelin, Disabled 1, and beta 1 integrins are required for the formation of the radial glial scaffold in the hippocampus. Proc Natl Acad Sci U S A 99 (2002), pp. 13178-83.

Franco, S.J., Martinez-Garay, I., Gil-Sanz, C., Harkins-Perry, S.R. and Muller, U. Reelin regulates cadherin function via Dab1/Rap1 to control neuronal migration and lamination in the neocortex. Neuron 69 (2011), pp. 482-97.

Franke, T.F. PI3K/Akt: getting it right matters. Oncogene 27 (2008), pp. 6473-88.

Frotscher, M. Cajal-Retzius cells, Reelin, and the formation of layers. Curr Opin Neurobiol 8 (1998), pp. 570-5.

Frotscher, M., Haas, C.A. and Forster, E. Reelin controls granule cell migration in the dentate gyrus by acting on the radial glial scaffold. Cereb Cortex 13 (2003), pp. 634-40.

Fu, W.Y., Chen, Y., Sahin, M., Zhao, X.S., Shi, L., Bikoff, J.B., Lai, K.O., Yung, W.H., Fu, A.K., Greenberg, M.E. and Ip, N.Y. Cdk5 regulates EphA4-mediated dendritic spine retraction through an ephexin1-dependent mechanism. Nat Neurosci 10 (2007), pp. 67-76.

Fukuda, S., Kato, F., Tozuka, Y., Yamaguchi, M., Miyamoto, Y. and Hisatsune, T. Two distinct subpopulations of nestin-positive cells in adult mouse dentate gyrus. J Neurosci 23 (2003), pp. 9357-66.

Furukawa, K., Sopher, B.L., Rydel, R.E., Begley, J.G., Pham, D.G., Martin, G.M., Fox, M. and Mattson, M.P. Increased activity-regulating and neuroprotective efficacy of alpha-secretase-derived secreted amyloid precursor protein conferred by a C-terminal heparin-binding domain. J Neurochem 67 (1996), pp. 1882-96.

Gahwiler, B.H., Capogna, M., Debanne, D., McKinney, R.A. and Thompson, S.M. Organotypic slice cultures: a technique has come of age. Trends Neurosci 20 (1997), pp. 471-7.

Gale, N.W., Holland, S.J., Valenzuela, D.M., Flenniken, A., Pan, L., Ryan, T.E., Henkemeyer, M., Strebhardt, K., Hirai, H., Wilkinson, D.G., Pawson, T., Davis, S. and Yancopoulos, G.D. Eph receptors and ligands comprise two major specificity subclasses and are reciprocally compartmentalized during embryogenesis. Neuron 17 (1996), pp. 9-19.

Gheusi, G., Cremer, H., McLean, H., Chazal, G., Vincent, J.D. and Lledo, P.M. Importance of newly generated neurons in the adult olfactory bulb for odor discrimination. Proc Natl Acad Sci U S A 97 (2000), pp. 1823-8.

Glenner, G.G. and Wong, C.W. Alzheimer's disease: initial report of the purification and characterization of a novel cerebrovascular amyloid protein. Biochem Biophys Res Commun 120 (1984), pp. 885-90.

Glodowski, D.R., Chen, C.C., Schaefer, H., Grant, B.D. and Rongo, C. RAB-10 regulates glutamate receptor recycling in a cholesterol-dependent endocytosis pathway. Mol Biol Cell 18 (2007), pp. 4387-96.

Goffinet, A.M., So, K.F., Yamamoto, M., Edwards, M. and Caviness, V.S., Jr. Architectonic and hodological organization of the cerebellum in reeler mutant mice. Brain Res 318 (1984), pp. 263-76.

Goldowitz, D., Cushing, R.C., Laywell, E., D'Arcangelo, G., Sheldon, M., Sweet, H.O., Davisson, M., Steindler, D. and Curran, T. Cerebellar disorganization characteristic of reeler in scrambler mutant mice despite presence of reelin. J Neurosci 17 (1997), pp. 8767-77.

Gong, C., Wang, T.W., Huang, H.S. and Parent, J.M. Reelin regulates neuronal progenitor migration in intact and epileptic hippocampus. J Neurosci 27 (2007), pp. 1803-11.

Gonzalez, J.L., Russo, C.J., Goldowitz, D., Sweet, H.O., Davisson, M.T. and Walsh, C.A. Birthdate and cell marker analysis of scrambler: a novel mutation affecting cortical development with a reeler-like phenotype. J Neurosci 17 (1997), pp. 9204-11.

Good, M.C., Zalatan, J.G. and Lim, W.A. Scaffold proteins: hubs for controlling the flow of cellular information. Science 332 (2011), pp. 680-6.

Gotthardt, M., Trommsdorff, M., Nevitt, M.F., Shelton, J., Richardson, J.A., Stockinger, W., Nimpf, J. and Herz, J. Interactions of the low density lipoprotein receptor gene family with cytosolic adaptor and scaffold proteins suggest diverse biological functions in cellular communication and signal transduction. J Biol Chem 275 (2000), pp. 25616-24.

Gould, E., Beylin, A., Tanapat, P., Reeves, A. and Shors, T.J. Learning enhances adult neurogenesis in the hippocampal formation. Nat Neurosci 2 (1999), pp. 260-5.

Groc, L., Choquet, D., Stephenson, F.A., Verrier, D., Manzoni, O.J. and Chavis, P. NMDA receptor surface trafficking and synaptic subunit composition are developmentally regulated by the extracellular matrix protein Reelin. J Neurosci 27 (2007), pp. 10165-75.

Grundke-Iqbal, I., Iqbal, K., Tung, Y.C., Quinlan, M., Wisniewski, H.M. and Binder, L.I. Abnormal phosphorylation of the microtubule-associated protein tau (tau) in Alzheimer cytoskeletal pathology. Proc Natl Acad Sci U S A 83 (1986), pp. 4913-7.

Gubar, O., Morderer, D., Tsyba, L., Croise, P., Houy, S., Ory, S., Gasman, S. and Rynditch, A. Intersectin: The Crossroad between Vesicle Exocytosis and Endocytosis. Front Endocrinol (Lausanne) 4 (2013), p. 109.

Guidotti, A., Auta, J., Davis, J.M., Di-Giorgi-Gerevini, V., Dwivedi, Y., Grayson, D.R., Impagnatiello, F., Pandey, G., Pesold, C., Sharma, R., Uzunov, D. and Costa, E. Decrease in reelin and glutamic acid decarboxylase67 (GAD67) expression in schizophrenia and bipolar disorder: a postmortem brain study. Arch Gen Psychiatry 57 (2000), pp. 1061-9.

Guipponi, M., Scott, H.S., Chen, H., Schebesta, A., Rossier, C. and Antonarakis, S.E. Two isoforms of a human intersectin (ITSN) protein are produced by brain-specific alternative splicing in a stop codon. Genomics 53 (1998), pp. 369-76.

Gupta, A., Tsai, L.H. and Wynshaw-Boris, A. Life is a journey: a genetic look at neocortical development. Nat Rev Genet 3 (2002), pp. 342-55.

Haass, C., Koo, E.H., Mellon, A., Hung, A.Y. and Selkoe, D.J. Targeting of cell-surface beta-amyloid precursor protein to lysosomes: alternative processing into amyloid-bearing fragments. Nature 357 (1992), pp. 500-3.

Hack, I., Bancila, M., Loulier, K., Carroll, P. and Cremer, H. Reelin is a detachment signal in tangential chain-migration during postnatal neurogenesis. Nat Neurosci 5 (2002), pp. 939-45.
Hack, I., Hellwig, S., Junghans, D., Brunne, B., Bock, H.H., Zhao, S. and Frotscher, M. Divergent roles of ApoER2 and Vldlr in the migration of cortical neurons. Development 134 (2007), pp. 3883-91.
Hamburgh, M. Analysis of the Postnatal Developmental Effects of "Reeler," a Neurological Mutation in Mice. A Study in Developmental Genetics. Dev Biol 8 (1963), pp. 165-85.
Hampel, H., Burger, K., Teipel, S.J., Bokde, A.L., Zetterberg, H. and Blennow, K. Core candidate neurochemical and imaging biomarkers of Alzheimer's disease. Alzheimers Dement 4 (2008), pp. 38-48.
Hansen, C.G. and Nichols, B.J. Molecular mechanisms of clathrin-independent endocytosis. J Cell Sci 122 (2009), pp. 1713-21.
Hara, Y., Nomura, T., Yoshizaki, K., Frisen, J. and Osumi, N. Impaired hippocampal neurogenesis and vascular formation in ephrin-A5-deficient mice. Stem Cells 28 (2010), pp. 974-83.
Harrison, P.J. The hippocampus in schizophrenia: a review of the neuropathological evidence and its pathophysiological implications. Psychopharmacology (Berl) 174 (2004), pp. 151-62.
Hashimoto-Torii, K., Torii, M., Sarkisian, M.R., Bartley, C.M., Shen, J., Radtke, F., Gridley, T., Sestan, N. and Rakic, P. Interaction between Reelin and Notch signaling regulates neuronal migration in the cerebral cortex. Neuron 60 (2008), pp. 273-84.
Hayashi, K., Kubo, K., Kitazawa, A. and Nakajima, K. Cellular dynamics of neuronal migration in the hippocampus. Front Neurosci 9 (2015), p. 135.
Henley, J.R., Krueger, E.W., Oswald, B.J. and McNiven, M.A. Dynamin-mediated internalization of caveolae. J Cell Biol 141 (1998), pp. 85-99.
Henne, W.M., Boucrot, E., Meinecke, M., Evergren, E., Vallis, Y., Mittal, R. and McMahon, H.T. FCHo proteins are nucleators of clathrin-mediated endocytosis. Science 328 (2010), pp. 1281-4.
Herrick, T.M. and Cooper, J.A. A hypomorphic allele of dab1 reveals regional differences in reelin-Dab1 signaling during brain development. Development 129 (2002), pp. 787-96.
Herrick, T.M. and Cooper, J.A. High affinity binding of Dab1 to Reelin receptors promotes normal positioning of upper layer cortical plate neurons. Brain Res Mol Brain Res 126 (2004), pp. 121-8.
Herz, J. and Chen, Y. Reelin, lipoprotein receptors and synaptic plasticity. Nat Rev Neurosci 7 (2006), pp. 850-9.
Hibi, T. and Hattori, M. The N-terminal fragment of Reelin is generated after endocytosis and released through the pathway regulated by Rab11. FEBS Lett 583 (2009), pp. 1299-303.
Hibi, T., Mizutani, M., Baba, A. and Hattori, M. Splicing variations in the ligand-binding domain of ApoER2 results in functional differences in the binding properties to Reelin. Neurosci Res 63 (2009), pp. 251-8.
Hiesberger, T., Trommsdorff, M., Howell, B.W., Goffinet, A., Mumby, M.C., Cooper, J.A. and Herz, J. Direct binding of Reelin to VLDL receptor and ApoE receptor 2 induces tyrosine phosphorylation of disabled-1 and modulates tau phosphorylation. Neuron 24 (1999), pp. 481-9.
Himanen, J.P., Chumley, M.J., Lackmann, M., Li, C., Barton, W.A., Jeffrey, P.D., Vearing, C., Geleick, D., Feldheim, D.A., Boyd, A.W., Henkemeyer, M. and Nikolov, D.B. Repelling class discrimination: ephrin-A5 binds to and activates EphB2 receptor signaling. Nat Neurosci 7 (2004), pp. 501-9.
Himanen, J.P., Rajashankar, K.R., Lackmann, M., Cowan, C.A., Henkemeyer, M. and Nikolov, D.B. Crystal structure of an Eph receptor-ephrin complex. Nature 414 (2001), pp. 933-8.
Hirotsune, S., Fleck, M.W., Gambello, M.J., Bix, G.J., Chen, A., Clark, G.D., Ledbetter, D.H., McBain, C.J. and Wynshaw-Boris, A. Graded reduction of Pafah1b1 (Lis1) activity results in neuronal migration defects and early embryonic lethality. Nat Genet 19 (1998), pp. 333-9.
Hirotsune, S., Takahara, T., Sasaki, N., Hirose, K., Yoshiki, A., Ohashi, T., Kusakabe, M., Murakami, Y., Muramatsu, M., Watanabe, S. and et al. The reeler gene encodes a protein with an EGF-like motif expressed by pioneer neurons. Nat Genet 10 (1995), pp. 77-83.
Hoe, H.S. and Rebeck, G.W. Regulation of ApoE receptor proteolysis by ligand binding. Brain Res Mol Brain Res 137 (2005), pp. 31-9.
Hoe, H.S., Tran, T.S., Matsuoka, Y., Howell, B.W. and Rebeck, G.W. DAB1 and Reelin effects on amyloid precursor protein and ApoE receptor 2 trafficking and processing. J Biol Chem 281 (2006), pp. 35176-85.
Holen, H.L., Shadidi, M., Narvhus, K., Kjosnes, O., Tierens, A. and Aasheim, H.C. Signaling through ephrin-A ligand leads to activation of Src-family kinases, Akt phosphorylation, and inhibition of antigen receptor-induced apoptosis. J Leukoc Biol 84 (2008), pp. 1183-91.

Holmberg, J., Armulik, A., Senti, K.A., Edoff, K., Spalding, K., Momma, S., Cassidy, R., Flanagan, J.G. and Frisen, J. Ephrin-A2 reverse signaling negatively regulates neural progenitor proliferation and neurogenesis. Genes Dev 19 (2005), pp. 462-71.

Honda, T., Kobayashi, K., Mikoshiba, K. and Nakajima, K. Regulation of cortical neuron migration by the Reelin signaling pathway. Neurochem Res 36 (2011), pp. 1270-9.

Hong, C., Duit, S., Jalonen, P., Out, R., Scheer, L., Sorrentino, V., Boyadjian, R., Rodenburg, K.W., Foley, E., Korhonen, L., Lindholm, D., Nimpf, J., van Berkel, T.J., Tontonoz, P. and Zelcer, N. The E3 ubiquitin ligase IDOL induces the degradation of the low density lipoprotein receptor family members VLDLR and ApoER2. J Biol Chem 285 (2010), pp. 19720-6.

Hong, S.E., Shugart, Y.Y., Huang, D.T., Shahwan, S.A., Grant, P.E., Hourihane, J.O., Martin, N.D. and Walsh, C.A. Autosomal recessive lissencephaly with cerebellar hypoplasia is associated with human RELN mutations. Nat Genet 26 (2000), pp. 93-6.

Howell, B.W., Gertler, F.B. and Cooper, J.A. Mouse disabled (mDab1): a Src binding protein implicated in neuronal development. EMBO J 16 (1997a), pp. 121-32.

Howell, B.W., Hawkes, R., Soriano, P. and Cooper, J.A. Neuronal position in the developing brain is regulated by mouse disabled-1. Nature 389 (1997b), pp. 733-7.

Howell, B.W., Herrick, T.M., Hildebrand, J.D., Zhang, Y. and Cooper, J.A. Dab1 tyrosine phosphorylation sites relay positional signals during mouse brain development. Curr Biol 10 (2000), pp. 877-85.

Hu, T., Shi, G., Larose, L., Rivera, G.M., Mayer, B.J. and Zhou, R. Regulation of process retraction and cell migration by EphA3 is mediated by the adaptor protein Nck1. Biochemistry 48 (2009), pp. 6369-78.

Huang, X., Wu, D., Jin, H., Stupack, D. and Wang, J.Y. Induction of cell retraction by the combined actions of Abl-CrkII and Rho-ROCK1 signaling. J Cell Biol 183 (2008), pp. 711-23.

Huang, Y., Magdaleno, S., Hopkins, R., Slaughter, C., Curran, T. and Keshvara, L. Tyrosine phosphorylated Disabled 1 recruits Crk family adapter proteins. Biochem Biophys Res Commun 318 (2004), pp. 204-12.

Huang, Y., Shah, V., Liu, T. and Keshvara, L. Signaling through Disabled 1 requires phosphoinositide binding. Biochem Biophys Res Commun 331 (2005), pp. 1460-8.

Hunter, M.P., Russo, A. and O'Bryan, J.P. Emerging roles for intersectin (ITSN) in regulating signaling and disease pathways. Int J Mol Sci 14 (2013), pp. 7829-52.

Hussain, N.K., Jenna, S., Glogauer, M., Quinn, C.C., Wasiak, S., Guipponi, M., Antonarakis, S.E., Kay, B.K., Stossel, T.P., Lamarche-Vane, N. and McPherson, P.S. Endocytic protein intersectin-l regulates actin assembly via Cdc42 and N-WASP. Nat Cell Biol 3 (2001), pp. 927-32.

Hussain, N.K., Yamabhai, M., Ramjaun, A.R., Guy, A.M., Baranes, D., O'Bryan, J.P., Der, C.J., Kay, B.K. and McPherson, P.S. Splice variants of intersectin are components of the endocytic machinery in neurons and nonneuronal cells. J Biol Chem 274 (1999), pp. 15671-7.

Impagnatiello, F., Guidotti, A.R., Pesold, C., Dwivedi, Y., Caruncho, H., Pisu, M.G., Uzunov, D.P., Smalheiser, N.R., Davis, J.M., Pandey, G.N., Pappas, G.D., Tueting, P., Sharma, R.P. and Costa, E. A decrease of reelin expression as a putative vulnerability factor in schizophrenia. Proc Natl Acad Sci U S A 95 (1998), pp. 15718-23.

Irie, F. and Yamaguchi, Y. EphB receptors regulate dendritic spine development via intersectin, Cdc42 and N-WASP. Nat Neurosci 5 (2002), pp. 1117-8.

Jenna, S., Hussain, N.K., Danek, E.I., Triki, I., Wasiak, S., McPherson, P.S. and Lamarche-Vane, N. The activity of the GTPase-activating protein CdGAP is regulated by the endocytic protein intersectin. J Biol Chem 277 (2002), pp. 6366-73.

Jiao, J.W., Feldheim, D.A. and Chen, D.F. Ephrins as negative regulators of adult neurogenesis in diverse regions of the central nervous system. Proc Natl Acad Sci U S A 105 (2008), pp. 8778-83.

Jossin, Y. and Cooper, J.A. Reelin, Rap1 and N-cadherin orient the migration of multipolar neurons in the developing neocortex. Nat Neurosci 14 (2011), pp. 697-703.

Jossin, Y. and Goffinet, A.M. Reelin signals through phosphatidylinositol 3-kinase and Akt to control cortical development and through mTor to regulate dendritic growth. Mol Cell Biol 27 (2007), pp. 7113-24.

Jossin, Y., Ignatova, N., Hiesberger, T., Herz, J., Lambert de Rouvroit, C. and Goffinet, A.M. The central fragment of Reelin, generated by proteolytic processing in vivo, is critical to its function during cortical plate development. J Neurosci 24 (2004), pp. 514-21.

Kaplan, M.S. and Hinds, J.W. Neurogenesis in the adult rat: electron microscopic analysis of light radioautographs. Science 197 (1977), pp. 1092-4.

Katakowski, M., Zhang, Z., deCarvalho, A.C. and Chopp, M. EphB2 induces proliferation and promotes a neuronal fate in adult subventricular neural precursor cells. Neurosci Lett 385 (2005), pp. 204-9.

Kayser, M.S., McClelland, A.C., Hughes, E.G. and Dalva, M.B. Intracellular and trans-synaptic regulation of glutamatergic synaptogenesis by EphB receptors. J Neurosci 26 (2006), pp. 12152-64.

Kempermann, G., Jessberger, S., Steiner, B. and Kronenberg, G. Milestones of neuronal development in the adult hippocampus. Trends Neurosci 27 (2004), pp. 447-52.

Kempermann, G., Song, H. and Gage, F.H. Neurogenesis in the Adult Hippocampus. Cold Spring Harb Perspect Biol 7 (2015), p. a018812.

Khalaf-Nazzal, R. and Francis, F. Hippocampal development - old and new findings. Neuroscience 248 (2013), pp. 225-42.

Khodosevich, K., Watanabe, Y. and Monyer, H. EphA4 preserves postnatal and adult neural stem cells in an undifferentiated state in vivo. J Cell Sci 124 (2011), pp. 1268-79.

Kim, H.M., Qu, T., Kriho, V., Lacor, P., Smalheiser, N., Pappas, G.D., Guidotti, A., Costa, E. and Sugaya, K. Reelin function in neural stem cell biology. Proc Natl Acad Sci U S A 99 (2002), pp. 4020-5.

Kim, J.J., Rison, R.A. and Fanselow, M.S. Effects of amygdala, hippocampus, and periaqueductal gray lesions on short- and long-term contextual fear. Behav Neurosci 107 (1993), pp. 1093-8.

Koch, S., Strasser, V., Hauser, C., Fasching, D., Brandes, C., Bajari, T.M., Schneider, W.J. and Nimpf, J. A secreted soluble form of ApoE receptor 2 acts as a dominant-negative receptor and inhibits Reelin signaling. EMBO J 21 (2002), pp. 5996-6004.

Kocherhans, S., Madhusudan, A., Doehner, J., Breu, K.S., Nitsch, R.M., Fritschy, J.M. and Knuesel, I. Reduced Reelin expression accelerates amyloid-beta plaque formation and tau pathology in transgenic Alzheimer's disease mice. J Neurosci 30 (2010), pp. 9228-40.

Koh, T.W., Korolchuk, V.I., Wairkar, Y.P., Jiao, W., Evergren, E., Pan, H., Zhou, Y., Venken, K.J., Shupliakov, O., Robinson, I.M., O'Kane, C.J. and Bellen, H.J. Eps15 and Dap160 control synaptic vesicle membrane retrieval and synapse development. J Cell Biol 178 (2007), pp. 309-22.

Koh, T.W., Verstreken, P. and Bellen, H.J. Dap160/intersectin acts as a stabilizing scaffold required for synaptic development and vesicle endocytosis. Neuron 43 (2004), pp. 193-205.

Koie, M., Okumura, K., Hisanaga, A., Kamei, T., Sasaki, K., Deng, M., Baba, A., Kohno, T. and Hattori, M. Cleavage within Reelin repeat 3 regulates the duration and range of the signaling activity of Reelin protein. J Biol Chem 289 (2014), pp. 12922-30.

Konstantinova, I., Nikolova, G., Ohara-Imaizumi, M., Meda, P., Kucera, T., Zarbalis, K., Wurst, W., Nagamatsu, S. and Lammert, E. EphA-Ephrin-A-mediated beta cell communication regulates insulin secretion from pancreatic islets. Cell 129 (2007), pp. 359-70.

Kronenberg, G., Reuter, K., Steiner, B., Brandt, M.D., Jessberger, S., Yamaguchi, M. and Kempermann, G. Subpopulations of proliferating cells of the adult hippocampus respond differently to physiologic neurogenic stimuli. J Comp Neurol 467 (2003), pp. 455-63.

Kullander, K., Butt, S.J., Lebret, J.M., Lundfald, L., Restrepo, C.E., Rydstrom, A., Klein, R. and Kiehn, O. Role of EphA4 and EphrinB3 in local neuronal circuits that control walking. Science 299 (2003), pp. 1889-92.

Kuo, G., Arnaud, L., Kronstad-O'Brien, P. and Cooper, J.A. Absence of Fyn and Src causes a reeler-like phenotype. J Neurosci 25 (2005), pp. 8578-86.

Labrador, J.P., Brambilla, R. and Klein, R. The N-terminal globular domain of Eph receptors is sufficient for ligand binding and receptor signaling. EMBO J 16 (1997), pp. 3889-97.

Lai, K.O. and Ip, N.Y. Synapse development and plasticity: roles of ephrin/Eph receptor signaling. Curr Opin Neurobiol 19 (2009), pp. 275-83.

Lakatosova, S. and Ostatnikova, D. Reelin and its complex involvement in brain development and function. Int J Biochem Cell Biol 44 (2012), pp. 1501-4.

Lambert de Rouvroit, C., de Bergeyck, V., Cortvrindt, C., Bar, I., Eeckhout, Y. and Goffinet, A.M. Reelin, the extracellular matrix protein deficient in reeler mutant mice, is processed by a metalloproteinase. Exp Neurol 156 (1999), pp. 214-7.

Larouche, M., Beffert, U., Herz, J. and Hawkes, R. The Reelin receptors Apoer2 and Vldlr coordinate the patterning of Purkinje cell topography in the developing mouse cerebellum. PLoS One 3 (2008), p. e1653.

Laussu, J., Khuong, A., Gautrais, J. and Davy, A. Beyond boundaries--Eph:ephrin signaling in neurogenesis. Cell Adh Migr 8 (2014), pp. 349-59.

Lee, G.H. and D'Arcangelo, G. New Insights into Reelin-Mediated Signaling Pathways. Front Cell Neurosci 10 (2016), p. 122.

Lee, H.S., Nishanian, T.G., Mood, K., Bong, Y.S. and Daar, I.O. EphrinB1 controls cell-cell junctions through the Par polarity complex. Nat Cell Biol 10 (2008), pp. 979-86.

Leemhuis, J., Bouche, E., Frotscher, M., Henle, F., Hein, L., Herz, J., Meyer, D.K., Pichler, M., Roth, G., Schwan, C. and Bock, H.H. Reelin signals through apolipoprotein E receptor 2 and Cdc42 to increase growth cone motility and filopodia formation. J Neurosci 30 (2010), pp. 14759-72.

Li, G., Ji, X.D., Gao, H., Zhao, J.S., Xu, J.F., Sun, Z.J., Deng, Y.Z., Shi, S., Feng, Y.X., Zhu, Y.Q., Wang, T., Li, J.J. and Xie, D. EphB3 suppresses non-small-cell lung cancer metastasis via a PP2A/RACK1/Akt signalling complex. Nat Commun 3 (2012), p. 667.

Li, J.J., Liu, D.P., Liu, G.T. and Xie, D. EphrinA5 acts as a tumor suppressor in glioma by negative regulation of epidermal growth factor receptor. Oncogene 28 (2009), pp. 1759-68.

Lim, Y.S., McLaughlin, T., Sung, T.C., Santiago, A., Lee, K.F. and O'Leary, D.D. p75(NTR) mediates ephrin-A reverse signaling required for axon repulsion and mapping. Neuron 59 (2008), pp. 746-58.

Lisabeth, E.M., Falivelli, G. and Pasquale, E.B. Eph receptor signaling and ephrins. Cold Spring Harb Perspect Biol 5 (2013).

Lois, C. and Alvarez-Buylla, A. Long-distance neuronal migration in the adult mammalian brain. Science 264 (1994), pp. 1145-8.

Lu, Q., Sun, E.E., Klein, R.S. and Flanagan, J.G. Ephrin-B reverse signaling is mediated by a novel PDZ-RGS protein and selectively inhibits G protein-coupled chemoattraction. Cell 105 (2001), pp. 69-79.

Lucassen, P.J., Oomen, C.A., Naninck, E.F., Fitzsimons, C.P., van Dam, A.M., Czeh, B. and Korosi, A. Regulation of Adult Neurogenesis and Plasticity by (Early) Stress, Glucocorticoids, and Inflammation. Cold Spring Harb Perspect Biol 7 (2015), p. a021303.

Luskin, M.B. Restricted proliferation and migration of postnatally generated neurons derived from the forebrain subventricular zone. Neuron 11 (1993), pp. 173-89.

Maddigan, A., Truitt, L., Arsenault, R., Freywald, T., Allonby, O., Dean, J., Narendran, A., Xiang, J., Weng, A., Napper, S. and Freywald, A. EphB receptors trigger Akt activation and suppress Fas receptor-induced apoptosis in malignant T lymphocytes. J Immunol 187 (2011), pp. 5983-94.

Makinen, T., Adams, R.H., Bailey, J., Lu, Q., Ziemiecki, A., Alitalo, K., Klein, R. and Wilkinson, G.A. PDZ interaction site in ephrinB2 is required for the remodeling of lymphatic vasculature. Genes Dev 19 (2005), pp. 397-410.

Malacombe, M., Ceridono, M., Calco, V., Chasserot-Golaz, S., McPherson, P.S., Bader, M.F. and Gasman, S. Intersectin-1L nucleotide exchange factor regulates secretory granule exocytosis by activating Cdc42. EMBO J 25 (2006), pp. 3494-503.

Margolis, S.S., Salogiannis, J., Lipton, D.M., Mandel-Brehm, C., Wills, Z.P., Mardinly, A.R., Hu, L., Greer, P.L., Bikoff, J.B., Ho, H.Y., Soskis, M.J., Sahin, M. and Greenberg, M.E. EphB-mediated degradation of the RhoA GEF Ephexin5 relieves a developmental brake on excitatory synapse formation. Cell 143 (2010), pp. 442-55.

Marie, B., Sweeney, S.T., Poskanzer, K.E., Roos, J., Kelly, R.B. and Davis, G.W. Dap160/intersectin scaffolds the periactive zone to achieve high-fidelity endocytosis and normal synaptic growth. Neuron 43 (2004), pp. 207-19.

Marler, K.J., Becker-Barroso, E., Martinez, A., Llovera, M., Wentzel, C., Poopalasundaram, S., Hindges, R., Soriano, E., Comella, J. and Drescher, U. A TrkB/EphrinA interaction controls retinal axon branching and synaptogenesis. J Neurosci 28 (2008), pp. 12700-12.

Marston, D.J., Dickinson, S. and Nobes, C.D. Rac-dependent trans-endocytosis of ephrinBs regulates Eph-ephrin contact repulsion. Nat Cell Biol 5 (2003), pp. 879-88.

Martin, N.P., Mohney, R.P., Dunn, S., Das, M., Scappini, E. and O'Bryan, J.P. Intersectin regulates epidermal growth factor receptor endocytosis, ubiquitylation, and signaling. Mol Pharmacol 70 (2006), pp. 1643-53.

Martina, J.A., Bonangelino, C.J., Aguilar, R.C. and Bonifacino, J.S. Stonin 2: an adaptor-like protein that interacts with components of the endocytic machinery. J Cell Biol 153 (2001), pp. 1111-20.

Maurer, M.E. and Cooper, J.A. The adaptor protein Dab2 sorts LDL receptors into coated pits independently of AP-2 and ARH. J Cell Sci 119 (2006), pp. 4235-46.

May, P., Bock, H.H., Nimpf, J. and Herz, J. Differential glycosylation regulates processing of lipoprotein receptors by gamma-secretase. J Biol Chem 278 (2003), pp. 37386-92.

May, P., Reddy, Y.K. and Herz, J. Proteolytic processing of low density lipoprotein receptor-related protein mediates regulated release of its intracellular domain. J Biol Chem 277 (2002), pp. 18736-43.

Mayer, B.J. and Eck, M.J. SH3 domains. Minding your p's and q's. Curr Biol 5 (1995), pp. 364-7.

Mayer, H., Duit, S., Hauser, C., Schneider, W.J. and Nimpf, J. Reconstitution of the Reelin signaling pathway in fibroblasts demonstrates that Dab1 phosphorylation is independent of receptor localization in lipid rafts. Mol Cell Biol 26 (2006), pp. 19-27.

McGavin, M.K., Badour, K., Hardy, L.A., Kubiseski, T.J., Zhang, J. and Siminovitch, K.A. The intersectin 2 adaptor links Wiskott Aldrich Syndrome protein (WASp)-mediated actin polymerization to T cell antigen receptor endocytosis. J Exp Med 194 (2001), pp. 1777-87.

McMahon, H.T. and Boucrot, E. Molecular mechanism and physiological functions of clathrin-mediated endocytosis. Nat Rev Mol Cell Biol 12 (2011), pp. 517-33.

Meier, C., Anastasiadou, S. and Knoll, B. Ephrin-A5 suppresses neurotrophin evoked neuronal motility, ERK activation and gene expression. PLoS One 6 (2011), p. e26089.

Mendes, S.W., Henkemeyer, M. and Liebl, D.J. Multiple Eph receptors and B-class ephrins regulate midline crossing of corpus callosum fibers in the developing mouse forebrain. J Neurosci 26 (2006), pp. 882-92.

Menges, C.W. and McCance, D.J. Constitutive activation of the Raf-MAPK pathway causes negative feedback inhibition of Ras-PI3K-AKT and cellular arrest through the EphA2 receptor. Oncogene 27 (2008), pp. 2934-40.

Miao, H., Li, D.Q., Mukherjee, A., Guo, H., Petty, A., Cutter, J., Basilion, J.P., Sedor, J., Wu, J., Danielpour, D., Sloan, A.E., Cohen, M.L. and Wang, B. EphA2 mediates ligand-dependent inhibition and ligand-independent promotion of cell migration and invasion via a reciprocal regulatory loop with Akt. Cancer Cell 16 (2009), pp. 9-20.

Miao, H., Wei, B.R., Peehl, D.M., Li, Q., Alexandrou, T., Schelling, J.R., Rhim, J.S., Sedor, J.R., Burnett, E. and Wang, B. Activation of EphA receptor tyrosine kinase inhibits the Ras/MAPK pathway. Nat Cell Biol 3 (2001), pp. 527-30.

Minami, M., Koyama, T., Wakayama, Y., Fukuhara, S. and Mochizuki, N. EphrinA/EphA signal facilitates insulin-like growth factor-I-induced myogenic differentiation through suppression of the Ras/extracellular signal-regulated kinase 1/2 cascade in myoblast cell lines. Mol Biol Cell 22 (2011), pp. 3508-19.

Ming, G.L. and Song, H. Adult neurogenesis in the mammalian central nervous system. Annu Rev Neurosci 28 (2005), pp. 223-50.

Mishra, S.K., Keyel, P.A., Hawryluk, M.J., Agostinelli, N.R., Watkins, S.C. and Traub, L.M. Disabled-2 exhibits the properties of a cargo-selective endocytic clathrin adaptor. EMBO J 21 (2002), pp. 4915-26.

Mitsunari, T., Nakatsu, F., Shioda, N., Love, P.E., Grinberg, A., Bonifacino, J.S. and Ohno, H. Clathrin adaptor AP-2 is essential for early embryonal development. Mol Cell Biol 25 (2005), pp. 9318-23.

Miyakawa, T., Yagi, T., Kitazawa, H., Yasuda, M., Kawai, N., Tsuboi, K. and Niki, H. Fyn-kinase as a determinant of ethanol sensitivity: relation to NMDA-receptor function. Science 278 (1997), pp. 698-701.

Miyata, T., Nakajima, K., Mikoshiba, K. and Ogawa, M. Regulation of Purkinje cell alignment by reelin as revealed with CR-50 antibody. J Neurosci 17 (1997), pp. 3599-609.

Moeller, M.L., Shi, Y., Reichardt, L.F. and Ethell, I.M. EphB receptors regulate dendritic spine morphogenesis through the recruitment/phosphorylation of focal adhesion kinase and RhoA activation. J Biol Chem 281 (2006), pp. 1587-98.

Moheb, L.A., Tzschach, A., Garshasbi, M., Kahrizi, K., Darvish, H., Heshmati, Y., Kordi, A., Najmabadi, H., Ropers, H.H. and Kuss, A.W. Identification of a nonsense mutation in the very low-density lipoprotein receptor gene (VLDLR) in an Iranian family with dysequilibrium syndrome. Eur J Hum Genet 16 (2008), pp. 270-3.

Mohney, R.P., Das, M., Bivona, T.G., Hanes, R., Adams, A.G., Philips, M.R. and O'Bryan, J.P. Intersectin activates Ras but stimulates transcription through an independent pathway involving JNK. J Biol Chem 278 (2003), pp. 47038-45.

Momboisse, F., Ory, S., Calco, V., Malacombe, M., Bader, M.F. and Gasman, S. Calcium-regulated exocytosis in neuroendocrine cells: intersectin-1L stimulates actin polymerization and exocytosis by activating Cdc42. Ann N Y Acad Sci 1152 (2009), pp. 209-14.

Morderer, D., Nikolaienko, O., Skrypkina, I., Cherkas, V., Tsyba, L., Belan, P. and Rynditch, A. Endocytic adaptor protein intersectin 1 forms a complex with microtubule stabilizer STOP in neurons. Gene 505 (2012), pp. 360-4.

Morimura, T., Hattori, M., Ogawa, M. and Mikoshiba, K. Disabled1 regulates the intracellular trafficking of reelin receptors. J Biol Chem 280 (2005), pp. 16901-8.

Morimura, T. and Ogawa, M. Relative importance of the tyrosine phosphorylation sites of Disabled-1 to the transmission of Reelin signaling. Brain Res 1304 (2009), pp. 26-37.
Morris, R.G., Garrud, P., Rawlins, J.N. and O'Keefe, J. Place navigation impaired in rats with hippocampal lesions. Nature 297 (1982), pp. 681-3.
Morris, S.M. and Cooper, J.A. Disabled-2 colocalizes with the LDLR in clathrin-coated pits and interacts with AP-2. Traffic 2 (2001), pp. 111-23.
Murai, K.K., Nguyen, L.N., Irie, F., Yamaguchi, Y. and Pasquale, E.B. Control of hippocampal dendritic spine morphology through ephrin-A3/EphA4 signaling. Nat Neurosci 6 (2003), pp. 153-60.
Nakahira, E. and Yuasa, S. Neuronal generation, migration, and differentiation in the mouse hippocampal primoridium as revealed by enhanced green fluorescent protein gene transfer by means of in utero electroporation. J Comp Neurol 483 (2005), pp. 329-40.
Nakajima, K., Mikoshiba, K., Miyata, T., Kudo, C. and Ogawa, M. Disruption of hippocampal development in vivo by CR-50 mAb against reelin. Proc Natl Acad Sci U S A 94 (1997), pp. 8196-201.
Nakano, Y., Kohno, T., Hibi, T., Kohno, S., Baba, A., Mikoshiba, K., Nakajima, K. and Hattori, M. The extremely conserved C-terminal region of Reelin is not necessary for secretion but is required for efficient activation of downstream signaling. J Biol Chem 282 (2007), pp. 20544-52.
Nishimura, T., Yamaguchi, T., Tokunaga, A., Hara, A., Hamaguchi, T., Kato, K., Iwamatsu, A., Okano, H. and Kaibuchi, K. Role of numb in dendritic spine development with a Cdc42 GEF intersectin and EphB2. Mol Biol Cell 17 (2006), pp. 1273-85.
Niu, S., Renfro, A., Quattrocchi, C.C., Sheldon, M. and D'Arcangelo, G. Reelin promotes hippocampal dendrite development through the VLDLR/ApoER2-Dab1 pathway. Neuron 41 (2004), pp. 71-84.
Niu, S., Yabut, O. and D'Arcangelo, G. The Reelin signaling pathway promotes dendritic spine development in hippocampal neurons. J Neurosci 28 (2008), pp. 10339-48.
Noren, N.K., Foos, G., Hauser, C.A. and Pasquale, E.B. The EphB4 receptor suppresses breast cancer cell tumorigenicity through an Abl-Crk pathway. Nat Cell Biol 8 (2006), pp. 815-25.
Ogawa, M., Miyata, T., Nakajima, K., Yagyu, K., Seike, M., Ikenaka, K., Yamamoto, H. and Mikoshiba, K. The reeler gene-associated antigen on Cajal-Retzius neurons is a crucial molecule for laminar organization of cortical neurons. Neuron 14 (1995), pp. 899-912.
Oh, P., McIntosh, D.P. and Schnitzer, J.E. Dynamin at the neck of caveolae mediates their budding to form transport vesicles by GTP-driven fission from the plasma membrane of endothelium. J Cell Biol 141 (1998), pp. 101-14.
Ohkubo, N., Lee, Y.D., Morishima, A., Terashima, T., Kikkawa, S., Tohyama, M., Sakanaka, M., Tanaka, J., Maeda, N., Vitek, M.P. and Mitsuda, N. Apolipoprotein E and Reelin ligands modulate tau phosphorylation through an apolipoprotein E receptor/disabled-1/glycogen synthase kinase-3beta cascade. FASEB J 17 (2003), pp. 295-7.
Okamoto, M., Schoch, S. and Sudhof, T.C. EHSH1/intersectin, a protein that contains EH and SH3 domains and binds to dynamin and SNAP-25. A protein connection between exocytosis and endocytosis? J Biol Chem 274 (1999), pp. 18446-54.
Palmer, A., Zimmer, M., Erdmann, K.S., Eulenburg, V., Porthin, A., Heumann, R., Deutsch, U. and Klein, R. EphrinB phosphorylation and reverse signaling: regulation by Src kinases and PTP-BL phosphatase. Mol Cell 9 (2002), pp. 725-37.
Palmer, T.D., Takahashi, J. and Gage, F.H. The adult rat hippocampus contains primordial neural stem cells. Mol Cell Neurosci 8 (1997), pp. 389-404.
Park, I. and Lee, H.S. EphB/ephrinB signaling in cell adhesion and migration. Mol Cells 38 (2015), pp. 14-9.
Park, T.J. and Curran, T. Crk and Crk-like play essential overlapping roles downstream of disabled-1 in the Reelin pathway. J Neurosci 28 (2008), pp. 13551-62.
Pasquale, E.B. Eph-ephrin bidirectional signaling in physiology and disease. Cell 133 (2008), pp. 38-52.
Patten, A.R., Yau, S.Y., Fontaine, C.J., Meconi, A., Wortman, R.C. and Christie, B.R. The Benefits of Exercise on Structural and Functional Plasticity in the Rodent Hippocampus of Different Disease Models. Brain Plasticity 1 (2015), pp. 97-127.
Pechstein, A., Bacetic, J., Vahedi-Faridi, A., Gromova, K., Sundborger, A., Tomlin, N., Krainer, G., Vorontsova, O., Schafer, J.G., Owe, S.G., Cousin, M.A., Saenger, W., Shupliakov, O. and Haucke, V. Regulation of synaptic vesicle recycling by complex formation between intersectin 1 and the clathrin adaptor complex AP2. Proc Natl Acad Sci U S A 107 (2010a), pp. 4206-11.
Pechstein, A., Gerth, F., Milosevic, I., Japel, M., Eichhorn-Grunig, M., Vorontsova, O., Bacetic, J., Maritzen, T., Shupliakov, O., Freund, C. and Haucke, V. Vesicle uncoating regulated by SH3-SH3 domain-

mediated complex formation between endophilin and intersectin at synapses. EMBO Rep 16 (2015), pp. 232-9.

Pechstein, A., Shupliakov, O. and Haucke, V. Intersectin 1: a versatile actor in the synaptic vesicle cycle. Biochem Soc Trans 38 (2010b), pp. 181-6.

Penzes, P., Beeser, A., Chernoff, J., Schiller, M.R., Eipper, B.A., Mains, R.E. and Huganir, R.L. Rapid induction of dendritic spine morphogenesis by trans-synaptic ephrinB-EphB receptor activation of the Rho-GEF kalirin. Neuron 37 (2003), pp. 263-74.

Pesold, C., Impagnatiello, F., Pisu, M.G., Uzunov, D.P., Costa, E., Guidotti, A. and Caruncho, H.J. Reelin is preferentially expressed in neurons synthesizing gamma-aminobutyric acid in cortex and hippocampus of adult rats. Proc Natl Acad Sci U S A 95 (1998), pp. 3221-6.

Poirier, S., Mayer, G., Benjannet, S., Bergeron, E., Marcinkiewicz, J., Nassoury, N., Mayer, H., Nimpf, J., Prat, A. and Seidah, N.G. The proprotein convertase PCSK9 induces the degradation of low density lipoprotein receptor (LDLR) and its closest family members VLDLR and ApoER2. J Biol Chem 283 (2008), pp. 2363-72.

Poliakov, A., Cotrina, M.L., Pasini, A. and Wilkinson, D.G. Regulation of EphB2 activation and cell repulsion by feedback control of the MAPK pathway. J Cell Biol 183 (2008), pp. 933-47.

Pramatarova, A., Ochalski, P.G., Chen, K., Gropman, A., Myers, S., Min, K.T. and Howell, B.W. Nck beta interacts with tyrosine-phosphorylated disabled 1 and redistributes in Reelin-stimulated neurons. Mol Cell Biol 23 (2003), pp. 7210-21.

Predescu, S.A., Predescu, D.N., Knezevic, I., Klein, I.K. and Malik, A.B. Intersectin-1s regulates the mitochondrial apoptotic pathway in endothelial cells. J Biol Chem 282 (2007), pp. 17166-78.

Predescu, S.A., Predescu, D.N., Timblin, B.K., Stan, R.V. and Malik, A.B. Intersectin regulates fission and internalization of caveolae in endothelial cells. Mol Biol Cell 14 (2003), pp. 4997-5010.

Pucharcos, C., Casas, C., Nadal, M., Estivill, X. and de la Luna, S. The human intersectin genes and their spliced variants are differentially expressed. Biochim Biophys Acta 1521 (2001), pp. 1-11.

Pucharcos, C., Estivill, X. and de la Luna, S. Intersectin 2, a new multimodular protein involved in clathrin-mediated endocytosis. FEBS Lett 478 (2000), pp. 43-51.

Pujadas, L., Gruart, A., Bosch, C., Delgado, L., Teixeira, C.M., Rossi, D., de Lecea, L., Martinez, A., Delgado-Garcia, J.M. and Soriano, E. Reelin regulates postnatal neurogenesis and enhances spine hypertrophy and long-term potentiation. J Neurosci 30 (2010), pp. 4636-49.

Pujadas, L., Rossi, D., Andres, R., Teixeira, C.M., Serra-Vidal, B., Parcerisas, A., Maldonado, R., Giralt, E., Carulla, N. and Soriano, E. Reelin delays amyloid-beta fibril formation and rescues cognitive deficits in a model of Alzheimer's disease. Nat Commun 5 (2014), p. 3443.

Qiao, F. and Bowie, J.U. The many faces of SAM. Sci STKE 2005 (2005), p. re7.

Qiu, R., Wang, X., Davy, A., Wu, C., Murai, K., Zhang, H., Flanagan, J.G., Soriano, P. and Lu, Q. Regulation of neural progenitor cell state by ephrin-B. J Cell Biol 181 (2008), pp. 973-83.

Rakic, P. Evolution of the neocortex: a perspective from developmental biology. Nat Rev Neurosci 10 (2009), pp. 724-35.

Ramos-Moreno, T., Galazo, M.J., Porrero, C., Martinez-Cerdeno, V. and Clasca, F. Extracellular matrix molecules and synaptic plasticity: immunomapping of intracellular and secreted Reelin in the adult rat brain. Eur J Neurosci 23 (2006), pp. 401-22.

Reddy, S.S., Connor, T.E., Weeber, E.J. and Rebeck, W. Similarities and differences in structure, expression, and functions of VLDLR and ApoER2. Mol Neurodegener 6 (2011), p. 30.

Ricard, J., Salinas, J., Garcia, L. and Liebl, D.J. EphrinB3 regulates cell proliferation and survival in adult neurogenesis. Mol Cell Neurosci 31 (2006), pp. 713-22.

Rice, D.S., Sheldon, M., D'Arcangelo, G., Nakajima, K., Goldowitz, D. and Curran, T. Disabled-1 acts downstream of Reelin in a signaling pathway that controls laminar organization in the mammalian brain. Development 125 (1998), pp. 3719-29.

Richter, M., Murai, K.K., Bourgin, C., Pak, D.T. and Pasquale, E.B. The EphA4 receptor regulates neuronal morphology through SPAR-mediated inactivation of Rap GTPases. J Neurosci 27 (2007), pp. 14205-15.

Riddell, D.R., Sun, X.M., Stannard, A.K., Soutar, A.K. and Owen, J.S. Localization of apolipoprotein E receptor 2 to caveolae in the plasma membrane. J Lipid Res 42 (2001), pp. 998-1002.

Riedl, J.A., Brandt, D.T., Batlle, E., Price, L.S., Clevers, H. and Bos, J.L. Down-regulation of Rap1 activity is involved in ephrinB1-induced cell contraction. Biochem J 389 (2005), pp. 465-9.

Roos, J. and Kelly, R.B. Dap160, a neural-specific Eps15 homology and multiple SH3 domain-containing protein that interacts with Drosophila dynamin. J Biol Chem 273 (1998), pp. 19108-19.

Rose, S., Malabarba, M.G., Krag, C., Schultz, A., Tsushima, H., Di Fiore, P.P. and Salcini, A.E. Caenorhabditis elegans intersectin: a synaptic protein regulating neurotransmission. Mol Biol Cell 18 (2007), pp. 5091-9.

Rothberg, K.G., Heuser, J.E., Donzell, W.C., Ying, Y.S., Glenney, J.R. and Anderson, R.G. Caveolin, a protein component of caveolae membrane coats. Cell 68 (1992), pp. 673-82.

Royaux, I., Lambert de Rouvroit, C., D'Arcangelo, G., Demirov, D. and Goffinet, A.M. Genomic organization of the mouse reelin gene. Genomics 46 (1997), pp. 240-50.

Sahin, M., Greer, P.L., Lin, M.Z., Poucher, H., Eberhart, J., Schmidt, S., Wright, T.M., Shamah, S.M., O'Connell, S., Cowan, C.W., Hu, L., Goldberg, J.L., Debant, A., Corfas, G., Krull, C.E. and Greenberg, M.E. Eph-dependent tyrosine phosphorylation of ephexin1 modulates growth cone collapse. Neuron 46 (2005), pp. 191-204.

Sakaba, T., Kononenko, N.L., Bacetic, J., Pechstein, A., Schmoranzer, J., Yao, L., Barth, H., Shupliakov, O., Kobler, O., Aktories, K. and Haucke, V. Fast neurotransmitter release regulated by the endocytic scaffold intersectin. Proc Natl Acad Sci U S A 110 (2013), pp. 8266-71.

Sakai, K., Tiebel, O., Ljungberg, M.C., Sullivan, M., Lee, H.J., Terashima, T., Li, R., Kobayashi, K., Lu, H.C., Chan, L. and Oka, K. A neuronal VLDLR variant lacking the third complement-type repeat exhibits high capacity binding of apoE containing lipoproteins. Brain Res 1276 (2009), pp. 11-21.

Santolini, E., Salcini, A.E., Kay, B.K., Yamabhai, M. and Di Fiore, P.P. The EH network. Exp Cell Res 253 (1999), pp. 186-209.

Sawamiphak, S., Seidel, S., Essmann, C.L., Wilkinson, G.A., Pitulescu, M.E., Acker, T. and Acker-Palmer, A. Ephrin-B2 regulates VEGFR2 function in developmental and tumour angiogenesis. Nature 465 (2010), pp. 487-91.

Schiffmann, S.N., Bernier, B. and Goffinet, A.M. Reelin mRNA expression during mouse brain development. Eur J Neurosci 9 (1997), pp. 1055-71.

Schurig, V., Orman, A.V. and Bowen, P. Nonprogressive cerebellar disorder with mental retardation and autosomal recessive inheritance in Hutterites. Am J Med Genet 9 (1981), pp. 43-53.

Seaberg, R.M. and van der Kooy, D. Adult rodent neurogenic regions: the ventricular subependyma contains neural stem cells, but the dentate gyrus contains restricted progenitors. J Neurosci 22 (2002), pp. 1784-93.

Segura, I., Essmann, C.L., Weinges, S. and Acker-Palmer, A. Grb4 and GIT1 transduce ephrinB reverse signals modulating spine morphogenesis and synapse formation. Nat Neurosci 10 (2007), pp. 301-10.

Sengar, A.S., Ellegood, J., Yiu, A.P., Wang, H., Wang, W., Juneja, S.C., Lerch, J.P., Josselyn, S.A., Henkelman, R.M., Salter, M.W. and Egan, S.E. Vertebrate intersectin1 is repurposed to facilitate cortical midline connectivity and higher order cognition. J Neurosci 33 (2013), pp. 4055-65.

Sengar, A.S., Wang, W., Bishay, J., Cohen, S. and Egan, S.E. The EH and SH3 domain Ese proteins regulate endocytosis by linking to dynamin and Eps15. EMBO J 18 (1999), pp. 1159-71.

Senturk, A., Pfennig, S., Weiss, A., Burk, K. and Acker-Palmer, A. Ephrin Bs are essential components of the Reelin pathway to regulate neuronal migration. Nature 472 (2011), pp. 356-60.

Seri, B., Garcia-Verdugo, J.M., Collado-Morente, L., McEwen, B.S. and Alvarez-Buylla, A. Cell types, lineage, and architecture of the germinal zone in the adult dentate gyrus. J Comp Neurol 478 (2004), pp. 359-78.

Seri, B., Garcia-Verdugo, J.M., McEwen, B.S. and Alvarez-Buylla, A. Astrocytes give rise to new neurons in the adult mammalian hippocampus. J Neurosci 21 (2001), pp. 7153-60.

Shamah, S.M., Lin, M.Z., Goldberg, J.L., Estrach, S., Sahin, M., Hu, L., Bazalakova, M., Neve, R.L., Corfas, G., Debant, A. and Greenberg, M.E. EphA receptors regulate growth cone dynamics through the novel guanine nucleotide exchange factor ephexin. Cell 105 (2001), pp. 233-44.

Sheldon, M., Rice, D.S., D'Arcangelo, G., Yoneshima, H., Nakajima, K., Mikoshiba, K., Howell, B.W., Cooper, J.A., Goldowitz, D. and Curran, T. Scrambler and yotari disrupt the disabled gene and produce a reeler-like phenotype in mice. Nature 389 (1997), pp. 730-3.

Shi, L., Fu, W.Y., Hung, K.W., Porchetta, C., Hall, C., Fu, A.K. and Ip, N.Y. Alpha2-chimaerin interacts with EphA4 and regulates EphA4-dependent growth cone collapse. Proc Natl Acad Sci U S A 104 (2007), pp. 16347-52.

Sibbe, M., Forster, E., Basak, O., Taylor, V. and Frotscher, M. Reelin and Notch1 cooperate in the development of the dentate gyrus. J Neurosci 29 (2009), pp. 8578-85.

Sinagra, M., Verrier, D., Frankova, D., Korwek, K.M., Blahos, J., Weeber, E.J., Manzoni, O.J. and Chavis, P. Reelin, very-low-density lipoprotein receptor, and apolipoprotein E receptor 2 control somatic

NMDA receptor composition during hippocampal maturation in vitro. J Neurosci 25 (2005), pp. 6127-36.

Song, J., Vranken, W., Xu, P., Gingras, R., Noyce, R.S., Yu, Z., Shen, S.H. and Ni, F. Solution structure and backbone dynamics of the functional cytoplasmic subdomain of human ephrin B2, a cell-surface ligand with bidirectional signaling properties. Biochemistry 41 (2002), pp. 10942-9.

Srivastava, N., Robichaux, M.A., Chenaux, G., Henkemeyer, M. and Cowan, C.W. EphB2 receptor forward signaling controls cortical growth cone collapse via Nck and Pak. Mol Cell Neurosci 52 (2013), pp. 106-16.

Steiner, B., Klempin, F., Wang, L., Kott, M., Kettenmann, H. and Kempermann, G. Type-2 cells as link between glial and neuronal lineage in adult hippocampal neurogenesis. Glia 54 (2006), pp. 805-14.

Stockinger, W., Brandes, C., Fasching, D., Hermann, M., Gotthardt, M., Herz, J., Schneider, W.J. and Nimpf, J. The reelin receptor ApoER2 recruits JNK-interacting proteins-1 and -2. J Biol Chem 275 (2000), pp. 25625-32.

Stolt, P.C., Chen, Y., Liu, P., Bock, H.H., Blacklow, S.C. and Herz, J. Phosphoinositide binding by the disabled-1 PTB domain is necessary for membrane localization and Reelin signal transduction. J Biol Chem 280 (2005), pp. 9671-7.

Stolt, P.C., Jeon, H., Song, H.K., Herz, J., Eck, M.J. and Blacklow, S.C. Origins of peptide selectivity and phosphoinositide binding revealed by structures of disabled-1 PTB domain complexes. Structure 11 (2003), pp. 569-79.

Stranahan, A.M., Erion, J.R. and Wosiski-Kuhn, M. Reelin signaling in development, maintenance, and plasticity of neural networks. Ageing Res Rev 12 (2013), pp. 815-22.

Strasser, V., Fasching, D., Hauser, C., Mayer, H., Bock, H.H., Hiesberger, T., Herz, J., Weeber, E.J., Sweatt, J.D., Pramatarova, A., Howell, B., Schneider, W.J. and Nimpf, J. Receptor clustering is involved in Reelin signaling. Mol Cell Biol 24 (2004), pp. 1378-86.

Suh, H., Consiglio, A., Ray, J., Sawai, T., D'Amour, K.A. and Gage, F.H. In vivo fate analysis reveals the multipotent and self-renewal capacities of Sox2+ neural stem cells in the adult hippocampus. Cell Stem Cell 1 (2007), pp. 515-28.

Suh, H., Deng, W. and Gage, F.H. Signaling in adult neurogenesis. Annu Rev Cell Dev Biol 25 (2009), pp. 253-75.

Sun, X.M. and Soutar, A.K. The transmembrane domain and PXXP motifs of ApoE receptor 2 exclude it from carrying out clathrin-mediated endocytosis. J Biol Chem 278 (2003), pp. 19926-32.

Suzuki, T. and Okumura-Noji, K. NMDA receptor subunits epsilon 1 (NR2A) and epsilon 2 (NR2B) are substrates for Fyn in the postsynaptic density fraction isolated from the rat brain. Biochem Biophys Res Commun 216 (1995), pp. 582-8.

Sweet, H.O., Bronson, R.T., Johnson, K.R., Cook, S.A. and Davisson, M.T. Scrambler, a new neurological mutation of the mouse with abnormalities of neuronal migration. Mamm Genome 7 (1996), pp. 798-802.

Tanaka, M., Kamata, R. and Sakai, R. Phosphorylation of ephrin-B1 via the interaction with claudin following cell-cell contact formation. EMBO J 24 (2005), pp. 3700-11.

Teckchandani, A., Mulkearns, E.E., Randolph, T.W., Toida, N. and Cooper, J.A. The clathrin adaptor Dab2 recruits EH domain scaffold proteins to regulate integrin beta1 endocytosis. Mol Biol Cell 23 (2012), pp. 2905-16.

Teixeira, C.M., Kron, M.M., Masachs, N., Zhang, H., Lagace, D.C., Martinez, A., Reillo, I., Duan, X., Bosch, C., Pujadas, L., Brunso, L., Song, H., Eisch, A.J., Borrell, V., Howell, B.W., Parent, J.M. and Soriano, E. Cell-autonomous inactivation of the reelin pathway impairs adult neurogenesis in the hippocampus. J Neurosci 32 (2012), pp. 12051-65.

Thomas, S., Ritter, B., Verbich, D., Sanson, C., Bourbonniere, L., McKinney, R.A. and McPherson, P.S. Intersectin regulates dendritic spine development and somatodendritic endocytosis but not synaptic vesicle recycling in hippocampal neurons. J Biol Chem 284 (2009), pp. 12410-9.

Tissir, F. and Goffinet, A.M. Reelin and brain development. Nat Rev Neurosci 4 (2003), pp. 496-505.

Tolias, K.F., Bikoff, J.B., Kane, C.G., Tolias, C.S., Hu, L. and Greenberg, M.E. The Rac1 guanine nucleotide exchange factor Tiam1 mediates EphB receptor-dependent dendritic spine development. Proc Natl Acad Sci U S A 104 (2007), pp. 7265-70.

Tong, X.K., Hussain, N.K., Adams, A.G., O'Bryan, J.P. and McPherson, P.S. Intersectin can regulate the Ras/MAP kinase pathway independent of its role in endocytosis. J Biol Chem 275 (2000a), pp. 29894-9.

Tong, X.K., Hussain, N.K., de Heuvel, E., Kurakin, A., Abi-Jaoude, E., Quinn, C.C., Olson, M.F., Marais, R., Baranes, D., Kay, B.K. and McPherson, P.S. The endocytic protein intersectin is a major binding partner for the Ras exchange factor mSos1 in rat brain. EMBO J 19 (2000b), pp. 1263-71.

Torres, R., Firestein, B.L., Dong, H., Staudinger, J., Olson, E.N., Huganir, R.L., Bredt, D.S., Gale, N.W. and Yancopoulos, G.D. PDZ proteins bind, cluster, and synaptically colocalize with Eph receptors and their ephrin ligands. Neuron 21 (1998), pp. 1453-63.

Trommsdorff, M., Gotthardt, M., Hiesberger, T., Shelton, J., Stockinger, W., Nimpf, J., Hammer, R.E., Richardson, J.A. and Herz, J. Reeler/Disabled-like disruption of neuronal migration in knockout mice lacking the VLDL receptor and ApoE receptor 2. Cell 97 (1999), pp. 689-701.

Tsyba, L., Nikolaienko, O., Dergai, O., Dergai, M., Novokhatska, O., Skrypkina, I. and Rynditch, A. Intersectin multidomain adaptor proteins: regulation of functional diversity. Gene 473 (2011), pp. 67-75.

Turkmen, S., Hoffmann, K., Demirhan, O., Aruoba, D., Humphrey, N. and Mundlos, S. Cerebellar hypoplasia, with quadrupedal locomotion, caused by mutations in the very low-density lipoprotein receptor gene. Eur J Hum Genet 16 (2008), pp. 1070-4.

Utsunomiya-Tate, N., Kubo, K., Tate, S., Kainosho, M., Katayama, E., Nakajima, K. and Mikoshiba, K. Reelin molecules assemble together to form a large protein complex, which is inhibited by the function-blocking CR-50 antibody. Proc Natl Acad Sci U S A 97 (2000), pp. 9729-34.

van Praag, H., Schinder, A.F., Christie, B.R., Toni, N., Palmer, T.D. and Gage, F.H. Functional neurogenesis in the adult hippocampus. Nature 415 (2002), pp. 1030-4.

Vindis, C., Cerretti, D.P., Daniel, T.O. and Huynh-Do, U. EphB1 recruits c-Src and p52Shc to activate MAPK/ERK and promote chemotaxis. J Cell Biol 162 (2003), pp. 661-71.

Voss, A.K., Britto, J.M., Dixon, M.P., Sheikh, B.N., Collin, C., Tan, S.S. and Thomas, T. C3G regulates cortical neuron migration, preplate splitting and radial glial cell attachment. Development 135 (2008), pp. 2139-49.

Wahlsten, D. Deficiency of corpus callosum varies with strain and supplier of the mice. Brain Res 239 (1982), pp. 329-47.

Wang, J.B., Wu, W.J. and Cerione, R.A. Cdc42 and Ras cooperate to mediate cellular transformation by intersectin-L. J Biol Chem 280 (2005), pp. 22883-91.

Wang, W., Bouhours, M., Gracheva, E.O., Liao, E.H., Xu, K., Sengar, A.S., Xin, X., Roder, J., Boone, C., Richmond, J.E., Zhen, M. and Egan, S.E. ITSN-1 controls vesicle recycling at the neuromuscular junction and functions in parallel with DAB-1. Traffic 9 (2008), pp. 742-54.

Wang, Y., Nakayama, M., Pitulescu, M.E., Schmidt, T.S., Bochenek, M.L., Sakakibara, A., Adams, S., Davy, A., Deutsch, U., Luthi, U., Barberis, A., Benjamin, L.E., Makinen, T., Nobes, C.D. and Adams, R.H. Ephrin-B2 controls VEGF-induced angiogenesis and lymphangiogenesis. Nature 465 (2010), pp. 483-6.

Warner-Schmidt, J.L. and Duman, R.S. Hippocampal neurogenesis: opposing effects of stress and antidepressant treatment. Hippocampus 16 (2006), pp. 239-49.

Weeber, E.J., Beffert, U., Jones, C., Christian, J.M., Forster, E., Sweatt, J.D. and Herz, J. Reelin and ApoE receptors cooperate to enhance hippocampal synaptic plasticity and learning. J Biol Chem 277 (2002), pp. 39944-52.

Wegmeyer, H., Egea, J., Rabe, N., Gezelius, H., Filosa, A., Enjin, A., Varoqueaux, F., Deininger, K., Schnutgen, F., Brose, N., Klein, R., Kullander, K. and Betz, A. EphA4-dependent axon guidance is mediated by the RacGAP alpha2-chimaerin. Neuron 55 (2007), pp. 756-67.

Weiss, K.H., Johanssen, C., Tielsch, A., Herz, J., Deller, T., Frotscher, M. and Forster, E. Malformation of the radial glial scaffold in the dentate gyrus of reeler mice, scrambler mice, and ApoER2/VLDLR-deficient mice. J Comp Neurol 460 (2003), pp. 56-65.

Wilmot, B., McWeeney, S.K., Nixon, R.R., Montine, T.J., Laut, J., Harrington, C.A., Kaye, J.A. and Kramer, P.L. Translational gene mapping of cognitive decline. Neurobiol Aging 29 (2008), pp. 524-41.

Winther, A.M., Jiao, W., Vorontsova, O., Rees, K.A., Koh, T.W., Sopova, E., Schulze, K.L., Bellen, H.J. and Shupliakov, O. The dynamin-binding domains of Dap160/intersectin affect bulk membrane retrieval in synapses. J Cell Sci 126 (2013), pp. 1021-31.

Winther, A.M., Vorontsova, O., Rees, K.A., Nareoja, T., Sopova, E., Jiao, W. and Shupliakov, O. An Endocytic Scaffolding Protein together with Synapsin Regulates Synaptic Vesicle Clustering in the Drosophila Neuromuscular Junction. J Neurosci 35 (2015), pp. 14756-70.

Wong, K.A., Wilson, J., Russo, A., Wang, L., Okur, M.N., Wang, X., Martin, N.P., Scappini, E., Carnegie, G.K. and O'Bryan, J.P. Intersectin (ITSN) family of scaffolds function as molecular hubs in protein interaction networks. PLoS One 7 (2012), p. e36023.

Wybenga-Groot, L.E., Baskin, B., Ong, S.H., Tong, J., Pawson, T. and Sicheri, F. Structural basis for autoinhibition of the Ephb2 receptor tyrosine kinase by the unphosphorylated juxtamembrane region. Cell 106 (2001), pp. 745-57.

Wynshaw-Boris, A. and Gambello, M.J. LIS1 and dynein motor function in neuronal migration and development. Genes Dev 15 (2001), pp. 639-51.

Xiao, Z., Carrasco, R., Kinneer, K., Sabol, D., Jallal, B., Coats, S. and Tice, D.A. EphB4 promotes or suppresses Ras/MEK/ERK pathway in a context-dependent manner: Implications for EphB4 as a cancer target. Cancer Biol Ther 13 (2012), pp. 630-7.

Xu, N.J. and Henkemeyer, M. Ephrin-B3 reverse signaling through Grb4 and cytoskeletal regulators mediates axon pruning. Nat Neurosci 12 (2009), pp. 268-76.

Yamabhai, M., Hoffman, N.G., Hardison, N.L., McPherson, P.S., Castagnoli, L., Cesareni, G. and Kay, B.K. Intersectin, a novel adaptor protein with two Eps15 homology and five Src homology 3 domains. J Biol Chem 273 (1998), pp. 31401-7.

Yang, D.H., Smith, E.R., Roland, I.H., Sheng, Z., He, J., Martin, W.D., Hamilton, T.C., Lambeth, J.D. and Xu, X.X. Disabled-2 is essential for endodermal cell positioning and structure formation during mouse embryogenesis. Dev Biol 251 (2002), pp. 27-44.

Yang, G., Pan, F. and Gan, W.B. Stably maintained dendritic spines are associated with lifelong memories. Nature 462 (2009), pp. 920-4.

Yang, N., Higuchi, O., Ohashi, K., Nagata, K., Wada, A., Kangawa, K., Nishida, E. and Mizuno, K. Cofilin phosphorylation by LIM-kinase 1 and its role in Rac-mediated actin reorganization. Nature 393 (1998), pp. 809-12.

Yang, N.Y., Fernandez, C., Richter, M., Xiao, Z., Valencia, F., Tice, D.A. and Pasquale, E.B. Crosstalk of the EphA2 receptor with a serine/threonine phosphatase suppresses the Akt-mTORC1 pathway in cancer cells. Cell Signal 23 (2011), pp. 201-12.

Yoneshima, H., Nagata, E., Matsumoto, M., Yamada, M., Nakajima, K., Miyata, T., Ogawa, M. and Mikoshiba, K. A novel neurological mutant mouse, yotari, which exhibits reeler-like phenotype but expresses CR-50 antigen/reelin. Neurosci Res 29 (1997), pp. 217-23.

Yoo, S., Kim, Y., Noh, H., Lee, H., Park, E. and Park, S. Endocytosis of EphA receptors is essential for the proper development of the retinocollicular topographic map. EMBO J 30 (2011), pp. 1593-607.

Yu, Y., Chu, P.Y., Bowser, D.N., Keating, D.J., Dubach, D., Harper, I., Tkalcevic, J., Finkelstein, D.I. and Pritchard, M.A. Mice deficient for the chromosome 21 ortholog Itsn1 exhibit vesicle-trafficking abnormalities. Hum Mol Genet 17 (2008), pp. 3281-90.

Zhang, G., Assadi, A.H., McNeil, R.S., Beffert, U., Wynshaw-Boris, A., Herz, J., Clark, G.D. and D'Arcangelo, G. The Pafah1b complex interacts with the reelin receptor VLDLR. PLoS One 2 (2007), p. e252.

Zhao, S., Chai, X., Forster, E. and Frotscher, M. Reelin is a positional signal for the lamination of dentate granule cells. Development 131 (2004), pp. 5117-25.

Zhao, S., Chai, X. and Frotscher, M. Balance between neurogenesis and gliogenesis in the adult hippocampus: role for reelin. Dev Neurosci 29 (2007), pp. 84-90.

Zimmer, M., Palmer, A., Kohler, J. and Klein, R. EphB-ephrinB bi-directional endocytosis terminates adhesion allowing contact mediated repulsion. Nat Cell Biol 5 (2003), pp. 869-78.

6. Appendix

6.1 List of abbreviations

AA/BA	Acrylamide/bis-acrylamide
ACSF	Artificial cerebrospinal fluid
Alk5	Activin receptor-like kinase 5
AMPAR	α-amino-3-hydroxy-5-methyl-4-isoxazolepropionic acid receptor
AP-2	Adaptor protein complex 2
ApoER2	Apolipoprotein E receptor 2
APS	Ammonium persulfate
Arp2/3	Actin-related protein-2/3 complex
BAR	Bin-Amphiphysin-Rvs
BDNF	Brain-derived neurotrophic factor
BMP	Bone morphogenetic protein
bp	Base pair
BrdU	Bromodeoxyuridine
C3G	CRK SH3-binding GNRP
CA	Cornu ammonis
Cbl	Casitas B-lineage lymphoma
CCP	Clathrin-coated pit
CCR	Coiled-coil region
Cdc42	Cell division cycle 42
CdGAP	Cdc42 GTPase-activating protein
CIP	Calf intestinal phosphatase
Crk	CT10 Regulator of Kinase
CTD	C-terminal domain
Cul5	Culin-5
Dab1	Disabled 1
Dap160	Dynamin-associated protein 160 kDa
DAPI	4',6-Diamidino-2-phenylindole
Dcx	Doublecortin
DG	Dentate gyrus
DH	Dbl homology
DIV	Day *in vitro*
DMEM	Dulbecco's modified Eagle medium
DMSO	Dimethyl sulfoxide
DNA	Deoxyribonucleic acid
dNTP	Deoxynucleotide triphosphates
DSDB	Donkey serum dilution buffer
E. coli	Escherichia coli
EC	Entorhinal cortex
EDTA	Ethylenediaminetetraacetic acid
EGF	Epidermal growth factor
EH	Eps15 homology
Ephexin	Eph-interacting exchange protein
Ephrin	Eph family receptor interacting protein
Erk	Extracellular signal–regulated kinase
F-actin	Filamentous actin
FBS	Fetal bovine serum
fEPSPs	Field excitatory postsynaptic potentials
FGF2	Fibroblast growth factor 2
fw	Forward
GABA	Gamma-aminobutyric acid
GAP	GTPase-activating protein

GCC	Growth cone collapse
GCL	Granular cell layer
GEF	Guanine nucleotide exchange factor
GFAP	Glial fibrillary acidic protein
GFP	Green fluorescent protein
GPI	Glycosylphosphatidylinositol
Grb2	Growth factor receptor-bound protein 2
GSDB	Goat serum dilution buffer
GSK3β	Glycogen synthase kinase 3 beta
GST	Glutathione S-transferase
HA	Hemagglutinin
HBSS	Hank's balanced salt solution
HC	Hippocampus
HEK 293	Human Embryonic Kidney 293 cells
HRP	Horseradish peroxidase
ICR	Intracellular region
IGF1	Insulin-like growth factor 1
IgG	Immunoglobulin G
IP	Immunoprecipitation
IPTG	Isopropyl thiogalactoside
ITSN	Intersectin
IZ	Intermediate zone
JIP	JNK interacting protein
JNK	c-Jun N-terminal kinase
kDa	Kilodalton
KO	Knockout
LB	Lysogeny broth
Lis1	Lissencephaly 1
LPP	Lateral perforant pathway
LTP	Long-term potentiation
Mek	MAPK/ERK kinase
MEM	Minimum essential medium Eagle
ML	Molecular layer
MPP	Medial perforant pathway
MZ	Marginal zone
Nck	Noncatalytic region of tyrosine kinase
NeuN	Neuronal nuclei
NeuroD	Neurogenic differentiation
NMDA	N-methyl-D-aspartate
NPF	Asn-Pro-Phe
NT3	Neurotrophin 3
N-WASP	Neuronal Wiskott–Aldrich syndrome protein
OB	Olfactory bulb
Pafah	Platelet-activating factor acetylhydrolase
PAGE	Polyacrylamide gel electrophoresis
PBS	Phosphate-buffered saline
PCR	Polymerase chain reaction
PD	Pulldown
PDGF	Platelet-derived growth factor
PDZ	PSD-95/Dlg1/ZO1
PFA	Paraformaldehyde
PH	Pleckstrin homology
PI3K	Phosphoinositide 3-kinase
$PI4,5P_2$	Phosphatidylinositol 4,5-bisphosphate
PRR	Proline-rich region
PTB	Phosphotyrosine-binding
Rac1	Ras-related C3 botulinum toxin substrate 1
Rap1	Ras-related protein 1
Ras	Rat sarcoma

rev	Reverse
Rho	Ras homolog gene family
RNA	Ribonucleic acid
RR	Reelin repeat
RTK	Receptor tyrosine kinase
SAM	Sterile-α motif
SCM	Serum-containing medium
SDM	Secondary dentate matrix
SDS	Sodium dodecyl sulfate
SEM	Standard error of the mean
SFK	Src family kinase
SFM	Serum-free medium
SGZ	Subgranular zone
SH2	Src homology 2
SH3	Src homology 3
Shh	Sonic hedgehog protein
siRNA	Small interfering RNA
SNAP25	Synaptosomal-associated protein 25 kDa
SNARE	Soluble NSF attachment protein receptor
SOCS	Suppressor of cytokine signaling
Sos1	Son Of Sevenless Homolog 1
Sox2	SRY (sex determining region Y)-box 2
Src	Sarcoma
STAT3	Signal transducer and activator of transcription 3
SV	Synaptic vesicle
SVZ	Subventricular zone
TBE	Tris-Borate-EDTA
TBS	Tris-buffered saline
TBS	Theta burst stimulation
TDM	Tertiary dentate matrix
TE	Tris-EDTA
TEMED	Tetramethylethylenediamine
TGFβ	Transforming growth factor beta
Tiam1	T-Cell Lymphoma Invasion And Metastasis 1
TrkB	Tyrosine receptor kinase B
UV	Ultraviolet
v/v	Volume per volume
VEGF	Vascular endothelial growth factor
Vinc	Vinculin
VLDLR	Very-low-density-lipoprotein receptor
VZ	Ventricular zone
w/o	Without
w/v	Weight per volume
WT	Wildtype

6.2 List of figures